LBL-33996
CONF-9304102
UC-411

Advanced
Light
Source

Working Group on Elliptical Wiggler

Report of the Workshop

Lawrence Berkeley Laboratory
April 19, 1993

Lawrence Berkeley Laboratory
University of California
Berkeley, California 94720

May 1993

Prepared for the U.S. Department of Energy under Contract No. DE-AC03-76SF00098

LOAN COPY
Circulates
for 4 weeks
Bldg. 50 Library.
LBL-33996
Copy 2

DISCLAIMER

This document was prepared as an account of work sponsored by the United States Government. While this document is believed to contain correct information, neither the United States Government nor any agency thereof, nor the Regents of the University of California, nor any of their employees, makes any warranty, express or implied, or assumes any legal responsibility for the accuracy, completeness, or usefulness of any information, apparatus, product, or process disclosed, or represents that its use would not infringe privately owned rights. Reference herein to any specific commercial product, process, or service by its trade name, trademark, manufacturer, or otherwise, does not necessarily constitute or imply its endorsement, recommendation, or favoring by the United States Government or any agency thereof, or the Regents of the University of California. The views and opinions of authors expressed herein do not necessarily state or reflect those of the United States Government or any agency thereof or the Regents of the University of California.

Working Group on Elliptical Wiggler

Report of the Workshop

at

Lawrence Berkeley Laboratory

April 19, 1993

Organized by:

Philip A. Heimann and Alfred S. Schlachter

Lawrence Berkeley Laboratory
University of California
Berkeley, California 94720

This report has been reproduced directly from the best possible copy.

This work was supported by the Director, Office of Energy Research, Office of Basic Energy Sciences, Materials Sciences Division, of the U.S. Department of Energy under Contract No. DE-AC03-76SF00098

Contents

Workshop Program v

List of Participants vii

Executive Summary 1
Philip Heimann and Alfred Schlachter

Welcome to the ALS 3
Alfred Schlachter

Brief Scientific Presentation by Workshop Participants
Francois Wuilleumier 11
Dennis Lindle 19
Markus Pahler 21
Chien-Te Chen 25
James Tobin 27
James Erskine 37
Charles Fadley 45
Carsten Westphal 55
Joseph Nordgren 61
Zhixun Shen 69
Jeffrey Kortright 73
Stephen Cramer 75
Roger Carr 79

Overview of Insertion Devices for Elliptical Polarization 83
Kwang-Je Kim

Performance of Elliptical Wiggler and Crossed Undulator 109
Chun Xi Wang

Hybrid–Electromagnet Elliptical Wiggler Design 131
Egon Hoyer

3-D Magnetic Calculations 157
Ross Schlueter

Beamlines for the Elliptical Wiggler 161
Philip Heimann

WORKING GROUP ON ELLIPTICAL WIGGLER MEETING

April 19, 1993

Building 2, Room 100B

AGENDA

8:30 - 9:00 a.m.	Coffee	
9:00 - 9:15	Welcome	Fred Schlachter
9:15 - 10:15	Brief Scientific Presentations	
10:15 - 10:30	Break	
10:30 - 11:30	Brief Scientific Presentations	
11:30 - 12:00 p.m.	Overview of Insertion Devices for Elliptical Polarization	Kwang-Je Kim
12:00 - 1:00	WORKING LUNCH	
1:00 - 2:00	Radiation Calculations	Chun Xi Wang
2:00 - 3:00	Elliptical Wiggler	Egon Hoyer
3:00 - 3:30	3-D Magnetic Calculations	Ross Schlueter
3:30 - 3:45	Break	
3:45 - 4:30	Beamlines	Phil Heimann
4:30 - 5:15	Discussion	
5:15 - 5:45	Brief Tour of ALS	

Working Group on Elliptical Wiggler

April 19, 1993
Lawrence Berkeley Laboratory
Berkeley, CA

David Attwood
Lawrence Berkeley Laboratory
1 Cyclotron Road, 2-400
Berkeley, CA 94720

Thomas A. Callcott
University of Tennessee
Physics Department
401 Nielsen Physics Bldg.
Knoxville, TN 37996

Roger G. Carr
Stanford Synchrotron Rad. Lab
SLAC/Bin 69
P.O. Box 4349
Stanford, CA 94309-0210

Chien-Te Chen
AT&T Bell Laboratories
600 Mountain Avenue
1A-103
Murray Hill, NJ 07974

Paul L. Cowan
Argonne National Laboratory
Physics Division
F-125, Bldg. 203
9700 S. Cass Avenue
Argonne, IL 60439

Stephen P. Cramer
Lawrence Berkeley Laboratory
1 Cyclotron Road, 2-400
Berkeley, CA 94720

David L. Ederer
Tulane University
Physics Department
6823 St. Charles Avenue
New Orleans, LA 70118

James L. Erskine
University of Texas
Department of Physics
Austin, TX 78712-1081

Charles S. Fadley
Lawrence Berkeley Laboratory
1 Cyclotron Road, 2-100
Berkeley, CA 94720

Siman George
University of California, Davis
Davis, CA 95616

William V. Hassenzahl
Lawrence Livermore National Lab
L-643
P.O. Box 5511
Livermore, CA 94551

Phil Heimann
Lawrence Berkeley Laboratory
1 Cyclotron Road, 2-400
Berkeley, CA 94720

Egon Hoyer
Lawrence Berkeley Laboratory
1 Cyclotron Road, 46-161
Berkeley, CA 94720

David E. Humphries
Lawrence Berkeley Laboratory
1 Cyclotron Road, 46-161
Berkeley, CA 94720

Zahid Hussain
Lawrence Berkeley Laboratory
1 Cyclotron Road, 2-300
Berkeley, CA 94720

Kwang-Je Kim
Lawrence Berkeley Laboratory
1 Cyclotron Road, 71-259
Berkeley, CA 94720

Yong Joo Kim
Lawrence Berkeley Laboratory
1 Cyclotron Road, 2-100
Berkeley, CA 94720

Jeffrey B. Kortright
Lawrence Berkeley Laboratory
1 Cyclotron Road, 2-400
Berkeley, CA 94720

Steve Lidia
Lawrence Berkeley Laboratory
1 Cyclotron Road, 71-259
Berkeley, CA 94720

Dennis W. Lindle
Univ. of Nevada, Las Vegas
(UNLV)
Department of Chemistry
4505 S. Maryland Parkway
Las Vegas, NV 89154

Steve Marks
Lawrence Berkeley Laboratory
1 Cyclotron Road, 46-161
Berkeley, CA 94720

Miklos Ed Melczer
Lawrence Berkeley Laboratory
1 Cyclotron Road, 2-400
Berkeley, CA 94720

Andero Nillsson
Department of Physics
University of Uppsala
Box 530
S-75121 Uppsala, SWEDEN

Joseph E. Nordgren
Department of Physics
University of Uppsala
Box 530
S-75121 Uppsala, SWEDEN

Howard Padmore
Lawrence Berkeley Laboratory
1 Cyclotron Road, 2-400
Berkeley, CA 94720

Markus Pahler
Nernstweg 22
W-2000
Hamburg 50, GERMANY

Piero A. Pianetta
Stanford Synchrotron Rad. Lab
Bin 69
P.O. Box 4349
Stanford, CA 94309

David Plate
Lawrence Berkeley Laboratory
1 Cyclotron Road, 46-161
Berkeley, CA 94720

Arthur L. Robinson
Lawrence Berkeley Laboratory
1 Cyclotron Road, 80-101
Berkeley, CA 94720

Philip N. Ross, Jr.
Lawrence Berkeley Laboratory
1 Cyclotron Road, 2-100
Berkeley, CA 94720

Alfred S. Schlachter
Lawrence Berkeley Laboratory
1 Cyclotron Road, 2-400
Berkeley, CA 94720

Ross Schlueter
Lawrence Berkeley Laboratory
1 Cyclotron Road, 46-161
Berkeley, CA 94720

Zhixun X. Shen
Stanford University
Electrical Engineering Department
Stanford Electronics Laboratories
Stanford, CA 94305

Neville V. Smith
AT&T Bell Laboratories
600 Mountain Avenue
IT-106
Murray Hill, NJ 07974

James G. Tobin
Lawrence Livermore National
Laboratory
L-357
P.O. Box 805
Livermore, CA 94550

Chunxi Wang
Lawrence Berkeley Laboratory
1 Cyclotron Road, 2-400
Berkeley, CA 94720

Zaitin Wang
Lawrence Berkeley Laboratory
1 Cyclotron Road, 2-100
Berkeley, CA 94720

Tony Warwick
Lawrence Berkeley Laboratory
1 Cyclotron Road, 2-400
Berkeley, CA 94720

Carsten Westphal
Lawrence Berkeley Laboratory
1 Cyclotron Road, 2-100
Berkeley, CA 94720

Francois Wuilleumier
Université de Paris-Sud
Lab. de Spectroscopie
Atom. et Ionique
Bâtiment 350
91405 Orsay Cedex, FRANCE

Executive Summary

The purpose of the elliptical wiggler working group meeting held at Lawrence Berkeley Laboratory was to discuss the production and use of elliptically polarized radiation at the ALS. The objective was to exchange views with users on the scientific and technical cases for an elliptical wiggler that is presently being designed at the ALS. An additional purpose was to discuss an eventual second insertion device to produce elliptically polarized radiation at the ALS, e.g., a crossed undulator. Approximately 40 scientists and engineers participated in the informal workshop.

Elliptically polarized vacuum-ultraviolet (VUV) and x-ray radiation is of considerable interest as a tool for probing matter. There are many areas of application such as materials and surface sciences; atomic and molecular physics and chemistry; and biology. Possible benefits to industry might include a better understanding of the characteristics of magnetic materials, and the development of new materials with greatly increased magnetic storage capacities.

A synchrotron light source can produce elliptically-polarized radiation in the VUV and soft-x-ray regions of the spectrum in many ways. Choices include: use of bend-magnet radiation out of the plane of the circulating electrons; a specialized undulator or wiggler; or by means of specialized optical systems for certain regions of the spectrum (e.g., multiple reflection or a transmission multi-layer). A wiggler typically produces high flux over a large energy range while an undulator generates high-brightness radiation over a smaller energy range.

Brief scientific presentations were given by several workshop participants describing experiments that would take advantage of elliptically polarized light produced by an elliptical wiggler. The proposals covered a variety of scientific disciplines and demonstrated a high level of interest in elliptically-polarized photons over a broad energy range. Some of the applications discussed were: circular dichroism and magnetic circular dichroism effects as manifested in x-ray absorption; photoelectron emission and diffraction; and x-ray fluorescence from a wide range of systems including gas-phase specimens (e.g., laser-aligned atoms and chiral molecules), biological molecules, adsorbates, and magnetic materials. For magnetic materials, these measurements include the element-specific imaging of individual structures in magnetic storage devices, as well as studies of dilute or weak magnetic systems, multilayer and low-dimensional magnetic structures, high-temperature superconductors, element-specific magnetic phase transitions, and so-called "complete" experiments in which all physical variables, including the direction and spin of the outgoing photoelectrons, are measured. Excitation of both core and valence levels were also of interest, leading to the conclusion that a very broad energy range of approximately 50 eV to 10,000 eV is desirable if all potential users are to be accommodated.

A degree of circular polarization of approximately 80% or higher was deemed to be sufficient for most applications. The accepted figure of merit (IP^2) for maximizing the signal-to-noise ratio in an experiment is the square of the polarization multiplied by the flux. The table on the next page shows the figure of merit for an ALS bend magnet, an ALS elliptical wiggler, and the EPU undulator at SSRL.

A general overview of elliptically-polarized radiation was presented; including bend magnets, helical and crossed undulators, and asymmetric and elliptical wigglers. A

comparison was made of calculated flux and brightness for bend-magnet, undulator, and wiggler sources at the ALS. Two insertion devices for the ALS appear to look favorable: an elliptical wiggler to produce high flux over a wide energy range, and an undulator to produce high-brightness radiation from low energies up to about 1 keV.

Afternoon talks by ALS staff members covered some of the engineering and physics design parameters of the wiggler and beamlines proposed at the ALS. It was generally agreed that the entire energy range of the ALS elliptical wiggler, approximately 50 eV to 10 keV, is important for research. The degree of polarization that can be obtained with a wiggler, and the desirability of modulating the sense of polarization and the desired rate of modulation, were also discussed.

At least two monochromators will be required to span the photon energy-range produced by an elliptical wiggler at the ALS. There was considerable discussion about optimizing the designs of various monochromators for spectroscopy and microscopy, using multilayer gratings in the 1–2 keV region, and preserving the degree of circular polarization through the monochromators. The ALS will devote additional design effort to these topics in the coming months, and intends to study square-wave modulation of the sense of the polarization at 1 Hz to meet user needs.

Users are excited about the prospects of research with elliptically polarized radiation at the ALS and the new research opportunities that will be available in this rapidly developing area.

Comparison of Different Sources of Elliptically Polarized Radiation

Parameter and Source	**Energy**			
	100 eV	500 eV	1000 eV	5000 eV
FLUX[1]				
ALS Elliptical Wiggler[2]	3×10^{14}	4×10^{14}	5×10^{14}	9×10^{13}
ALS Bend Magnet[3]	2×10^{13}	2×10^{13}	1×10^{13}	3×10^{11}
SSRL EPU (Undulator)[4]		3×10^{14}	8×10^{13}	
CIRCULAR POLARIZATION[5]				
ALS Elliptical Wiggler	0.79	0.79	0.82	0.83
ALS Bend Magnet	0.94	0.91	0.90	0.85
SSRL EPU (Undulator)		1.0	1.0	
IP[2]				
ALS Elliptical Wiggler	2×10^{14}	3×10^{14}	3×10^{14}	6×10^{13}
ALS Bend Magnet	2×10^{13}	2×10^{13}	1×10^{13}	2×10^{11}
SSRL EPU (Undulator)		3×10^{14}	8×10^{13}	

[1] The unit for flux is photon/(sec 0.1% bw). A current of 400 mA is assumed for the ALS and 100 mA for the Stanford Synchrotron Radiation Laboratory (SSRL).

[2] The angular acceptance for the elliptical wiggler is 5 mrad horizontally and 0.3 mrad vertically.

[3] The 7.5 mrad horizontal acceptance for the bend magnet is taken from ALS beamline 9.3.2.

[4] All SSRL values are from Roger Carr (SSRL).

[5] The circular polarization degree is expressed in terms of the Stokes parameters: S_3/S_0.

Welcome to the ALS

Alfred S. Schlachter

Lawrence Berkeley Laboratory

ELLIPTICAL WIGGLER WORKING GROUP: APRIL 19, 1993

- General objective: discuss production and use of elliptically polarized radiation at the ALS

- Specific objective: discuss scientific and technical cases for an elliptical wiggler at the ALS

- Scientific areas of application include:

  - magnetic materials
  - biological materials
  - atoms
  - molecules
  -

working group participants will present ideas for experiments

- Technical issues to discuss include:

  - choice of wiggler, undulator
  - parameters: energy range, flux, spot size, degree of polarization, modulation
  - beamlines: grating monochromator, double-crystal monochromator

Lawrence Berkeley Laboratory Scores Engineering Triumph

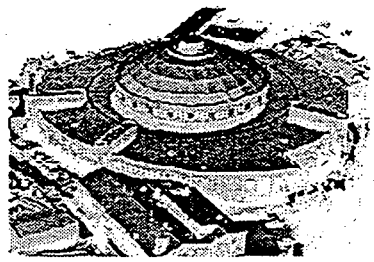

A full week ahead of schedule, the Advanced Light Source (ALS) at Lawrence Berkeley Laboratory (LBL) exceeded the baseline performance requirement for project completion while remaining within budget. The ALS achieved 65 milliamperes (mA) of electron-beam current in its storage ring, well above the 50-mA milestone set by the Department of Energy (DOE). On March 31, 1993, the actual deadline, the beam current far surpassed all expectations, reaching 290 mA. By April 9, the current exceeded the 400-mA design goal, reaching 407 mA. This performance is a testimony to the team of engineers, physicists, and technicians working on the project, whose near-perfect work in design, assembly, alignment, and electronic control enabled the ALS to operate as soon as it was turned on. This is a rare occurrence in high-tech projects as complex as this one.

Built with $100 million in DOE construction funds, the ALS is a national user facility providing high-brightness beams of ultraviolet and soft x-ray light. It has been eagerly awaited by researchers in the physical, chemical, materials, and life sciences. Its principal component is a storage ring 200 meters in circumference. A stored electron beam circulates in the ring at nearly the speed of light. The beam is guided and focused by hundreds of precision electromagnets situated around the ring. Special undulator magnets cause the electron beam to produce synchrotron radiation, making the ALS the world's brightest ultraviolet and soft x-ray light source.

The most remarkable aspect of commissioning the ALS storage ring is the speed with which it progressed (see table). For a project as large and complex as the ALS, this timetable would have been impossible if not for the high quality of the engineering that turned the ideas of physicist planners into reality. The fact that electron beam was stored on the same day the rf system was turned on clearly attests to this quality.

December 1992	*Storage ring installation completed.*
January 19, 1993	*Electrons injected into the ring. Beam coasts around the ring once.*
March 16, 1993	*Radio-frequency power system starts operation. Electron beam stored in ring for the first time; reaches current of 6 mA. Many millions of turns around the ring recorded.*
March 24, 1993	*Electron beam current passes 50-mA milestone; reaches 65 mA.*
March 31, 1993	*Electron beam current reaches 290 mA.*
April 9, 1993	*Electron beam current reaches 407 mA. Exceeds design goal of 400 mA.*

Once the conceptual design was established, perhaps the greatest engineering challenge was the requirement for extremely tight tolerances in building and aligning components. For instance, the typical tolerance for aligning the magnets around the storage ring was 150 μm (barely the thickness of two human hairs), and the tolerance for machining the 10-meter aluminum sectors that make up the storage-ring vacuum chamber was about the same.

At a time when some say U.S. expertise in science and technology is slipping, the ALS proves we have the knowledge, skill, and dedication to build a world-class scientific facility on time, within budget, and to a level of perfection rarely achieved on a comparable scale. ■

THE SECRETARY OF ENERGY
WASHINGTON, D.C.

March 30, 1993

Dr. Charles Shank
Director
Lawrence Berkeley Laboratory
University of California
Berkeley, California 94720

Dear Dr. Shank:

Congratulations on the successful completion of the new Advanced Light Source. Please convey my appreciation to the Lawrence Berkeley Laboratory staff members who contributed to this effort, especially Drs. Brian Kincaid and Jay Marx who guided the project. Achieving the first stored beam in the storage ring with all systems operating was a crucial milestone.

We are proud that this project will soon contribute to the Nation's technology base.

Sincerely,

Hazel R. O'Leary

ADVANCED LIGHT SOURCE: RESEARCH PROGRAM

- Operations begin now
  - Construction project completed: April 1993
  - Installation of undulators and beamlines: May–July 1993 (shutdown)
  - Research program begins: August 1993

- Six user beamlines for FY93 and FY94

Beamlines

7.0 —— U5 Undulator ------ materials
8.0 —— U5 Undulator ------ surfaces & materials
9.0 —— U8 Undulator ------ atomic physics & chemisty
9.3.1 —— Bend Magnet ------ soft x-ray beamline
9.3.2 —— Bend Magnet ------ surfaces and materials
10.3 —— Bend Magnet ------ microprobe

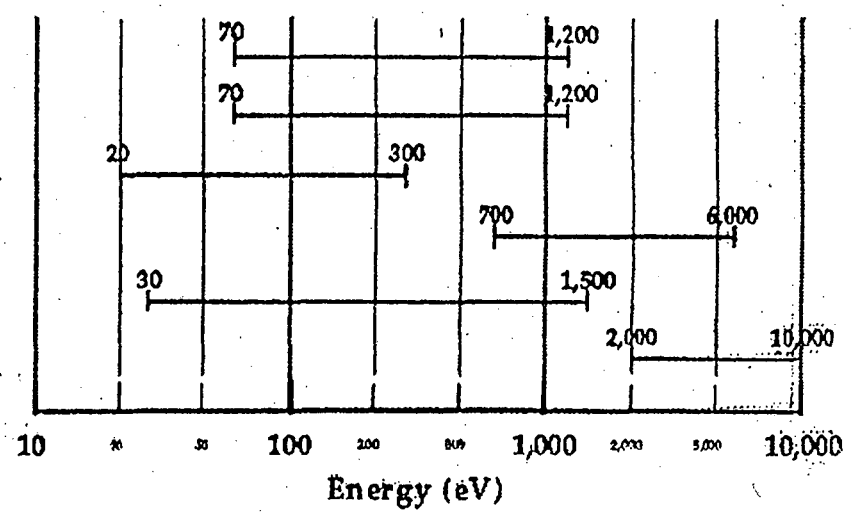

OPERATING PLANS FOR FY93 AND FY94

ALS

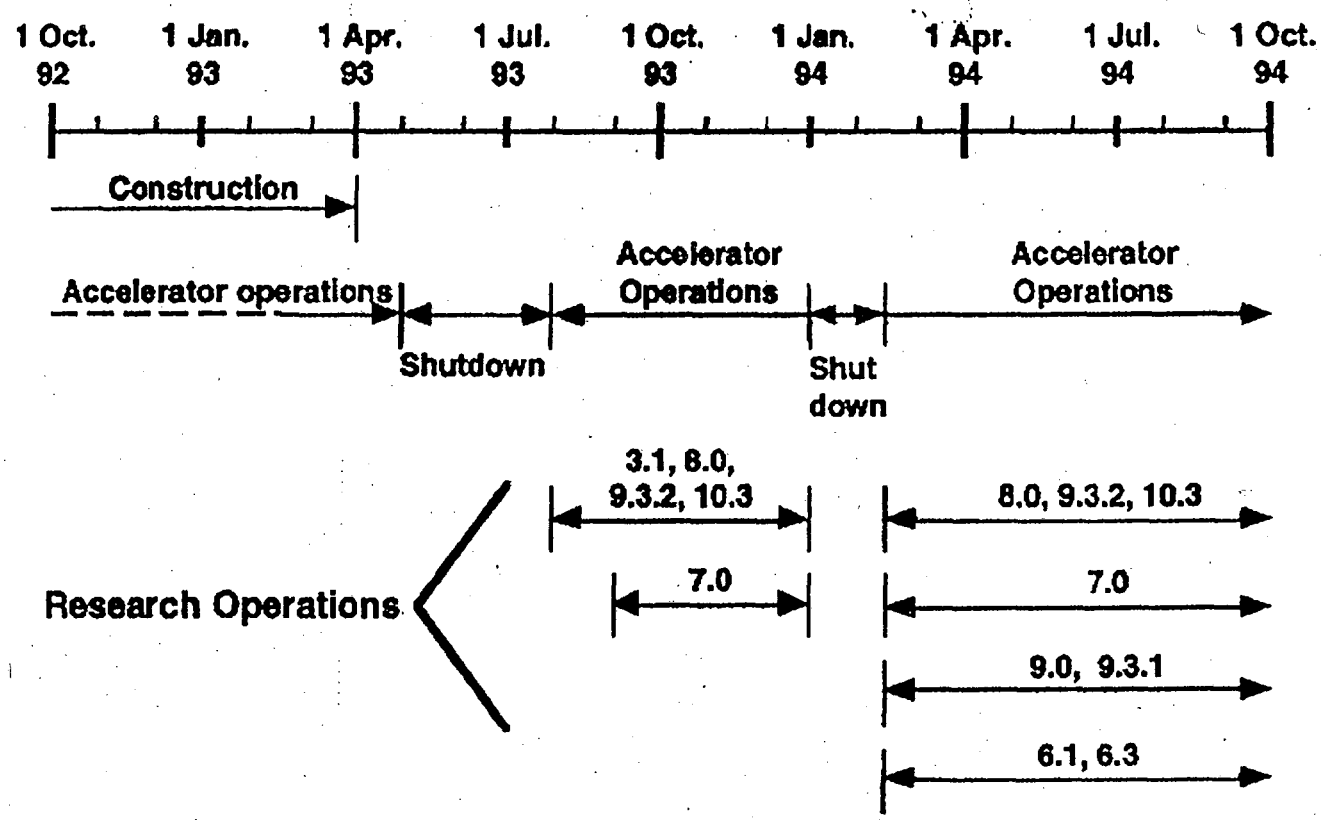

Beamlines

7.0	U5 Undulator—materials
8.0	U5 Undulator—surfaces & materials
9.0	U8 Undulator—atomic physics & chemistry
9.3.1	Bend Magnet—soft x-ray beamline
9.3.2	Bend Magnet—surfaces and materials
10.3	Bend Magnet—microprobe

Additional Bend-magnet Beamlines

3.1	Diagnostic
6.1	Microscopy
6.3	Metrology

Beamlines and Insertion Devices Funded for 1993—1995

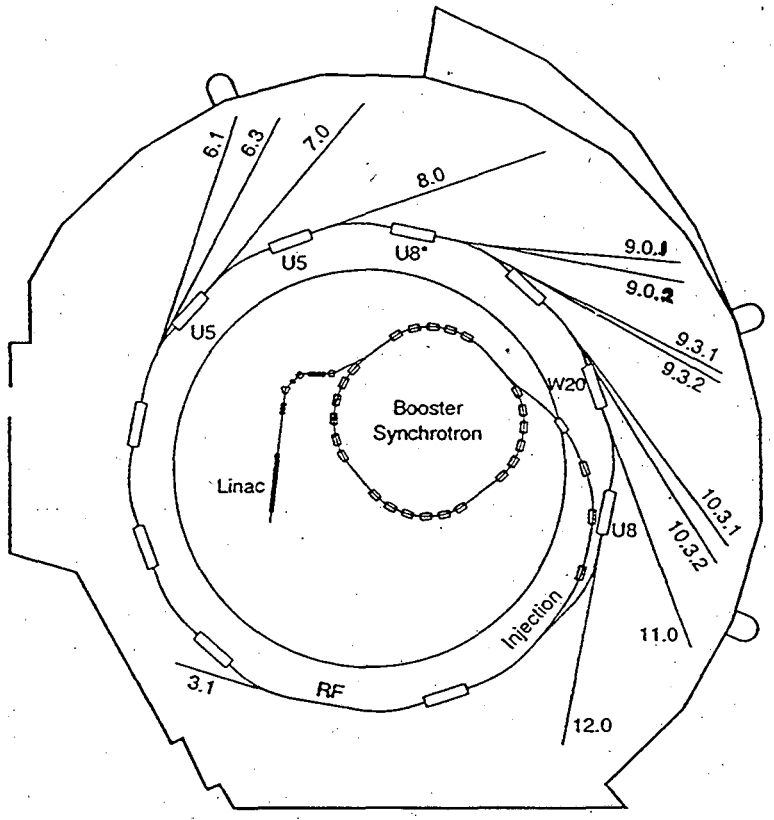

* Will change to U10 in 1995

Beamline	Source	Research
3.1	Bend magnet	Diagnostic beamline
6.1	Bend magnet	Biological microscopy
6.3	Bend magnet	Metrology and standards
7.0	U5.0 undulator	Surfaces and materials
8.0	U5.0 undulator	Surfaces and materials
9.0.1 9.0.2	U8.0 undulator (will become U10 in 1995)	Atomic physics and chemistry
9.3.1	Bend magnet	Atomic and materials science (double crystal)
9.3.2	Bend magnet	Chemical and materials science (SGM)
10.3.1 10.3.2	Bend magnet	Materials science (white light microprobe)
11.0	W20 elliptical wiggler	Materials science and biology
12.0	U8.0 undulator	X-ray lithography

Brief Scientific Presentation

Francois Wuilleumier

Université de Paris-Sud

Circular Dichroism in Double Photoionization

Jamal Berakdar and Hubert Klar
Fakultät für Physik, Universität Freiburg, 7800 Freiburg, Federal Republic of Germany
(Received 1 June 1992)

One-photon two-electron ionization of an atom by circularly polarized light yields triply differential cross sections different for left and right circular polarization. Necessary kinematical conditions for a finite dichroism are worked out. A numerical calculation for helium which employs correlated wave functions shows the angular correlations of the escaping electron pair to be very different for left and right circular polarization such that the effect should be observable in a coincidence experiment.

Proposed by F. Wuilleumier, F. Schlachter, M. Pahler

$$He\,(1s^2\ {}^1S_0) + h\nu \rightarrow He^{++} + e^- + e^-$$

Threshold for Double Ionization : 79.0 eV

$$\frac{d\sigma}{d\Omega_p} = \frac{\sigma_0}{4\pi}[1 - \tfrac{1}{2}\beta P_2(\hat{k}\cdot\hat{p})]\,,$$ for single ionization (for unpolarized, R or L circularly polarized radiation)

For double photoionization the triply differential cross section (TDCS) for the pair of photoelectrons detected in coincidence including energy analysis is then given by [2–4]

$$\frac{d^3\sigma}{d\Omega_a\, d\Omega_b\, dE_a} = C\sum_{M_f}\frac{1}{2J_i+1}\sum_{M_i}|\langle\Psi^-_{\mathbf{p}_a\mathbf{p}_b}|\hat{\epsilon}\cdot\mathbf{D}|\Phi_i\rangle|^2 \qquad (2)$$

with the constant $C = 4\pi^2\alpha a_0^2 E_\gamma p_a p_b$. Here, energies E and momenta p of the photoelectrons are labeled by indices a and b, α is the fine-structure constant, a_0 is the Bohr radius, E_γ is the incident radiation energy, $\mathbf{D} = \sum_n \mathbf{r}_n$ is the dipole operator in length form, and $\hat{\epsilon}$ is the polarization vector. Equation (2) averages over the initial magnetic sublevels M_i, and sums over the magnetic sublevels M_f of the photoion.

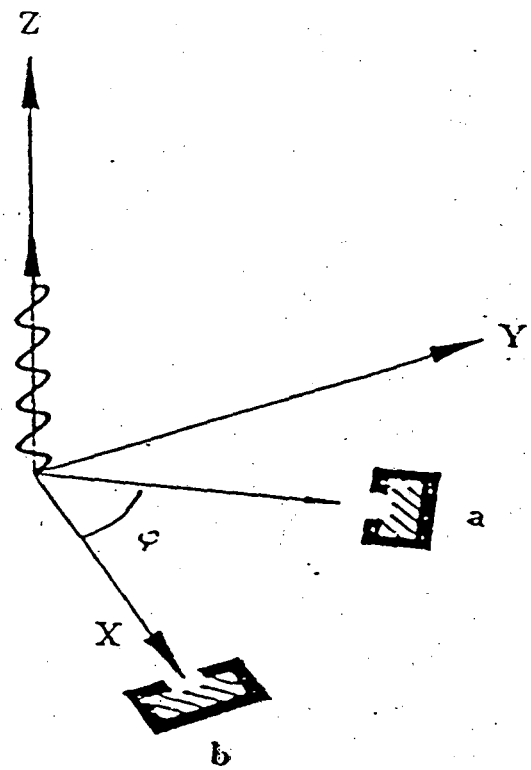

FIG. 1. Coordinate frame and experimental setup. Circularly polarized light is incident along the z direction. One electron counter (b) is in the x direction whereas the other one (a) can be rotated in the x-y plane.

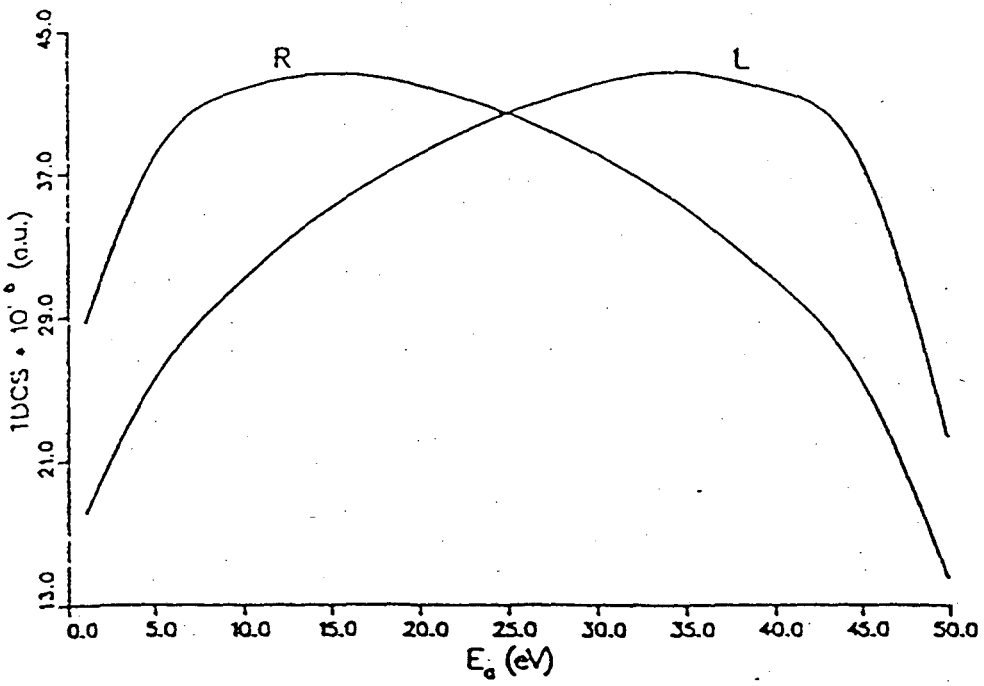

FIG. 2. The TDCS for He as a function of the energy E_a of the electron escaping in the y direction. The other electron escapes in the x direction; see Fig. 1. The total excess energy is 50 eV. L and R stand for left and right circular polarization.

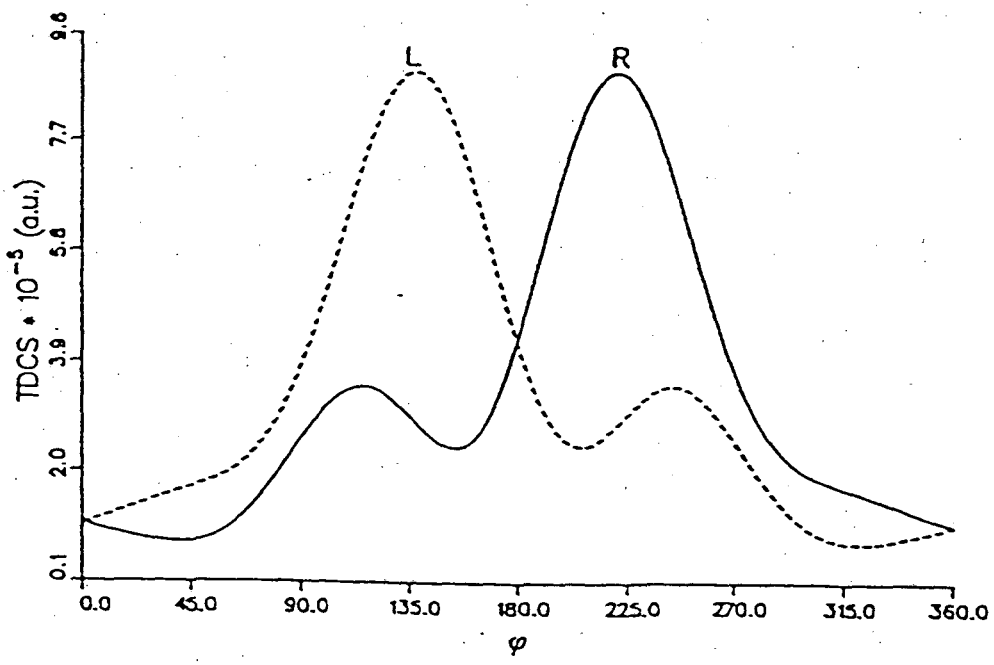

FIG. 3. Angular dependence of the TDCS for He. One electron with energy $E_b = 45$ eV is detected in the x direction, the other one with energy $E_a = 5$ eV is detected at the angle φ in the x-y plane; see Fig. 1. L and R stand for left and right circular polarization.

~ 9 kb

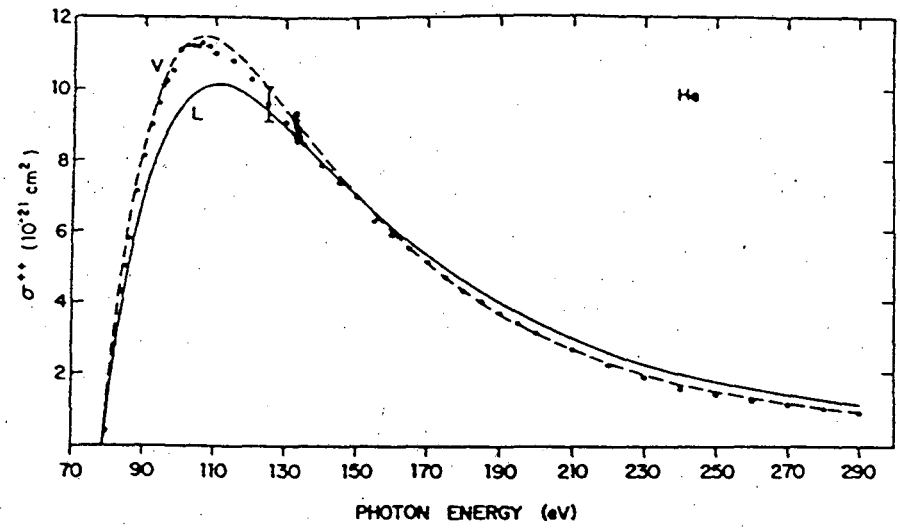

Fig 30. - *Section efficace de double photoionisation de He. Ces valeurs ont été obtenues à partir des mesures de photoélectrons de Wuilleumier et Krause (1972) et de Bizau et al (1981c), de photoions de Schmidt et al (1976) et Holland et Codling (1979), normalisées à la section efficace totale de photoabsorption. Les calculs MBPT de Carter et Kelly (1981) sont en accord étonnant avec les données expérimentales (Wuilleumier 1982a)*

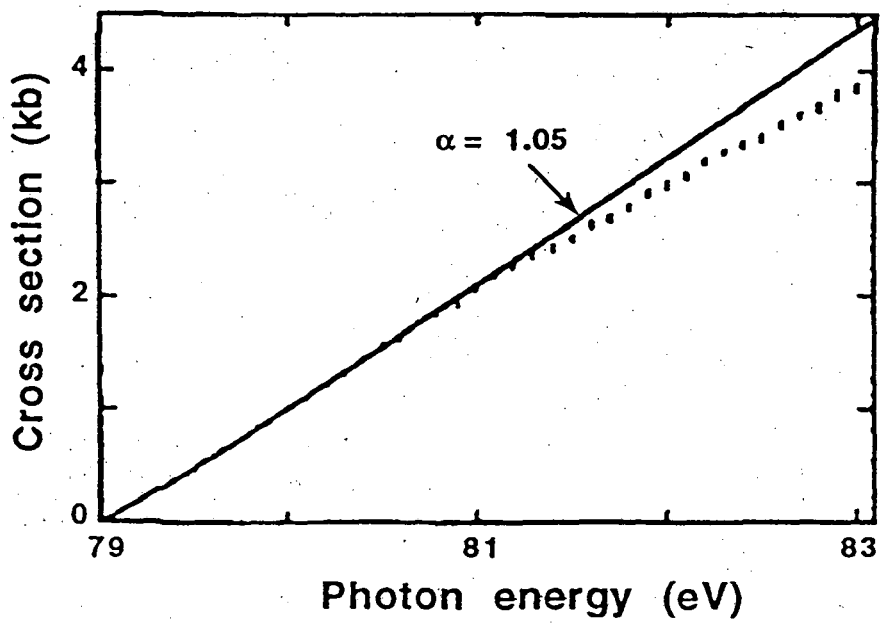

Figure 38. Double photoionization cross section in He just above the threshold. the solid line represents the least-square fit to the Wannier expression with the a coefficient a = 1.05. The Wannier law seems to be valid up to only 2 eV above

Coincidence experiments with linearly polarized radiation at Super ACO.

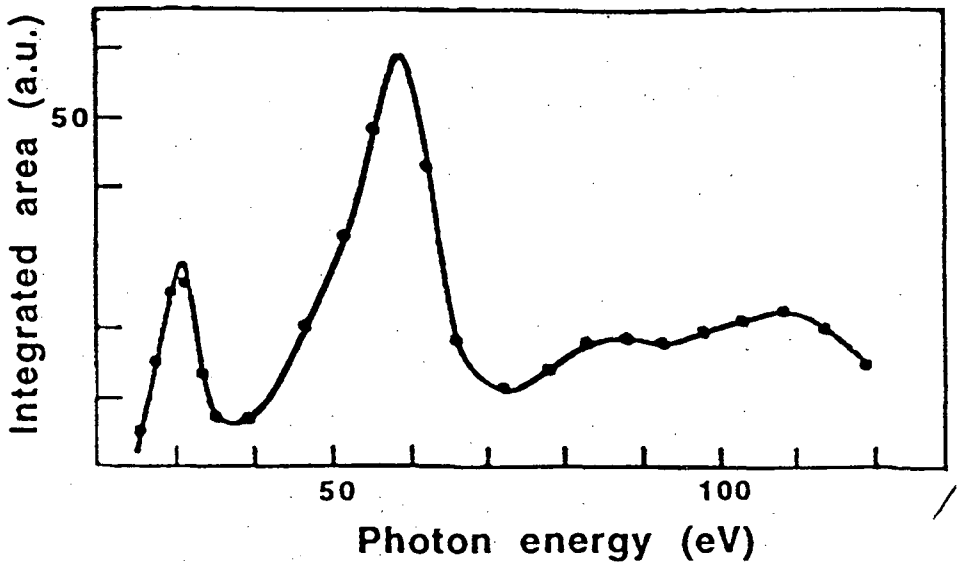

Figure 24. Spectral distribution of the photon flux emitted by the SU6 undulator (N = 16) of Super ACO (E = 0.8 GeV, average positron current of 200 mA). The measurements have been made with a CMA electron analyzer using the Ne 2p photoelectron line to calibrate the monochromatized photon flux [h].

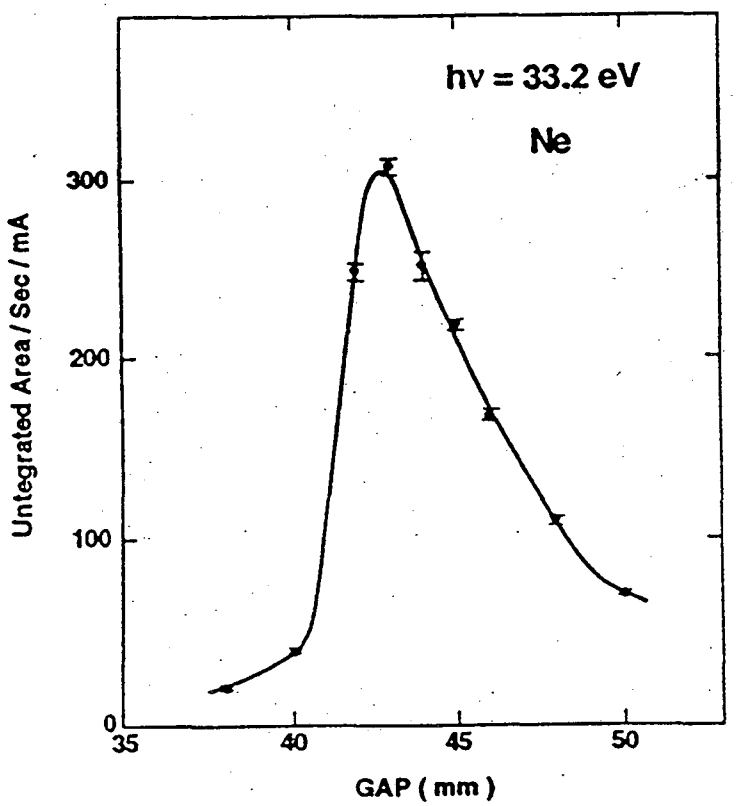

2×10^{13} φ / sec

TGM

400 mA

~ 0.1 eV BW

(0.3 %)

Figure 25. Variation, as a function of the undulator gap, of the photon flux emitted by the SU6 undulator of Super ACO, at a fixed photon energy, 33.2 eV here [h].

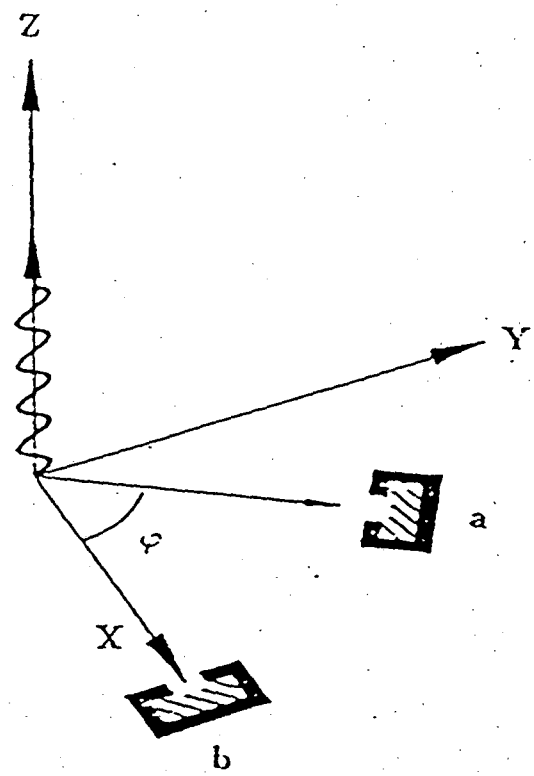

FIG. 1. Coordinate frame and experimental setup. Circularly polarized light is incident along the z direction. One electron counter (b) is in the x direction whereas the other one (a) can be rotated in the x-y plane.

A. Huetz, P. Lablanquie

Integrated cross section ~ 2-4 Kb

Differential cross section ~ 0.1-0.2 Kb

Conc. rate : 0.1 to 1 Herz

Brief Scientific Presentation

Dennis W. Lindle

University of Nevada, Las Vegas

Atomic & Molecular Science

- Fundamental measurements
  - circular dichroism
  - chiral systems
- Polarized X-Ray Emission
- "Complete" experiment

  <u>must</u> <u>know</u> polarization very well

Brief Scientific Presentation

Markus Pahler

ORIENTED ATOMS + CIRCULAR POLARIZED SR

M. Pahler

normal PES $\sigma(M_l^2)$; $\beta(M_l^2, M_{l-1}M_{l+1}|\cos\Delta l)$

PES from aligned atoms $d\sigma/d\Omega \cong \Sigma_i\Sigma_j \alpha_i P_{ij}(\cos\Theta)$

$\alpha_i(M_l^2; M_l; |\cos\Delta l)$

Oriented atoms

Example Sodium

$1s^2 2s^2 2p^6 3s\ ^2S_{1/2}$ ----> $1s^2 2s^2 2p^6 3p\ ^2P_{1/2}$ ----> $1s^2 2s^2 2p^5 3p\ ^{1,3}L_j + \varepsilon s;\varepsilon d$

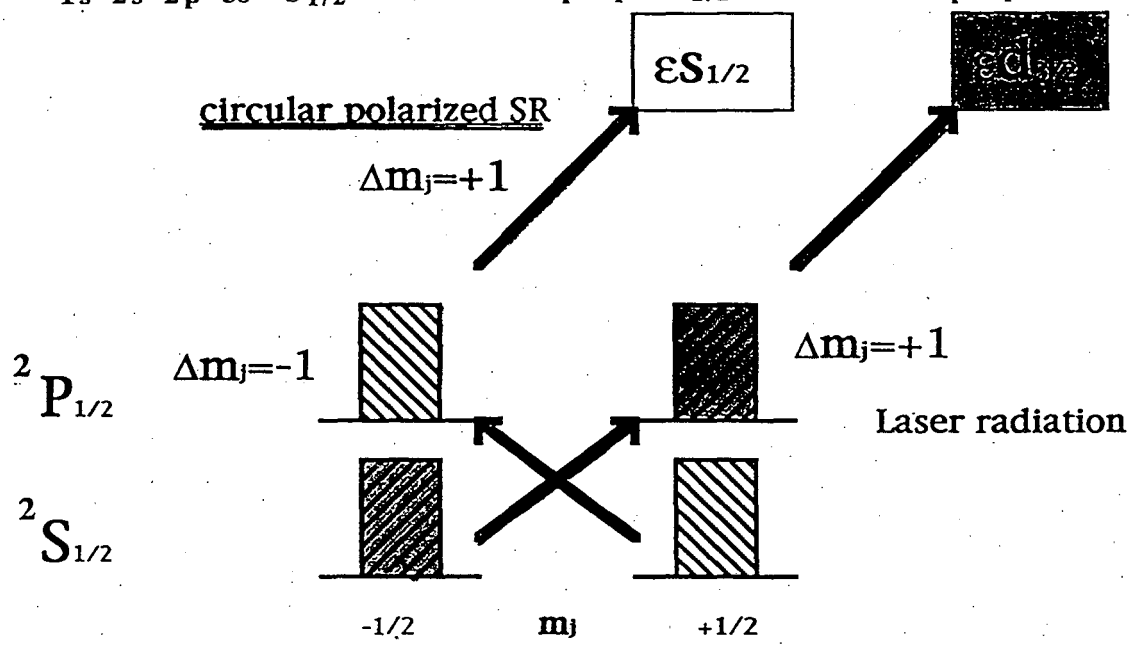

a) We are able to switch on and off different electron waves
b) Angular distribution depends only on one matrix element.
c) Photoionization from a pure quantum mechanic state (m_j).
d) Present: alkalis, alkaline earth
Future: transition metalls, rare earth giant resonances.

e) Going beyond normal PES with circular polarized SR =>

Experiment

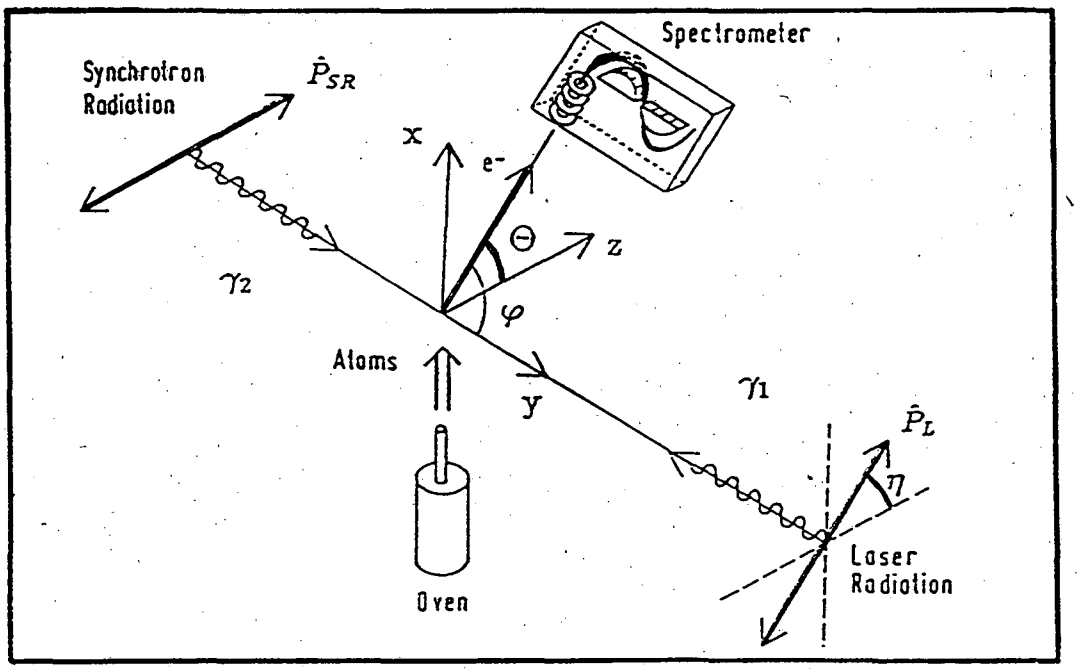

Bessy

TGM6 (undulator)
E_p=30-70 eV
$E/\Delta E=130$
$I=5*10^{12}$ $\Delta E*\gamma/E*s*100$ mA
P>98 %
$\lambda=0°$
10^{-7}-10^{-8} torr

Laser

CR699-21
670.8/589 nm
$E/\Delta E=10^7$
$I=100$ mW/mm^2
η=tunable
10 % excit. atoms

Brief Scientific Presentation

Chien-Te Chen

AT&T Bell Laboratories

WHAT TO DO with Elliptical Wiggler @ ALS?

* Magnetic Circular Dichroism of Dilute magnetic systems (Kondo + Bio.)

* Magnetic phase transitions ($T \sim T_c$; $\Delta I/I \sim 0$)

* Complete Experiment (Photon + Electron Spin-resolved photoemission)

* Circularly polarized magnetic Resonant Scattering (large ω, small I)

* pump & probe experiments (Laser + Synchrotron)

* MCD ⊕ Microscopy (Domain-Wall Dynamics)

* Natural Circular Dichroism

Brief Scientific Presentation

James G. Tobin

Lawrence Livermore National Laboratory

Magnetic Circular Dichroism in X-Ray Absorption and Core-Level Photoemission of Fe/Cu(001)

J.G. Tobin
Chemistry and Materials Science Department
Lawrence Livermore National Laboratory

Collaborators
G.D. Waddill, LLNL
D.P. Pappas, NRL
P.A. Sterne, LLNL
T. Gouder, LLNL
A. Jankowski, LLNL

L8.10 PDI
WED 4:15 PM

MCD Fe Pt MULT.
Q1 8.10
THUR 11:45 AM

1993 Spring Meeting of the Materials Research Society
San Francisco, CA • April 12–16, 1993

Magnetic Ultrathin Films

- Complicated chemistry

  Overlayers vs alloys vs clusters

- Need information on electronic and spin state population.

- Need exact positions as input for calculations of magnetic properties.

- "Magnetic" structure

  Magnetic effects
  → low ke ←
  → small effect ←
  Need spin dependent multiple scattering theory...
  Need ALS.....

- Prototype system
  Fe/Cu (001)

Fe/Cu(001) – Structure at Low Coverage

Overlayers versus surface-alloy versus cluster-on-surface versus cluster-in-surface

FCC → BCC
COV ↑

- XPD – S.A. Chambers, et. al., Phys. Rev. B 36, 8992 (1987)
- XPD – Steigerwald and Egelhoff, Phys. Rev. Lett., 60, 2558 (1988)
- STM – D. Chambliss, et. al. – MARCH APS MEETING, 1993
- SMOKE – Liu, Moog, and Bader, Phys. Rev. Lett., 60, 2422 (1988)
- SEXAFS – Magnan, Chanderis, Villette, Heckmann, and Lecante, Phys. Rev. Lett., 67, 859 (1991)

MAG MOM
⊥ → ∥
COV ↑

Overlayer | Surface Alloy | Cluster on Surface | Cluster in Surface

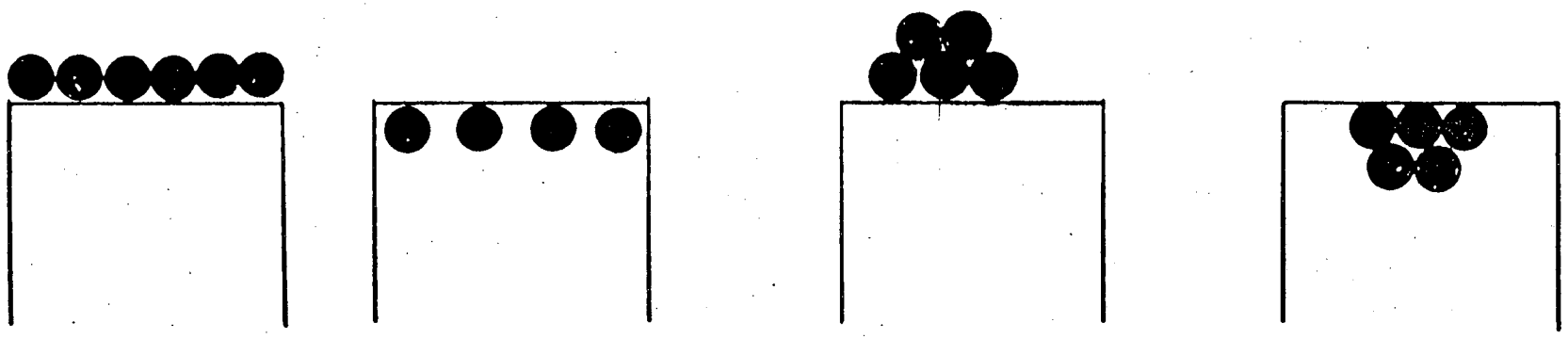

MCD–NEXAFS and photoemission of Fe/Cu(001)

X-RAY CIRCULAR POLARIZATION

- Giant effect in NEXAFS MCD
- Simplified approximate analysis: $BR_{TH} = \frac{3 + 2(1-\alpha)\beta + 2(1-\beta)\alpha}{6} = \frac{2}{3} - \frac{P_e P_{h\nu}}{6}$
- Perpendicular moment at low coverage–NEXAFS + TEMP. DEP.
- Parallel moment at high-coverage–NEXAFS
- Core-level photoemission → exchange splitting
  — Ultrathin film value < bulk Fe

→ PHOTOELECTRON DIFFRACTION: LOCAL GEOMETRIC AND MAGNETIC STRUCTURE...

PLUS SPIN-DETECTION

X-Ray Magnetic Circular Dichroism - Near Edge X-Ray Absorption Fine Structure

Electric dipole selection rules

right circular pol : $\Delta m_l = +l$, $\Delta m_j = +l$, $\Delta m_s = 0$

left circular pol: $\Delta m_l = -l$, $\Delta m_j = -l$, $\Delta m_s = 0$

Fe 2p → 3d

$$BR = \frac{I(2p^{3/2})}{I(2p^{3/2}) + I(2p^{1/2})}$$

P	M	PvsM	BR_{exp}	BR'_{exp}
L	O	+	0.64	0.58
L	I	−	0.83	0.75
R	I	+	0.65	0.59
R	O	−	0.83	0.75
LIN			0.74	0.67

$$BR' = BR * \frac{2/3}{BR^{LIN}_{EXP}}$$

Experiment
→ giant effect

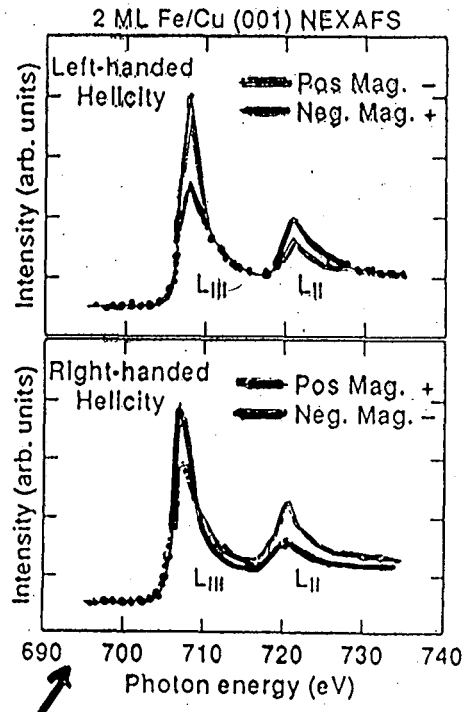

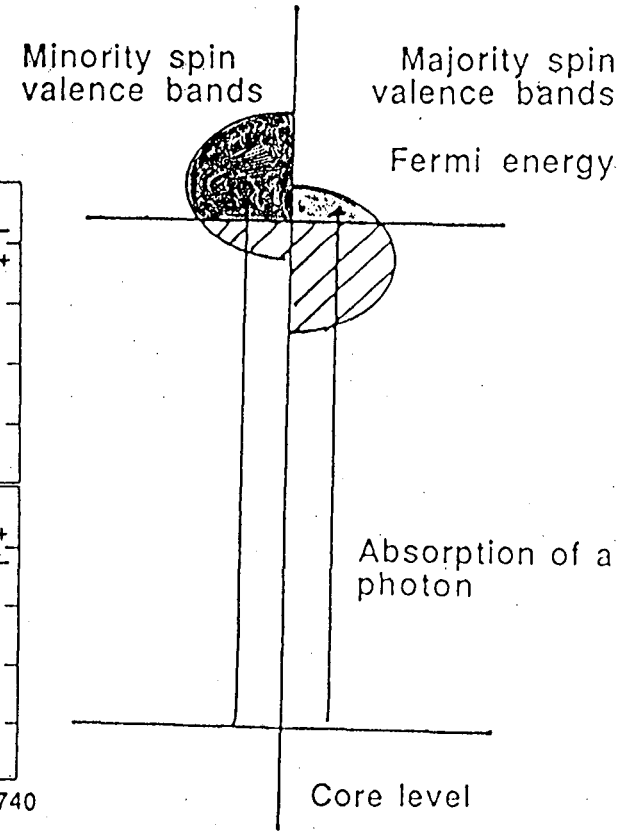

NO DATA MANIPULATION EXCEPT SET PRE-EDGE INTENSITY EQUAL.

Tobin, Waddill, and Pappas, Phys. Rev. Lett. 68, 3642 (1992)

Magnetic Ultrathin Films: Spin-DependentEffects in Photoemission

Fe3s

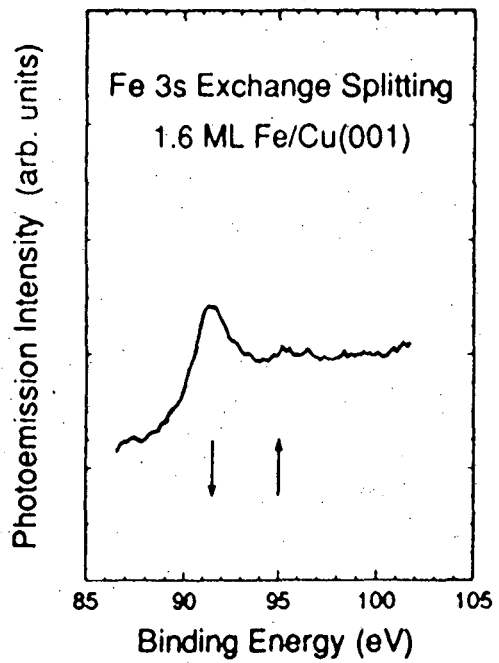

Fe3p MCD*

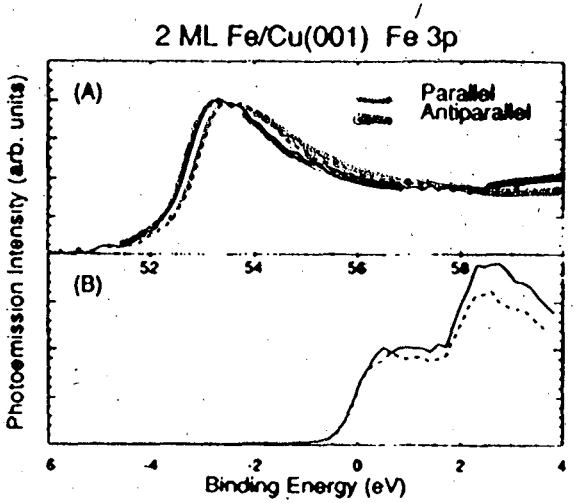

Fe2p MCD*

PRB - RAPID COMM.
JULY 92

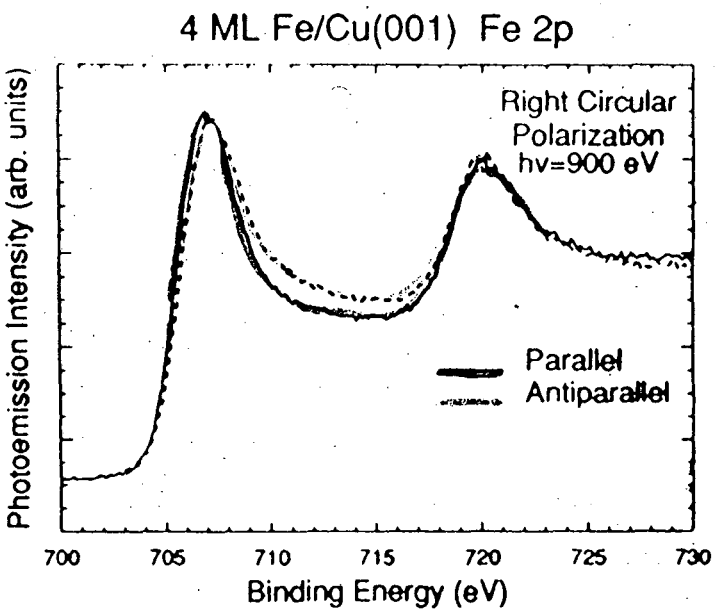

USE FOR
PD
AND
PDI

*** Requires circularly-polarized x-rays**

RARE EARTHS

ACTINIDES?
DEPLETED URANIUM

BAND MAP
CORE SHIFTS
KONDO EFFECT
⋮

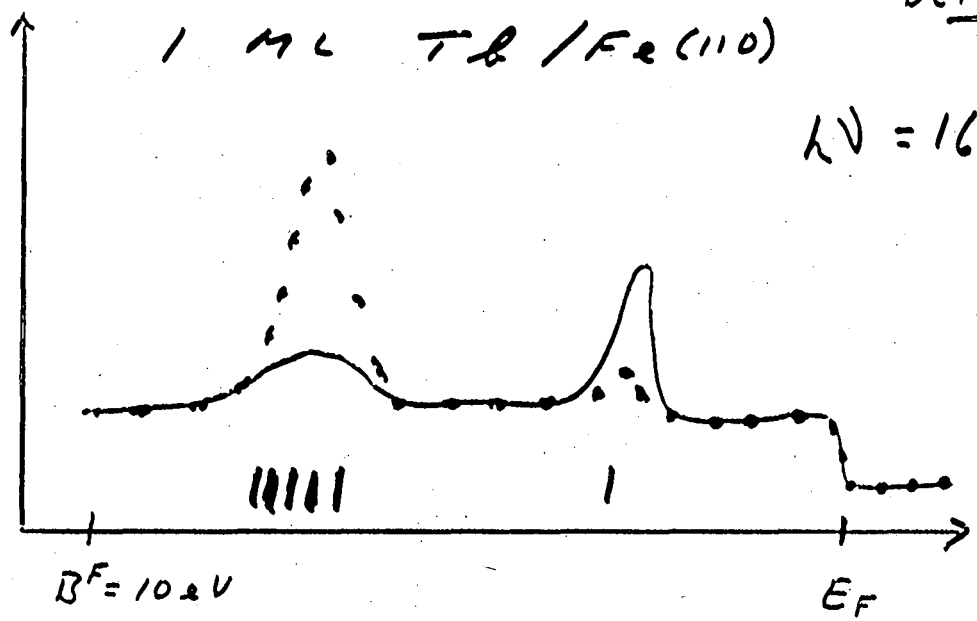

TERBIUM

PES MCD OF Tb / Fe(110)
MCD IN 4f PES
Tb $4f^7$
FACTOR OF 5 CHANGE OR DICHROISM

K. STARKE, G. KANOL et al
SPRING MRS, APRIL 93, S.F. CA

Magneto – PD Imaging

- Local magnetic structure
- Distinguish similar neighbors (e.g., Fe and Cu)
- Multiple scattering calculations of S.Y. Tong (with spin-dependence and at low Ke...)

Brief Scientific Presentation

James L. Erskine

University of Texas

BRIEF HISTORY OF MCD

(Key Publications)

Theoretical

J.L. Erskine and E.A. Stern, *PRB* **12**, 5016 (1975)
Prediction of strong MCD at p → d core absorption

F.C. Brown
J.L. Erskine
TANTALUS
EXPERIMENT

J.B. Goedkoop *et al.*, *PRB* 37, 2086 (1988)
Atomic MCD calculation (3d → 4f) for 4f rare-earth

H. Ebert, P. Strange, and B.L. Gyorffy, *Z. Phys. B* **73**, 77 (1988)
First principle calculation for hard x-ray MCD

C.T. Chen, N.V. Smith, and F. Sette, *PRB* **43**, 6785 (1991)
Relativistic tight binding MCD calculation (2p → 3d) of Ni

T. Jo and G.A. Sawatzky, *PRB* 43, 8771 (1991)
Atomic multiplet, configuration interaction MCD calculation (2→ 3d) of Ni

G. van der Laan and B.T. Thole, *PRB* **43**, 13401 (1991)
Atomic MCD calculation (2p → 3d) for ed transition metals (brief history)

N.V. Smith, C.T. Chen, F. Sette, and L.F. Mattheiss, *PRB* (in press)
Detail of the Fe and Ni relativistic tight binding MCD calculations

Experimental

G. Schütz *et al.* *PRL* 58, 737 (1987)
The first hard x-ray MCD; Fe K-edge absorption

C.T. Chen *et al.*, *PRB* 42, 7262 (1990)
The first soft x-ray MCD; Ni $L_{2,3}$ absorption

T. Koide *et al.*, *PRB* (1991 or 1992)
The first VUV MCD; Ni $M_{2,3}$ absorption

Journal of Magnetism and Magnetic Materials 109 (1992) 288–292
North-Holland

Soft-X-ray magnetic circular dichroism: a new technique for probing magnetic properties of magnetic surfaces and ultrathin films

L.H. Tjeng [a], Y.U. Idzerda [b], P. Rudolf [a], F. Sette [a] and C.T. Chen [a]

[a] *AT&T Bell Laboratories, Murray Hill, NJ 07974, USA*
[b] *Naval Research Laboratory, Washington, DC 20375, USA*

ULTRA THIN MAGNETIC FILMS / SUPERLATTICES

Received 12 July 1991; in revised form 10 October 1991

We demonstrate the feasibility of applying the novel soft-X-ray magnetic circular dichroism (SXMCD) technique to investigate the magnetic properties of magnetic surfaces and ultrathin films. Measurements have been carried out on Ni films of various thickness on a Cu(100) substrate at the Ni $L_{2,3}$ absorption edges. The SXMCD data exhibit strong temperature and thickness dependence, giving film thickness dependent Curie temperatures and suggesting that a single monolayer of Ni on a Cu(100) substrate may be non-magnetic.

Ni L_{23}

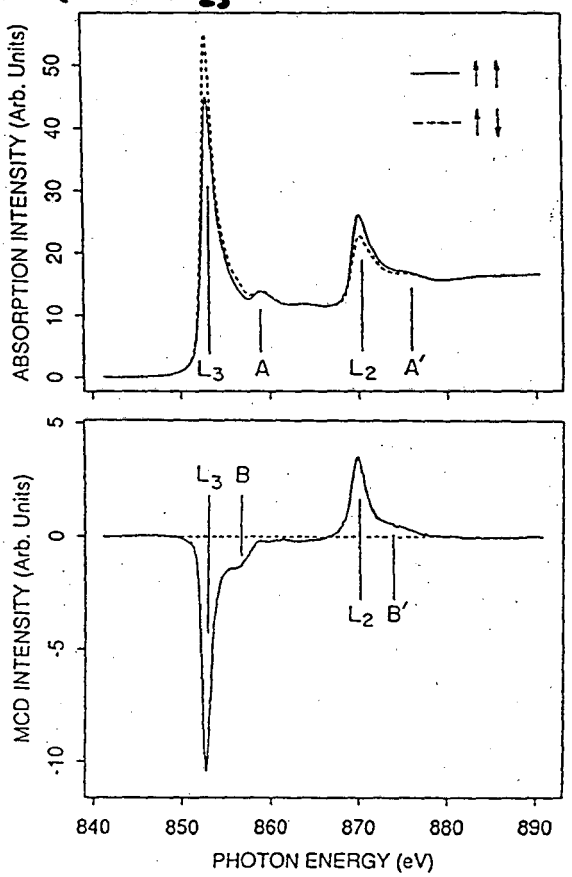

Fig. 2. $L_{2,3}$ X-ray absorption spectra (XAS) and the magnetic circular dichroism (MCD) of a thick Ni film taken with the spin directions of the photons and that of the majority 3d electrons parallel and anti-parallel to each other. Peaks observed at 853 and 871 eV are the L_3 and the L_2 white lines. The sum of the average L_3 XAS peak height is set at 100. The MCD spectrum shown in the power panel is obtained from the difference of the two XAS spectra shown in the upper panel. Fine features labeled as A, A′ and B, B′ are discussed in the text.

CRITICAL EXPONENTS

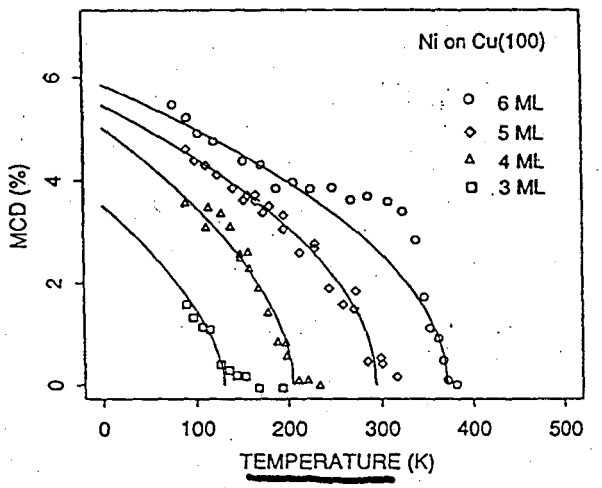

FINITE SIZE EFFECTS

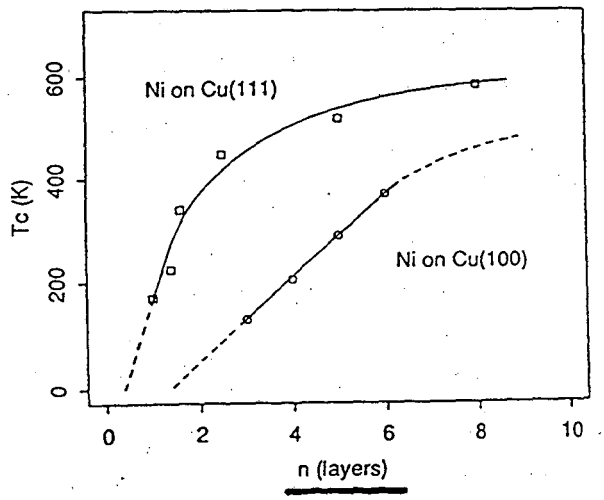

Surface Science 208 (1989) 245–266
North-Holland, Amsterdam

COORDINATION NUMBER AND SURFACE CORE-LEVEL SHIFT SPECTROSCOPY: STEPPED TUNGSTEN SURFACES

K.G. PURCELL *, J. JUPILLE ** and D.A. KING ***
The Donnan Laboratories, University of Liverpool, Liverpool L69 3BX, UK

Received 5 May 1988; accepted for publication 14 October 1988

ADD MAGNETIC SENSITIVITY

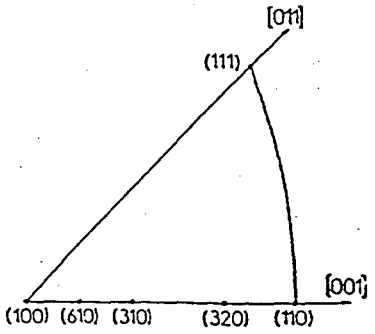

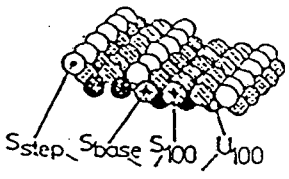

W(610)

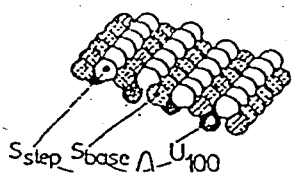

W(310)

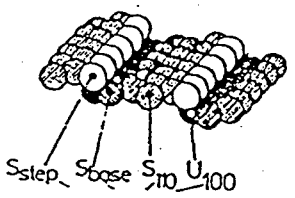

W(320)

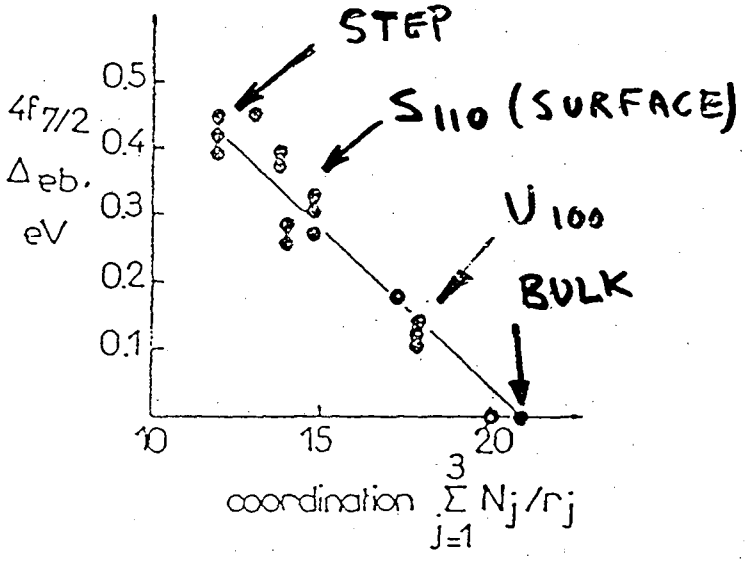

Dependence of binding energy shift on effective atomic coordination.

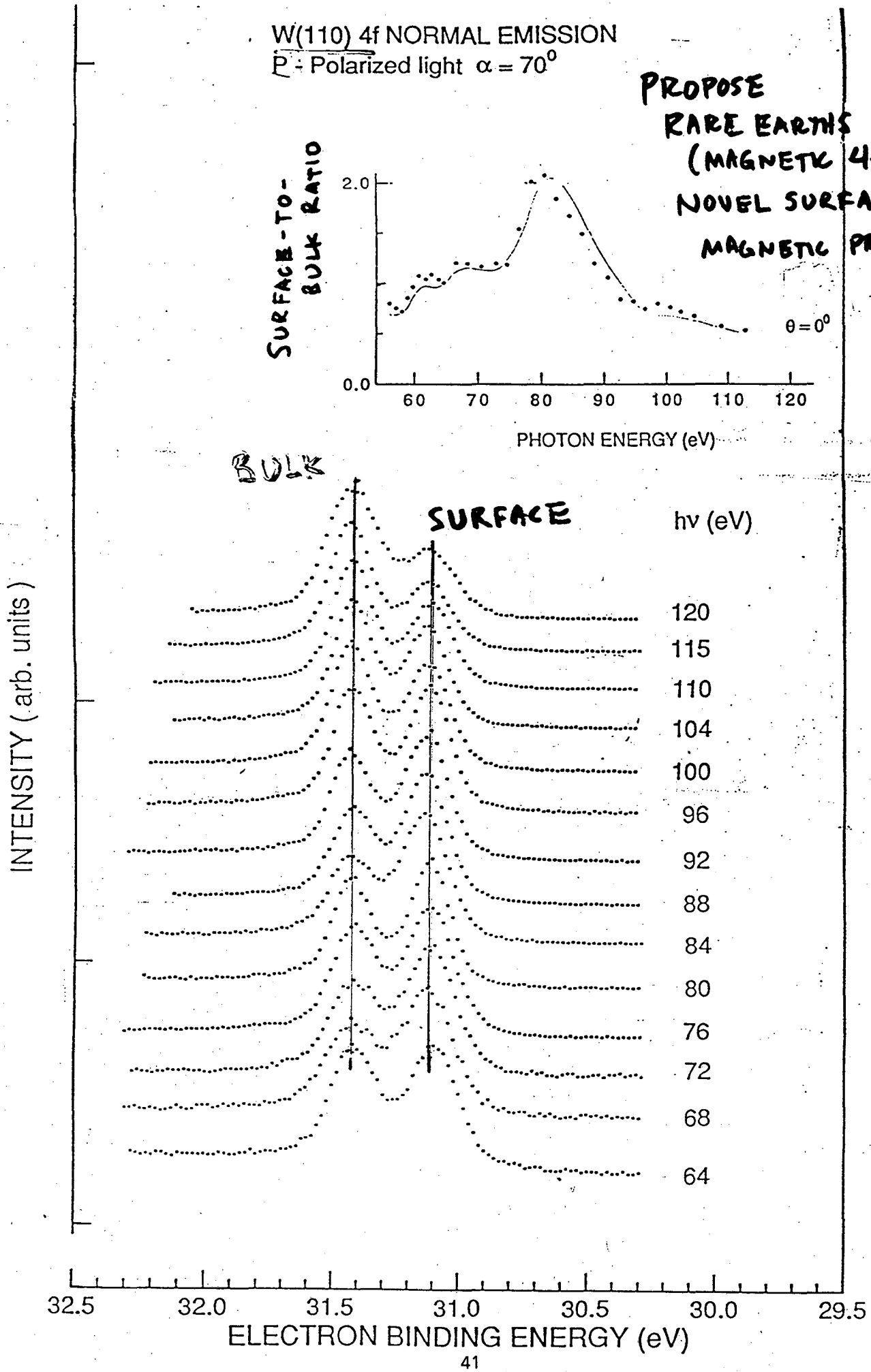
W(110) 4f NORMAL EMISSION
P - Polarized light α = 70°
PROPOSE
RARE EARTHS
(MAGNETIC 4f)
NOVEL SURFACE
MAGNETIC PROPERTY
SURFACE-TO-BULK RATIO
2.0
0.0
60
70
80
90
100
110
120
θ = 0°
PHOTON ENERGY (eV)
BULK
SURFACE
hv (eV)
120
115
110
104
100
96
92
88
84
80
76
72
68
64
INTENSITY (arb. units)
32.5
32.0
31.5
31.0
30.5
30.0
29.5
ELECTRON BINDING ENERGY (eV)

Magnetic X-Ray Dichroism in Core-Level Photoemission from Ferromagnets

L. Baumgarten and C. M. Schneider
Freie Universität Berlin, Institut für Experimentalphysik, Arnimallee 14, D-1000 Berlin 33, West Germany

H. Petersen and F. Schäfers
Berliner Elektronenspeicherring-Gesellschaft für Synchrotronstrahlung (BESSY) GmbH, Lentzeallee 100, D-1000 Berlin 33, West Germany

J. Kirschner
Freie Universität Berlin, Institut für Experimentalphysik, Arnimallee 14, D-1000 Berlin 33, West Germany
(Received 16 April 1990)

We report on the novel effect of magnetic x-ray dichroism in core-level photoemission from ferromagnets with circularly polarized radiation. Depending on the relative orientation of photon spin and sample magnetization (parallel or antiparallel), a single emission line may be resolved into two lines, due to exchange splitting of the core level. The mechanism is explained in terms of spin-selective dipole transitions in the presence of spin-orbit coupling. Possible applications of magnetic x-ray dichroism in photoemission from magnetic samples are pointed out.

PACS numbers: 79.60.Cn, 75.50.Bb, 78.20.Ls

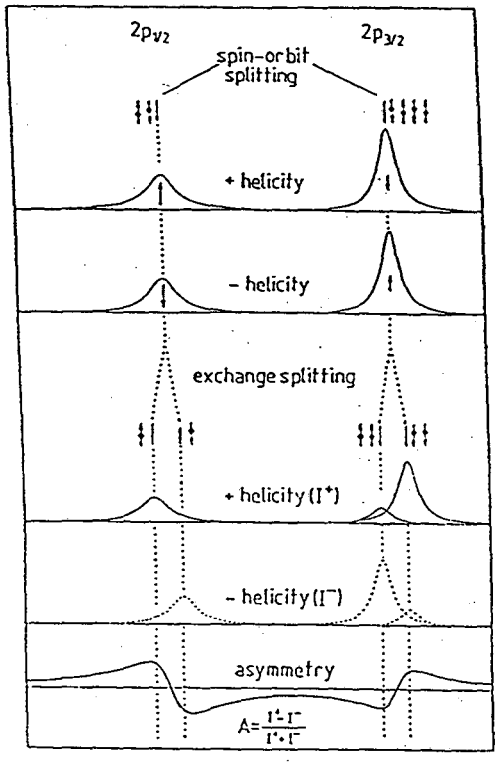

FIG. 2. Schematic explanation of the origin of magnetic x-ray dichroism in photoemission. The effect comes from the interference of spin-orbit interaction in the core levels and exchange interaction with the $3d$ valence electrons, together with the dipole selection rules for circularly polarized light. From top to bottom the figure shows the expected relative intensities of Lorentz-type photoelectron lines when excited by circularly polarized light in the presence of spin-orbit splitting only (top), and with additional exchange splitting (bottom). The low-intensity satellite in the $2p_{3/2}$ is not resolved in the experiment. For details see text.

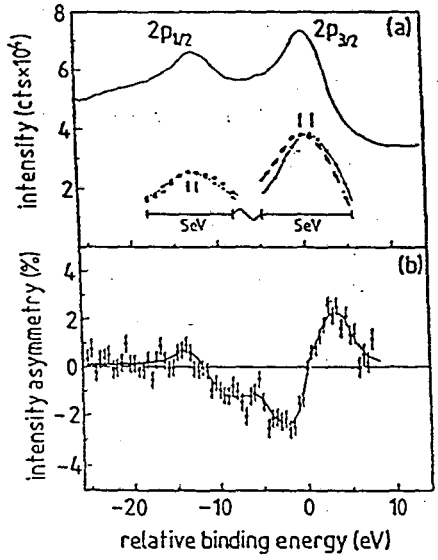

FIG. 1. The effect of magnetic x-ray dichroism in photoemission. (a) The upper part shows the total intensity spectrum in the region of the spin-orbit-split Fe $2p$ levels. The lower curves show, on enlarged scales, the partial intensities in the peak regions for photon spin parallel (solid lines) and antiparallel (dashed lines) to the sample magnetization. Note the apparent energetic peak shift in opposite directions (intensity zero suppressed). (b) Asymmetry A of the measured intensity for photon spin and sample magnetization parallel (I^+) and antiparallel (I^-). $A=(I^+-I^-)/(I^++I^-)$. The asymmetry curve was obtained from two separate runs with opposite photon helicity.

Ni, Co, and Fe 3s Core-Level Lineshapes

Poor Statistics — Fe 3s
Spin Resolved

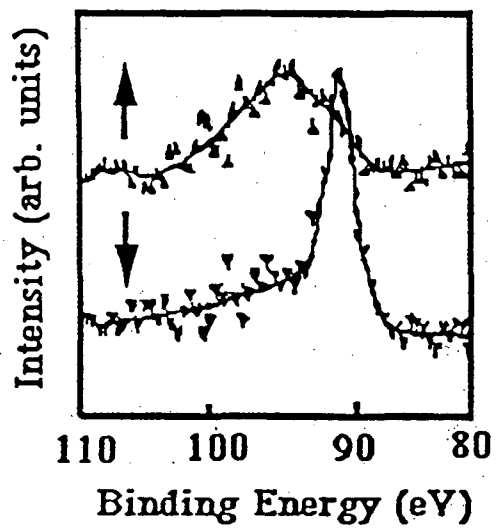

[Hillebrecht, et al., PRL 65, 2450 (1990)]

Good Statistics — Na 2p

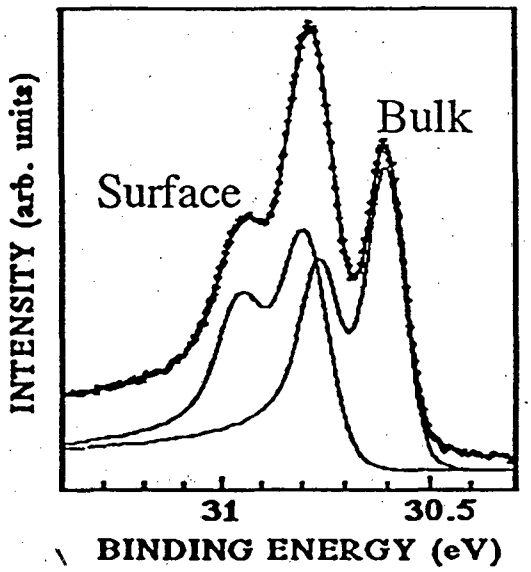

[Riffe, et al., PRL 67, 116 (1991)]

With High Quality Statistics can:

1) Determine **Spin-Dependent Lineshapes**:

a) Lifetime,

b) Screening,

c) Phonon Coupling — determine contribution to core-level lineshapes from magnetostriction-induced softening of phonon modes. [Benedek, et al., PRL 68, 2644 (1992)]

2) Quantatively investigate **Temperature-Dependent Magnetism**

a) Probe extraordinary-peak contribution to core-level lines,

b) Study loss of short-range order above T_c and concurrent collapse of exchange splitting.

*thin films have lower T_c than bulk.

RICE MINI-MOTT
(4-QUADRENT VERSION)

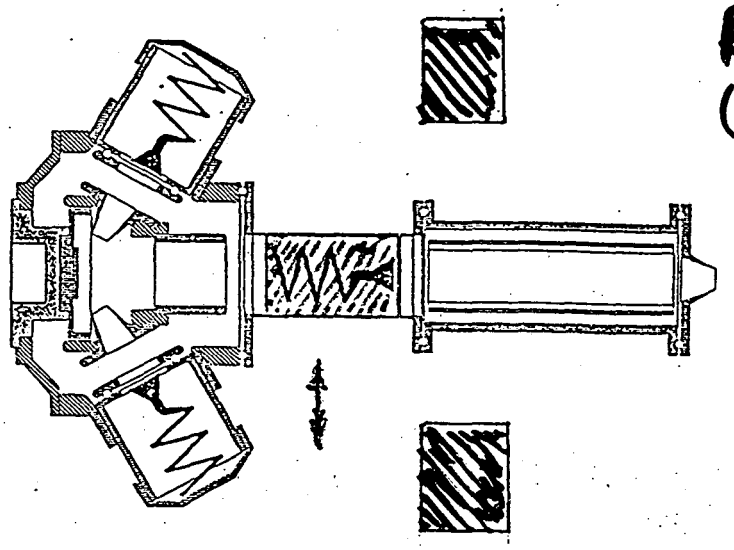

5TH CHANNELTRON CAN BE INSERTED FOR UNPOLARIZED ELECTRON DETECTION

MICROSCIENCE 150 mm ESCA ANALYZER

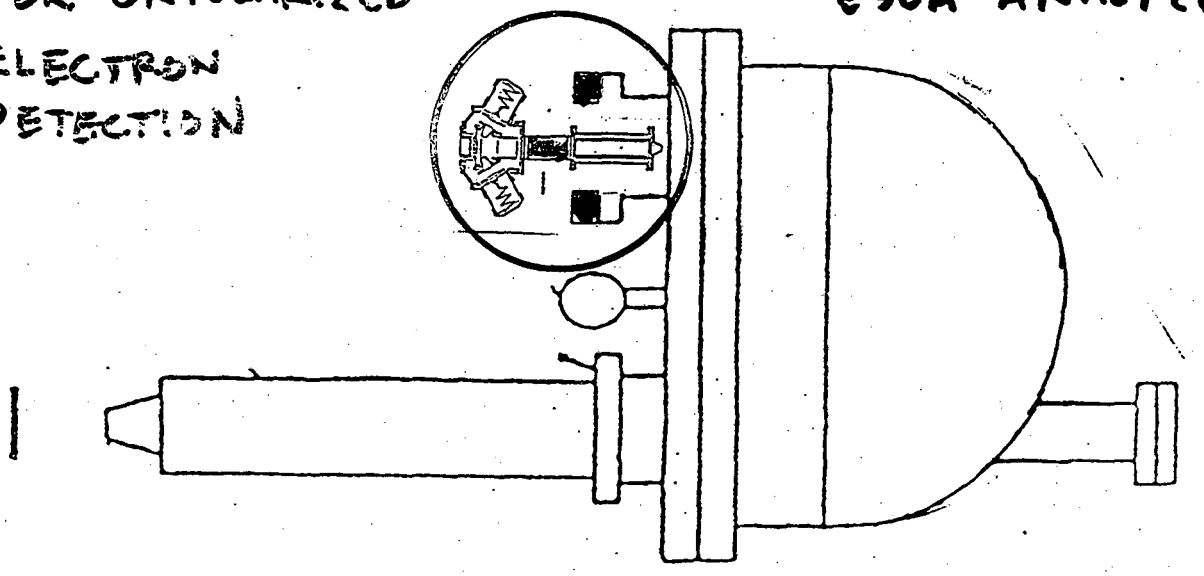

LENS COLUMN ELECTRON RAYTRACING TO OPTIMIZE TRANSMISSION FUNCTION

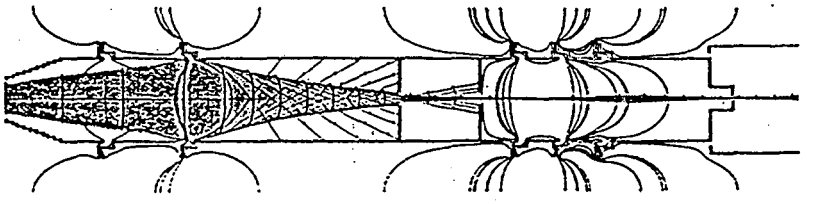

PROPOSED FOR U16 AND U5 CORE LEVEL

Brief Scientific Presentation

Charles S. Fadley

Lawrence Berkeley Laboratory

-Subgroup members (from original sx/vuv wiggler IDT):

T.-C. Chiang-Illinois
C. Fadley/C. Westphal-UCD/LBL
Z. Hussain-LBL
G.J. Lapeyre-Montana
P.N. Ross-LBL
J.G. Tobin-LLNL
K. Sattler--Hawaii (Clusters)
D.A. Shirley--Penn State

-Primary interests:

+Angle-resolved core and valence photoelectron spectroscopy with linear/circular polarization and (optional) spin resolution: 50 eV to 2000 eV

+Photoelectron diffraction and photoelectron holography

+Application to variety of surface/interface problems:
Adsorbates on metals/semiconductors
Metallic overlayers/superlattices/clusters
Metal/semiconductor and oxide/semiconductor
...

+ MEASURING SPIN:

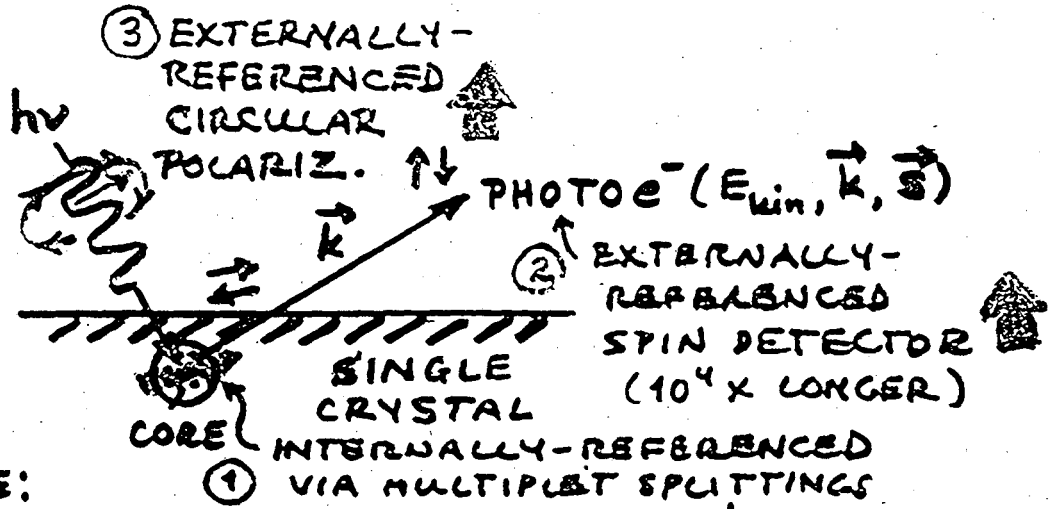

- MEASURE:

$$\text{INTENSITY} = I(E_{kin}, \vec{k}, \vec{s}) \propto \frac{d\sigma}{d\Omega}(E_{kin}, \vec{k}, \vec{s})$$

- TRY TO DERIVE:

ATOMIC POSITIONS, SURFACE STRUCTURE

LOCAL MAGNETIC ORDER

- EARLY HISTORY:

DIFFRACTION: 1970 – NaCl, SIEGBAHN ET AL.) XPS
1971 – Au, BERGSTRUM AND FADLEY)

1974 – ADSORBATES, THEORY, LIEBSCH) UPS

1978 – ADSORBATES, EXPT. –
SHIRLEY ET AL.) SYNCH. RAD.
WOODRUFF, SMITH ET AL.)
OUR GROUP) XPS

1985-87 – SPIN RESOLUTION/MAGNETISM, OUR GROUP

⋮

HOLOGRAPHY: 1986 – THEORY, SZÖKE
1988 – THEORY, BARTON
1990 – Cu EXPT., TONNER, SALDIN ET AL. XPS

⋮

ADVANCED PHOTOELECTRON SPECTROMETER/ DIFFRACTOMETER

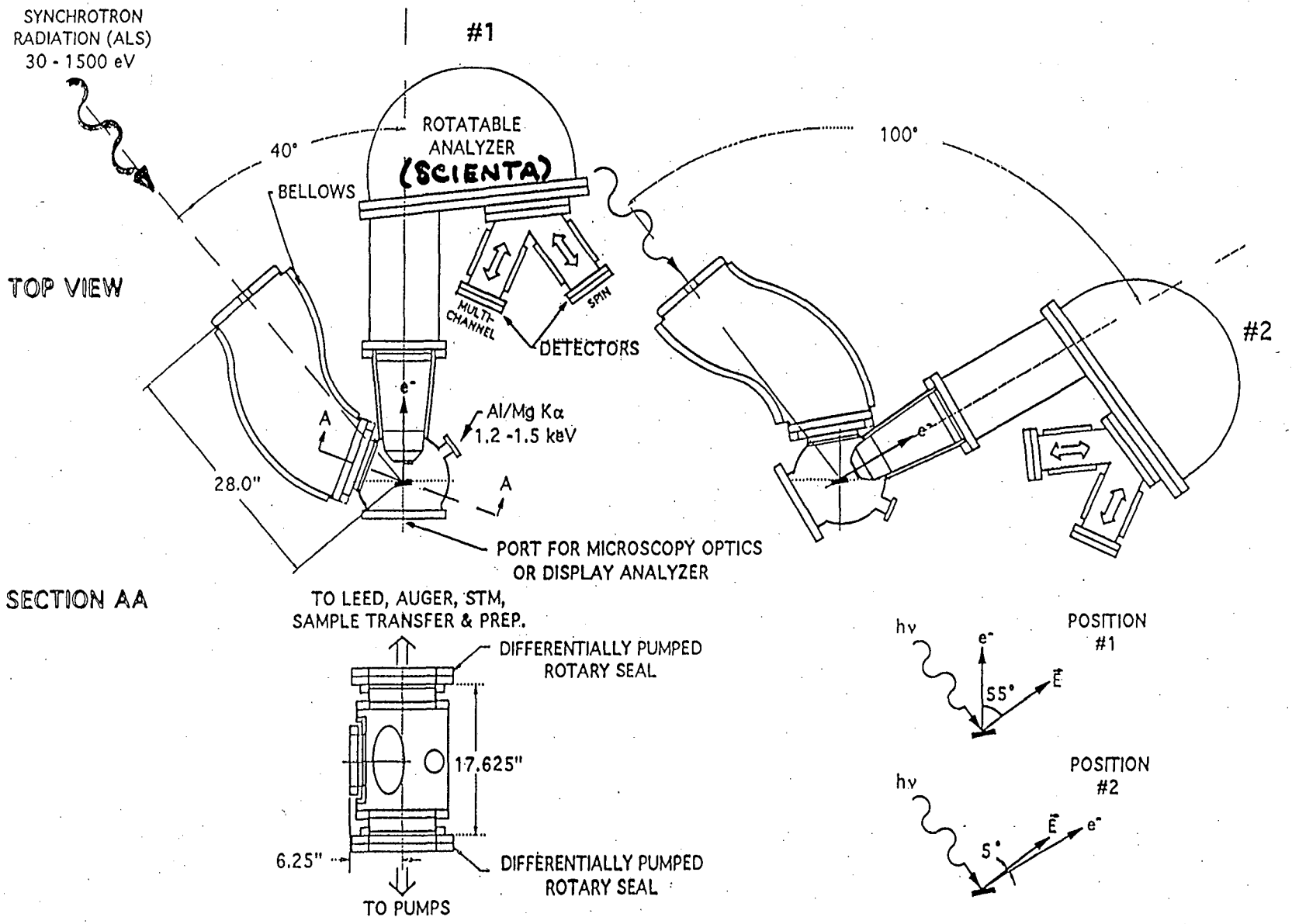

SPIN-POLARIZED PHOTOELECTRON DIFFRACTION

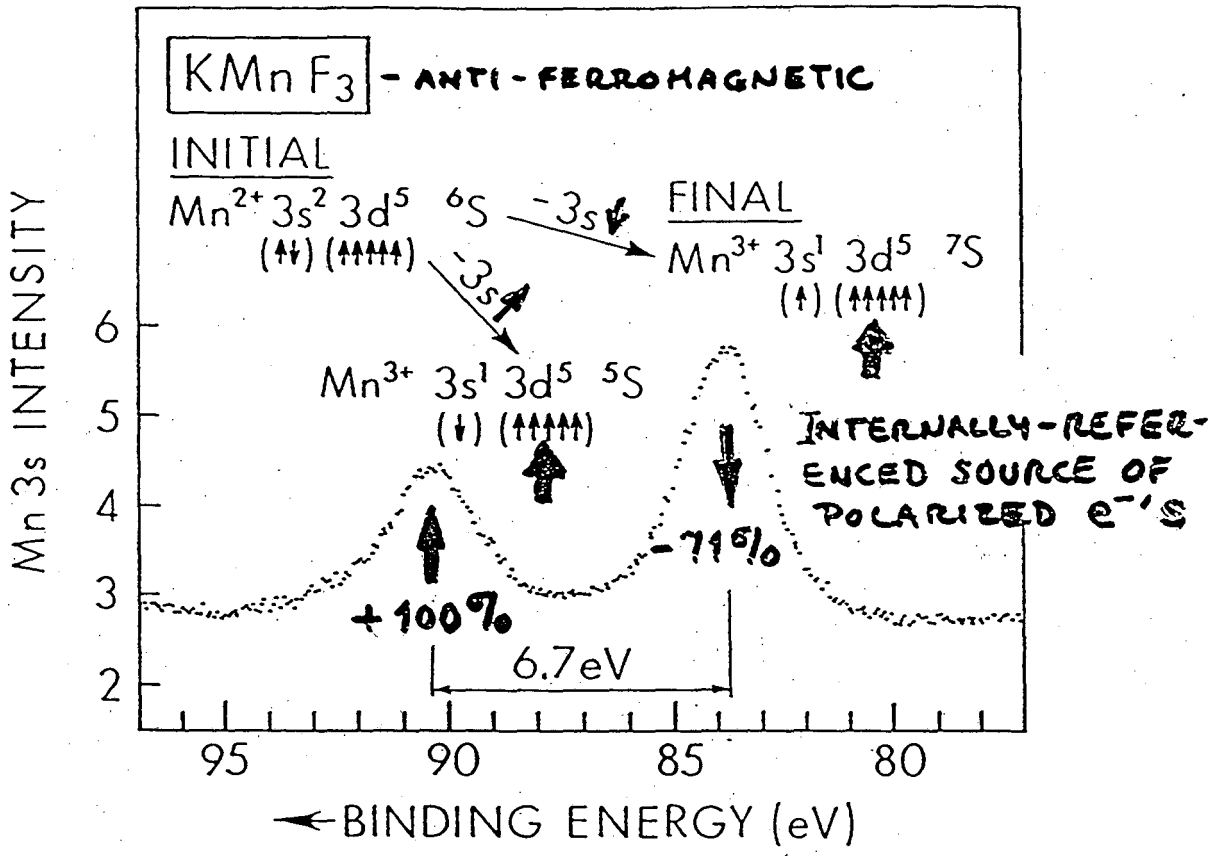

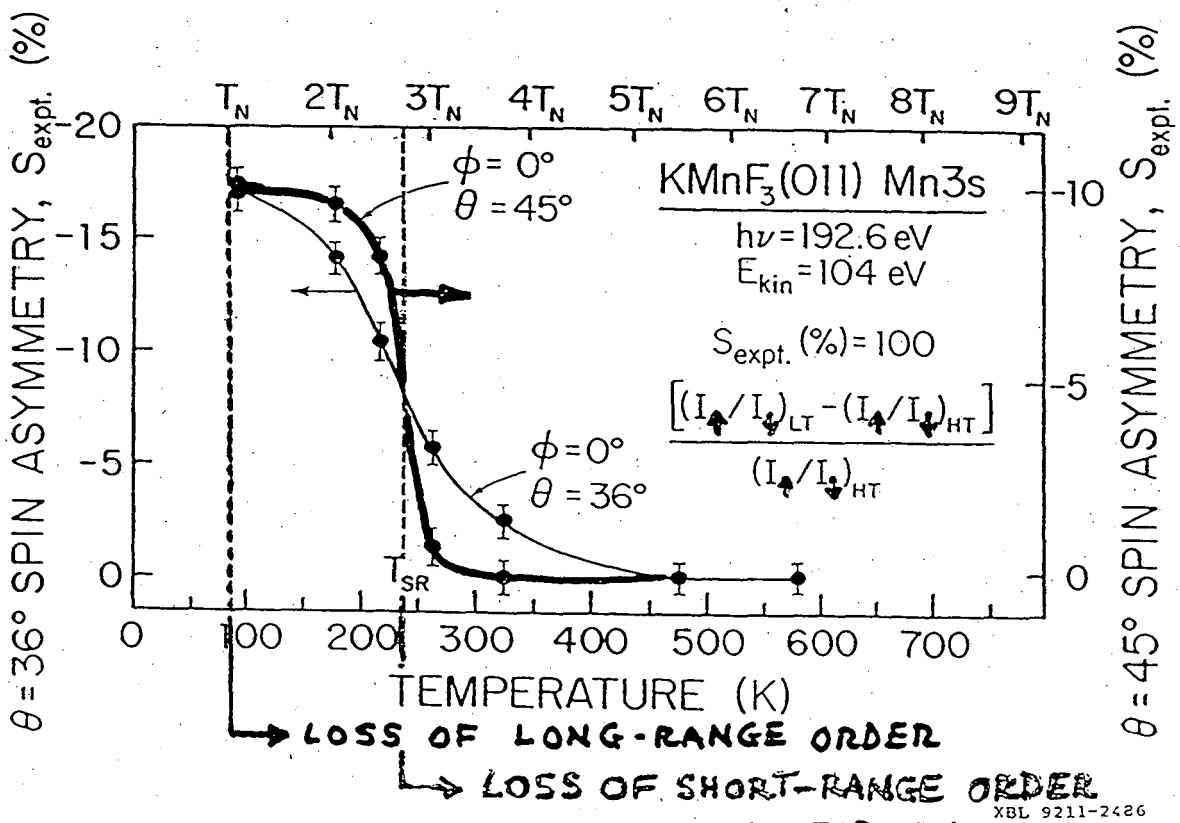

SINKOVIC, HERMSMEIER, FADLEY
P.R.L. 55, 1227('85)

DIRECT OBSERVATION OF SPIN-SPLIT CORE LEVELS IN A FERROMAGNET

$$\frac{I_\uparrow - I_\downarrow}{I_\uparrow + I_\downarrow}$$

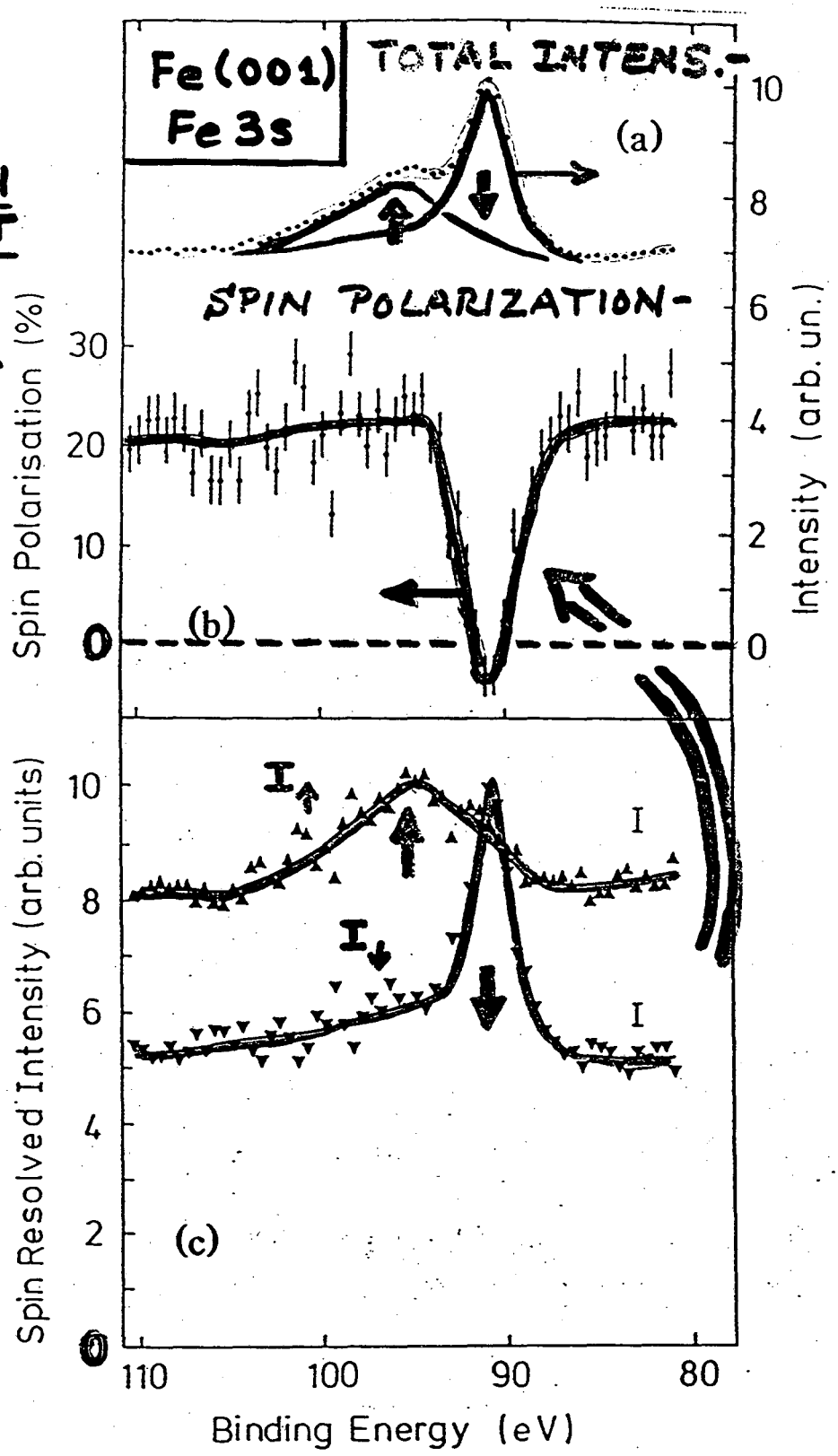

HILLEBRECHT ET AL., PHYS. REV. LETT. 65, 2450 (1990)

FIG. 1. Photoemission spectra of the Fe 3*s* core level taken with 250-eV photon energy at 0.9-eV total energy resolution. (a) Spin-integrated energy distribution curve. (b) Spin polarization with statistical error bars. (c) Spin-resolved energy distribution curves with statistical error bars.

...AND SPIN-POLARIZED PHOTOe⁻ HOLOGRAPHY?

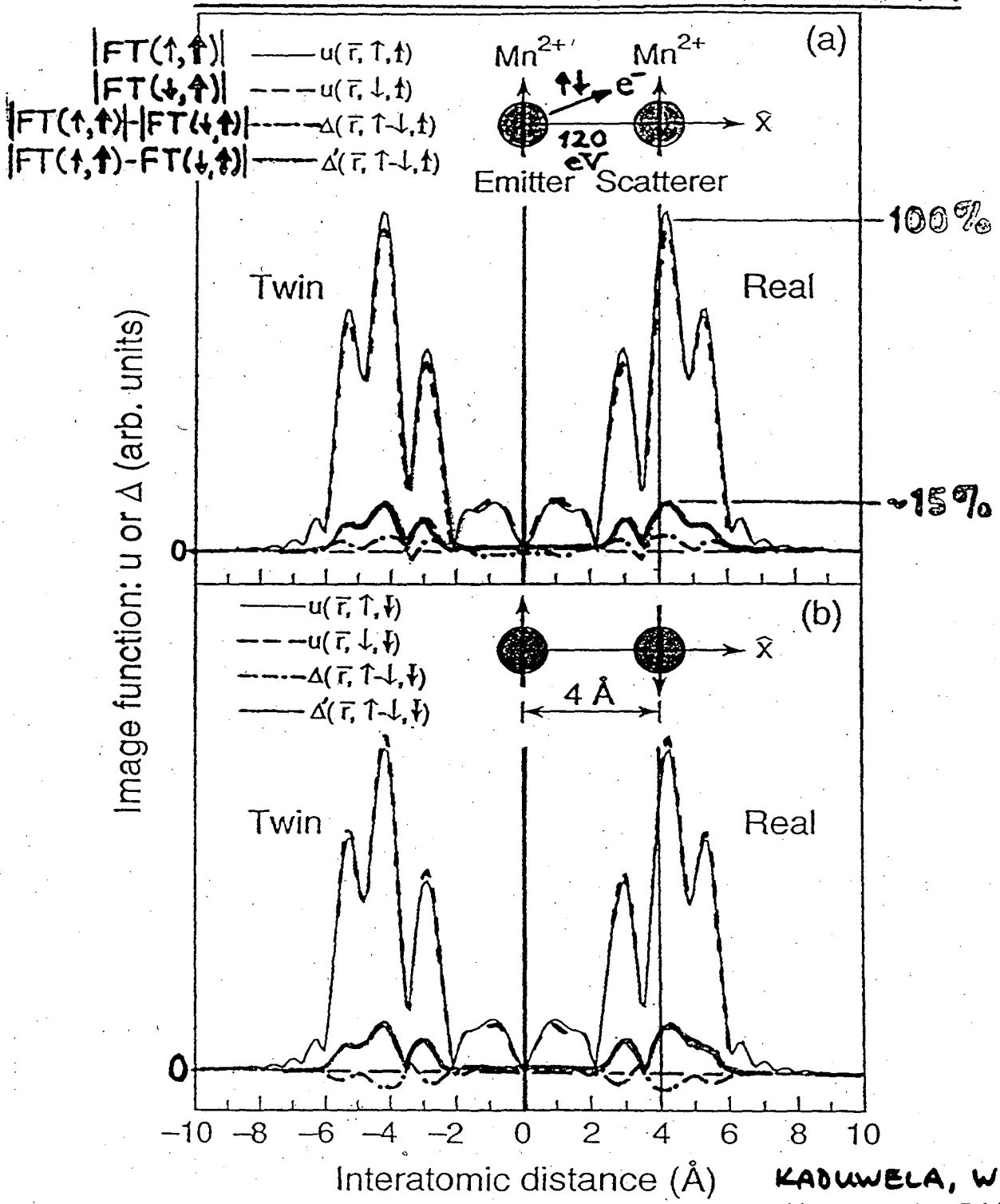

KADUWELA, WANG, VAN HOVE, FADLEY

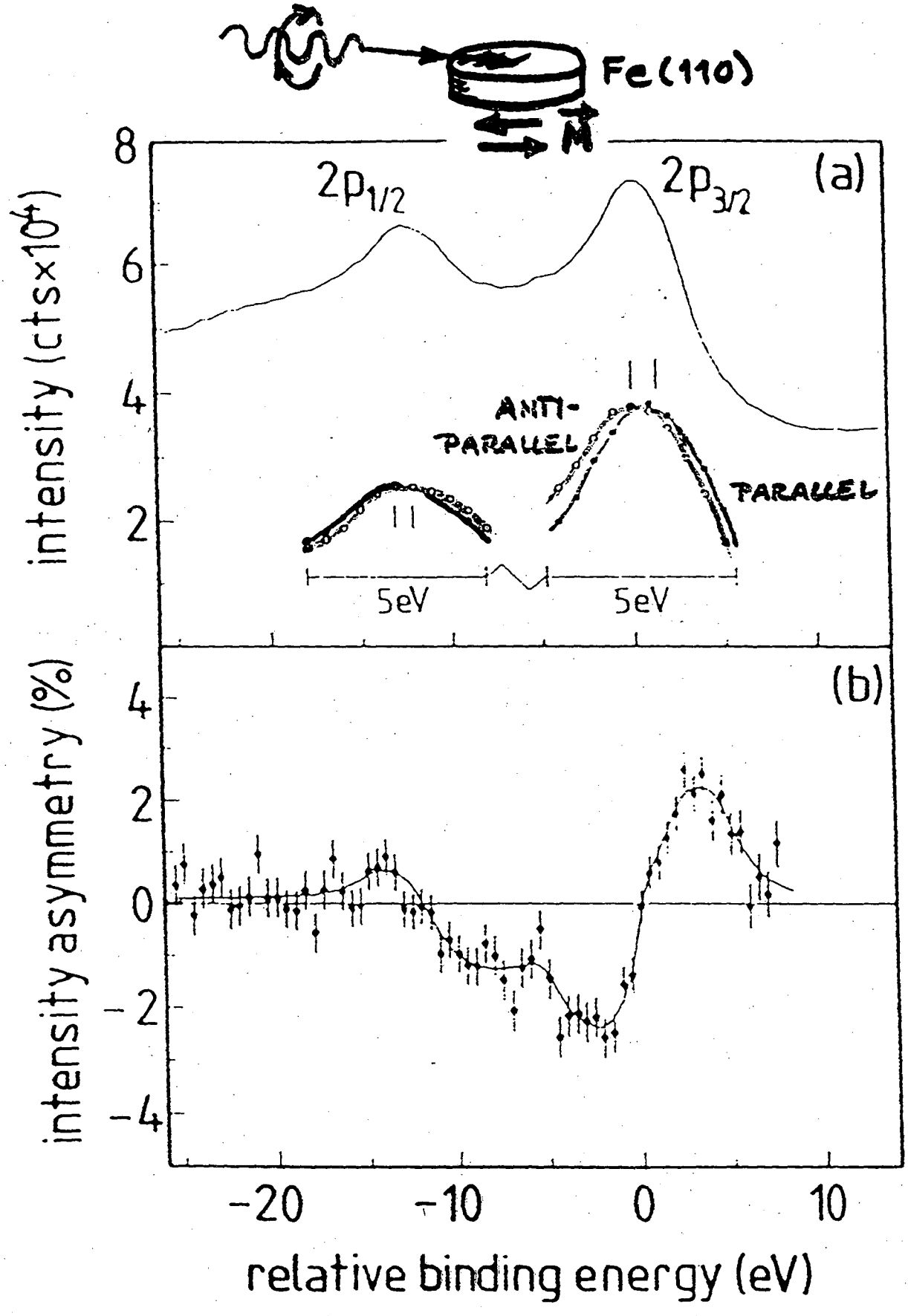

BAUMGARTEN ET AL., P.R.L. 65, 492('90)

ZEROTH-ORDER MODEL:

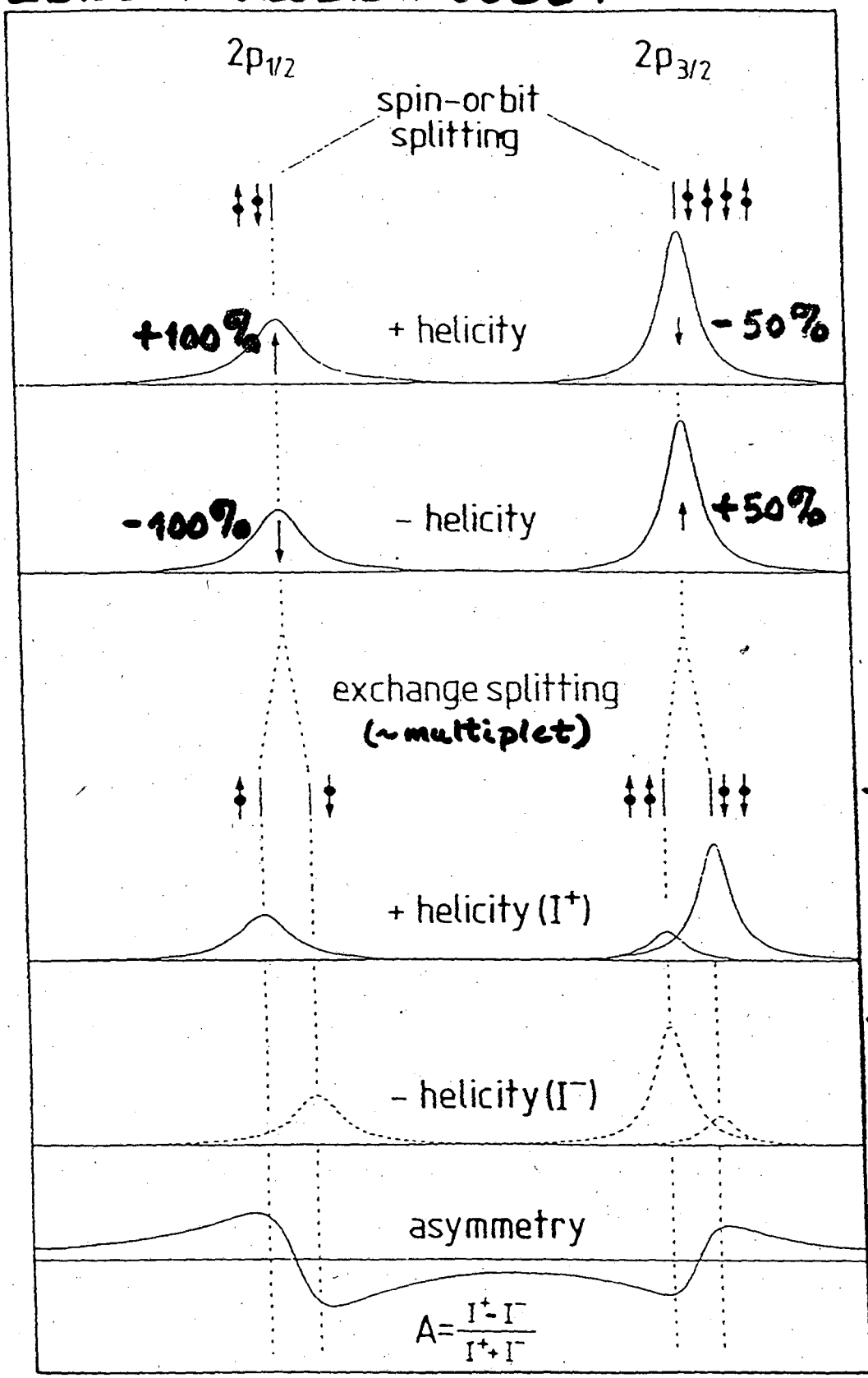

- NO $p \rightarrow s(1) + d(4)$ INTERFERENCE
- NO SPIN-DEPENDENT SCATTERING + DIFFRACTION
⋮

← BINDING ENERGY

Brief Scientific Presentation

Carsten Westphal

Lawrence Berkeley Laboratory

PHOTOELECTRON DIFFRACTION WITH CIRCULARLY-POLARIZED RADIATION:

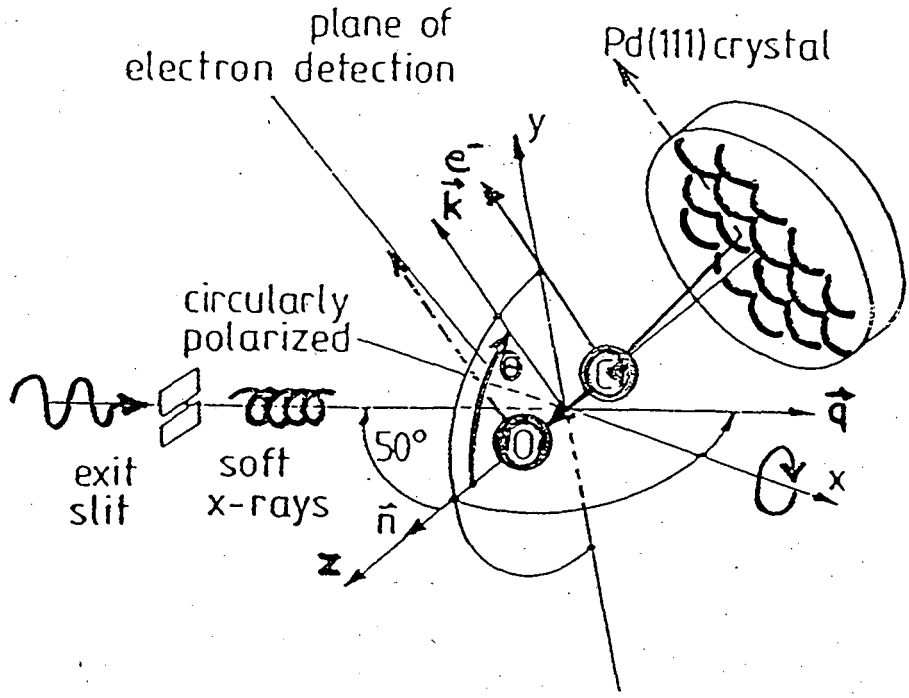

⇒ A CHIRAL GEOMETRY: $\vec{k}, \vec{z}, \vec{q}$ NOT CO-PLANAR

⇒ CIRCULAR DICHROISM: $I^{RCP} \neq I^{LCP}$

SCHÖNHENSE ET AL.,
PHYS. REV. B, NOV. 15, '92

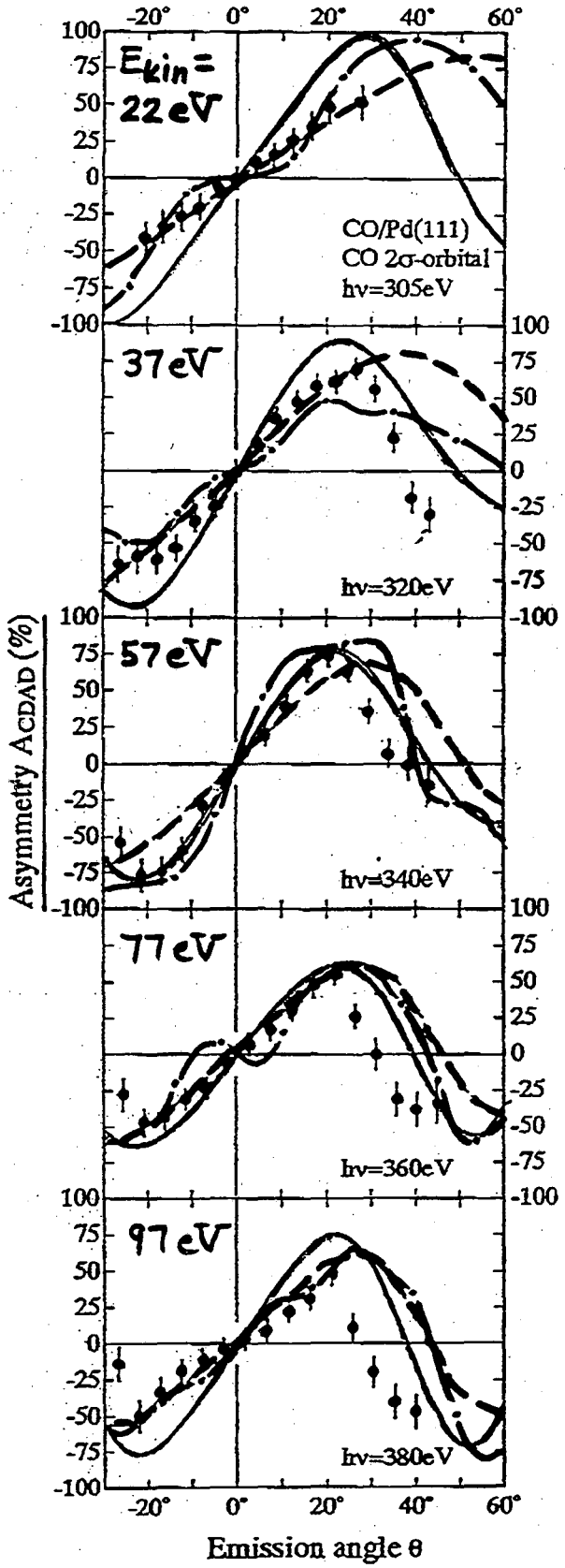

C1s EMISSION FROM CO/Pt(111) WITH CIRCULARLY-POLARIZED RADIATION ⇒

CIRCULAR DICHROISM ANGULAR DISTRIBUTIONS (CDAD)

$$A_{CDAD}(\theta) = \frac{I^{RCP}(\theta) - I^{LCP}(\theta)}{I^{RCP}(\theta) + I^{LCP}(\theta)}$$

ϕ = EXPT. (SCHÖNHENSE ET AL.)

THEORY:

—— = SCHWINGER-VARIATIONAL METHOD - CO ONLY (McCOY ET AL.)

- - - = SINGLE SCATT. CLUSTER-CO ONLY*

—— = SINGLE SCATT. CLUSTER-CO (hcp) + 18 Pt ATOMS*

* KADUWELA, WESTPHAL, VAN HOVE FADLEY

features:

- effect occurs for every material !
  (magnetic or non magnetic
  with or without spin-orbit interaction)

- effect is of the same order than the differential cross-section
  → ideal for use as a contrast

- first theoretical approach "sees" the phenomenon
  → important for the understanding of the photoemission process, phase-shift differences

Spin-polarized Auger Electron Spectrosc. with circularly pol. light

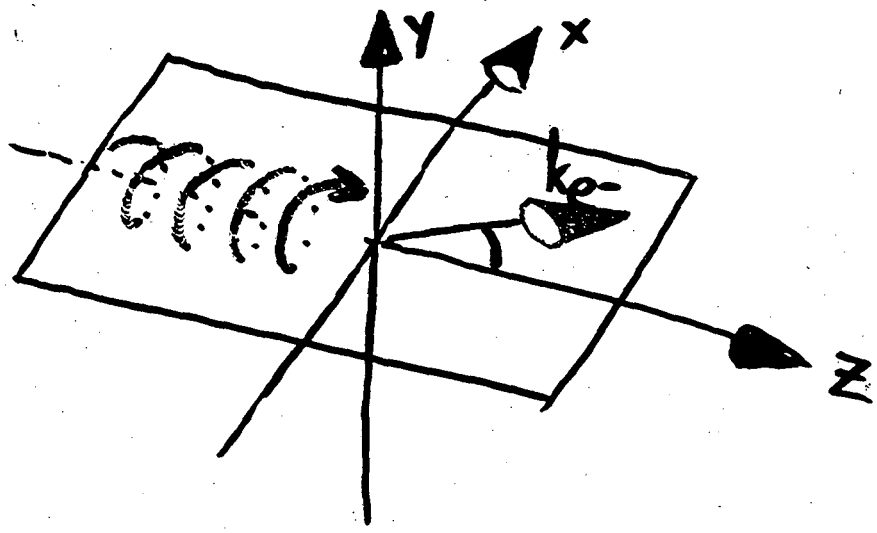

- circ. pol. light → inner shell vacancies may be aligned/oriented*

  → orientation is transfered to Auger-electron
  now: with spin-orbit
  ⇒ polarized electrons
  predicted: severel tens % !

- important for material science to study the Auger-decay

can be used as a probe for magnetism (needs lateral resolution)

* N.M Kabachnik, O.V. Lee, J. Phys B 22, 2705 (1989)

Brief Scientific Presentation

Joseph E. Nordgren

University of Uppsala, Sweden

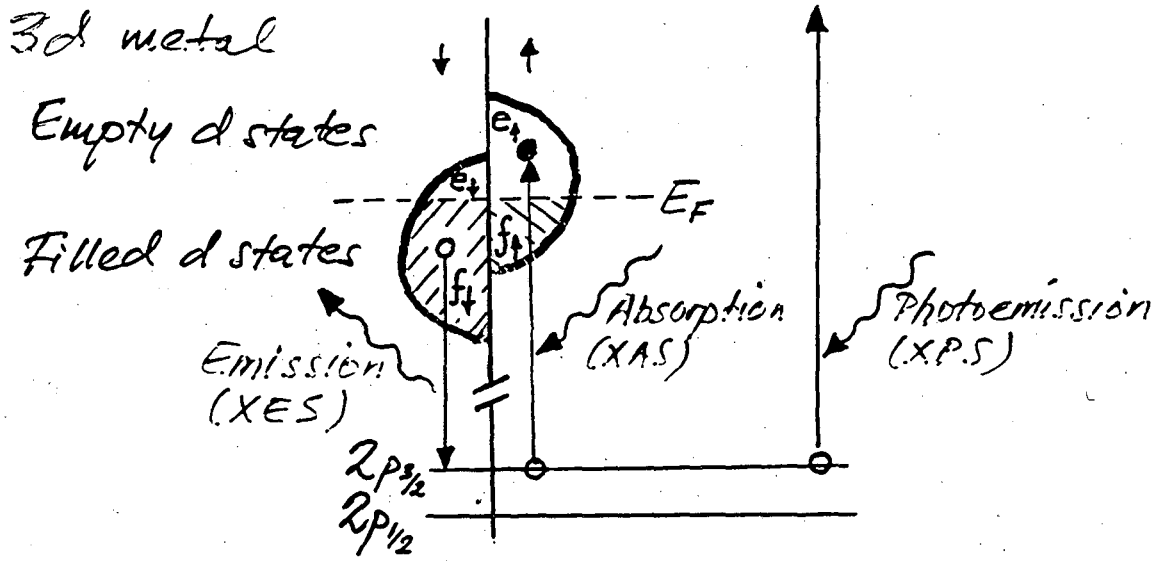

$$\sigma \propto \underbrace{|\langle \psi_f | \bar{D} | \psi_i \rangle|^2}_{M} \underbrace{\delta(E)}_{e,f} \qquad M_\downarrow^L = M_\uparrow^R \qquad M_\uparrow^L = M_\downarrow^R$$

DICHROISM (ABSORPTION) $= \sigma^L_{Abs.} - \sigma^R_{Abs.} =$

$$= M_\downarrow^L e_\downarrow + M_\uparrow^L e_\uparrow - M_\uparrow^L e_\downarrow - M_\downarrow^L e_\uparrow$$

$$= \underline{(\Delta M_{\downarrow\uparrow})(e_\downarrow - e_\uparrow)} = \underline{(\Delta M_{\downarrow\uparrow})\,\mu}$$

DICHROISM (EMISSION) $= \sigma^L_{Abs.} \cdot \sigma^L_{Em.} - \sigma^R_{Abs} \cdot \sigma^R_{Em.} =$

$$= M_\downarrow^L e_\downarrow \cdot M f_\downarrow + M_\uparrow^L e_\uparrow \cdot M f_\uparrow -$$

$$- M_\uparrow^L e_\downarrow \cdot M f_\downarrow - M_\downarrow^L e_\uparrow \cdot M f_\uparrow =$$

$$= \underline{M(\Delta M_{\downarrow\uparrow})(e_\downarrow f_\downarrow - e_\uparrow f_\uparrow)}$$

(M independent of $\uparrow\downarrow$ if no polarization detection is made)

1. Continuum excitation

$$e_{\downarrow} = e_{\uparrow} = e$$

$$\Rightarrow MCD_{Emission} = \underline{-M(\Delta M_{\downarrow\uparrow})\mu e}$$

2. $p \rightarrow d$ resonant excitation

$$e_{\downarrow} + f_{\downarrow} = e_{\uparrow} + f_{\uparrow}$$

$$\Rightarrow MCD_{Emission} = \underline{M(\Delta M_{\downarrow\uparrow})\mu(f_{\uparrow} - e_{\downarrow})}$$

X-RAY EMISSION MCD EXPERIMENTS

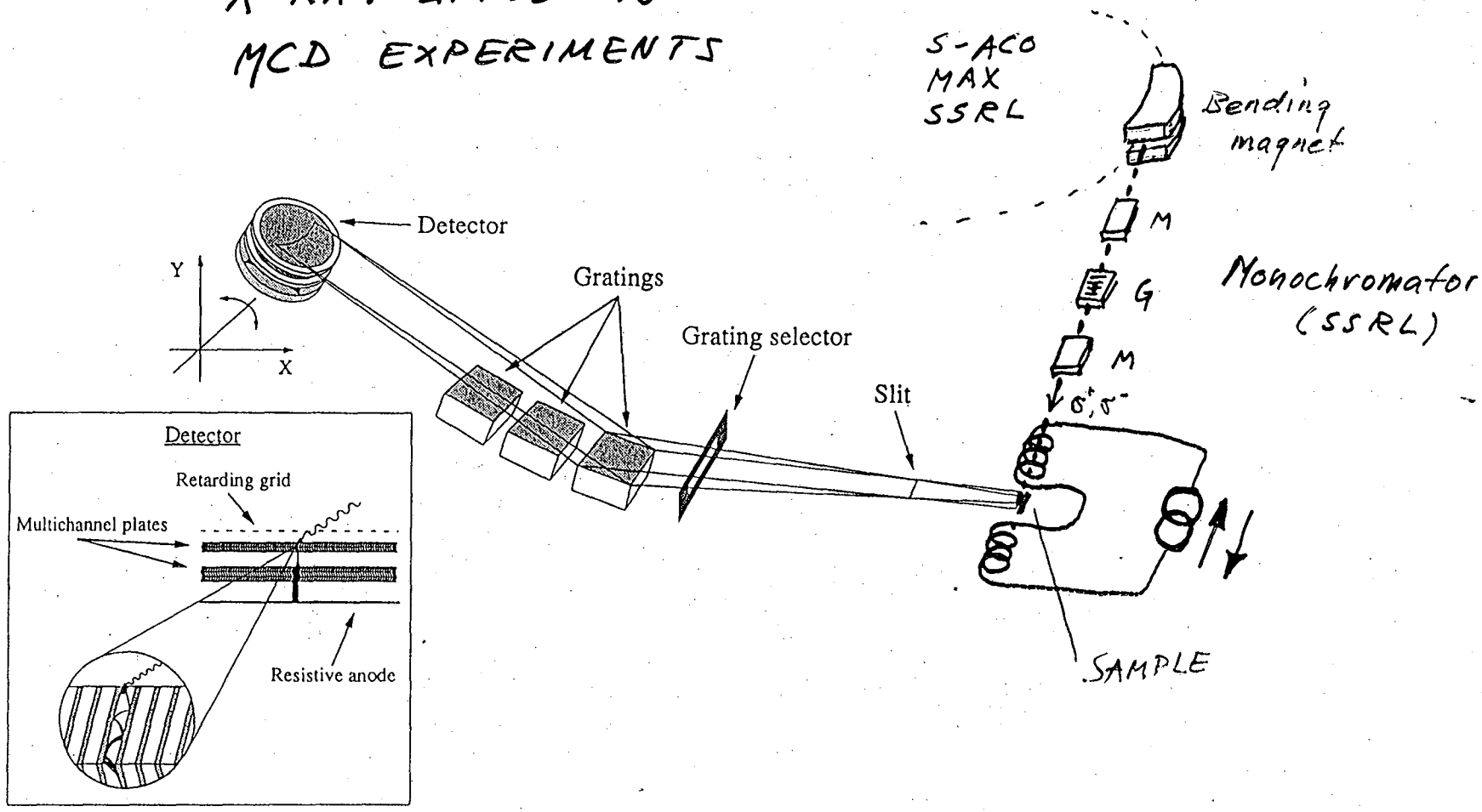

Co

COBALT SXES-difference spectra
(photon spin/magn. field:
parallel-antiparallel)

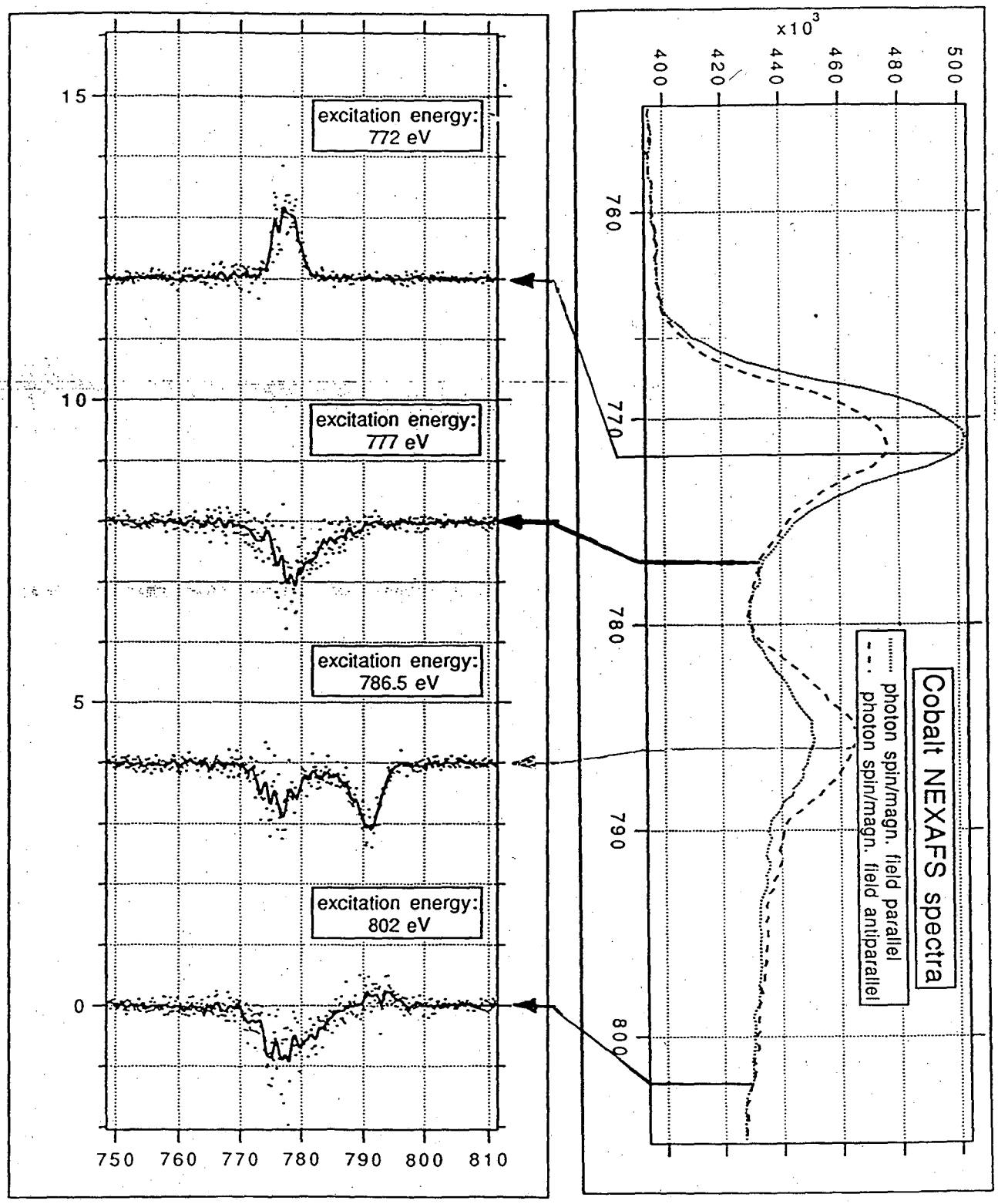

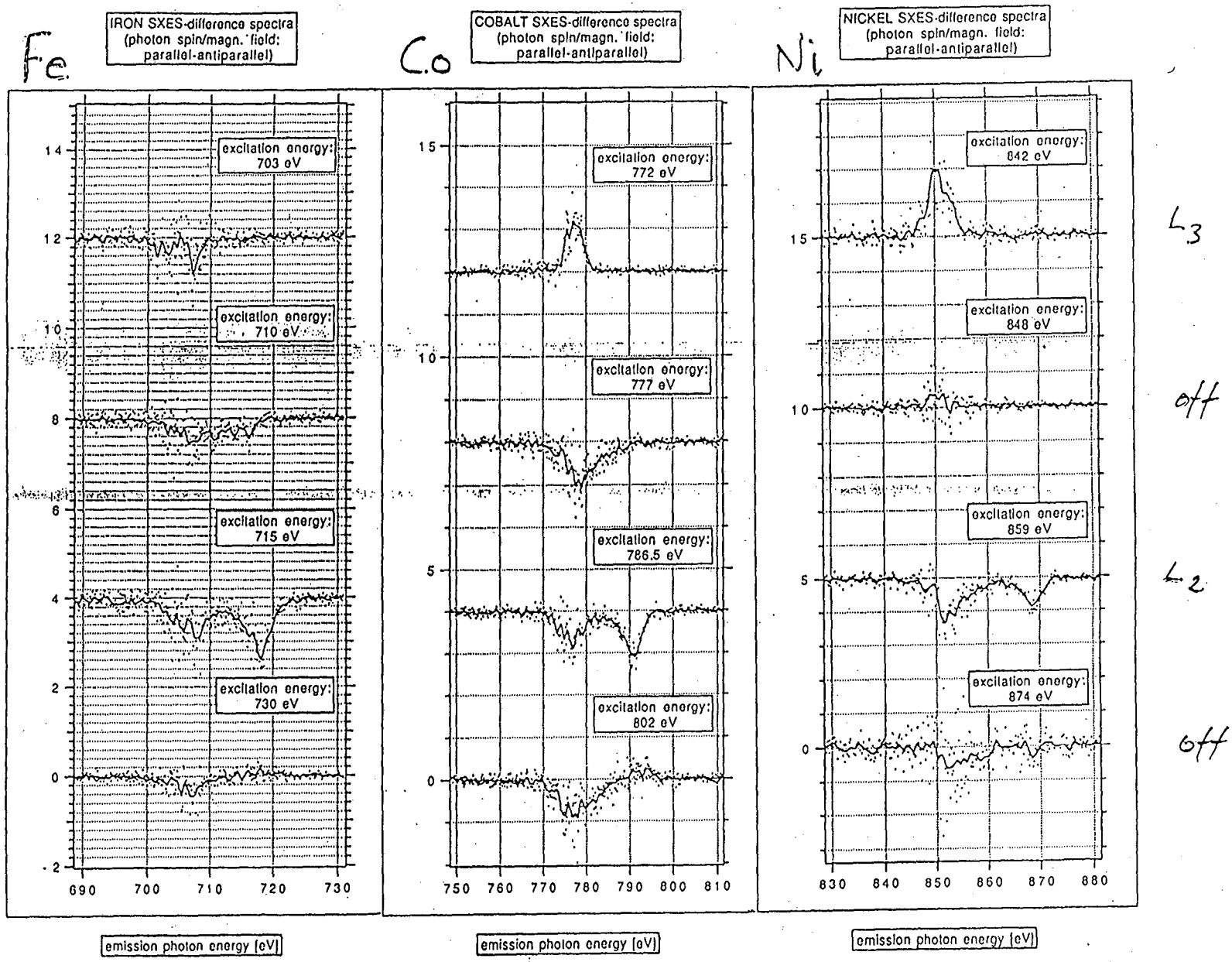
Fe
IRON SXES-difference spectra (photon spin/magn. field: parallel-antiparallel)
excitation energy: 703 eV
excitation energy: 710 eV
excitation energy: 715 eV
excitation energy: 730 eV
emission photon energy [eV]
Co
COBALT SXES-difference spectra (photon spin/magn. field: parallel-antiparallel)
excitation energy: 772 eV
excitation energy: 777 eV
excitation energy: 786.5 eV
excitation energy: 802 eV
emission photon energy [eV]
Ni
NICKEL SXES-difference spectra (photon spin/magn. field: parallel-antiparallel)
excitation energy: 842 eV
excitation energy: 848 eV
excitation energy: 859 eV
excitation energy: 874 eV
emission photon energy [eV]
L3
off
L2
off

CONCLUSIONS.

1. MCD in SXES feasible
2. Elemental and chem. specificity
3. Probe of spin densities of filled states
4. True bulk probe
5. Circ. polarized insertion device sources desired

Brief Scientific Presentation

Zhixun X. Shen

Stanford University

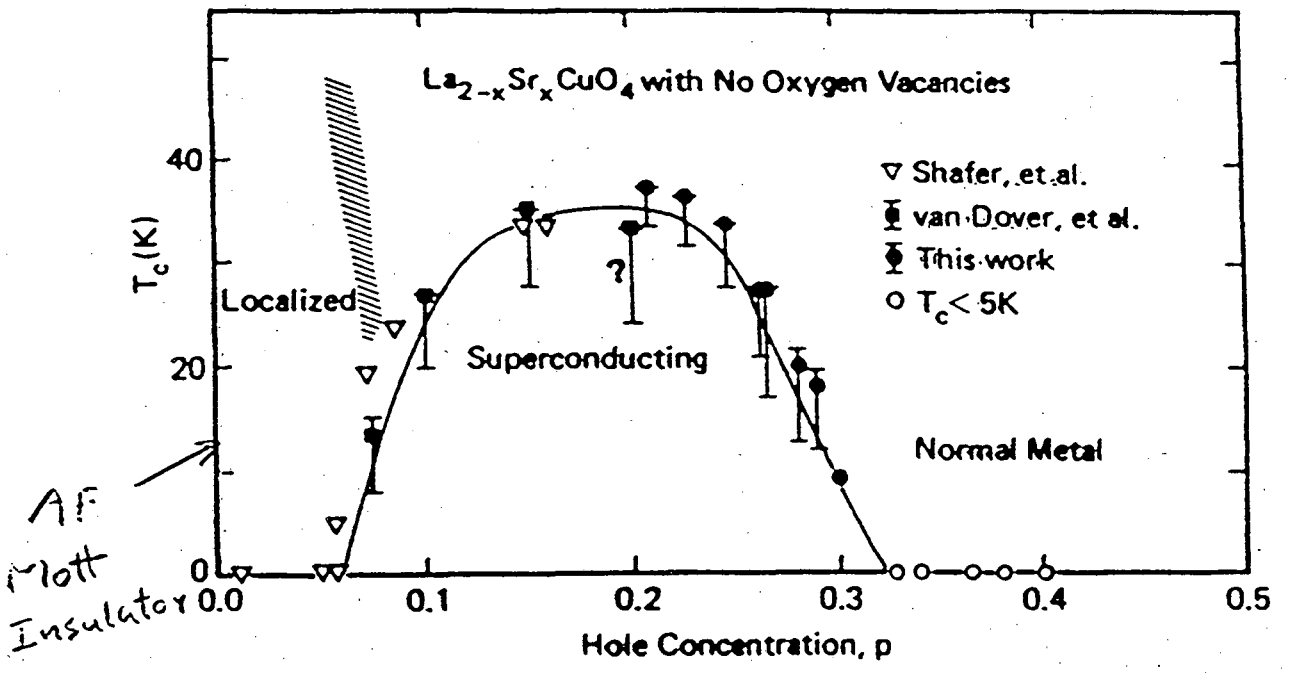
$La_{2-x}Sr_xCuO_4$ with No Oxygen Vacancies
Shafer, et al.
van Dover, et al.
This work
$T_c < 5K$
Localized
Superconducting
Normal Metal
?
T_c(K)
Hole Concentration, p
AF Mott Insulator

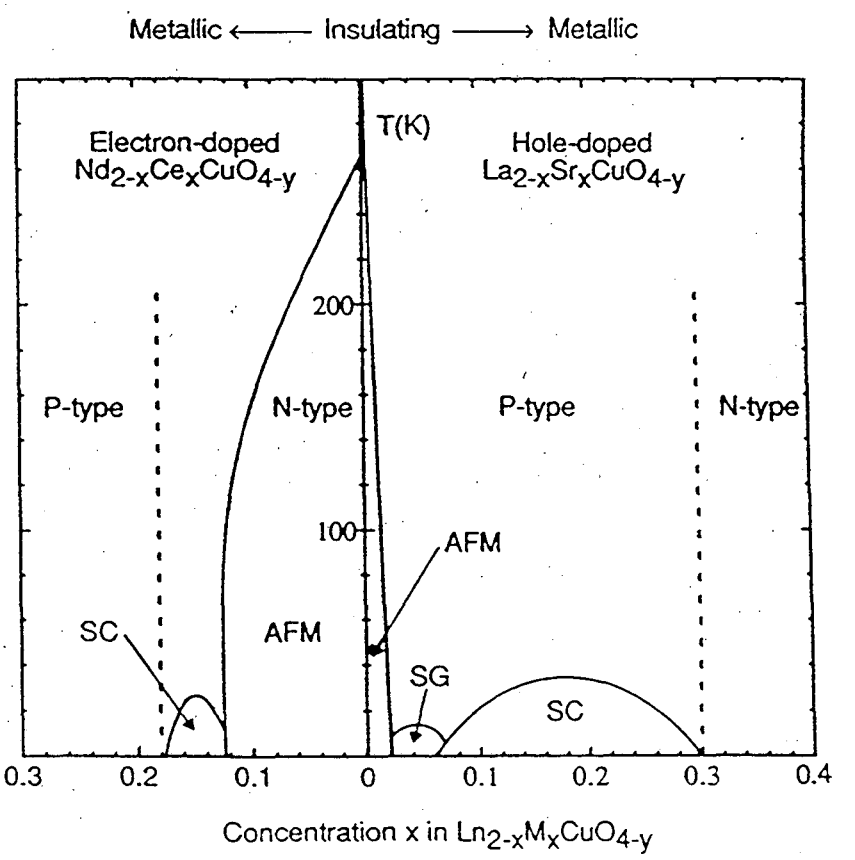
Metallic ← Insulating → Metallic
Electron-doped $Nd_{2-x}Ce_xCuO_{4-y}$
Hole-doped $La_{2-x}Sr_xCuO_{4-y}$
T(K)
P-type
N-type
P-type
N-type
AFM
SC
AFM
SG
SC
Concentration x in $Ln_{2-x}M_xCuO_{4-y}$

* Magnetic aspects in HTSC

AF spin fluctuations

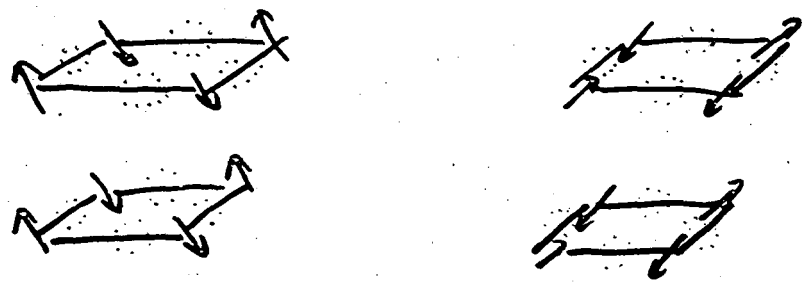

YBCO LSCO

* HTSC / F / HTSC

Pb / Fe / Pb

* Other oxides & Compounds

Brief Scientific Presentation

Jeffrey B. Kortright

Lawrence Berkeley Laboratory

Multilayer optics can generate and analyze polarization states over a range of energies in the XUV.

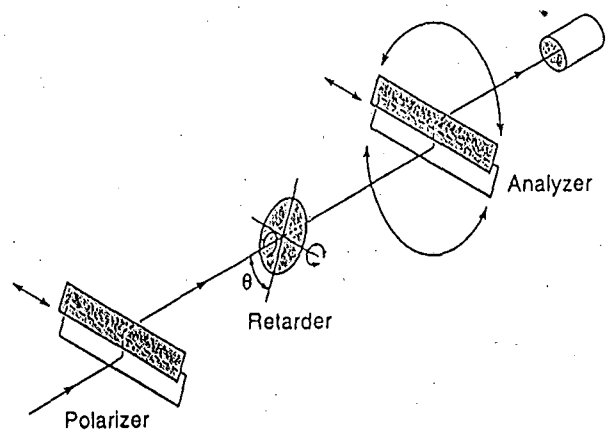

Polarization chamber capabilities:

- polarimetry
- optics development/characterization
- materials studies.

Useful hν range depends on experiment.

Polarization-resolved materials studies:

- XUV magneto-optical properties
  - M edges of Fe, Ni, Co
  - MCD, Kerr, Faraday effects, photoemission
- ellipsometric techniques in XUV
- absorption and scattering studies of chiral molecules and condensed systems (polymers)
- spectroscopies of lanthanides, actinides, superconductors, ...

Brief Scientific Presentation

Stephen P. Cramer

Lawrence Berkeley Laboratory

METALS IN PROTEINS

(paramagnets)

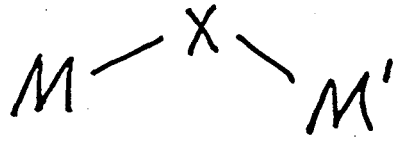

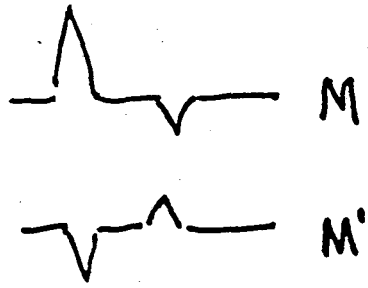

mixed metals e.g. N_2ase

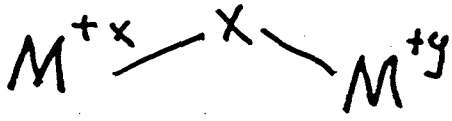

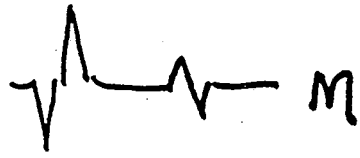

mixed valence e.g. MMO

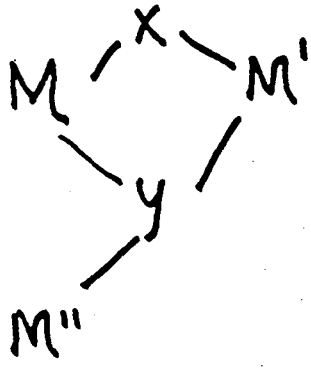

- spin orientations
- EXAFS simplification

SPEXAFS

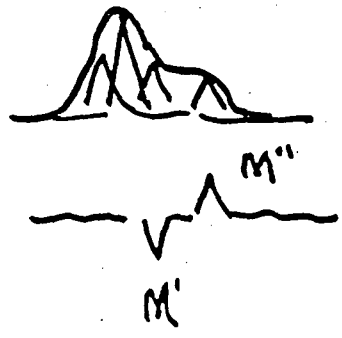

S. Cramer
G. George J. Chien
J. van Elp G. Peng

AN EXAMPLE OF XMCD FROM CURRENT INSTRUMENT

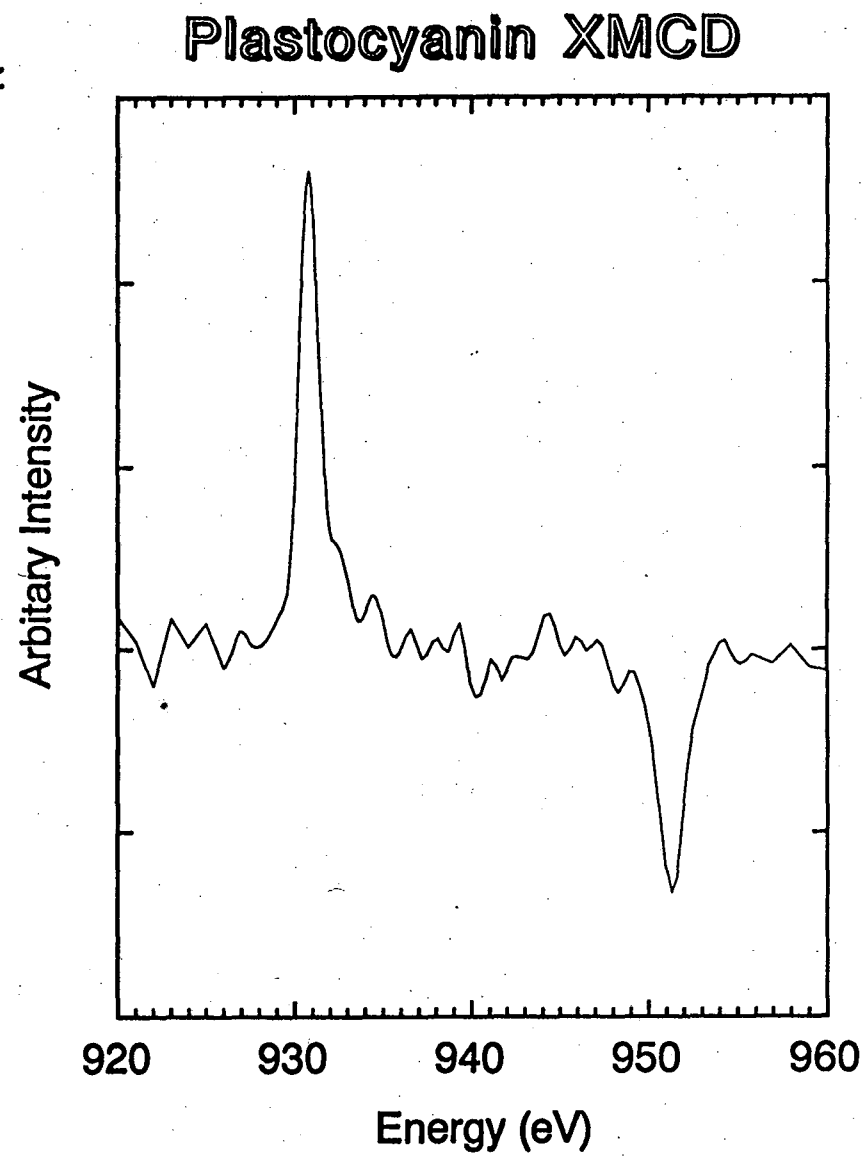

FUTURE XMCD DIRECTIONS

(1) LOWER TEMPERATURES
^{3}He cryostat

(2) 'fast magnets' - low inductance
~ 1 Hz switching

(3) faster detectors - arrays of
low capacitance
solid state detectors

(4) better sources ⟶ elliptical wiggler
beamlines

Brief Scientific Presentation

Roger G. Carr

Stanford Synchrotron Radiation Laboratory

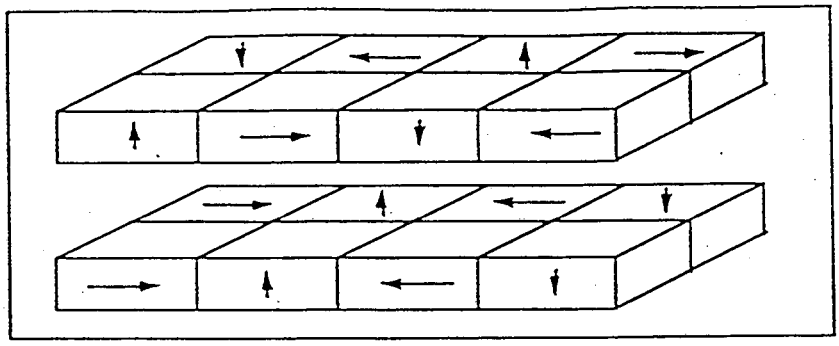

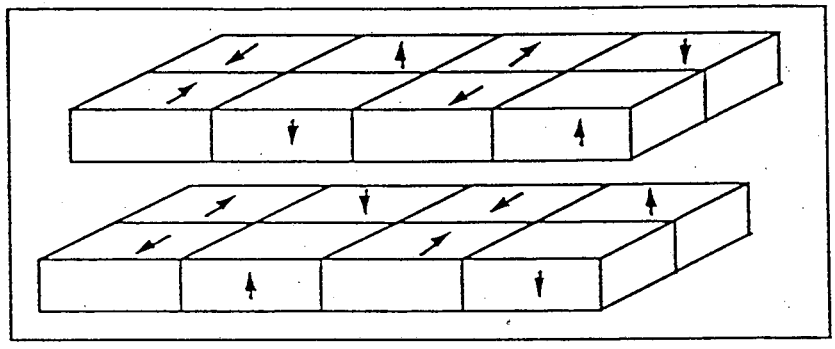

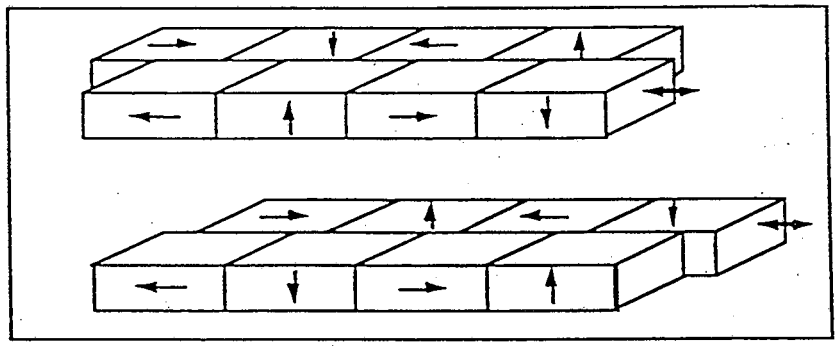

Undulator Type	Period Length	Kincaid Parameter	Number of Periods	Flux Watts/100mA
Halbach Single	6.9	1.72	27	7.95
Elleaume Single	7.6	1.57	24	5.32
Elleaume Chicane	7.6	1.57	10	2.22
Walker Chicane	7.4	1.67	10	2.58
Sasaki Single	6.5	1.79	28	9.49
Sasaki Chicane	6.5	1.79	11	3.73

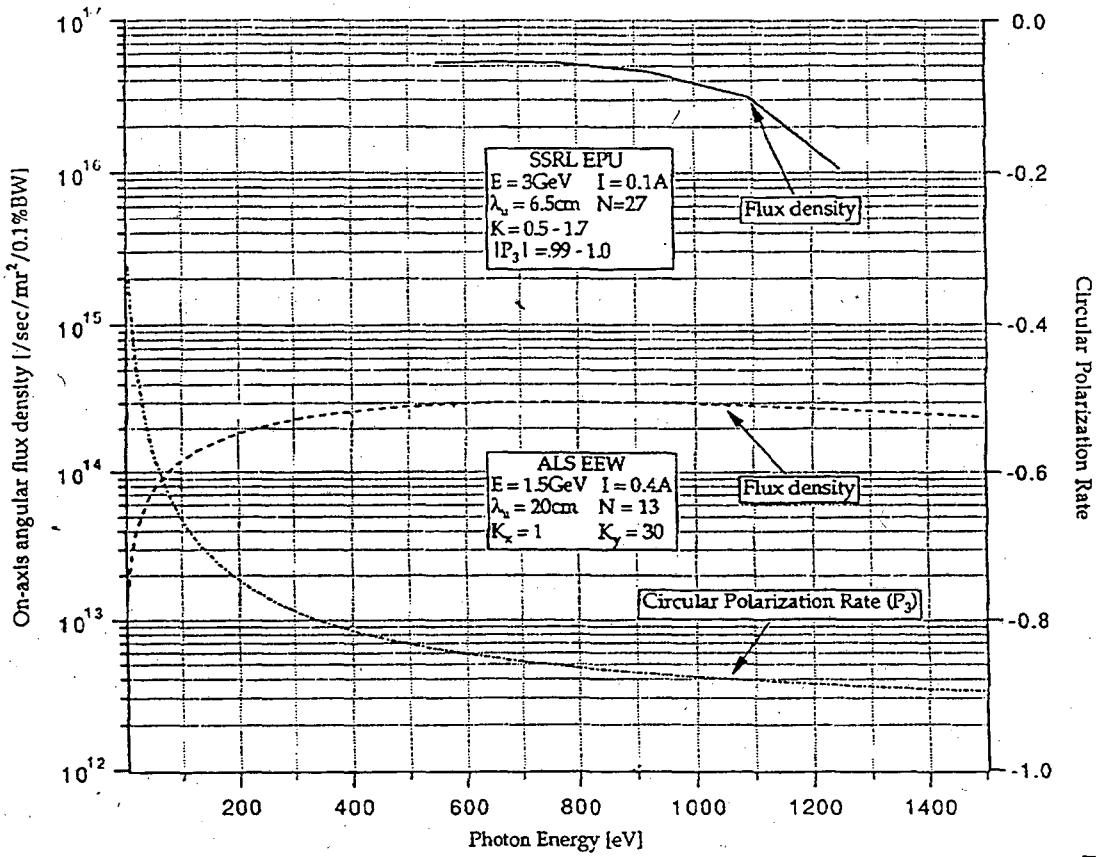
SSRL EPU
E = 3GeV I = 0.1A
λu = 6.5cm N=27
K = 0.5 - 1.7
|P3| = .99 - 1.0
Flux density
ALS EEW
E = 1.5GeV I = 0.4A
λu = 20cm N = 13
Kx = 1 Ky = 30
Flux density
Circular Polarization Rate (P3)
On-axis angular flux density [/sec/mr²/0.1%BW]
Circular Polarization Rate
Photon Energy [eV]

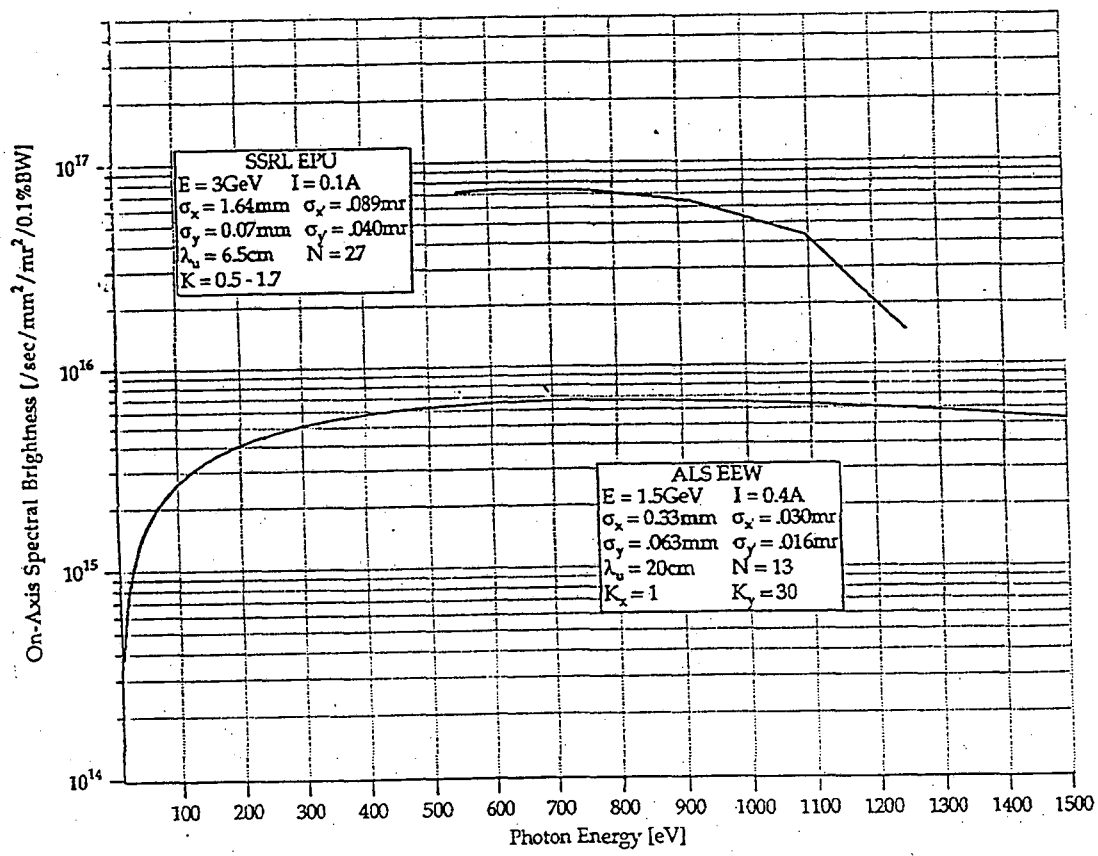
SSRL EPU
E = 3GeV I = 0.1A
σx = 1.64mm σx' = .089mr
σy = 0.07mm σy' = .040mr
λu = 6.5cm N = 27
K = 0.5 - 1.7
ALS EEW
E = 1.5GeV I = 0.4A
σx = 0.33mm σx' = .030mr
σy = .063mm σy' = .016mr
λu = 20cm N = 13
Kx = 1 Ky = 30
On-Axis Spectral Brightness [/sec/mm²/mr²/0.1%BW]
Photon Energy [eV]

Overview of Insertion Devices for Elliptical Polarization

Kwang-Je Kim

Lawrence Berkeley Laboratory

Experiment with Polarized Light

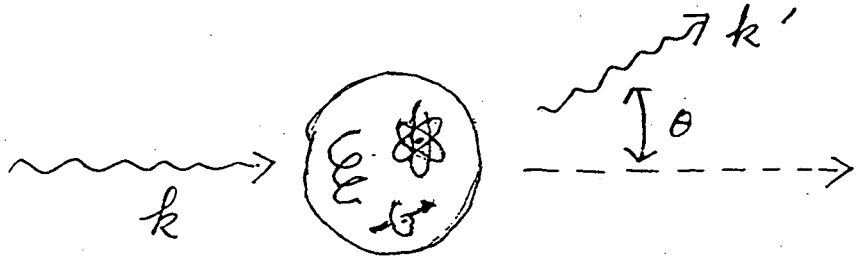

- Radiation beam characterized by Stokes Parameter

$$\mathcal{S} = (S_0, S_1, S_2, S_3)$$

$S_0 = |E_x|^2 + |E_y|^2$: total intensity

$S_1 = \langle |E_x|^2 - |E_y|^2 \rangle$

$S_2 = \langle E_x E_y^* + E_x^* E_y \rangle$

$S_3 = i \langle E_x E_y^* - E_x^* E_y \rangle$

- Degree of Polarization

$$P_i = \frac{S_i}{S_0}, \quad P = \sqrt{\Sigma P_i^2}$$

P_3 : degree of circular pol.

- Complete Experiment: Determine Mueller Matrix $\mathcal{M}$.

$$\mathcal{S}' = \mathcal{M}\,\mathcal{S}$$

Poincaré Sphere + Polarization Ellipse

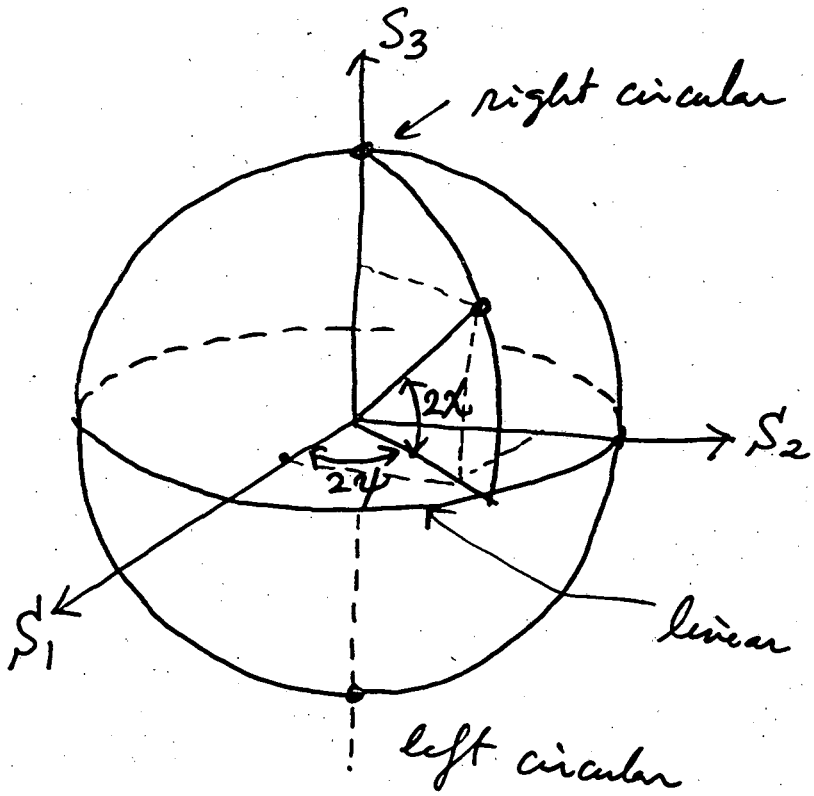

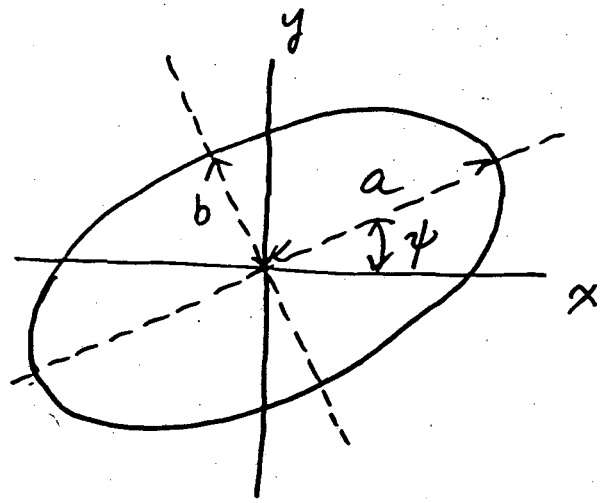

$$\tan \chi = \frac{b}{a}$$

Insertion Devices for Variable Polarization

- **Bending Magnet**
  Off plane observation($\psi \neq 0$). *BESSY, SRC, ..*

- **Wiggler**
  Asymetric wiggler (Goulon, Elleaume, Rauox), *HASYLAB, LURE,..*
  Elliptical wiggler (Yamamoto, Kitamura), *KEK*

- **Undulator**
  Devices producing helical field:

  Helical U..bifilar windindgs(Madey), permanent magnet(Halbach)
  Tilt-pole U(Halbach)
  Onuki, *ETL*
  Elleaume, *ESRF*
  Diviacco & Walker, *Elettra*
  Sasaki, *JAERI*

  Device based on interference effect:

  Crossed U(Moissev,Nikitin, Fedorov), (Kim) *BESSY, SRC*

Issues:
- Modulation versatility
- Vacuum chamber constraints(achievable K)
- Sensitivity to electron beam emittance
- Effect on electron trajectory
- Use of higher harmonics

Polarization of Bending Magnet Radiation

$$\begin{pmatrix} E_x \\ E_y \end{pmatrix} = e^{i\Phi} \begin{pmatrix} K_{2/3}(\eta) \\ \dfrac{i\gamma\psi}{\sqrt{1+(\gamma\psi)^2}} K_{1/3}(\eta) \end{pmatrix}$$

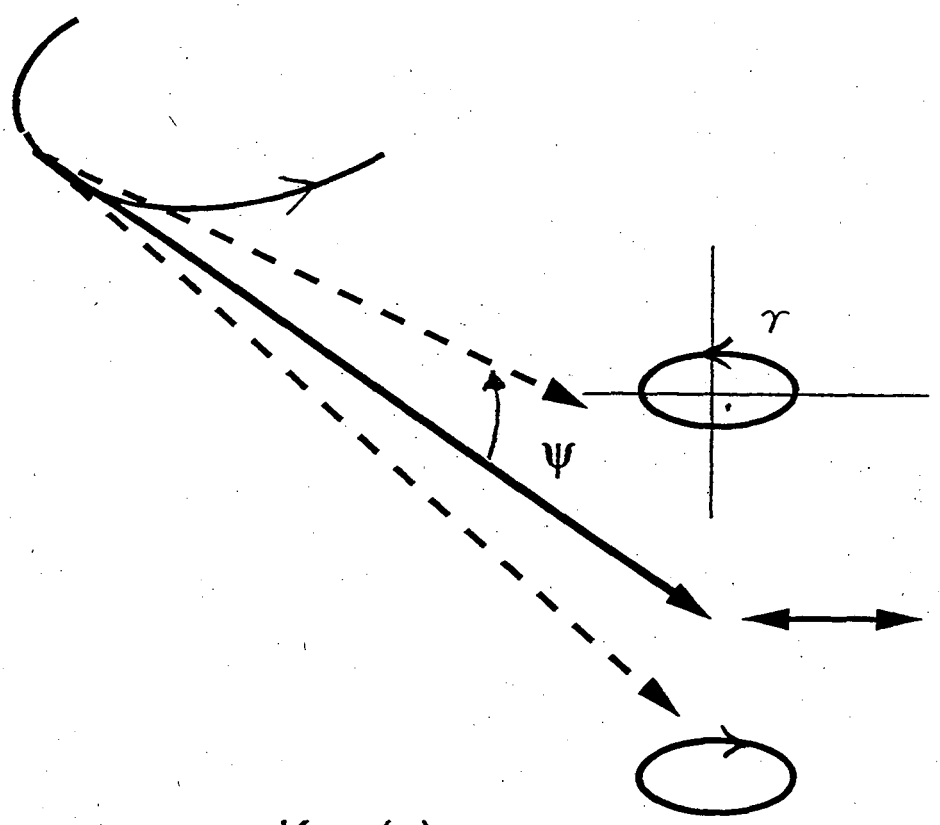

$$r = \frac{\gamma\psi}{\sqrt{1+(\gamma\psi)^2}} \frac{K_{1/3}(\eta)}{K_{2/3}(\eta)}$$

Elliptically polarized when observed at some vertical angle $\psi \neq 0$.

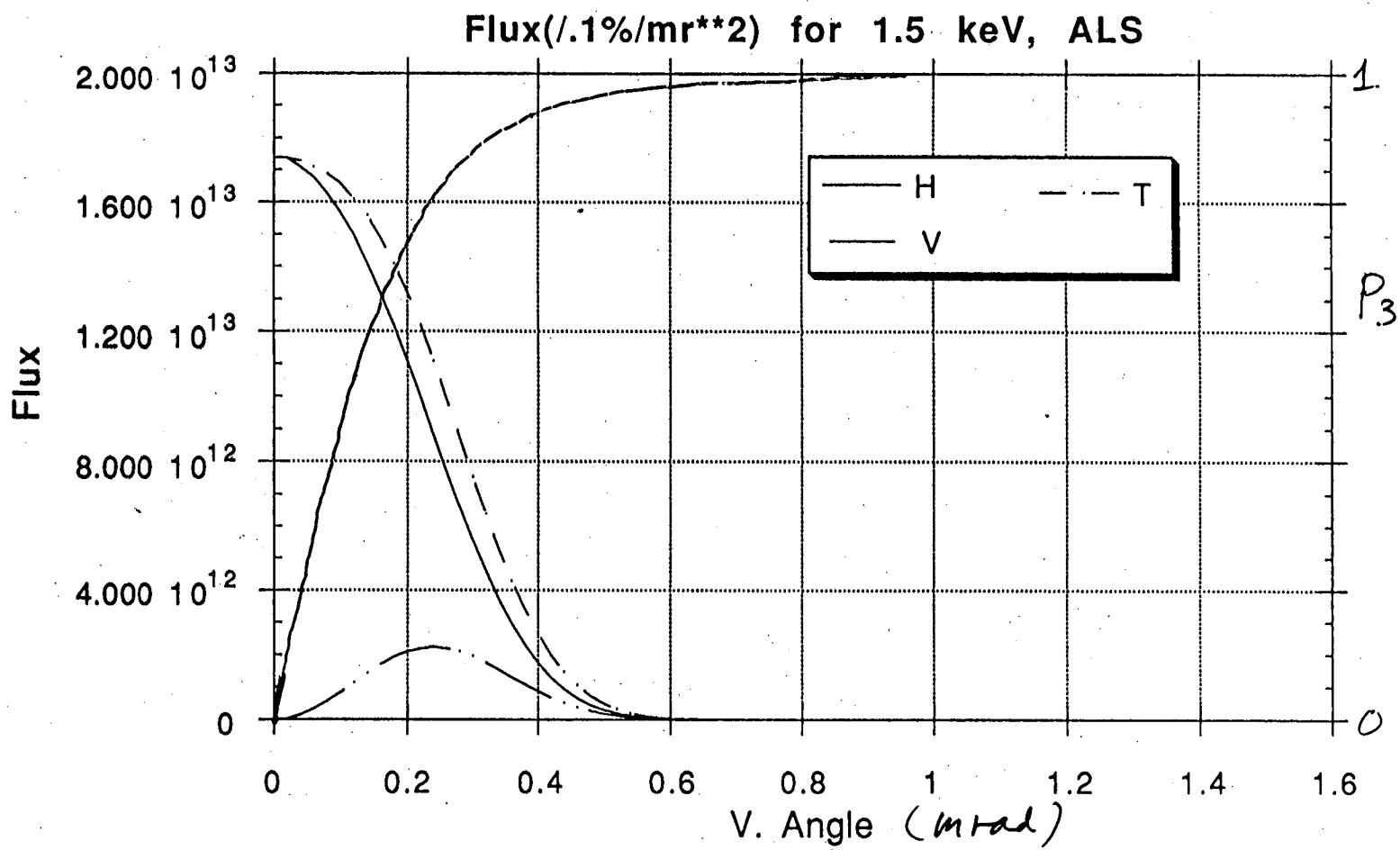
Flux(/.1%/mr**2) for 1.5 keV, ALS
Flux
2.000 10^13
1.600 10^13
1.200 10^13
8.000 10^12
4.000 10^12
0
0
0.2
0.4
0.6
0.8
1
1.2
1.4
1.6
V. Angle (mrad)
H
V
T
1
P3
0

Elliptical Polarization from Bending Magnets + Wigglers

- Bending magnet radiation, observed at a vertical angle $\psi \neq 0$, is elliptically polarized.

  Radiation from planar wiggler, due to interference from adjacent poles, is <u>linearly</u> polarized.

- To obtain elliptical polarization from wiggler

  i) break the symmetry of adjacent poles
  (Asymmetric wiggler)

  ii) or bend the trajectory plane by horizontal field
  (elliptical wiggler).

Radiation from Planar Wiggler is linearly Polarized

due to interference from adjacent poles.

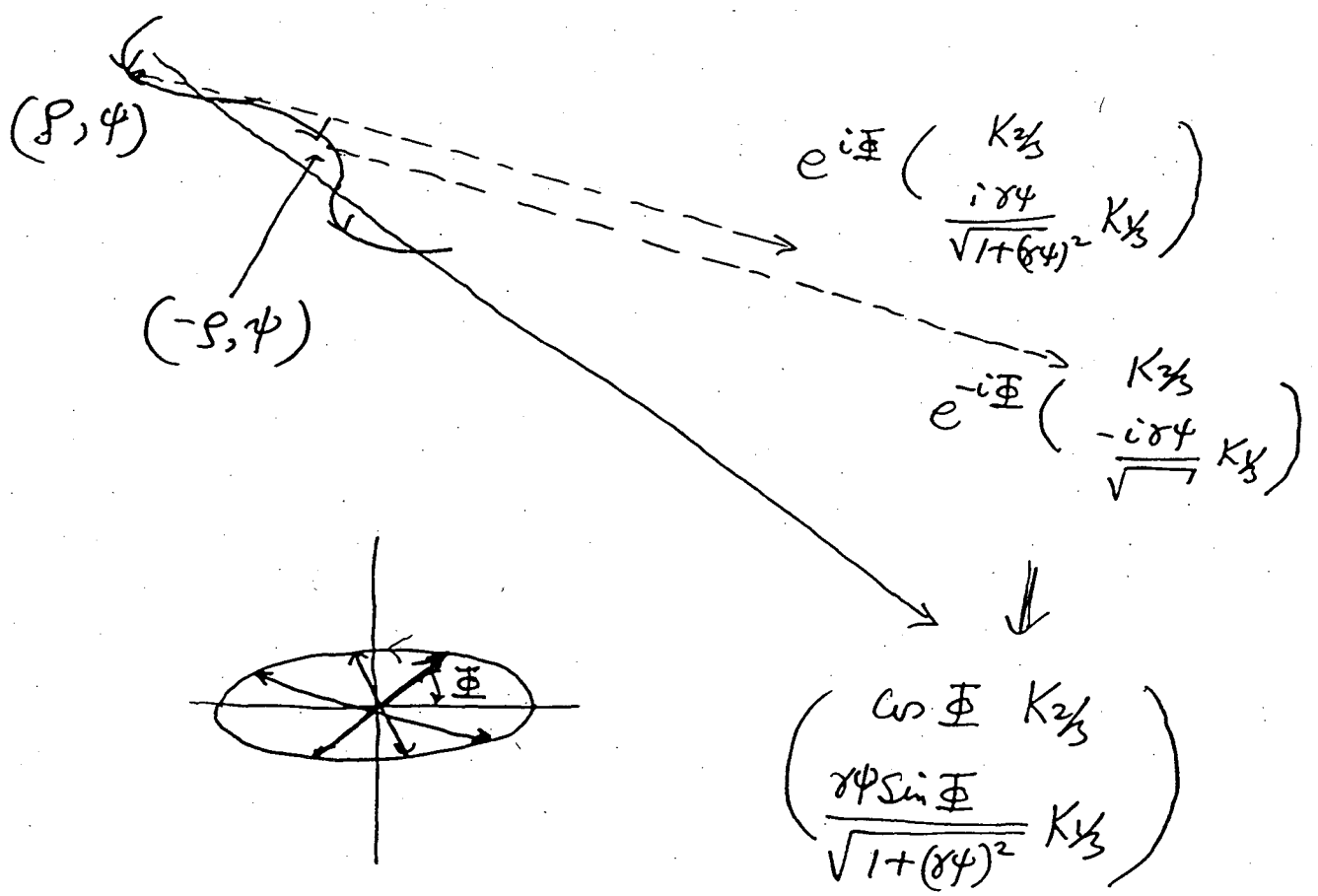

Can Even and Odd Poles Imaged Separately To obtain Circular Polarization from Planar Wiggler?

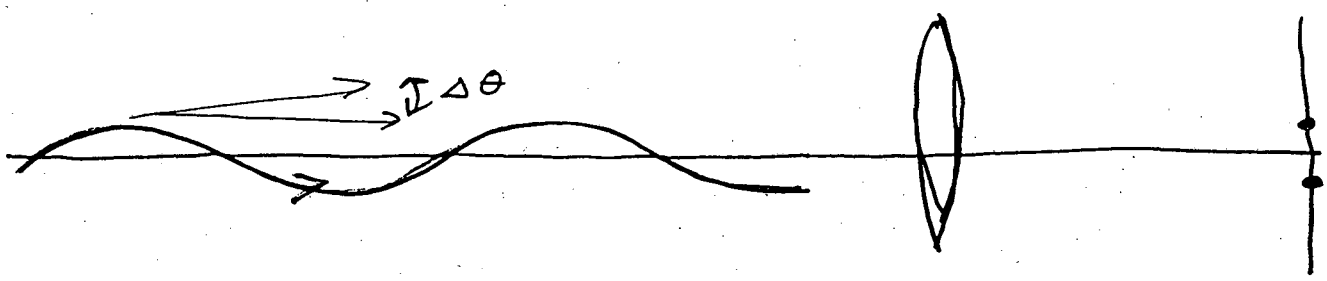

Blur due to depth of field should be less than source separation a

$$L\Delta\theta < a \quad ; \quad a = \frac{K\lambda u}{\gamma 2\pi}$$

$$\Delta\theta < \frac{K}{\gamma} \frac{1}{2\pi N}$$

$\therefore$ Total flux in each spot is less than that can be obtained from a single pole.

Asymmetric Wiggler

→ Break Symmetry.

Goulon + Ellearme.

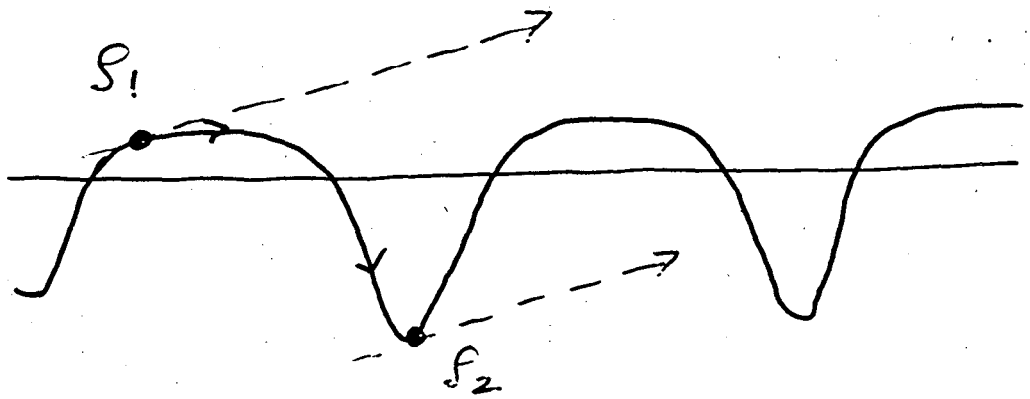

[HysyLab, DESY

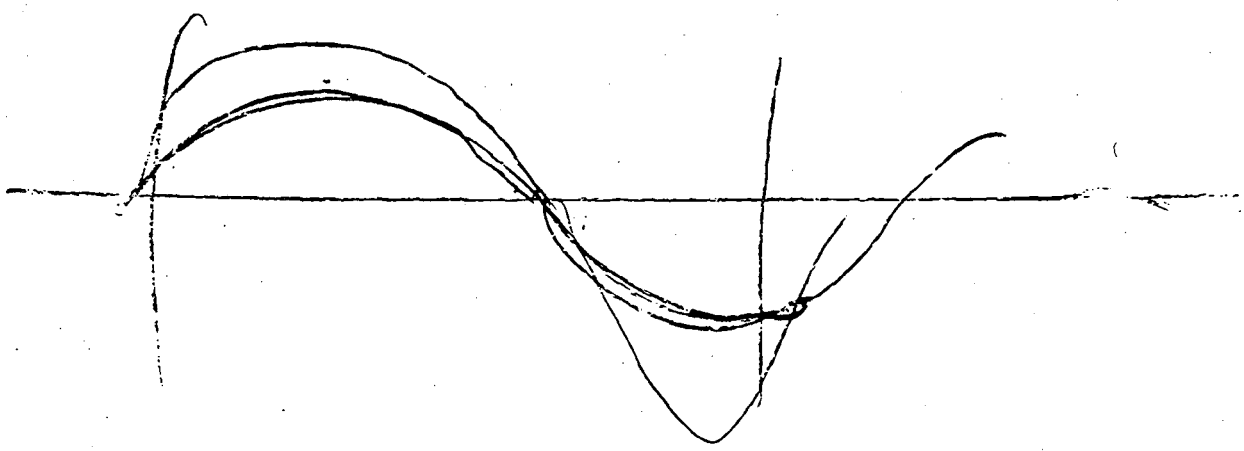

Elliptical Wiggler (Kitamura + Yamamoto)

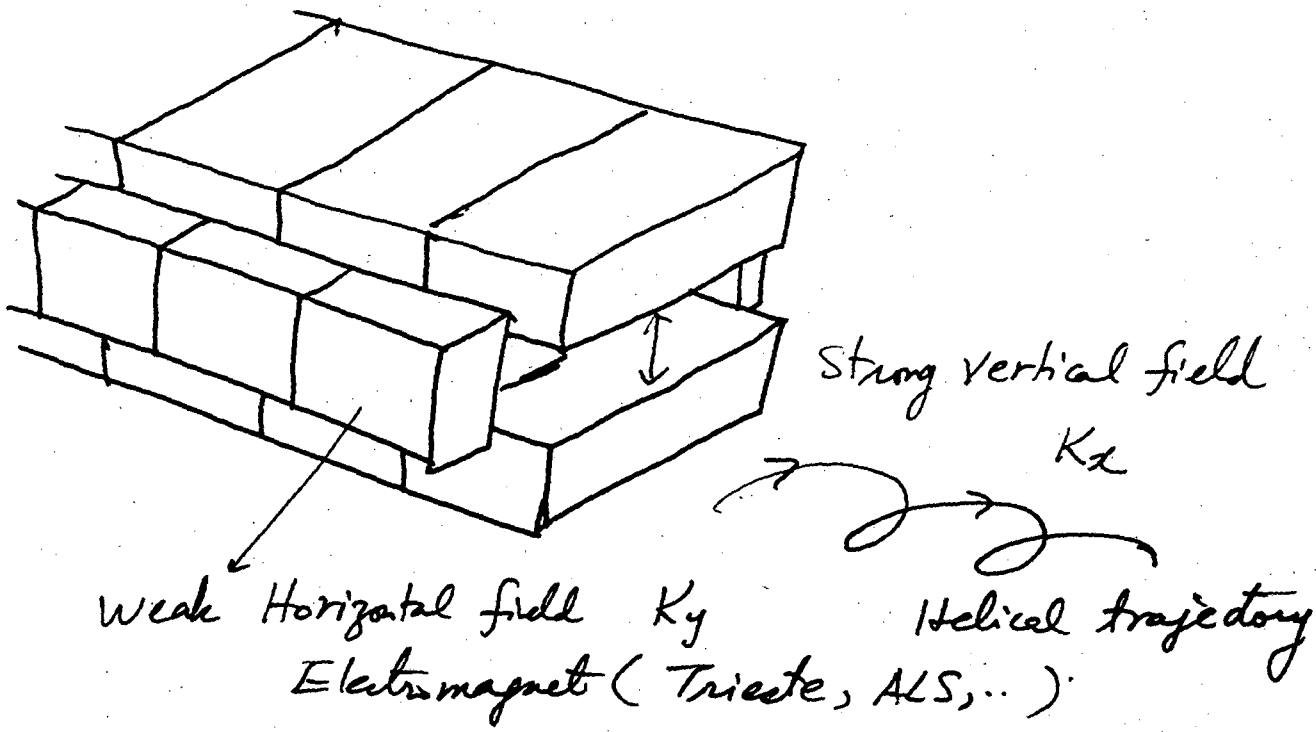

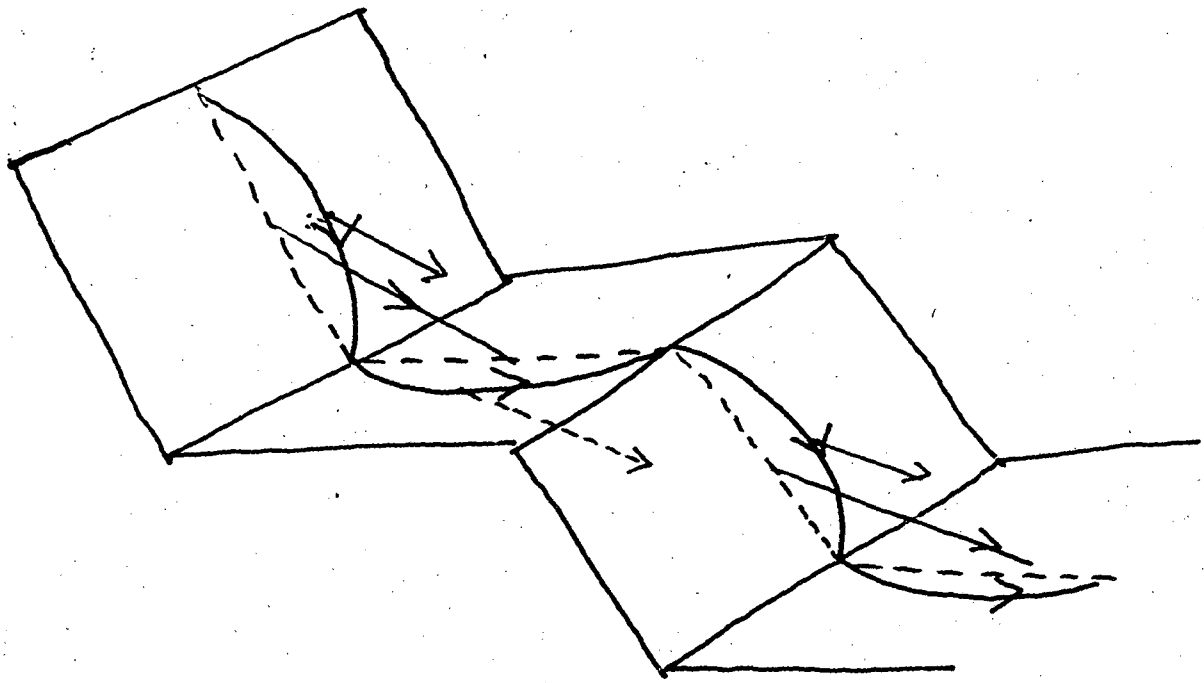

Elliptical polarization corresponding to $\psi = \frac{K_y}{\gamma}$ of Bending magnet radiation

Elliptical Wiggler: Similar to Bending Magnet But Stronger.

- Wide spectral coverage --- typical of wiggler

- Brightness -- typical of wiggler

$$\mathcal{B} = \underbrace{\frac{d^2\tilde{F}}{d^2\Omega}}_{\text{single pole}} \cdot \frac{1}{2\pi} \sum_j \frac{e^{-\frac{1}{2}\frac{x_0^2}{\sigma_x^2+\sigma_r^2+z_j^2\sigma_{x'}^2}}}{\sqrt{(\sigma_x^2+\sigma_r^2+z_j^2\sigma_{x'}^2)(\sigma_y^2+\sigma_r^2+z_j^2\sigma_{y'}^2)}}$$

- Polarization Coverage

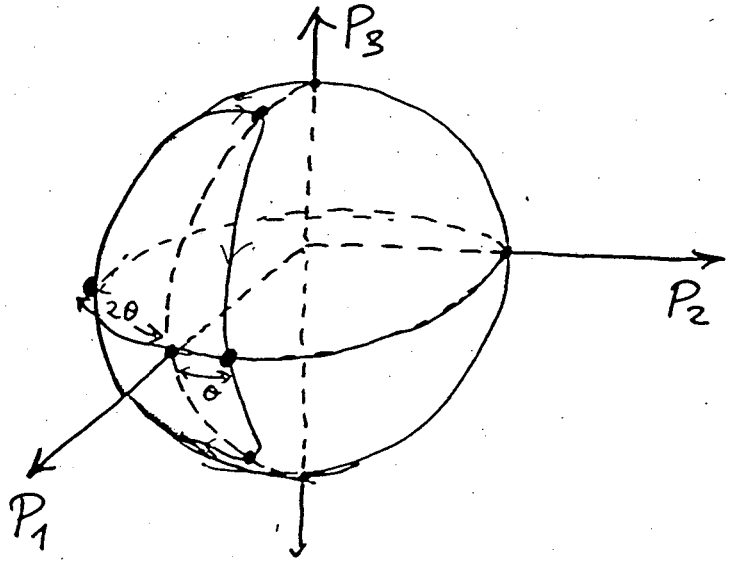

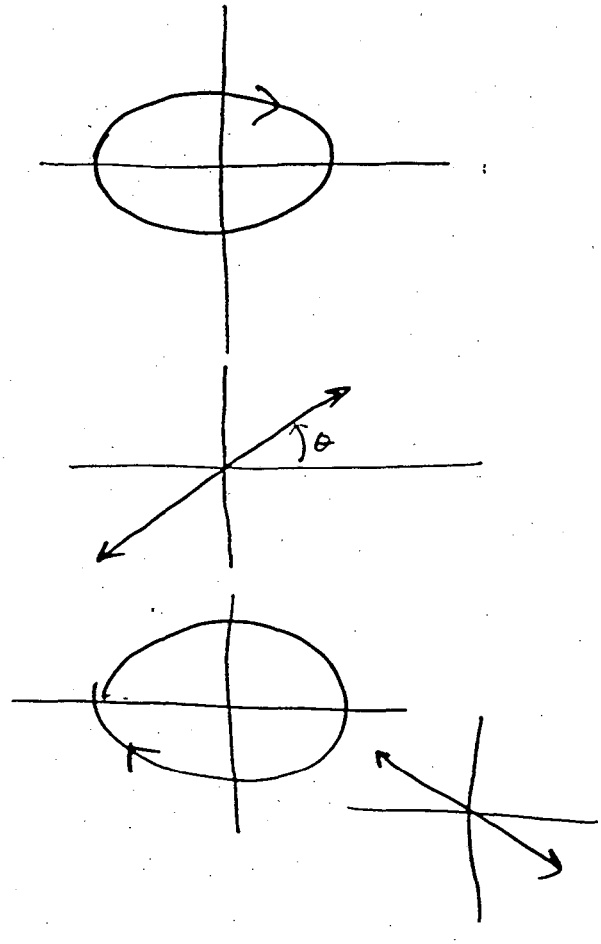

Undulators producing Helical Magnetic Field

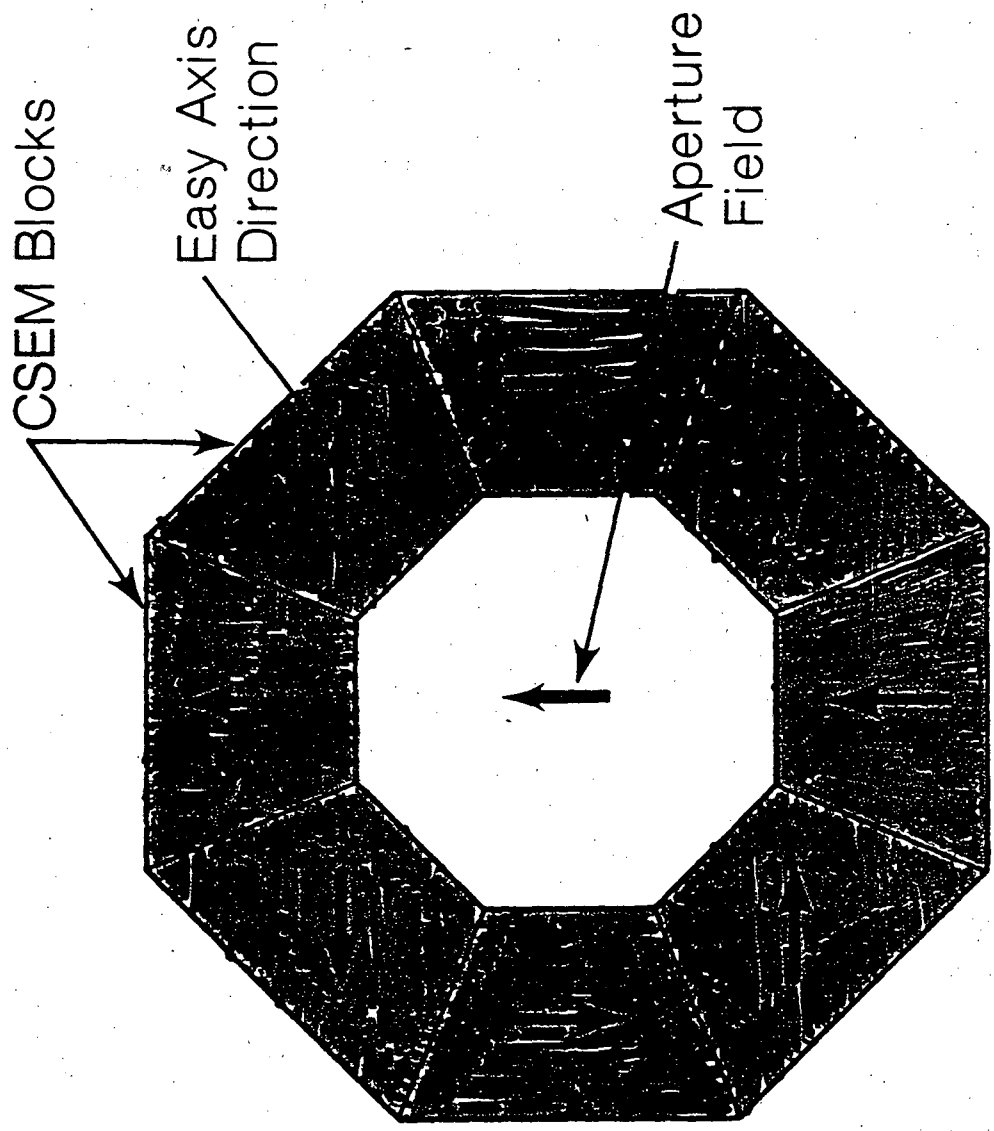

HELICAL UNDULATOR CROSS SECTION

Halbach

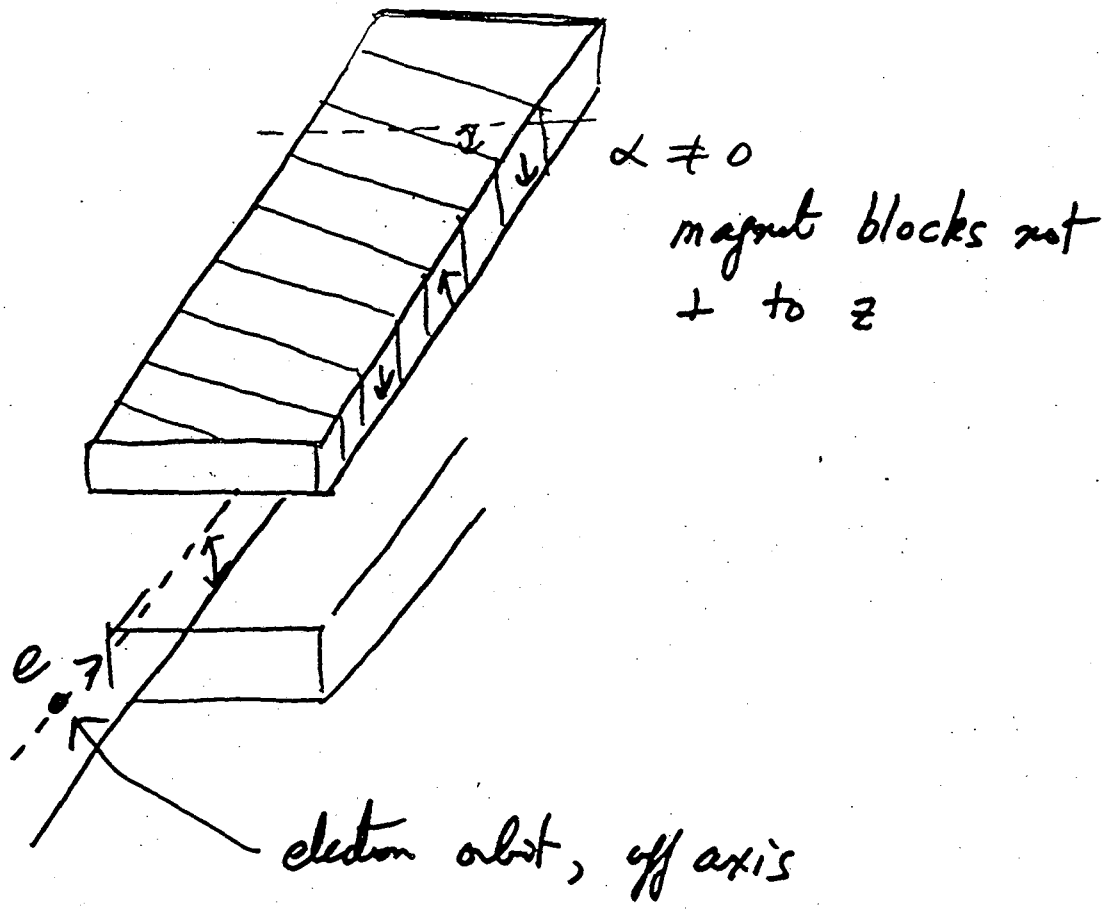
$\alpha \neq 0$
magnet blocks not
$\perp$ to z
e
electron orbit, off axis

Ohnuki

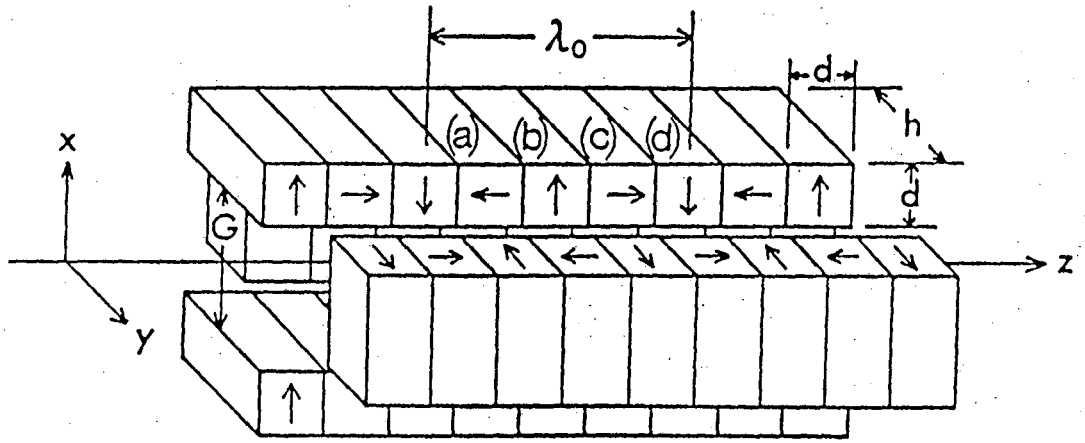

d : 14 mm
h : 28 mm
G : 29 mm

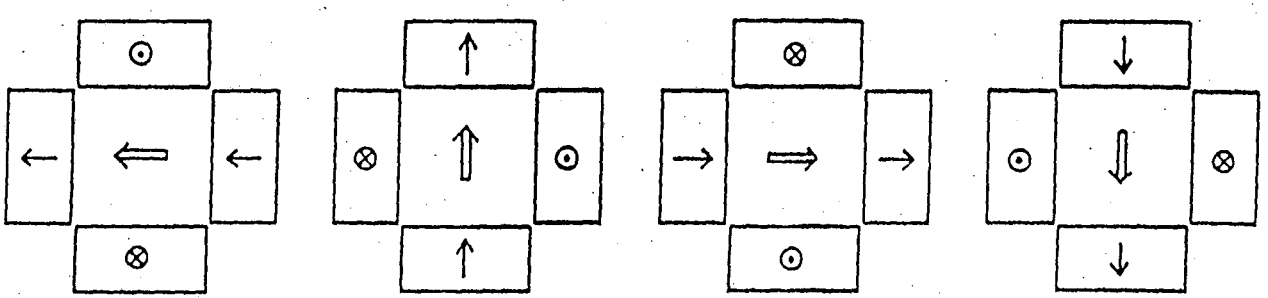

(a) (b) (c) (d)

(i)

Figure 5 (i)

ETL, Tsukuba, Japan.
$N=4$, $\lambda_u = 8$ cm,
gap (5.7 cm) $B_0 = 4.5$ kG
(5000–6000 Å)

P. Elleaume

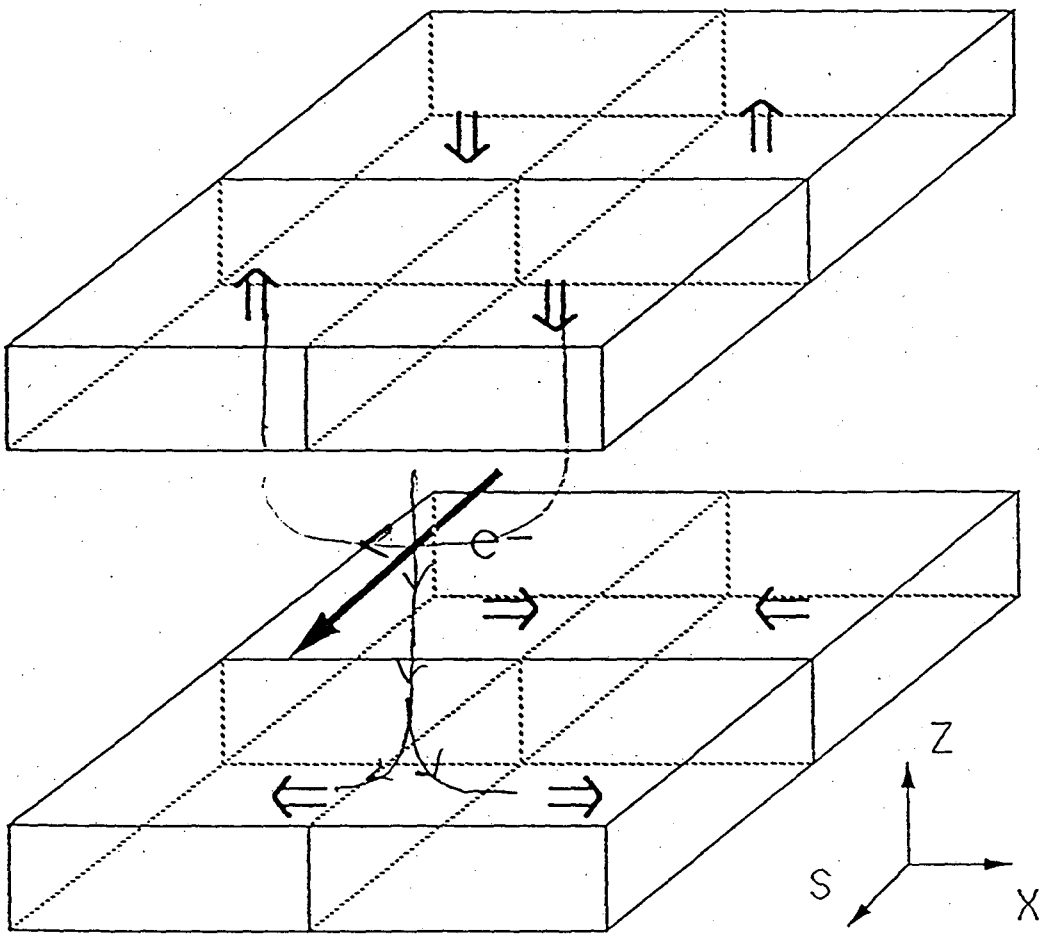

- Vacuum chamber requirement is easy
- effect on beam → may be dangerous for low energy machine
  - ⊙ Net deflection for linear polarization.
- helical field → no harmonics.

Sasaki Device

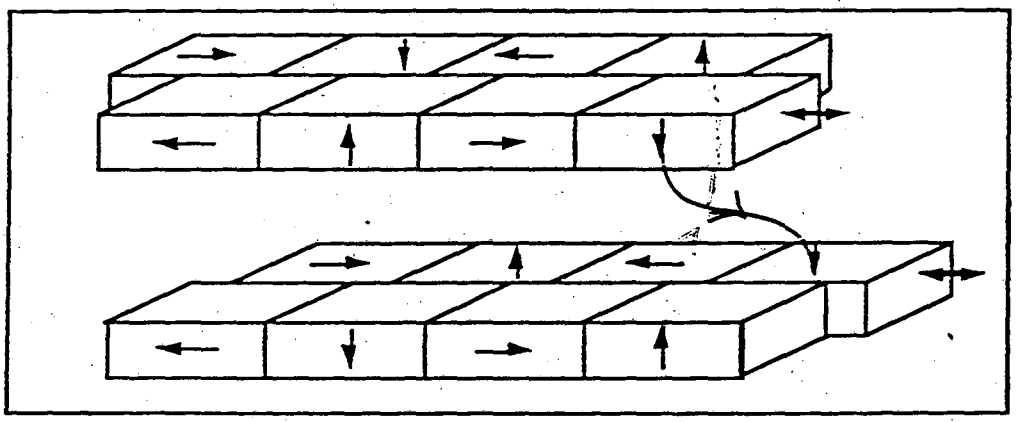

Undulators producing Helical Magnetic Field

- High degree of circular polarization

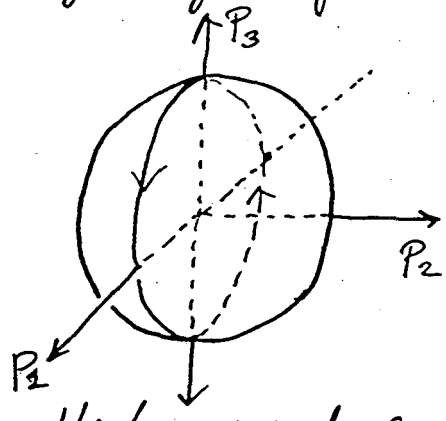

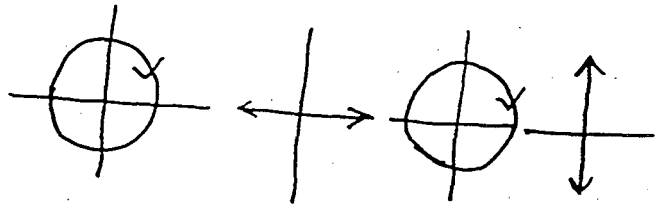

- High spectral brightness

- Deflection parameter K smaller than planar Undulator
- No higher harmonics

$\Rightarrow$ Limited spectral coverage

Variably Polarized Radiation can be Generated with Crossed Undulators in Low Emittance Storage Rings

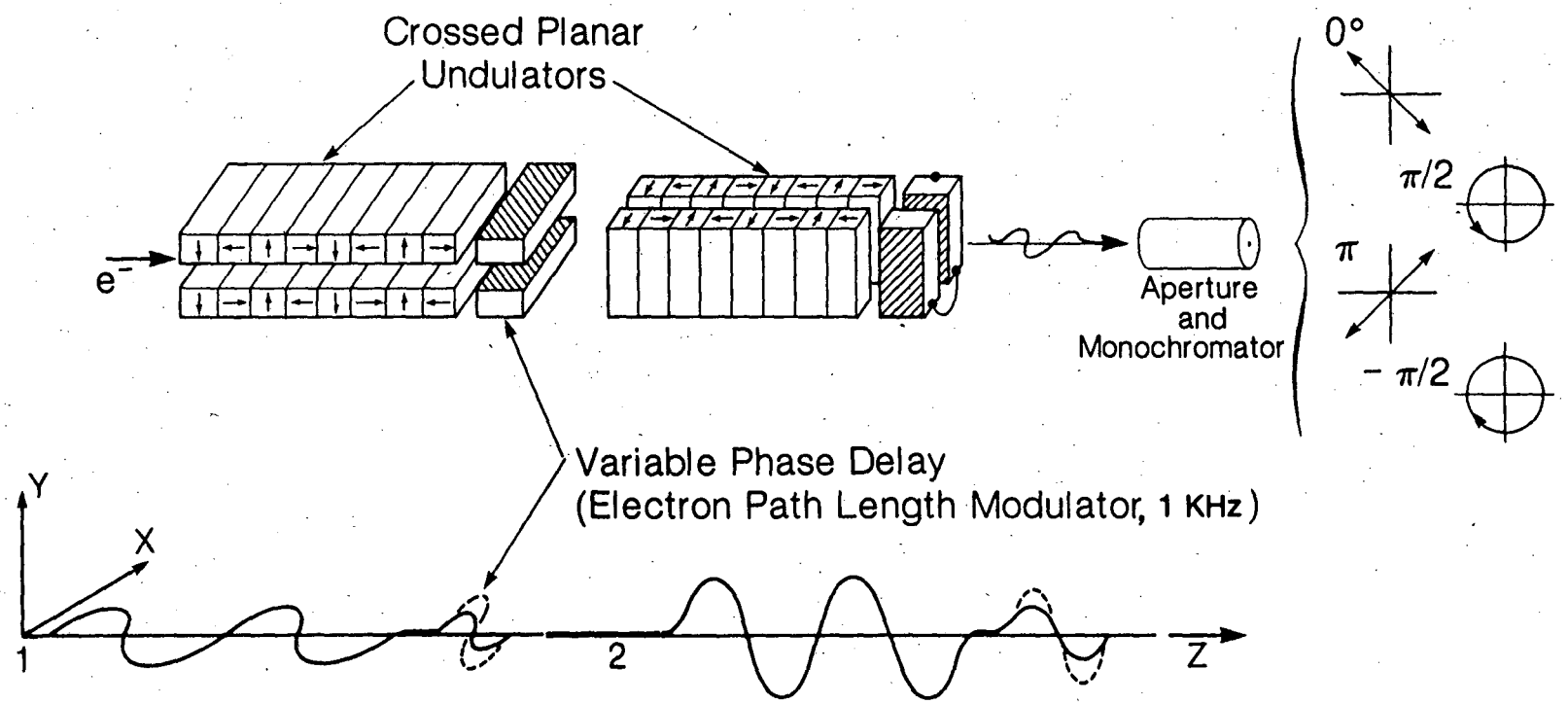

XBL 8311-4539-A

BESSY

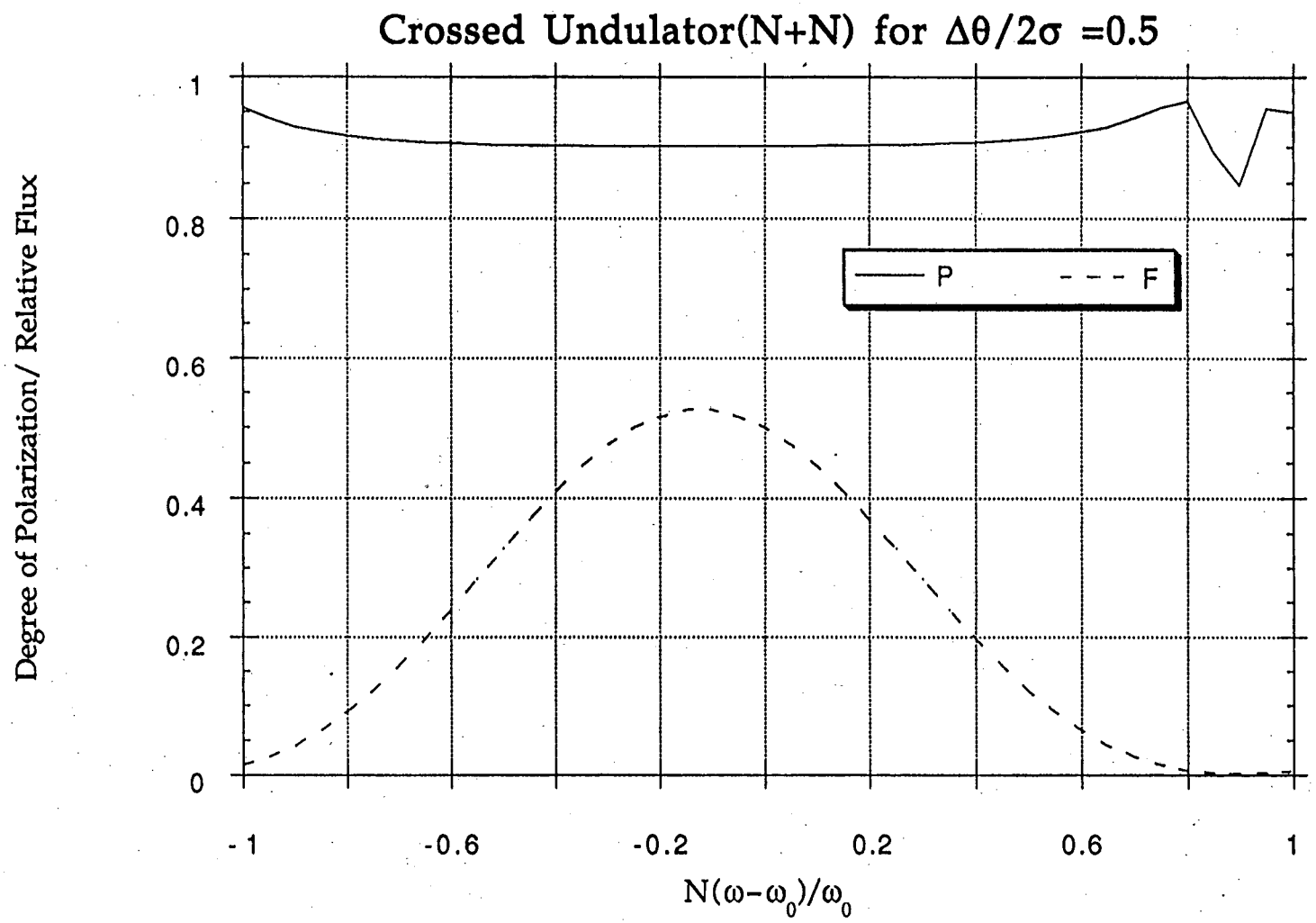
Crossed Undulator(N+N) for Δθ/2σ =0.5
Degree of Polarization/ Relative Flux
1
0.8
0.6
0.4
0.2
0
P
F
-1
-0.6
-0.2
0.2
0.6
1
N(ω−ω0)/ω0

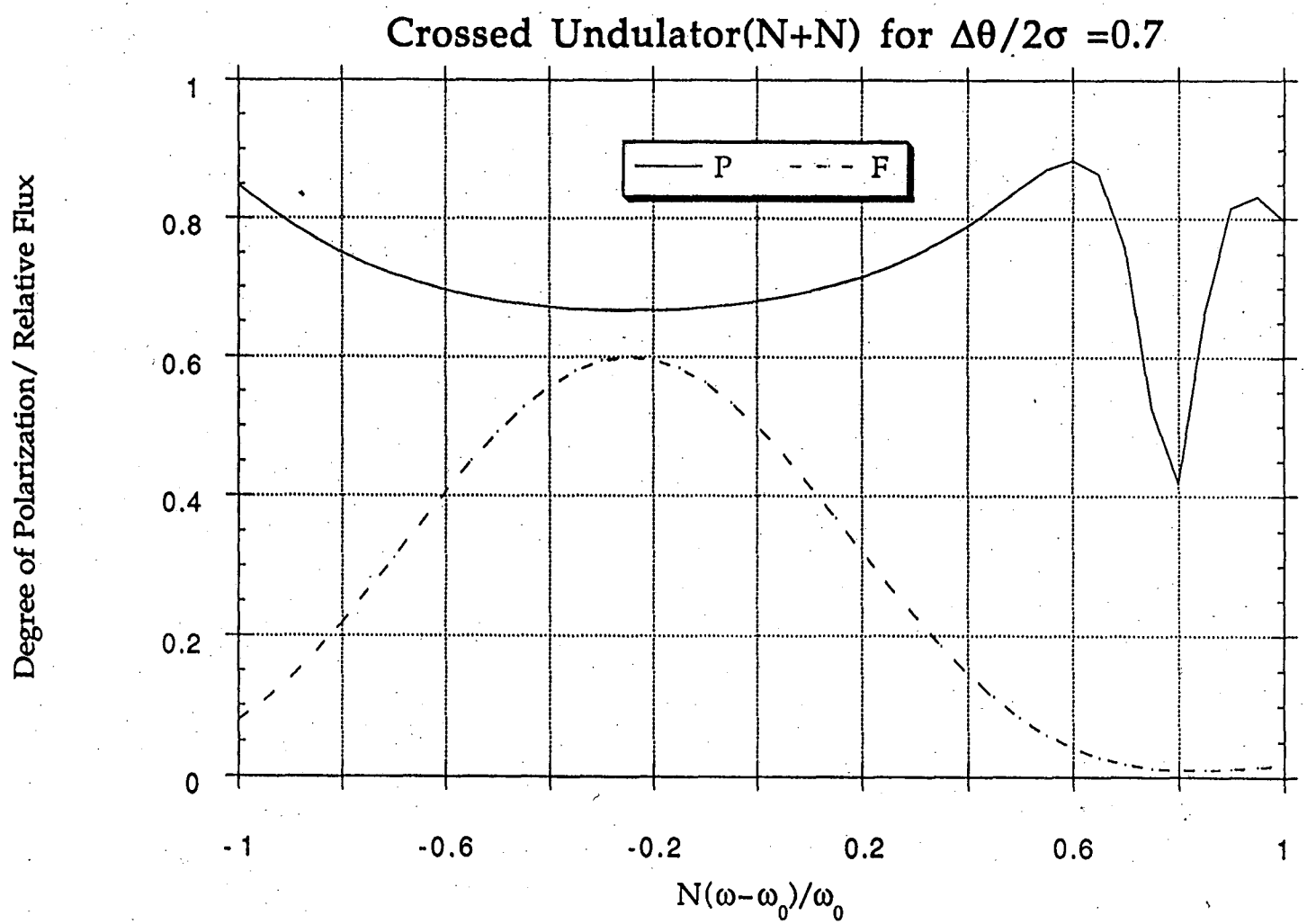
Crossed Undulator(N+N) for Δθ/2σ =0.7
P
F
Degree of Polarization/ Relative Flux
1
0.8
0.6
0.4
0.2
0
-1
-0.6
-0.2
0.2
0.6
1
N(ω−ω0)/ω0

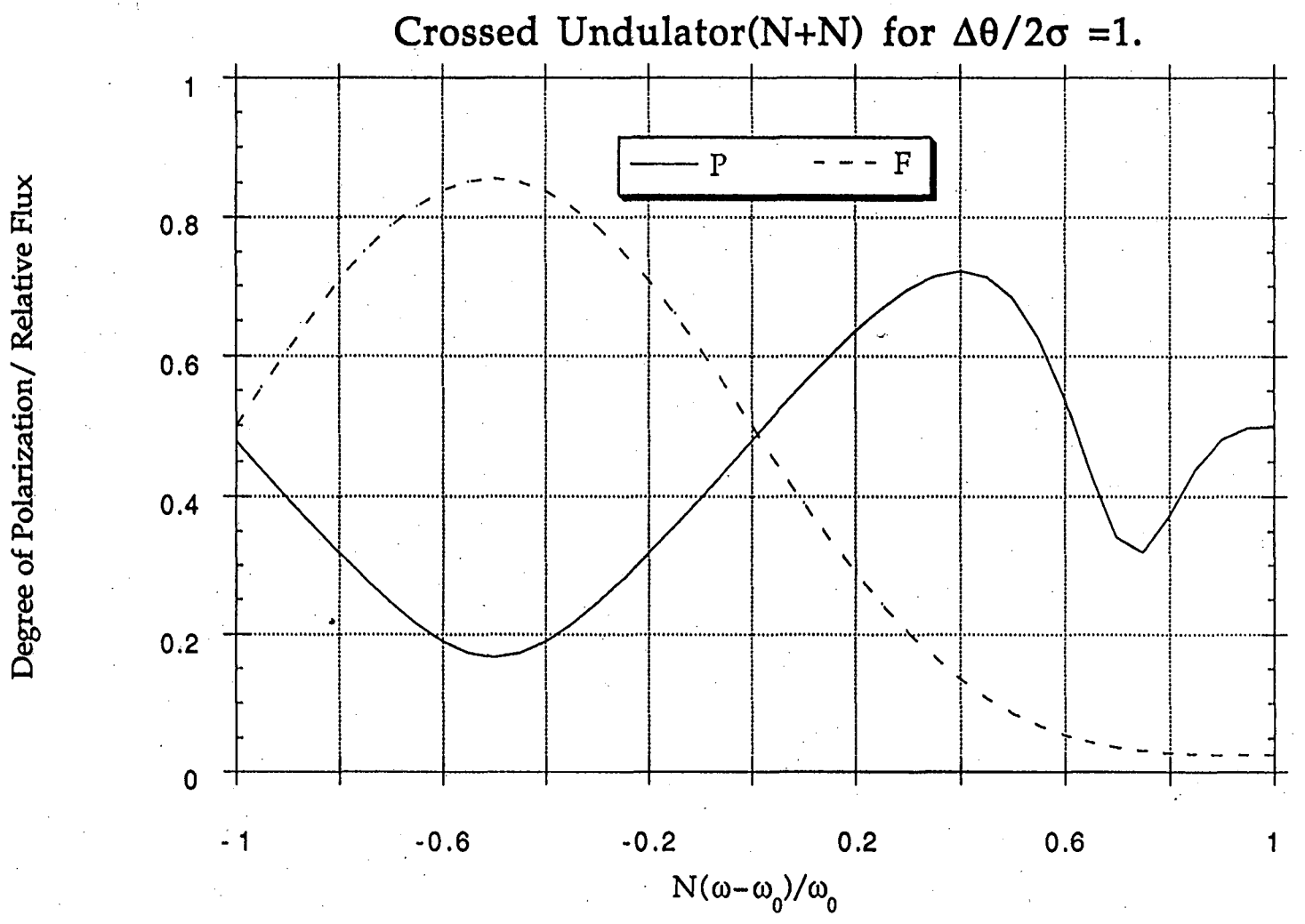
Crossed Undulator(N+N) for Δθ/2σ =1.
P
F
Degree of Polarization/ Relative Flux
1
0.8
0.6
0.4
0.2
0
-1
-0.6
-0.2
0.2
0.6
1
N(ω−ω0)/ω0

Crossed Undulator(N+N) Performance in the Short Wavelength Limit

(angular opening >> $(\lambda/L)^{1/2}$)

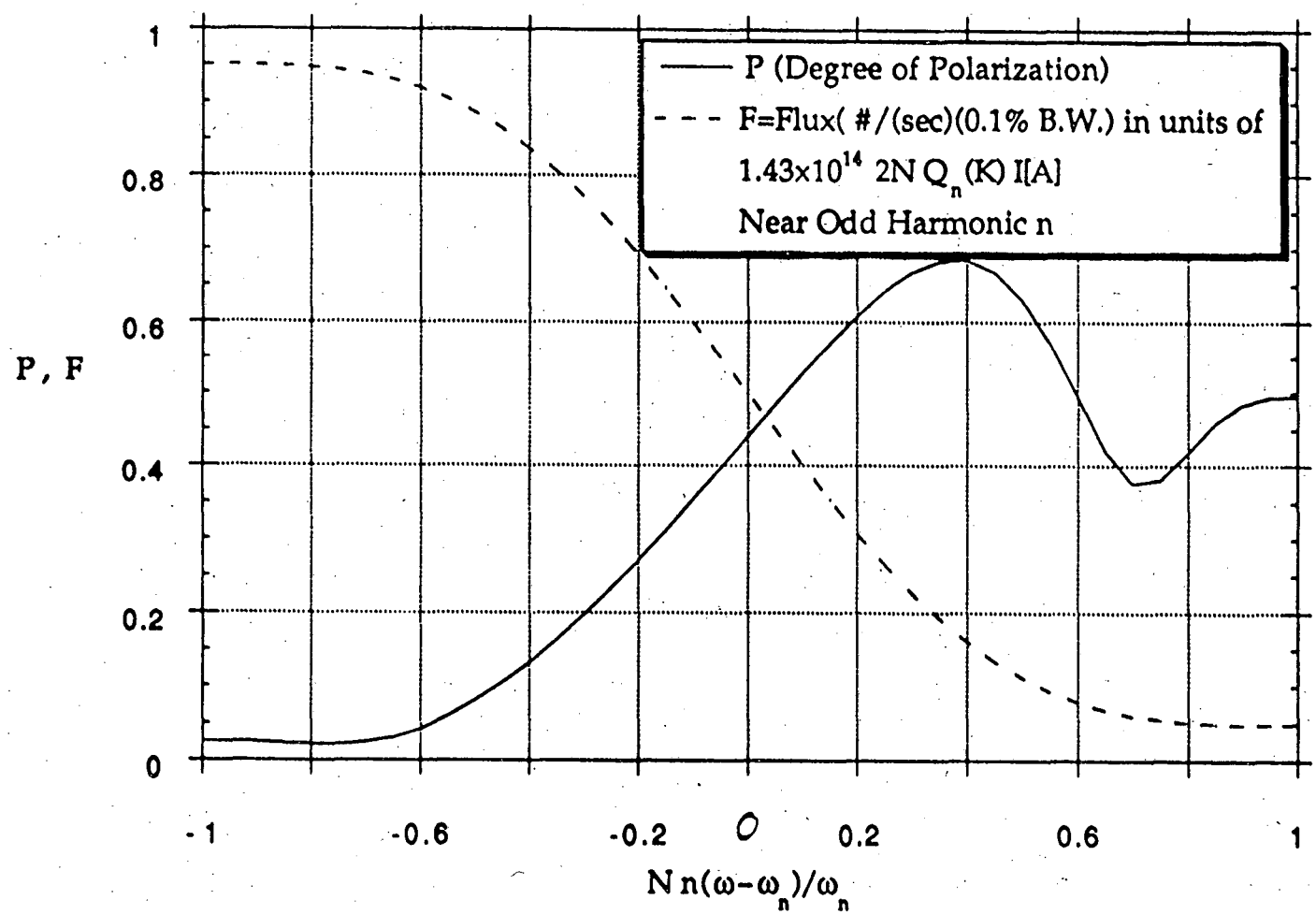

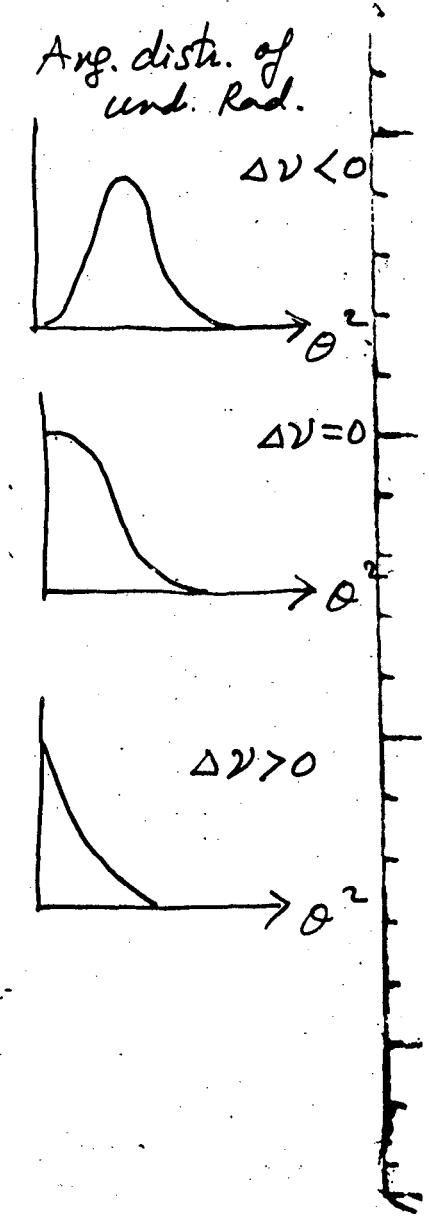

Fig. 2

Crossed Undulator

- Polarization Coverage similar to Helical U.

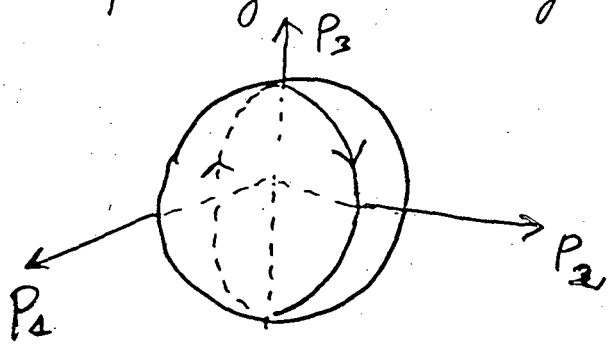

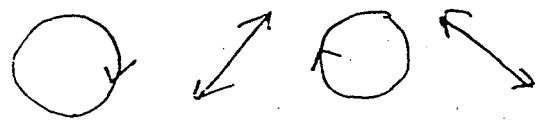

- Degree of Polarization depends on Angular Divergence.

  $P > 90\%$ at small ang. div.

  $P \Rightarrow 60\%$ at large ang. div. with some sacrifice of flux

  $\rightarrow$ optimize $\Delta\nu$.

- High Spectral flux

- Gap is larger (smaller K) than planar U.

- Can be operated at higher harmonics

  $\Rightarrow$ Wider spectral coverage than helical U.

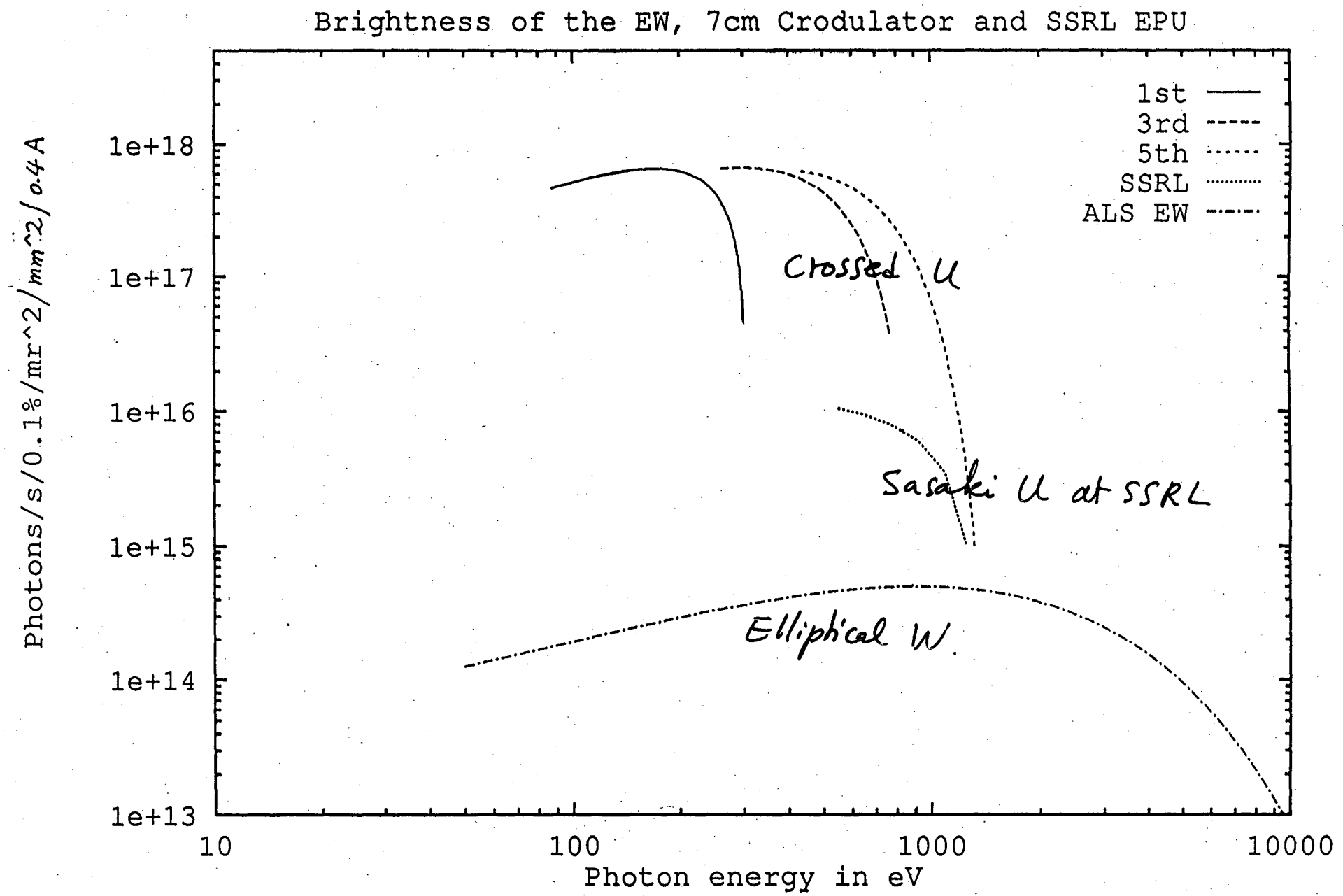
Brightness of the EW, 7cm Crodulator and SSRL EPU
1st
3rd
5th
SSRL
ALS EW
Crossed U
Sasaki U at SSRL
Elliptical W.
1e+18
1e+17
1e+16
1e+15
1e+14
1e+13
10
100
1000
10000
Photon energy in eV
Photons/s/0.1%/mr^2/mm^2/0.4A

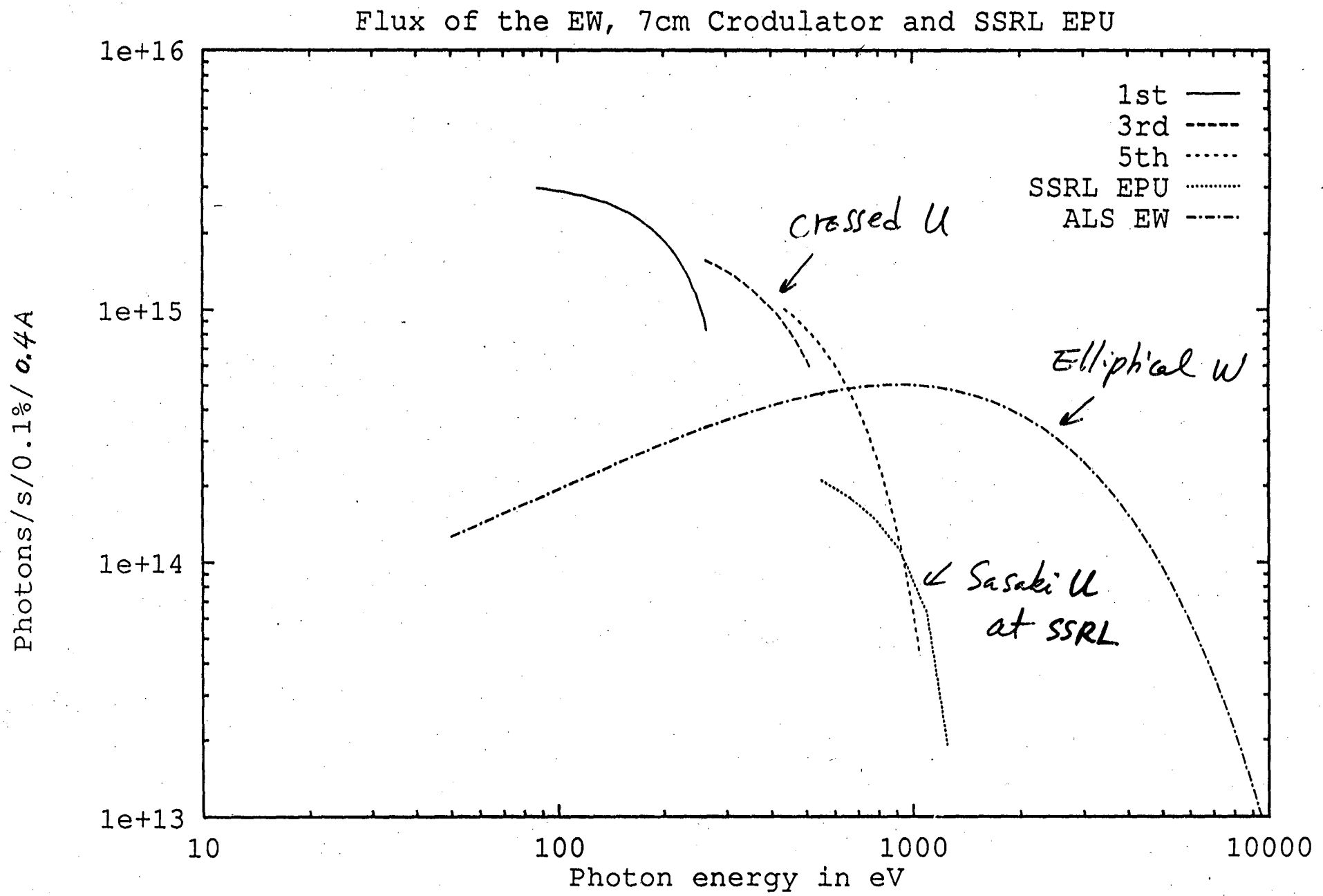
Flux of the EW, 7cm Crodulator and SSRL EPU
1st
3rd
5th
SSRL EPU
ALS EW
crossed U
Elliptical W
Sasaki U
at SSRL
1e+16
1e+15
1e+14
1e+13
10
100
1000
10000
Photon energy in eV
Photons/s/0.1%/0.4A

Performance of Elliptical Wiggler and Crossed Undulator

Chun Xi Wang

Lawrence Berkeley Laboratory

In order to satisfy the desire for elliptically polarized light sources, an electromagnet elliptical wiggler has been designing at ALS and a crossed undulator has been proposed as well. This talk will describe the performance of these two devices.

1. Elliptical wiggler (EW)

Goal: To provide elliptically polarized photons over a rather wide energy range from 50eV to 10keV with high flux and degree of polarization. Its best performance is over several hundreds eV to a few keV.

a) Panoramic view of the radiation properties

b) Optimization of EW performance

c) Horizontal angular distribution and beam line setup

2. Crossed undulator

Goal: To provide elliptically polarized VUV and extra-soft X-ray photons (say, a few tens eV to several hundred eV) with reasonable degree of polarization, flux comparable to the EW but brightness 3-4 order of magnitudes higher than the EW.

a) Basic principle and general properties.

b) Degree of polarization and depolarization due to electron beam emittance.

c) Comparison with the EW.

3. Summary of what we can obtain

?. User's suggestion.

plane radiation from a bend source. This is because each half period of the sinusoidal orbit due to the vertical field can be regarded as the arc in a bending magnet, and is tilted up or down alternately by the horizontal field by the angle K_x/γ, where γ is the relativistic energy of the electron. The angular flux density, $\mathcal{D}$, which is defined here as the photon flux per unit solid angle and stored current in the ring, and the degree of circular polarization, P_c, can be obtained with this bend-source approximation[6] for the wiggler radiation.

Immediately after the commissioning of EMPW (e.g., optimization of the electron orbit in the ring), the radiation in the hard-x-ray region with $K_y=15$ was characterized at the beam line BL NE1 (Ref. 7) in the 6-GeV operation of AR. Figure 2 shows the first direct observation of photons produced by EMPW. It is an image projected on a fluorescence screen right after a Cu attenuator with a thickness of 7 mm placed at 35 m from EMPW. Since the highest-energy portion of the photons is radiated along the tangential direction from the orbit, the bright line on the fluorescence screen is a locus of intersections of the orbital tangent and the screen. Therefore, the radiation obtained on the bright line has linear polarization, and the circular polarization of the radiation inside the bright elliptic line has an opposite sense to that outside the line. The elliptic patterns on the screen [Figs. 2(b) and 2(c)] prove that the electron orbit forms a deformed helix when the horizontal magnetic field is applied. The reason why the pattern is not a complete ellipse but separated into upper and lower parts is that the energy radiated towards the missing parts of the ellipse is not high enough to penetrate the Cu attenuator, since the vertical magnetic field at the corresponding point on the electron orbit is not so strong. Fattening of the elliptic pattern with increasing K_x shows the variation of the electron orbit from a plane sinusoidal type (i.e., an orbit in the usual plane multipole wiggler/undulator with vertical field only) to a deformed-helix type. In the present study the case with $K_x=K_y\leq 3$ is not shown, since an appropriate attenuator for the radiation for this case was not available.

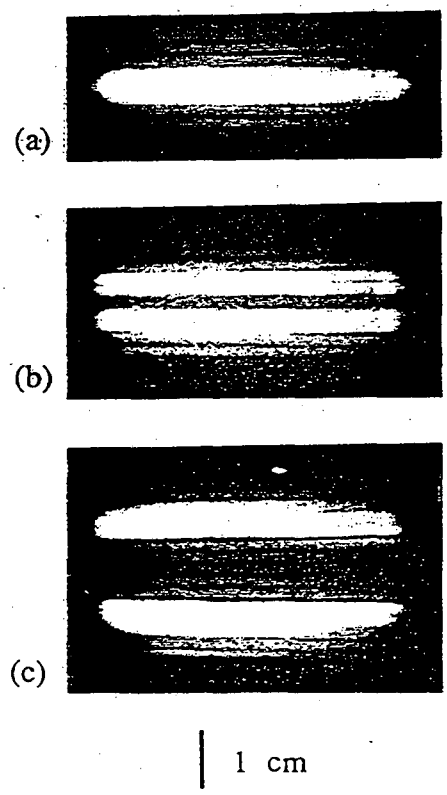

FIG. 2. Images on the fluorescence screen with $K_y=15$: (a) $K_x=0$, (b) $K_x=1.3$, and (c) $K_x=3.0$, with the stored current of 0.5 mA. Fattening of the bright pattern on the screen from a single segment (a) to ellipses (b) and (c) corresponds to variation of an electron orbit from a plane sinusoidal type to a deformed-helix type with the increasing horizontal field B_{x0}. The elliptically polarized radiation is obtained on the axis, where it is interrupted by a Cu attenuator.

The quantitative evaluation of P_c and $\mathcal{D}$ was made by Compton-scattering measurements with a magnetized polycrystalline Fe specimen. The measuring system for the evaluation is substantially the same as that used by Sakai, Terashima, and Sekizawa.[10] The radiation monochromatized by Ge 400 Bragg diffraction, was directed to the specimen inserted in an electromagnet which controls the spin vector, S, of the Fe specimen. The Compton-scattered x rays were detected by a Ge solid-state detector. P_c can be derived from the equation given by Lipps and Tolhoek,[11]

$$P_c=\frac{I^+-I^-}{I^++I^-}\left(\frac{n^\uparrow-n^\downarrow}{n^\uparrow+n^\downarrow}\right)^{-1}\frac{\Phi_0(E_0,\theta)}{\Phi_{\rm spin}(E_0,\theta,\mathbf{S},\mathbf{K}_0,\mathbf{K})}, \quad (3)$$

where I^+ and I^- denote the intensities of scattered x rays from the specimen magnetized up (S) and down (−S), respectively. $n^\uparrow$ and $n^\downarrow$ are the averaged electron numbers of the spin-up state and spin-down state, respectively. $\Phi_{\rm spin}$ and Φ_0 are the spin-dependent and ordinary Compton-scattering cross sections, respectively. E_0 is the incident x-ray energy and θ is the scattering angle between $\mathbf{K}_0$, the wave vector of the incident x ray, and $\mathbf{K}$, that of the scattered one. P_c is evaluated by the measured I^+ and I^- with the value of $(n^\uparrow-n^\downarrow)/(n^\uparrow+n^\downarrow)=0.080$ (Ref. 12) since Φ_0 and $\Phi_{\rm spin}$ are well known, whereas $\mathcal{D}$ is evaluated by $(I^+-I^-)/2$. The sense of either right- or left-handed circular polarization should be able to be predicted based on the electron trajectory deduced from the magnetic field of Eq. (1). The prediction was confirmed using Eq. (3) while changing the phase difference.

Figure 3 shows the dependences of P_c and $\mathcal{D}$ of the wiggler radiation on the vertical observation angle Ψ in the cases of (a) $K_x=1$ and (b) $K_x=1.5$ with K_y fixed at 15. The radiation for these cases (critical energy = 24 keV) is characterized at 60 keV, since the magnetic

Mechanism to generate elliptically polarized photons in wigglers

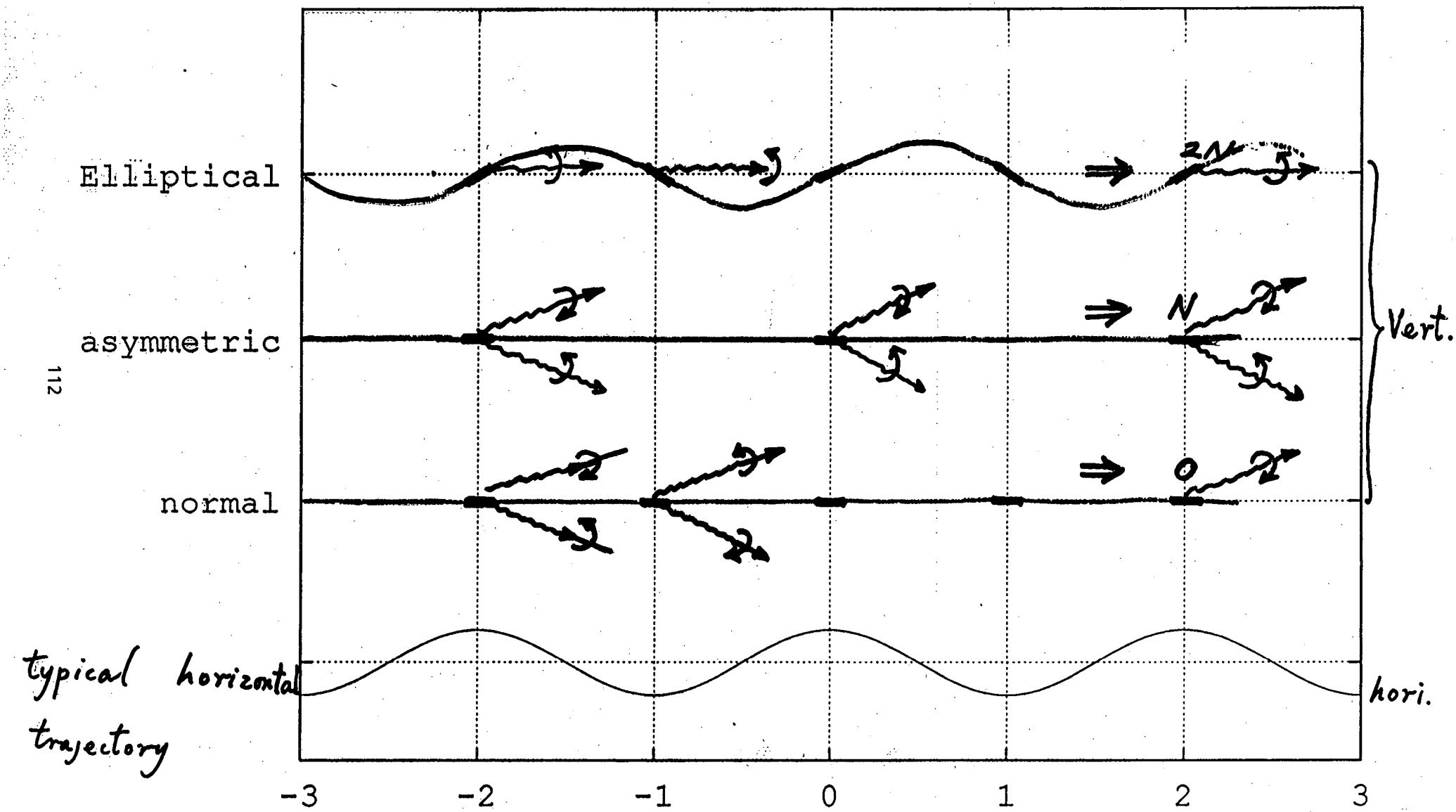

• Energy and vertical angle dependence of Flux and Polarization degree

• 2 radiation shoulders
– located at $\pm K_x/\gamma$;
– on which $P_c \simeq 0$

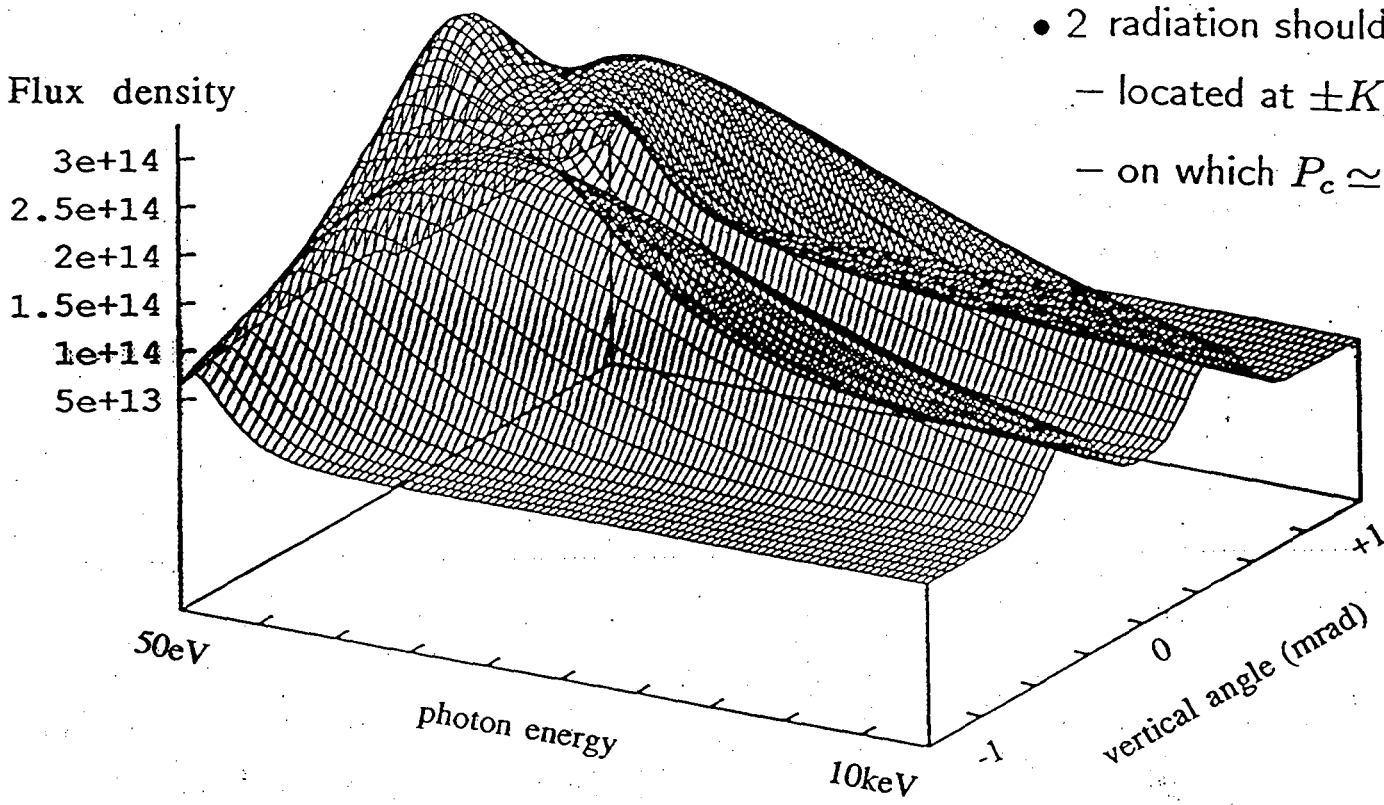

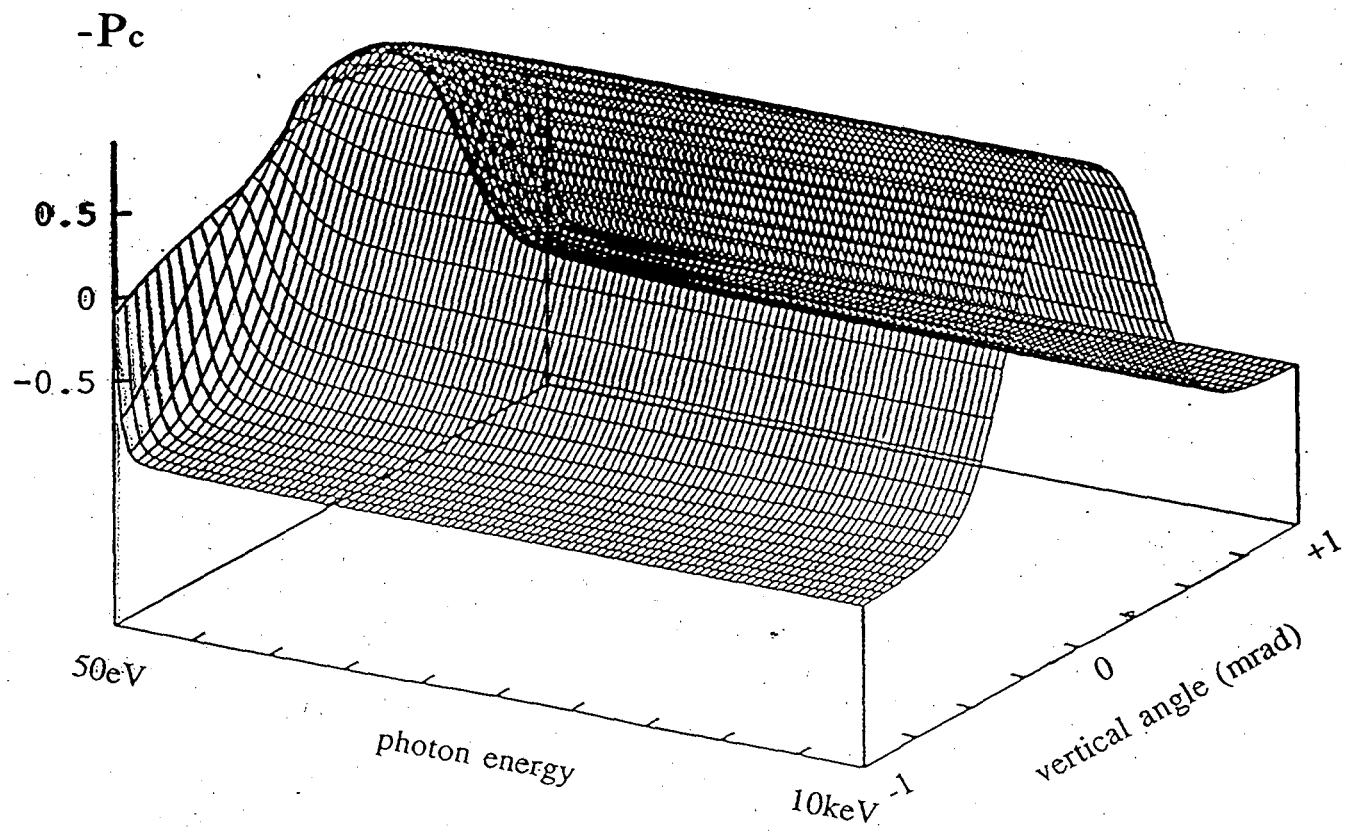

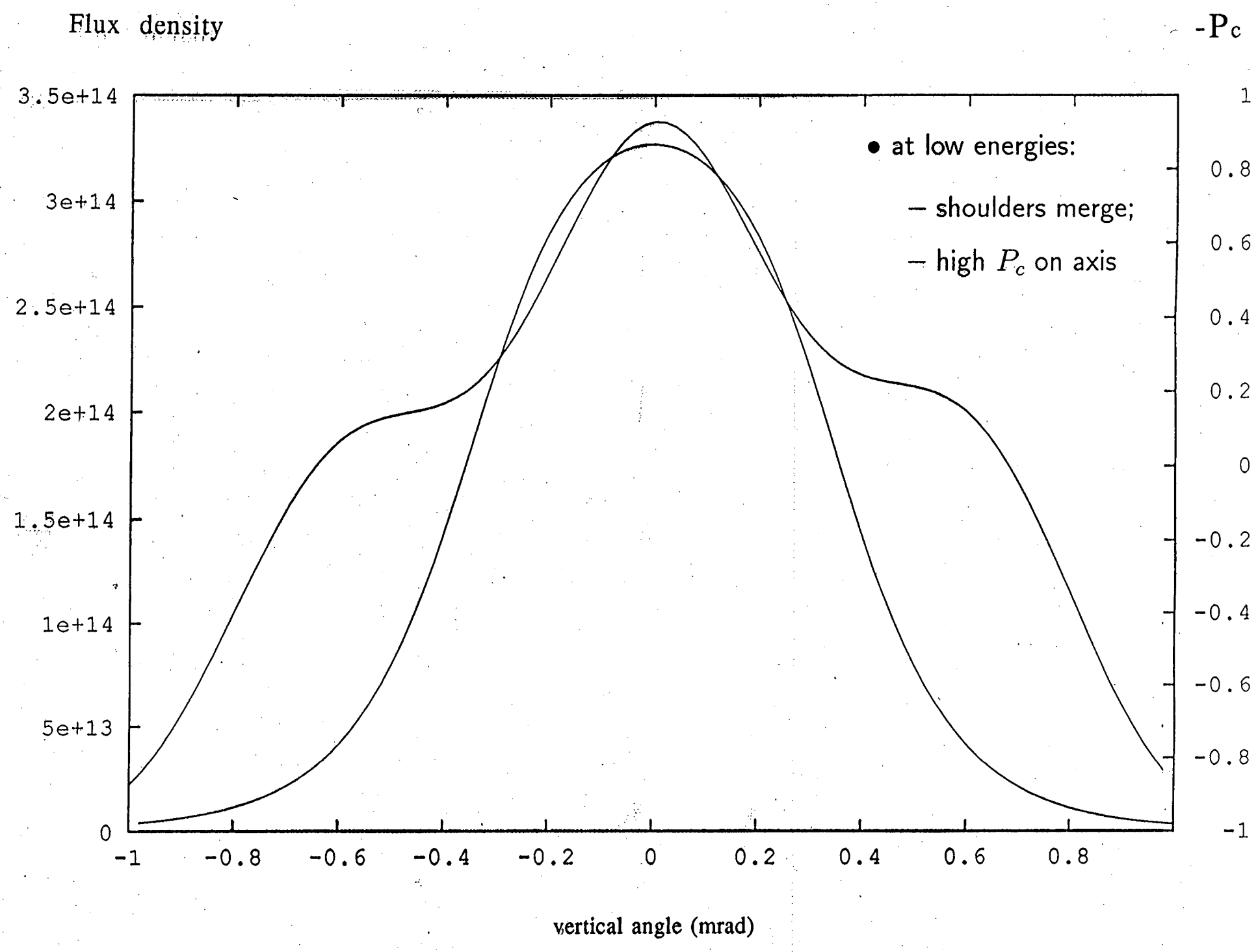
Flux density
-Pc
3.5e+14
3e+14
2.5e+14
2e+14
1.5e+14
1e+14
5e+13
0
1
0.8
0.6
0.4
0.2
0
-0.2
-0.4
-0.6
-0.8
-1
-1
-0.8
-0.6
-0.4
-0.2
0
0.2
0.4
0.6
0.8
• at low energies:
– shoulders merge;
– high P_c on axis
vertical angle (mrad)

- Flux & Polarization horizontal distribution
  - flat over horizontal angle
  - the fan width $\propto B_y$

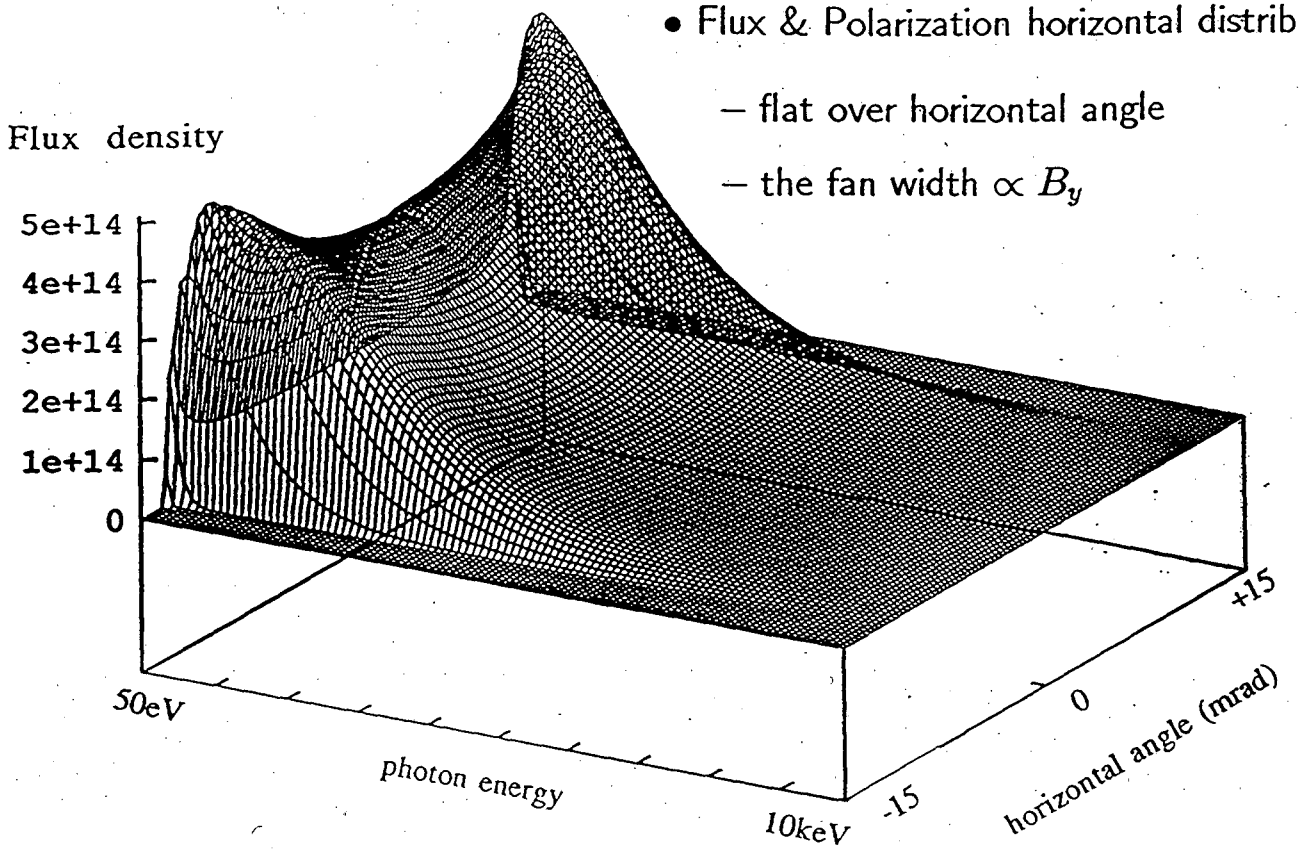

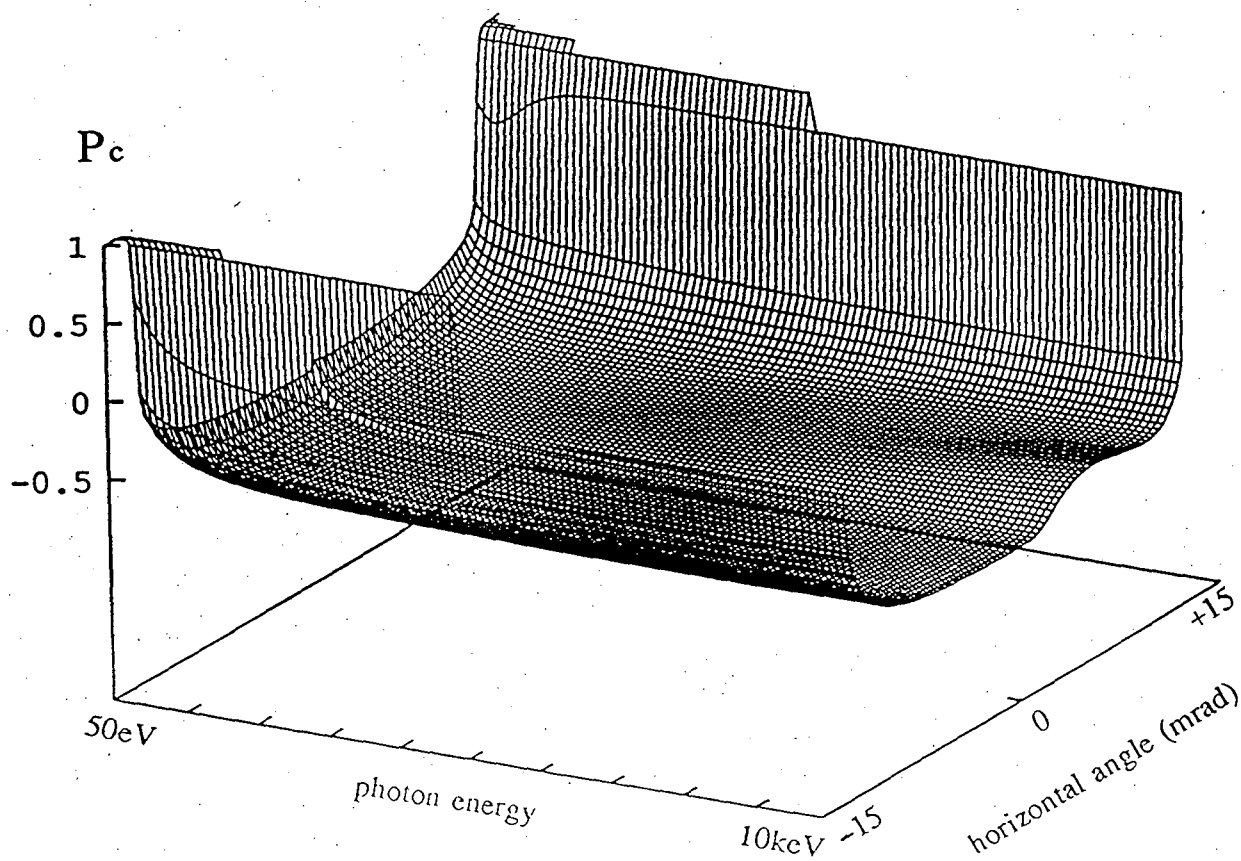

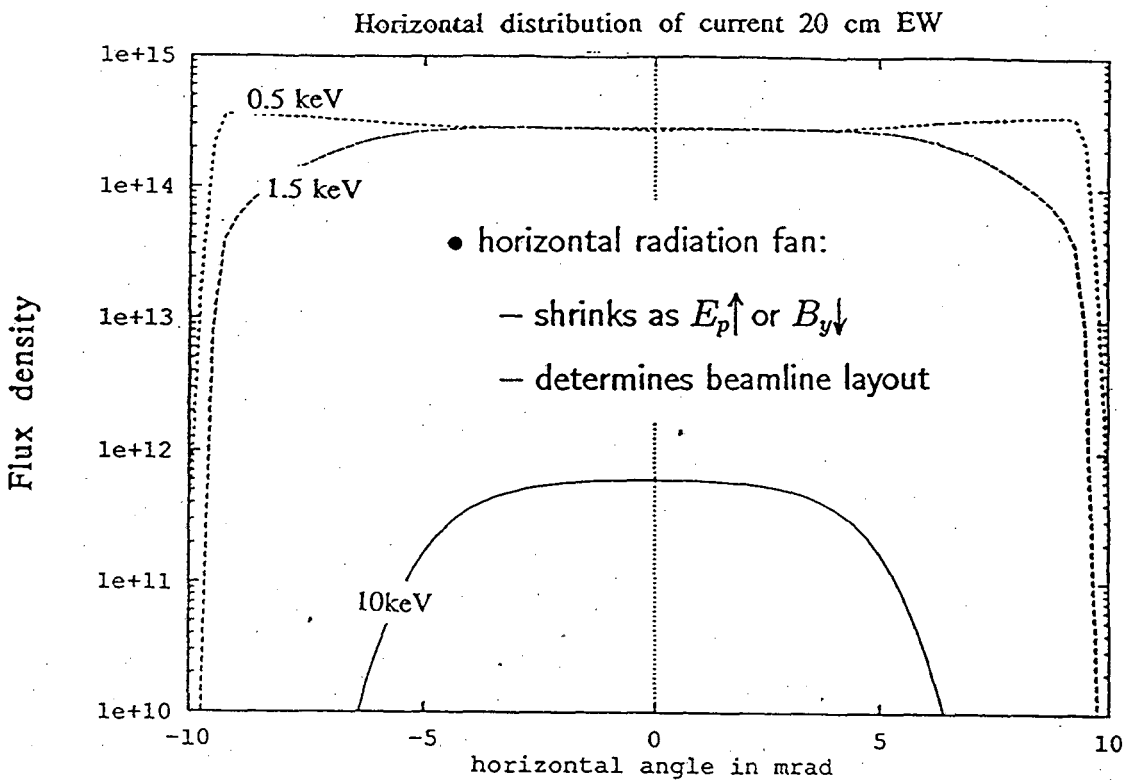
Horizontal distribution of current 20 cm EW
Flux density
1e+15
1e+14
1e+13
1e+12
1e+11
1e+10
0.5 keV
1.5 keV
10keV
• horizontal radiation fan:
– shrinks as $E_p\uparrow$ or $B_y\downarrow$
– determines beamline layout
-10
-5
0
5
10
horizontal angle in mrad

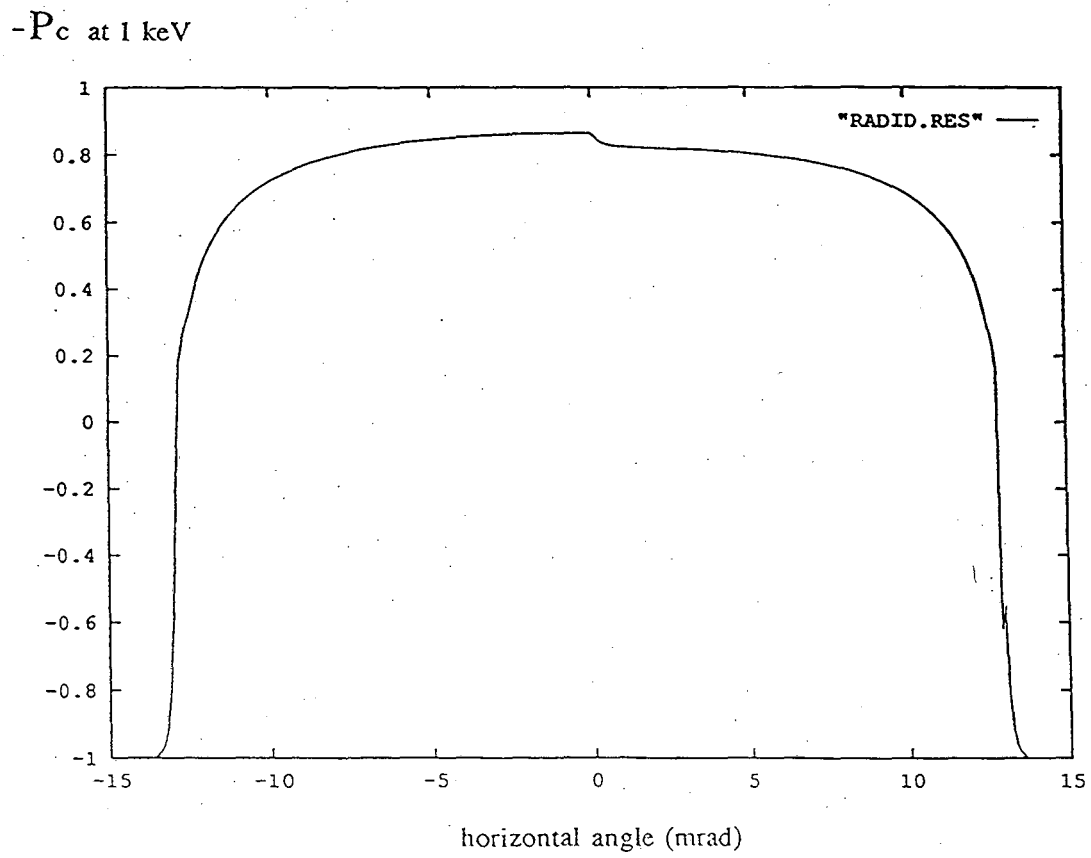
-Pc at 1 keV
"RADID.RES"
1
0.8
0.6
0.4
0.2
0
-0.2
-0.4
-0.6
-0.8
-1
-15
-10
-5
0
5
10
15
horizontal angle (mrad)

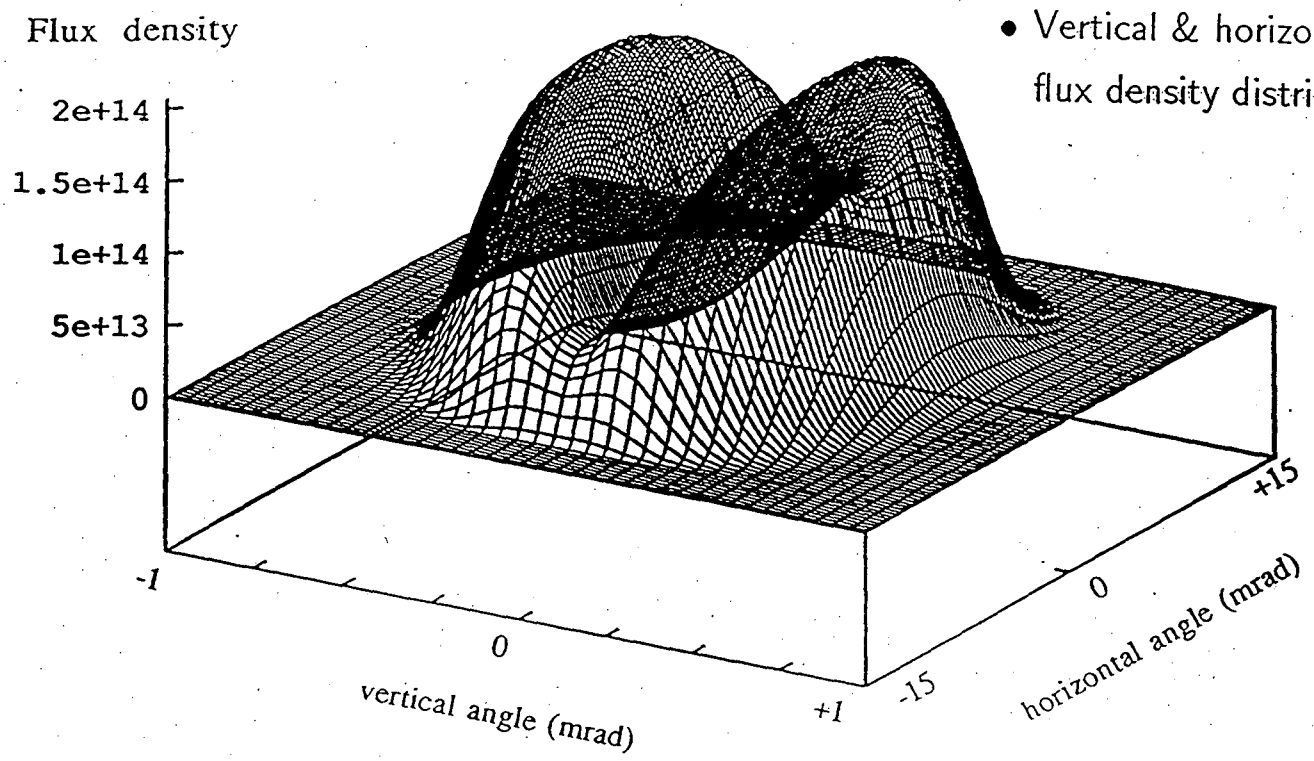

• Vertical & horizontal flux density distribution

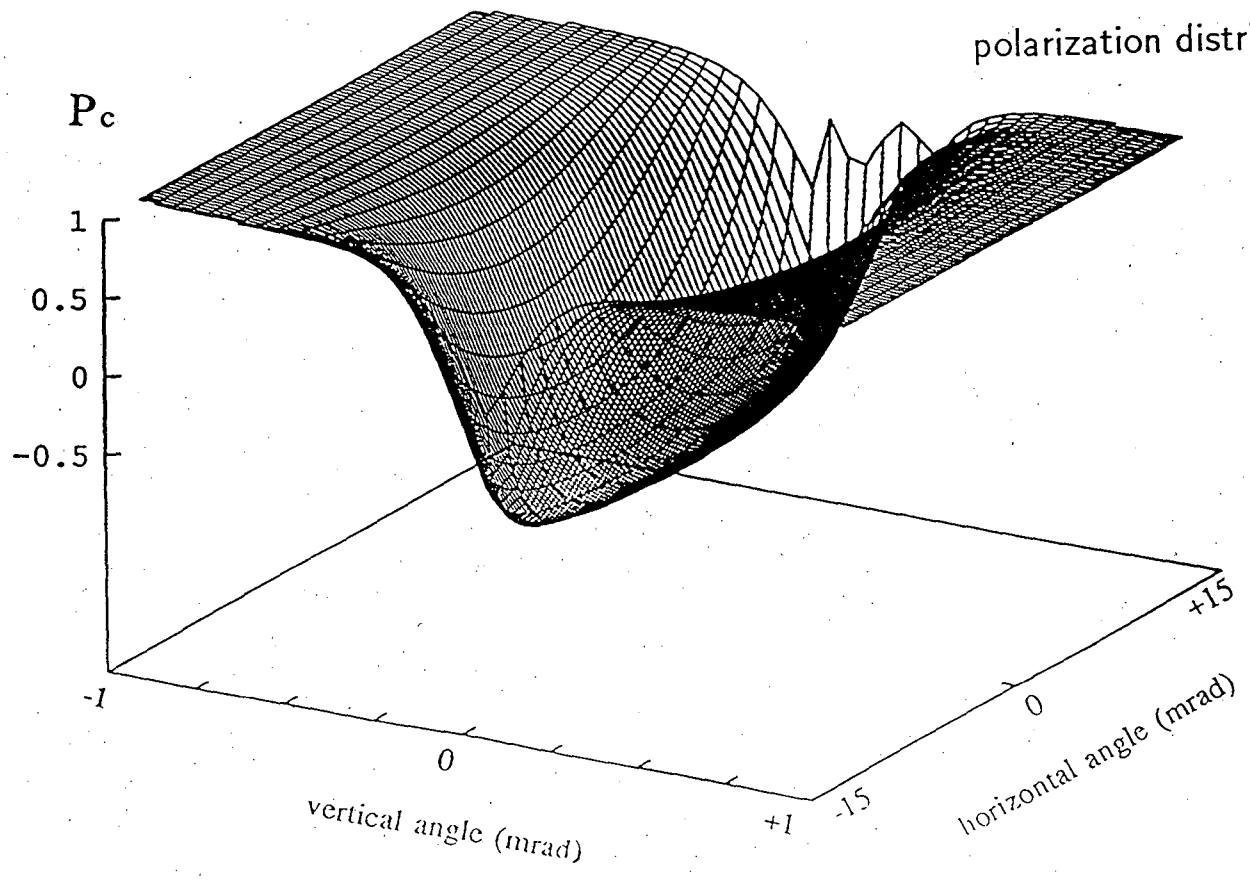

• Vertical & horizontal polarization distribution

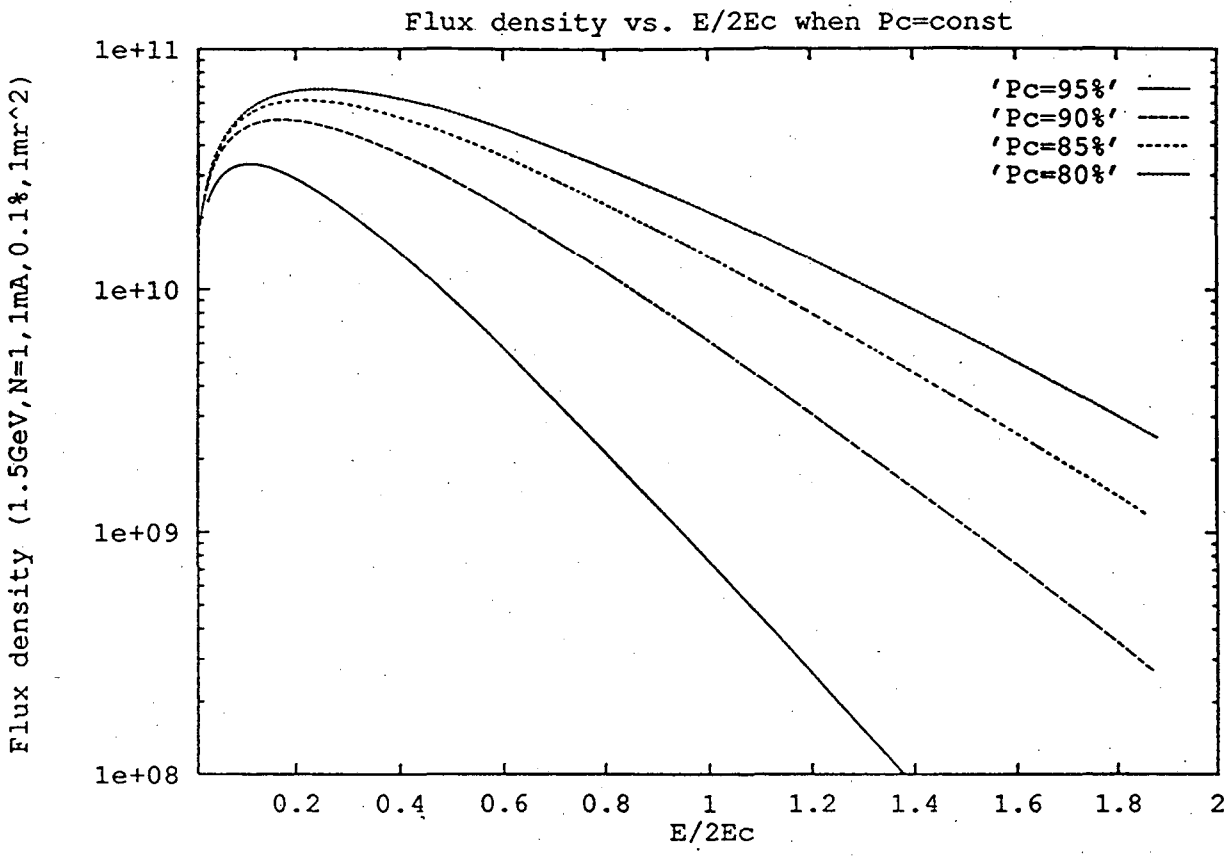
Flux density vs. E/2Ec when Pc=const
'Pc=95%'
'Pc=90%'
'Pc=85%'
'Pc=80%'
Flux density (1.5GeV,N=1,1mA,0.1%,1mr^2)
1e+11
1e+10
1e+09
1e+08
0.2
0.4
0.6
0.8
1
1.2
1.4
1.6
1.8
2
E/2Ec

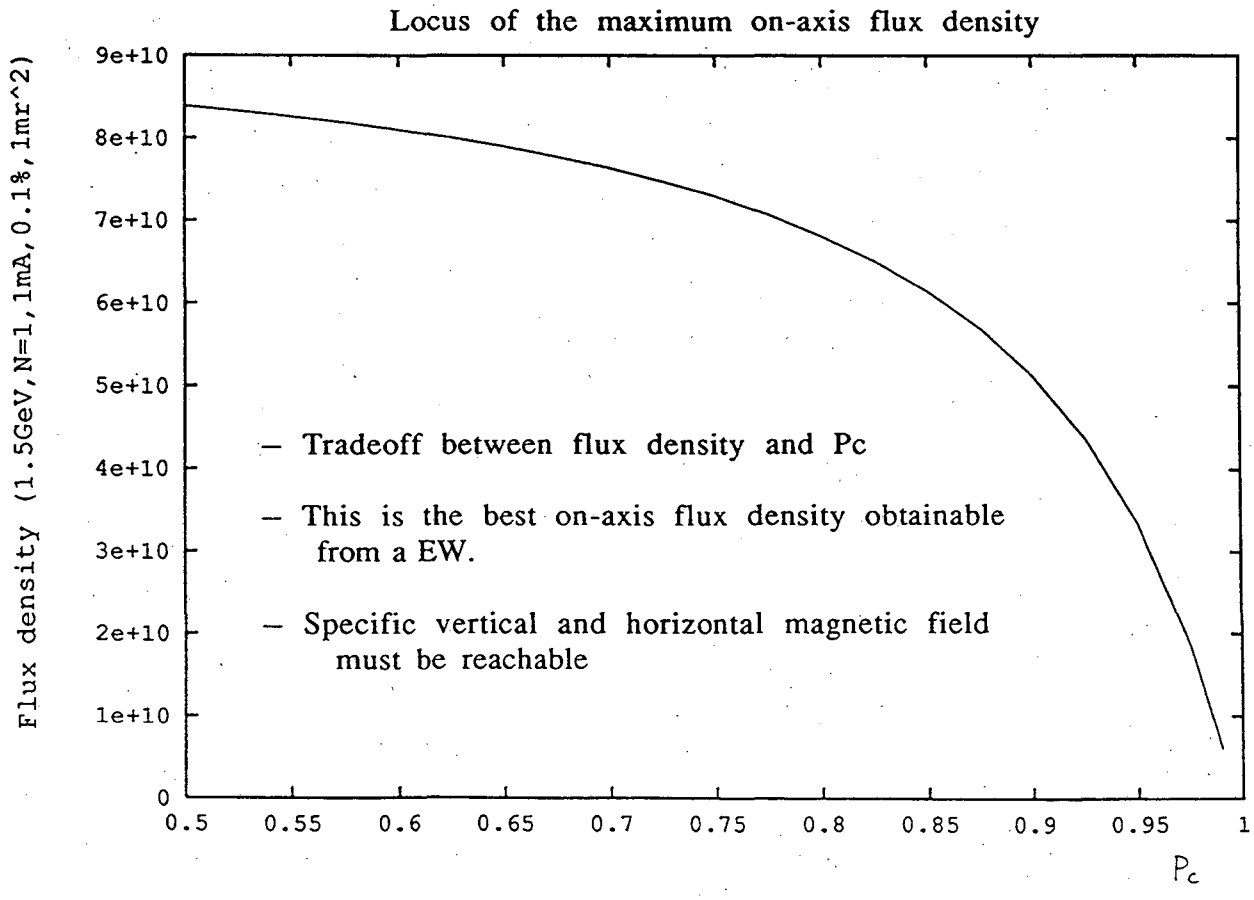
Locus of the maximum on-axis flux density
Flux density (1.5GeV,N=1,1mA,0.1%,1mr^2)
9e+10
8e+10
7e+10
6e+10
5e+10
4e+10
3e+10
2e+10
1e+10
0
0.5
0.55
0.6
0.65
0.7
0.75
0.8
0.85
0.9
0.95
1
Pc
– Tradeoff between flux density and Pc
– This is the best on-axis flux density obtainable from a EW.
– Specific vertical and horizontal magnetic field must be reachable

$E_e = 1.5$ GeV

#Universal optimization table for ellipitical wiggler

# Pc	Kx	0.5*E/Ec	Total Flux density (one period,1mA,mrad^2,0.1%)
0.500	0.353	0.366	8.39E10
0.525	0.376	0.360	8.33E10
0.550	0.401	0.352	8.26E10
0.575	0.426	0.346	8.19E10
0.600	0.453	0.339	8.10E10
0.625	0.482	0.330	8.01E10
0.650	0.512	0.322	7.90E10
0.675	0.545	0.312	7.78E10
0.700	0.581	0.302	7.64E10
0.725	0.621	0.290	7.48E10
0.750	0.664	0.279	7.30E10
0.775	0.713	0.266	7.08E10
0.800	0.769	0.250	6.82E10
0.825	0.833	0.234	6.52E10
0.850	0.912	0.213	6.15E10
0.875	1.006	0.194	5.70E10
0.900	1.128	0.172	5.13E10
0.925	1.302	0.143	4.38E10
0.950	1.580	0.109	3.35E10
0.975	2.171	0.066	1.85E10
0.990	3.290	0.032	6.01E9

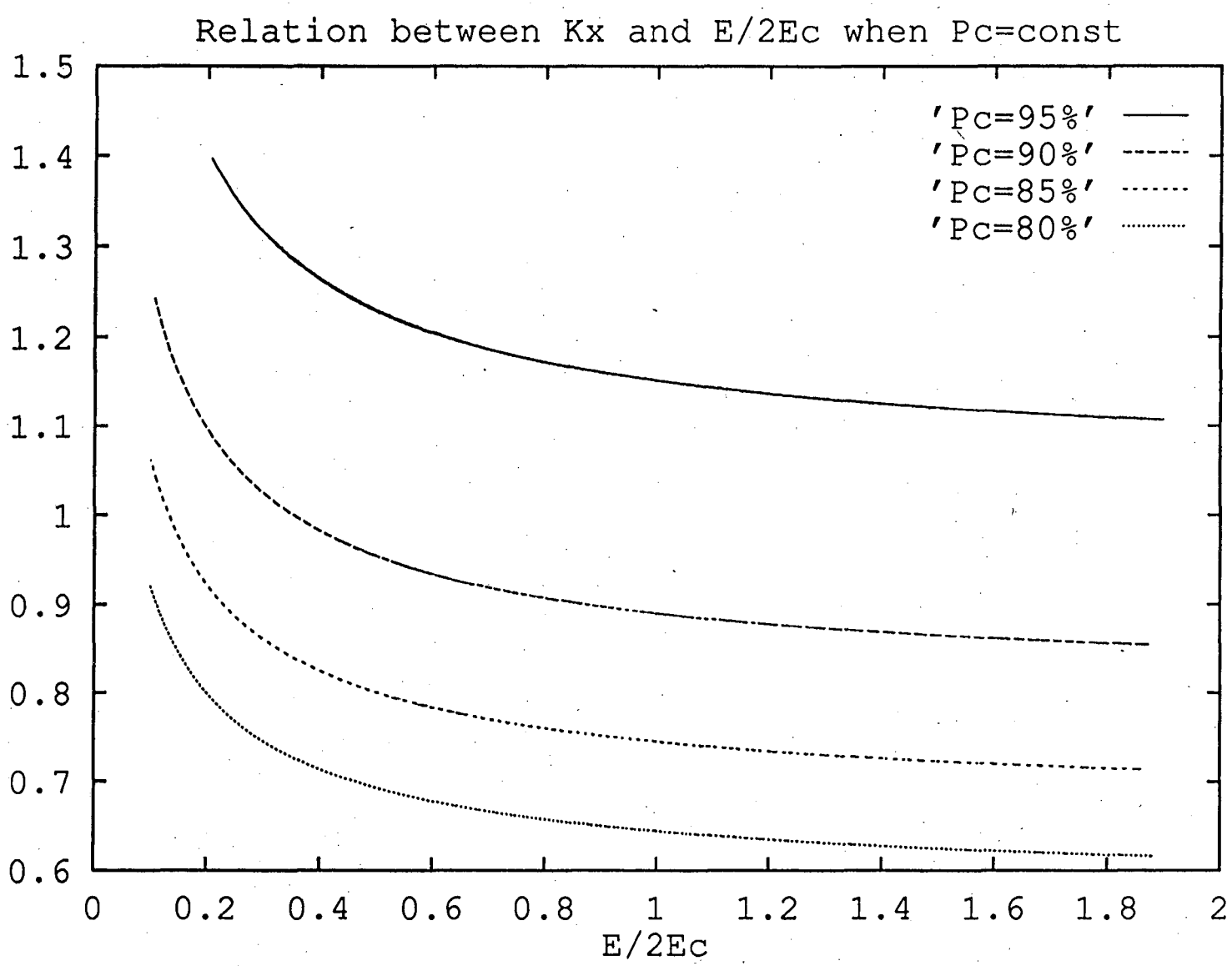
Relation between Kx and E/2Ec when Pc=const
'Pc=95%'
'Pc=90%'
'Pc=85%'
'Pc=80%'
Kx
1.5
1.4
1.3
1.2
1.1
1
0.9
0.8
0.7
0.6
0
0.2
0.4
0.6
0.8
1
1.2
1.4
1.6
1.8
2
E/2Ec

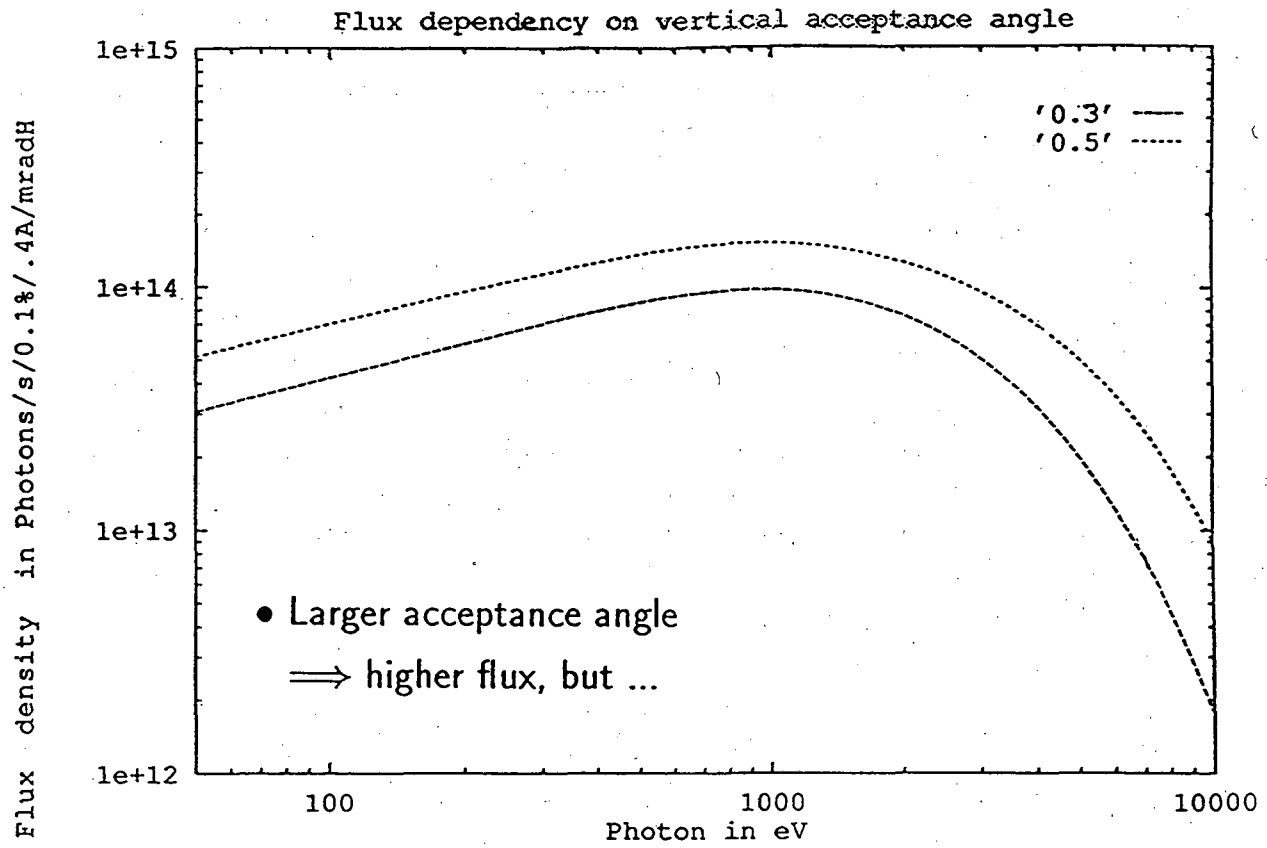
Flux dependency on vertical acceptance angle
1e+15
1e+14
1e+13
1e+12
Flux density in Photons/s/0.1%/.4A/mradH
'0.3'
'0.5'
• Larger acceptance angle
⟹ higher flux, but ...
100
1000
10000
Photon in eV

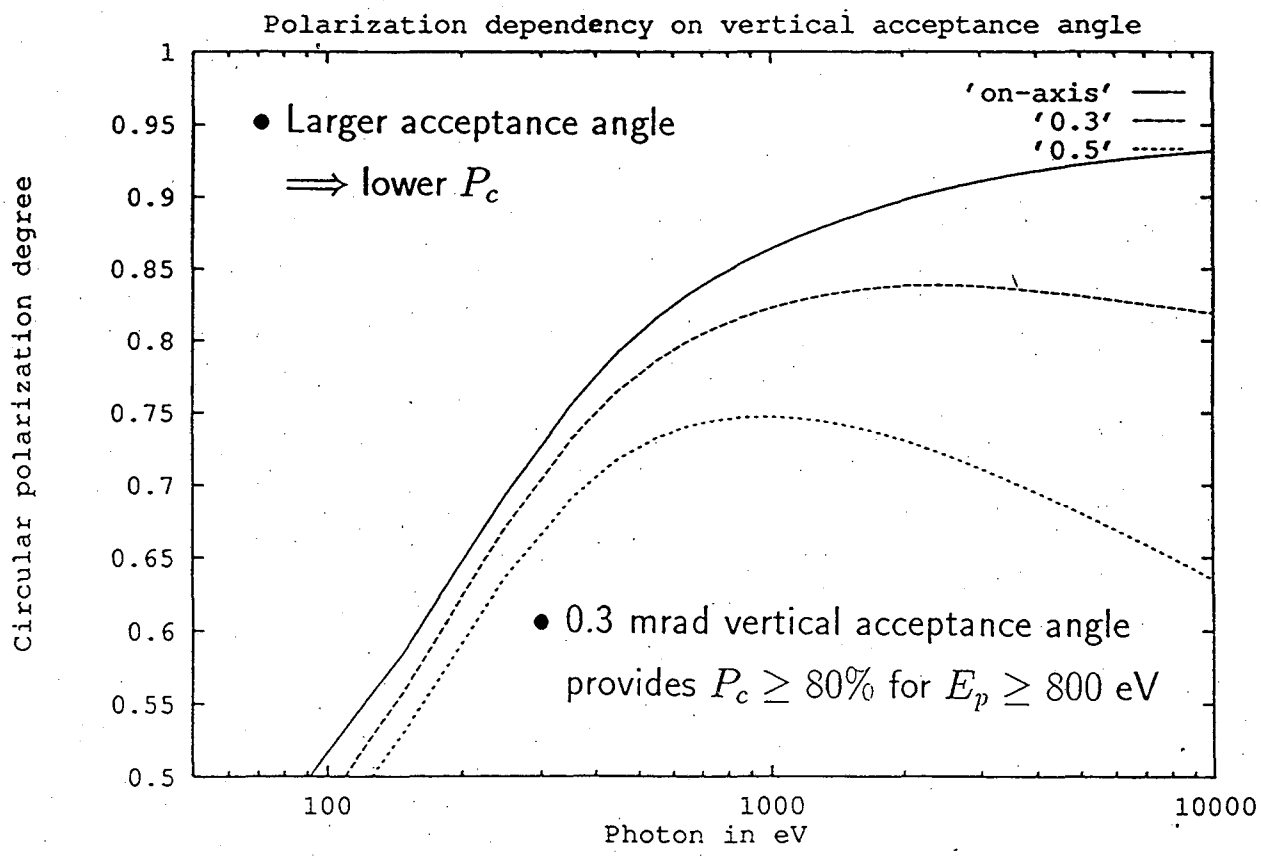
Polarization dependency on vertical acceptance angle
1
0.95
0.9
0.85
0.8
0.75
0.7
0.65
0.6
0.55
0.5
Circular polarization degree
'on-axis'
'0.3'
'0.5'
• Larger acceptance angle
⟹ lower P_c
• 0.3 mrad vertical acceptance angle
provides $P_c \geq 80\%$ for $E_p \geq 800$ eV
100
1000
10000
Photon in eV

A quarter Vertical Magnetic Field of EW

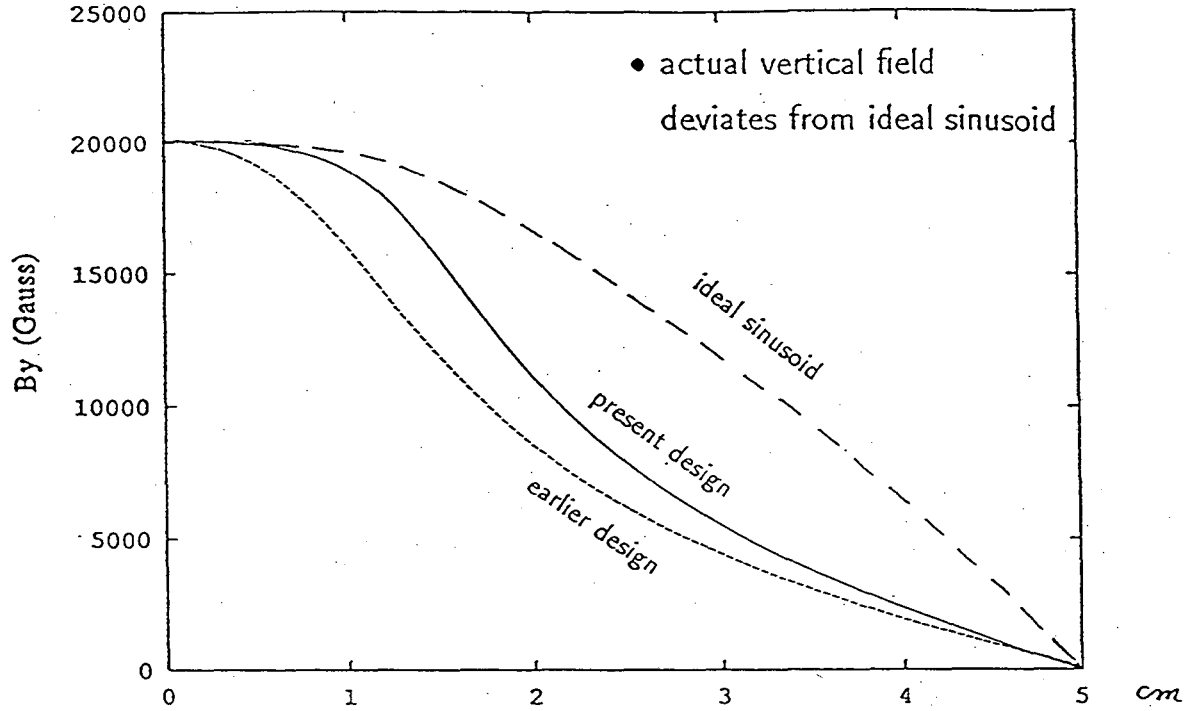

Sidebranch beamline flux

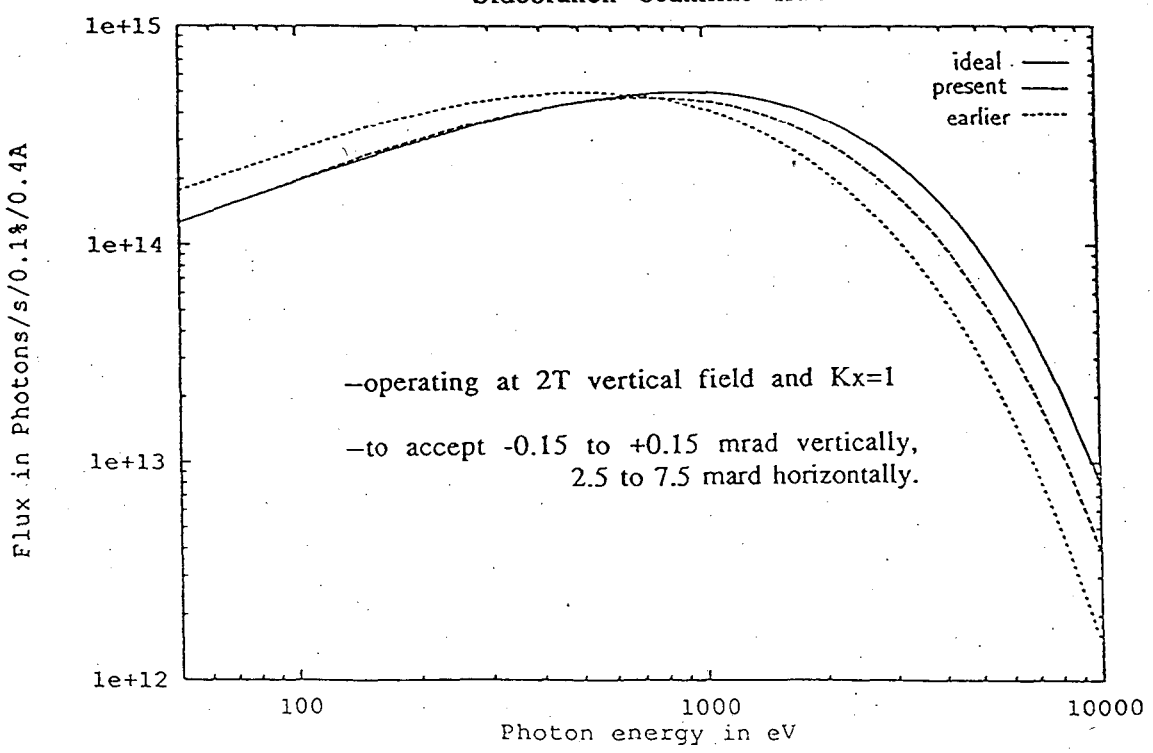

elliptical wiggler performance at limiting cases:

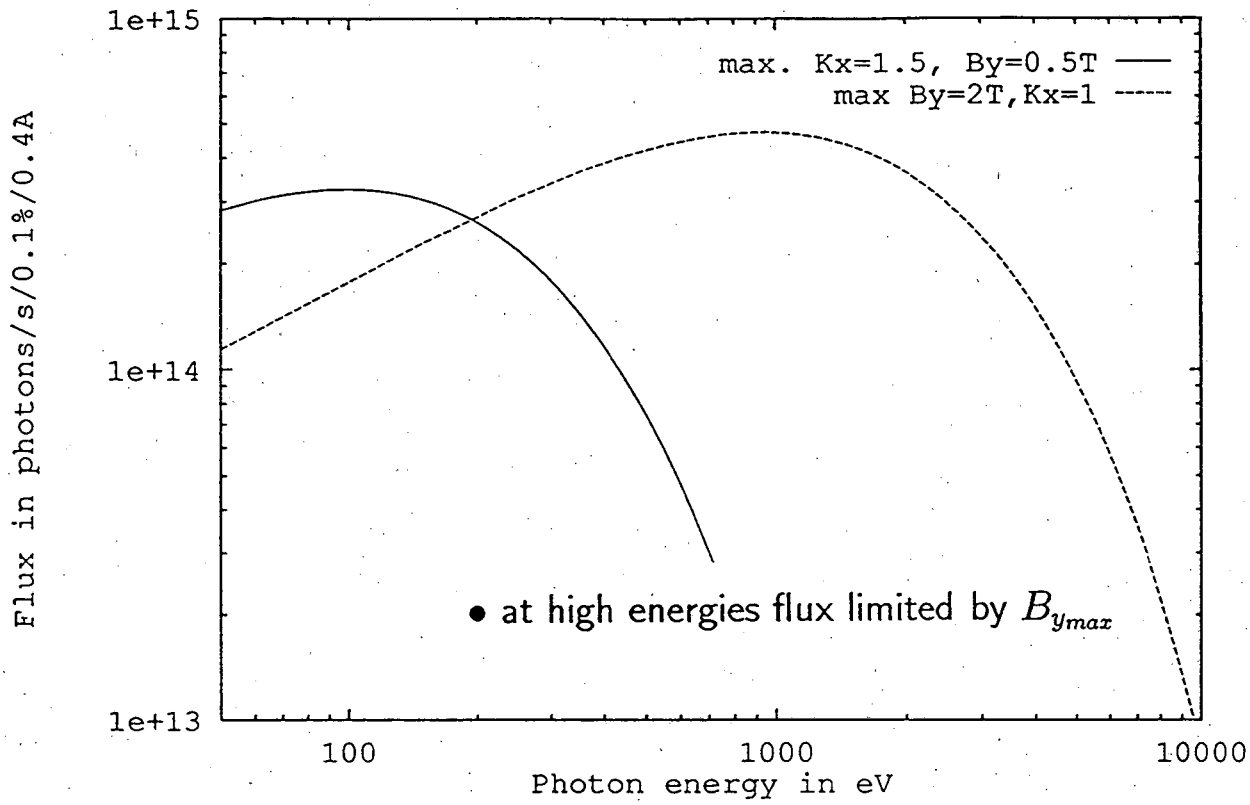

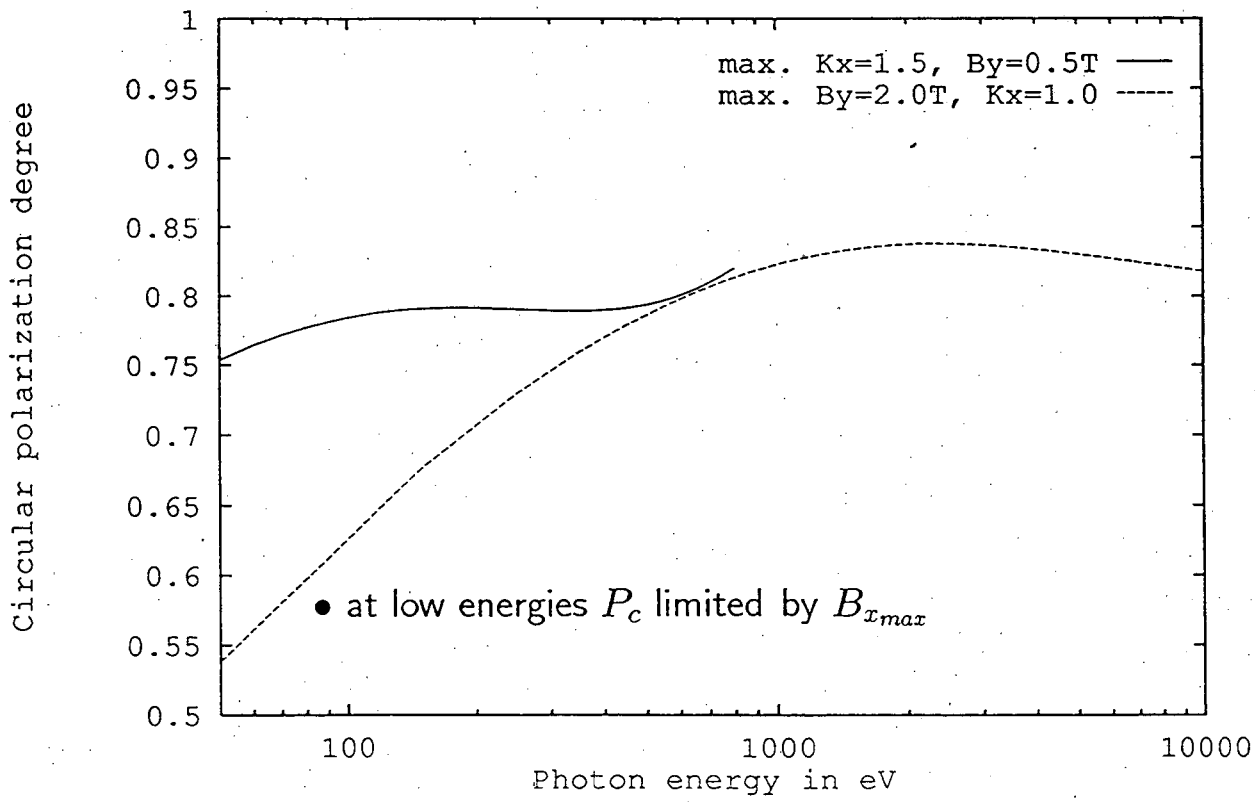

Mechanism of Crossed Undulator

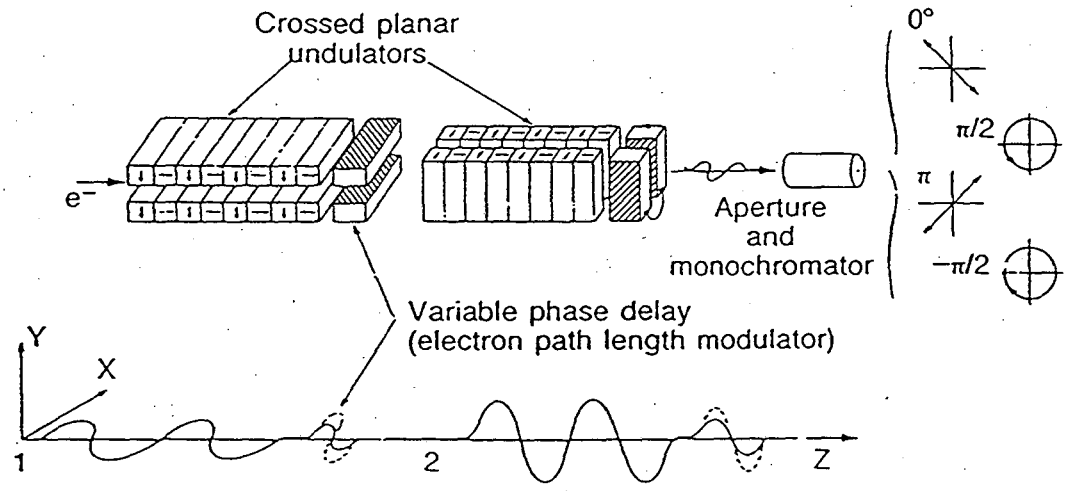

Fig. 3-14. Schematic drawing of a pair of crossed undulators that could be used to produce variably polarized radiation.

$$\vec{E} = E_x \vec{e}_x + E_y \vec{e}_y$$

two same planar undulators $E_x = E$, $E_y = E e^{i\Phi}$

$$\frac{E_y}{E_x} = e^{i\Phi} = \begin{cases} (-1)^m, & \Phi = m\pi, \text{ linearly Polarized} \\ -i, & \Phi = 2m\pi - \frac{\pi}{2}, \text{ R-Circularly Pol.} \\ +i, & \Phi = 2m\pi + \frac{\pi}{2}, \text{ L-C} \end{cases}$$

$$\Phi = \Phi_u + \Phi_M = \omega \Delta t$$

Δt = time interval between two linearly polarized photon pulses generated by an electron.

$$= \frac{D_e}{\beta c} - \frac{D_{photon}}{c}$$

D_e changed by modulato

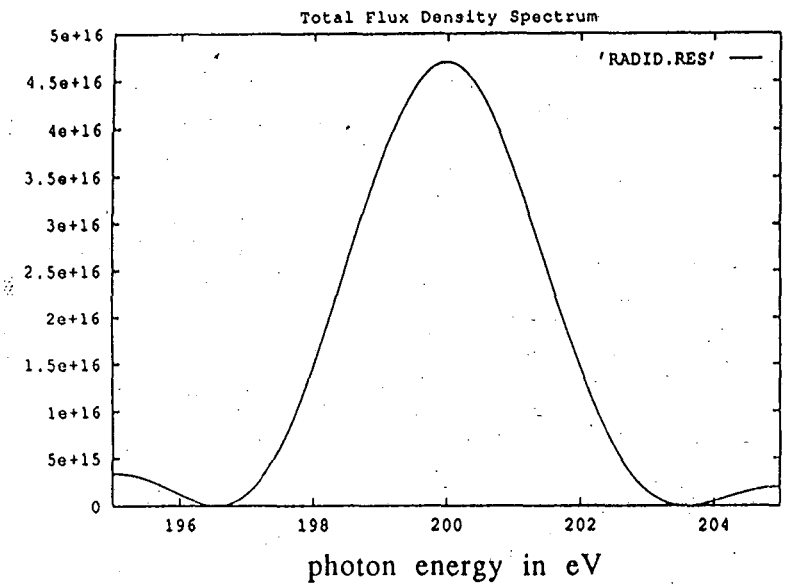

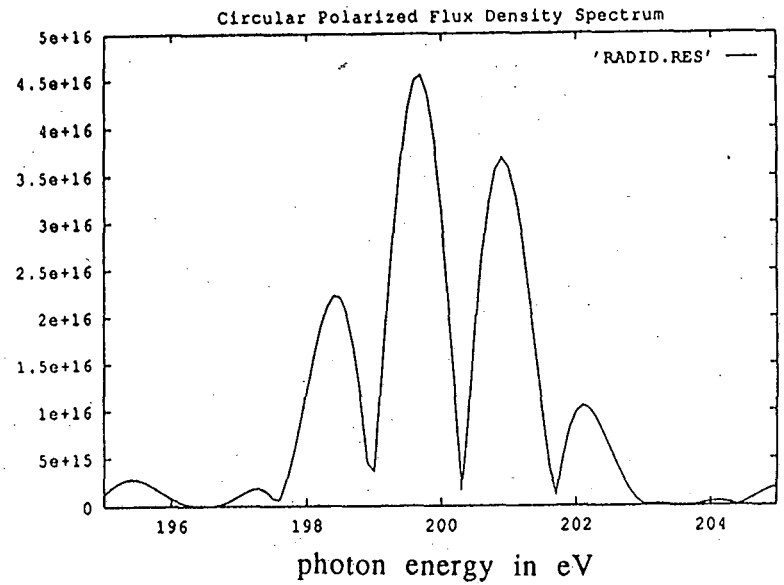

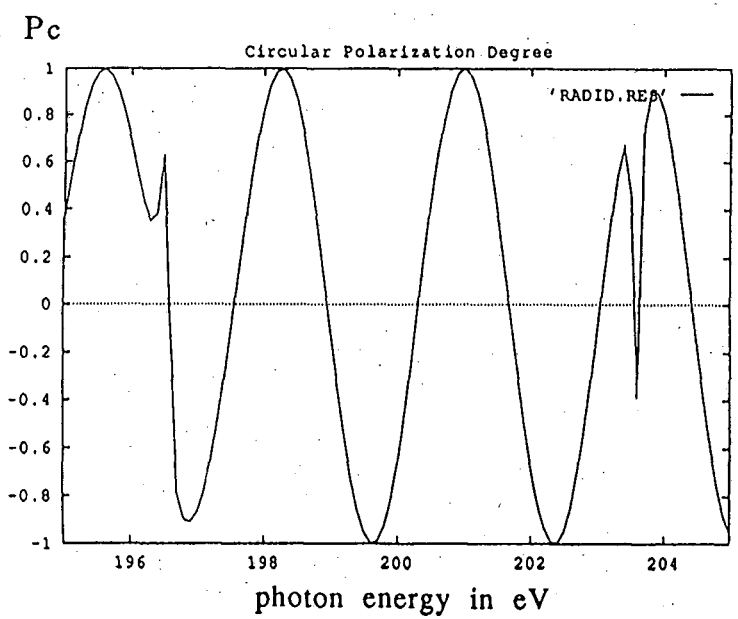

For a single electron...

- polarization oscillates over harmonic flux density peak
- $\Longrightarrow$ multiple peaks in circular polarized flux density spectrum
- $\Longrightarrow$ requires monochromator
- peak P_c position controllable with modulator

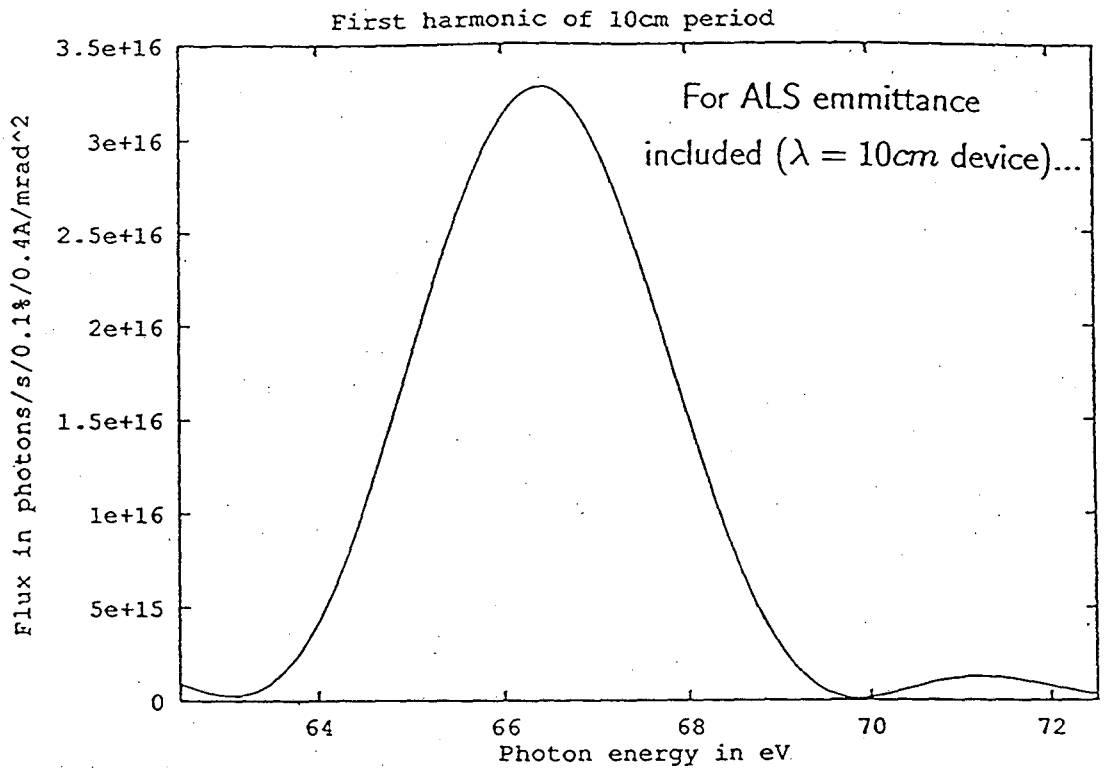
First harmonic of 10cm period
For ALS emmittance
included ($\lambda = 10cm$ device)...
Flux in photons/s/0.1%/0.4A/mrad^2
3.5e+16
3e+16
2.5e+16
2e+16
1.5e+16
1e+16
5e+15
0
64
66
68
70
72
Photon energy in eV

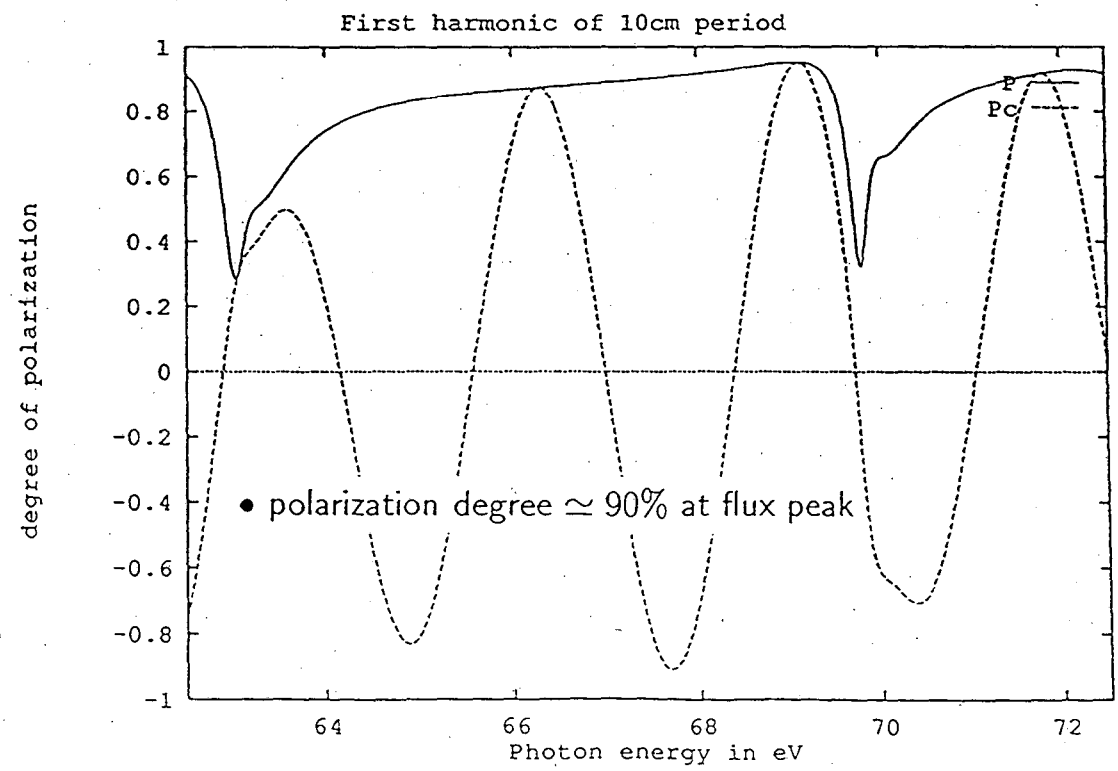
First harmonic of 10cm period
P
Pc
degree of polarization
1
0.8
0.6
0.4
0.2
0
-0.2
-0.4
-0.6
-0.8
-1
• polarization degree ≃ 90% at flux peak
64
66
68
70
72
Photon energy in eV

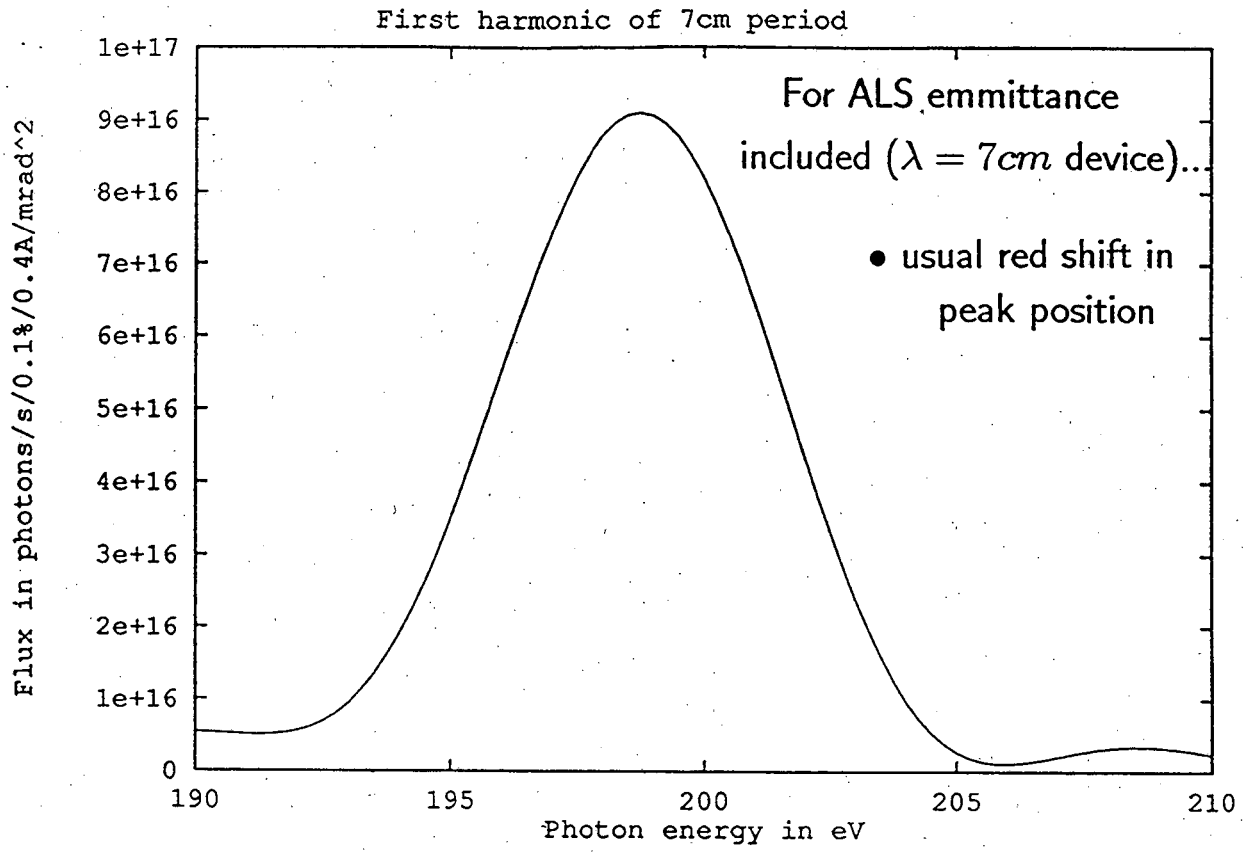
First harmonic of 7cm period
Flux in photons/s/0.1%/0.4A/mrad^2
1e+17
9e+16
8e+16
7e+16
6e+16
5e+16
4e+16
3e+16
2e+16
1e+16
0
190
195
200
205
210
Photon energy in eV
For ALS emmittance included ($\lambda = 7cm$ device)...
• usual red shift in peak position

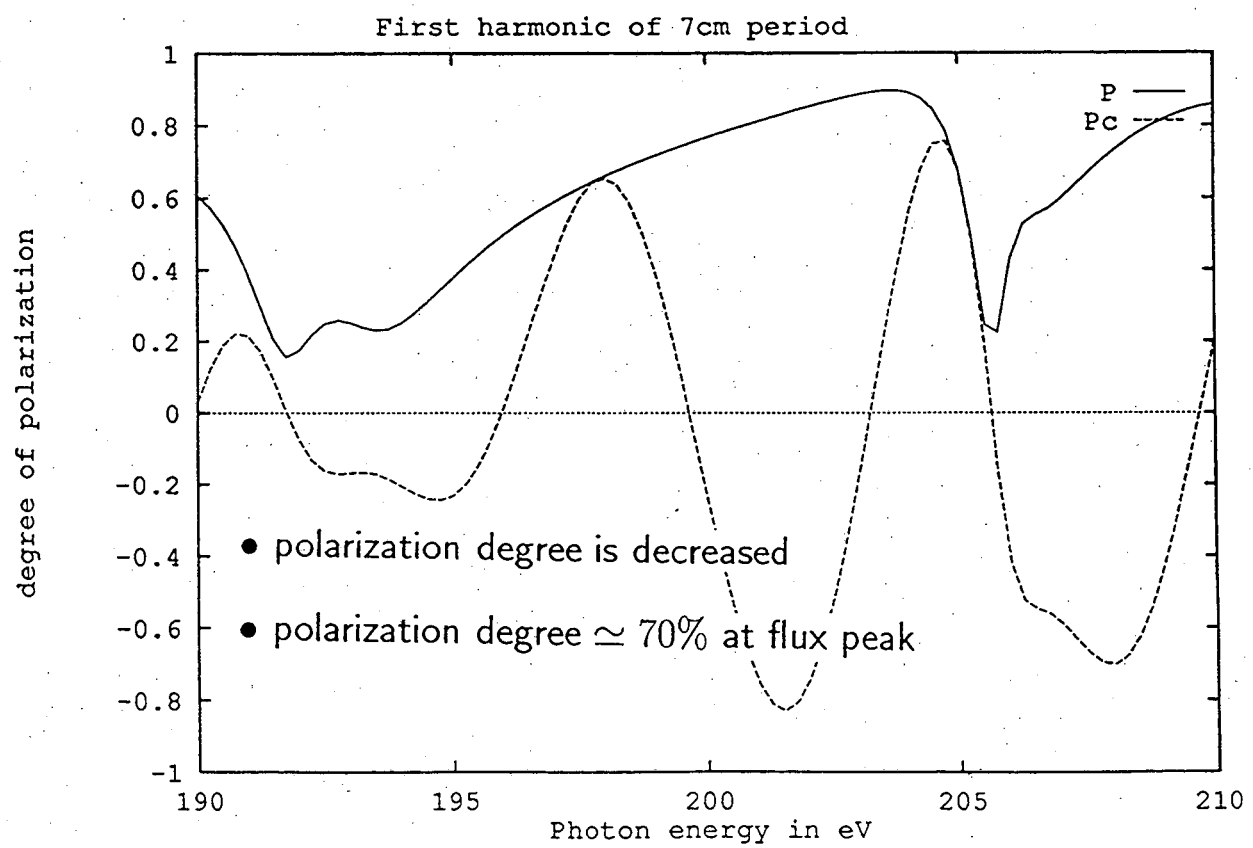
First harmonic of 7cm period
degree of polarization
1
0.8
0.6
0.4
0.2
0
-0.2
-0.4
-0.6
-0.8
-1
190
195
200
205
210
Photon energy in eV
P
Pc
• polarization degree is decreased
• polarization degree $\simeq$ 70% at flux peak

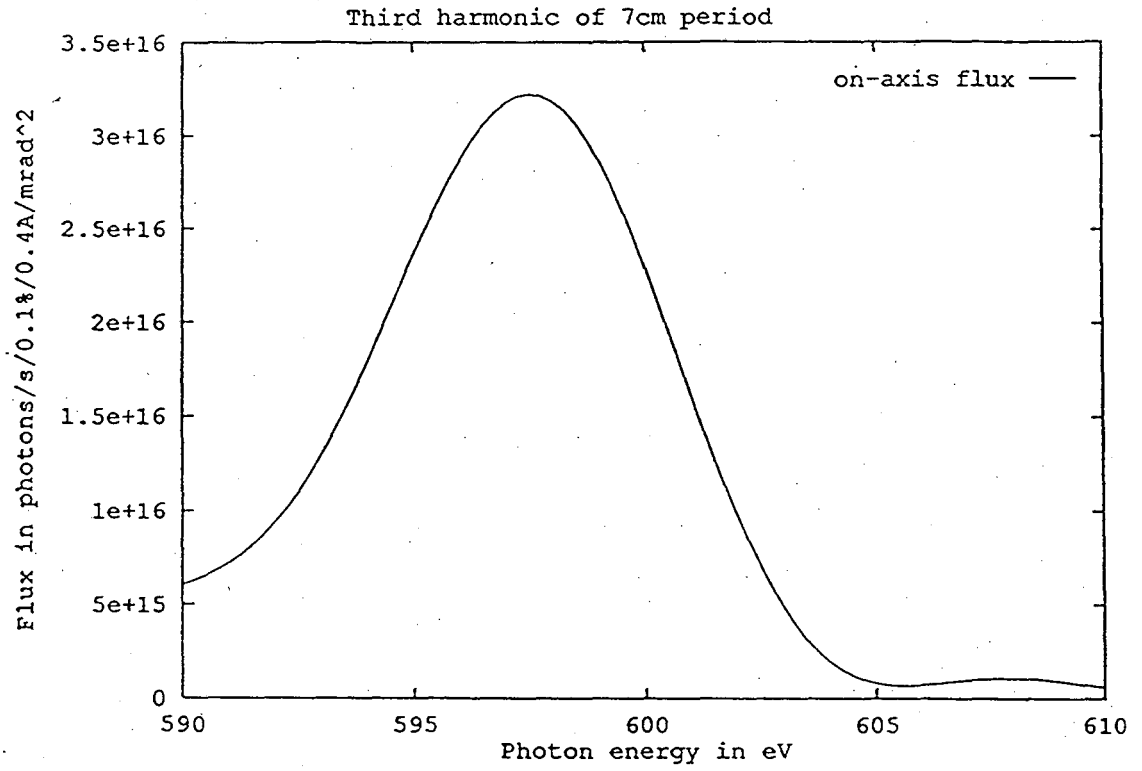
Third harmonic of 7cm period
on-axis flux
Flux in photons/s/0.1%/0.4A/mrad^2
3.5e+16
3e+16
2.5e+16
2e+16
1.5e+16
1e+16
5e+15
0
590
595
600
605
610
Photon energy in eV

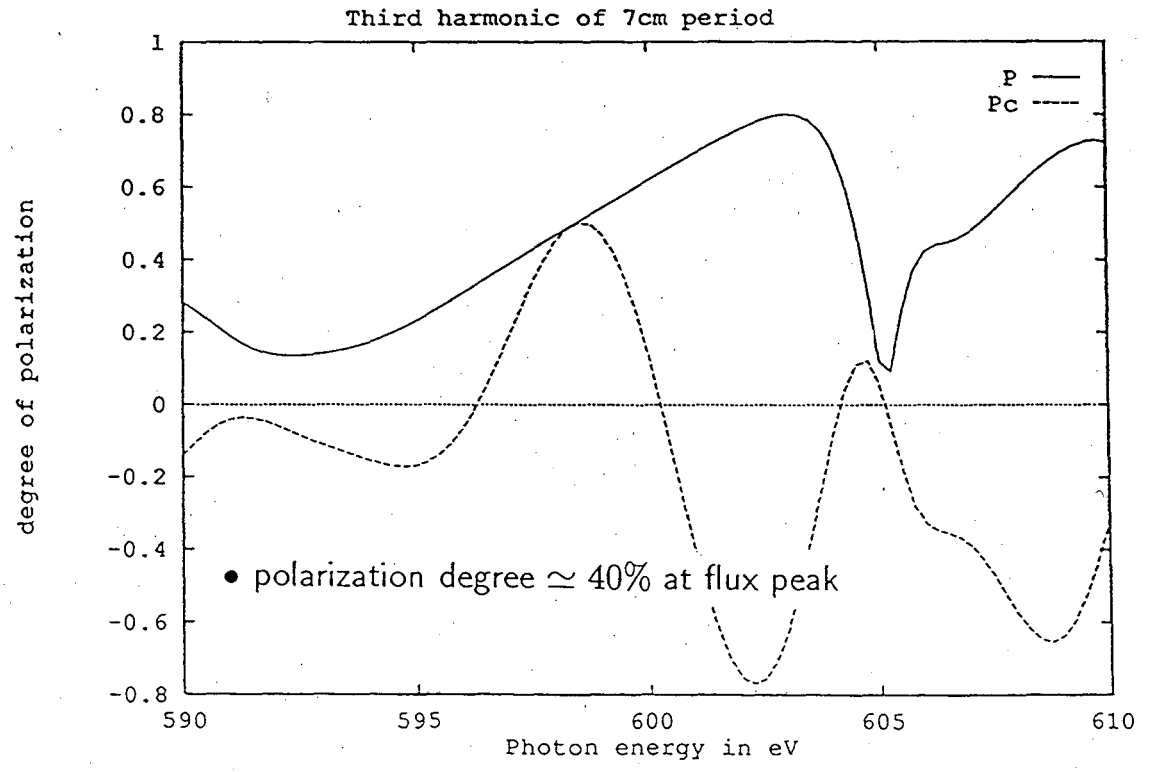
Third harmonic of 7cm period
P
Pc
degree of polarization
1
0.8
0.6
0.4
0.2
0
-0.2
-0.4
-0.6
-0.8
590
595
600
605
610
Photon energy in eV
• polarization degree ≃ 40% at flux peak

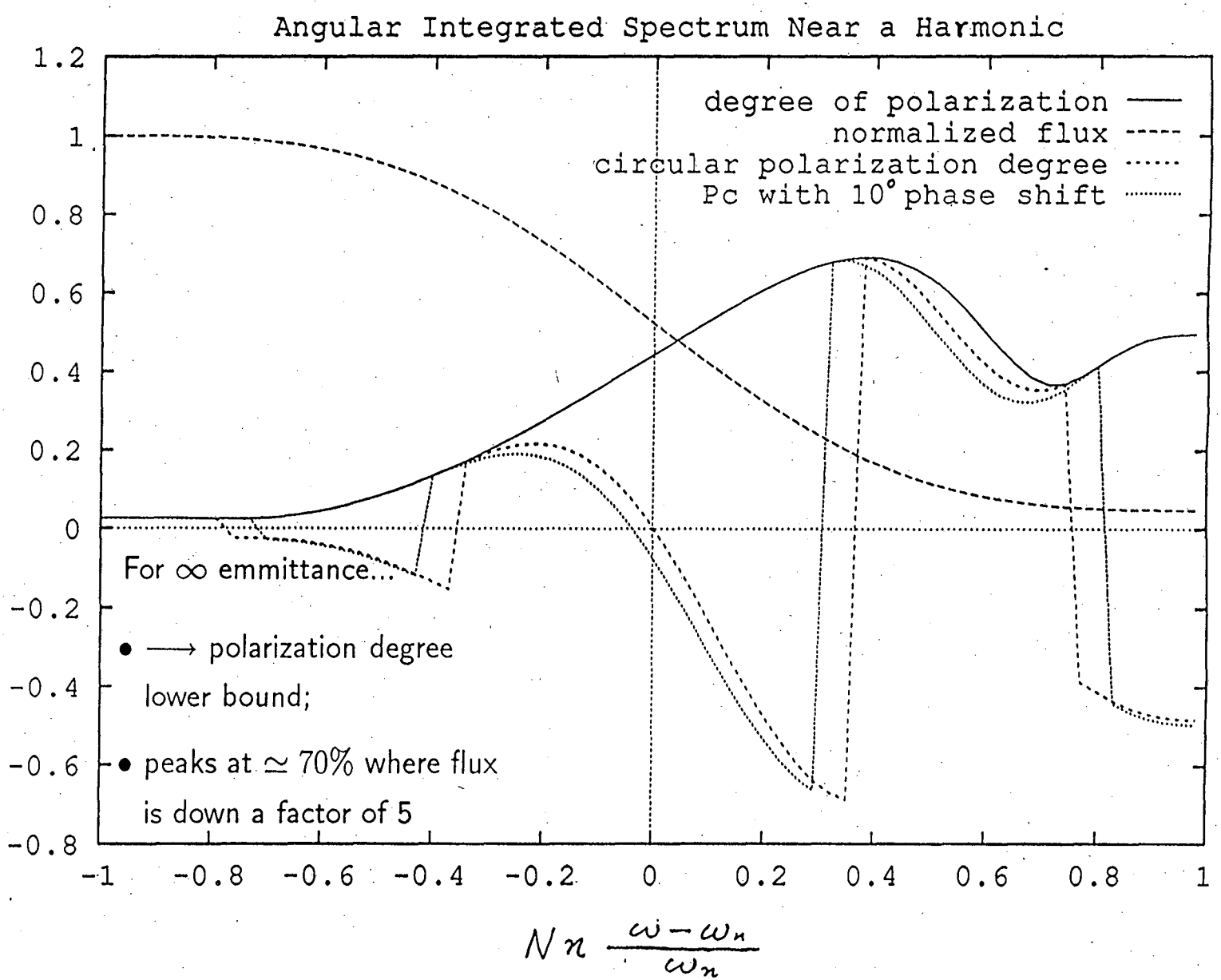
Angular Integrated Spectrum Near a Harmonic
degree of polarization
normalized flux
circular polarization degree
Pc with 10° phase shift
For ∞ emmittance...
• ⟶ polarization degree lower bound;
• peaks at ≃ 70% where flux is down a factor of 5
1.2
1
0.8
0.6
0.4
0.2
0
-0.2
-0.4
-0.6
-0.8
-1
-0.8
-0.6
-0.4
-0.2
0
0.2
0.4
0.6
0.8
1
$Nn\,\frac{\omega-\omega_n}{\omega_n}$

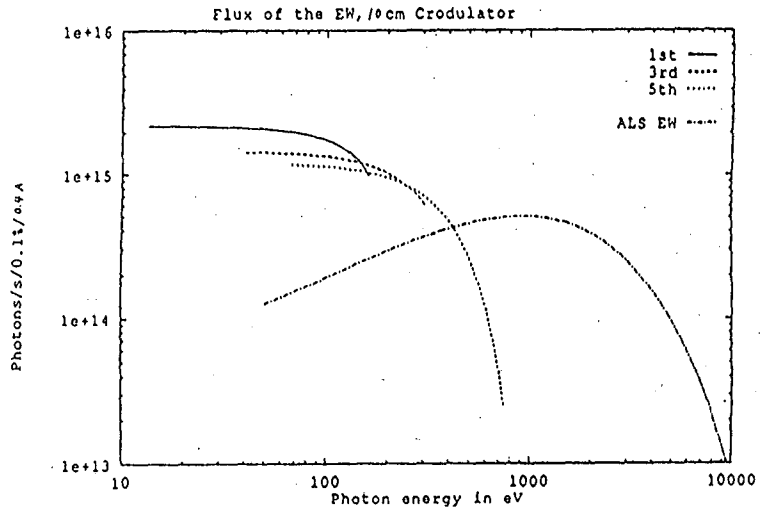
Flux of the EW, 10cm Crodulator
1st
3rd
5th
ALS EW
Photons/s/0.1%/0.4A
1e+16
1e+15
1e+14
1e+13
10
100
1000
10000
Photon energy in eV

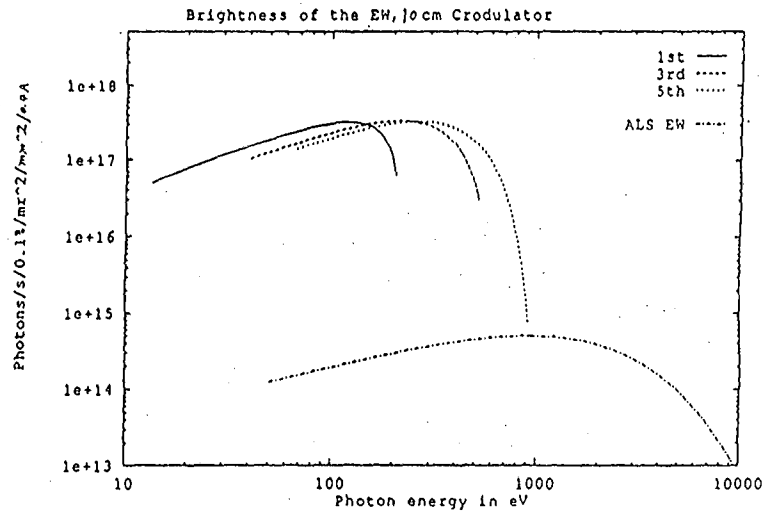
Brightness of the EW, 10cm Crodulator
1st
3rd
5th
ALS EW
Photons/s/0.1%/mr^2/mm^2/0.4A
1e+18
1e+17
1e+16
1e+15
1e+14
1e+13
10
100
1000
10000
Photon energy in eV

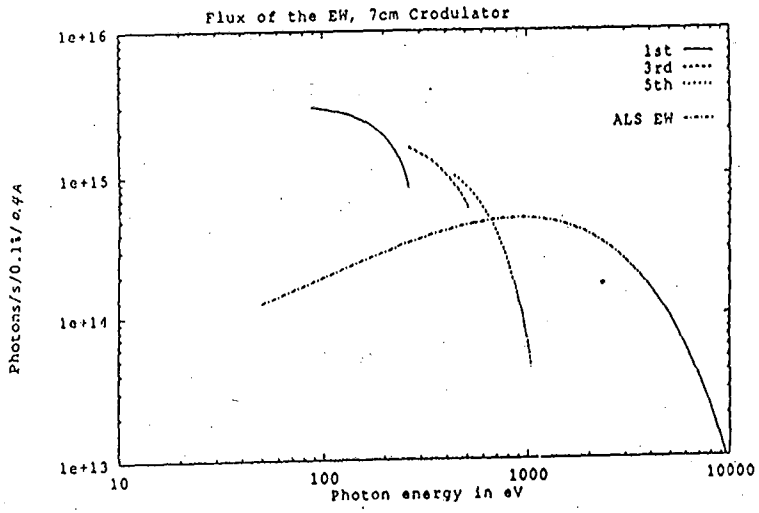
Flux of the EW, 7cm Crodulator
1st
3rd
5th
ALS EW
Photons/s/0.1%/0.4A
1e+16
1e+15
1e+14
1e+13
10
100
1000
10000
Photon energy in eV

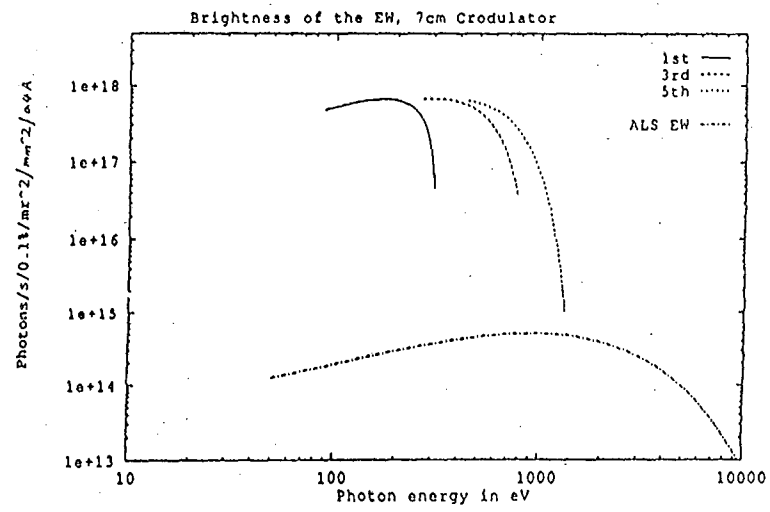
Brightness of the EW, 7cm Crodulator
1st
3rd
5th
ALS EW
Photons/s/0.1%/mr^2/mm^2/0.4A
1e+18
1e+17
1e+16
1e+15
1e+14
1e+13
10
100
1000
10000
Photon energy in eV

Hybrid–Electromagnet Elliptical Wiggler Design

Egon Hoyer

Lawrence Berkeley Laboratory

Hybrid - Electromagnet Elliptical Wiggler Design

E. Hoyer, D. Plate, R. Schlueter
LBL
April 19, 1993

Motivation for an Elliptical Wiggler

Outcome of informal meetings during Feb., 1992 with Hassenzahl, Hoyer, Marks & Schlueter, lead to the these requirements for a radiation source with elliptical polarization:

- Photon energy range: 50 eV to 8 keV
- Frequency of polarization handedness change: $\geq$ 10 Hz

For an insertion device on the ALS (1.5 GeV), this implies a wiggler with:

- Critical energy = 8 keV/ 3 = 2.67 keV
- Peak Field = 2.67 keV/ 0.665 * (1.5 GeV)**2 = 1.78 T

High Field Wiggler with Rapid Handedness Change - Options

- Assymetric Wiggler

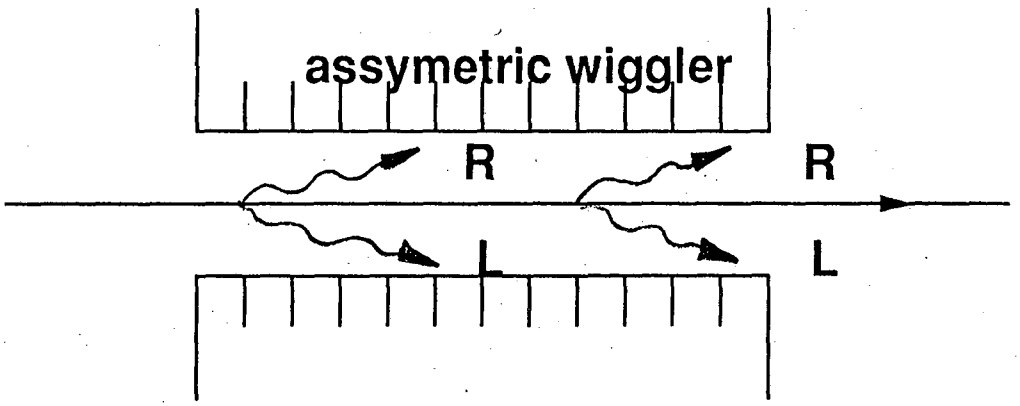

- Requires using off-midplane beams at near +/- K_x/gamma.
- Source distributed.
- Requires a chopper to achieve rapid handedness change.
- Requires special optics to combine the beams.

High Field Wiggler with Rapid Handedness Change - Options (#1 cont.)

- Modulated Assymetric Wiggler

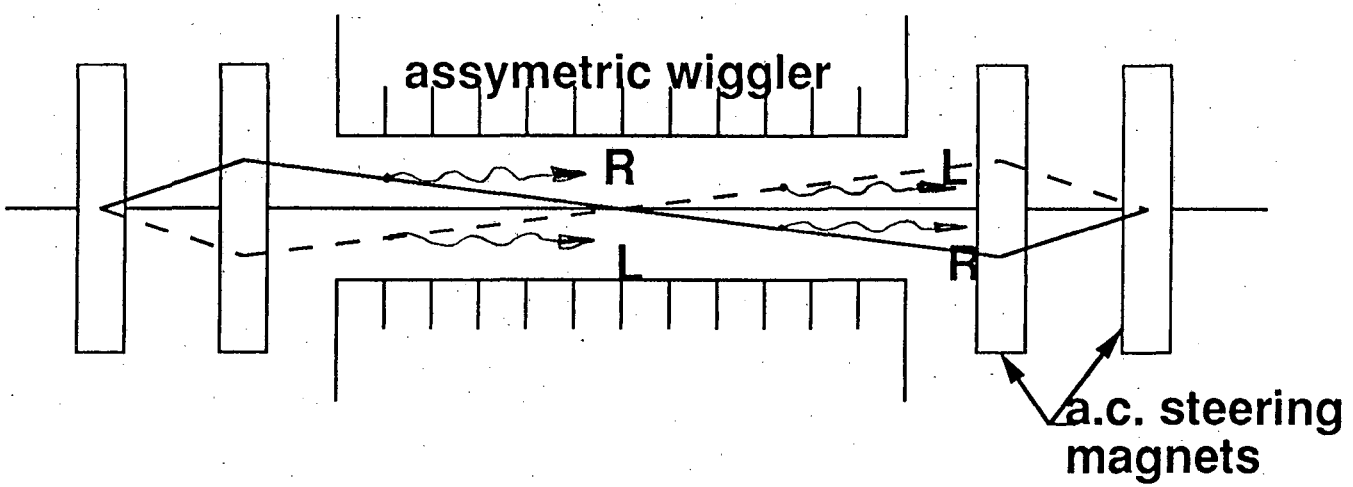

- Requires A/C electromagnets to steering the beam above & below the midplane at either end of the wiggler to achieve rapid handedness change.

- Beam is emitted parallel to the wiggler axis both above & below the midplane resulting in a large vertical beam size.

High Field Wiggler with Rapid Handedness Change - Options (#2 cont.)

- Hybrid - Electromagnet Elliptical Wiggler

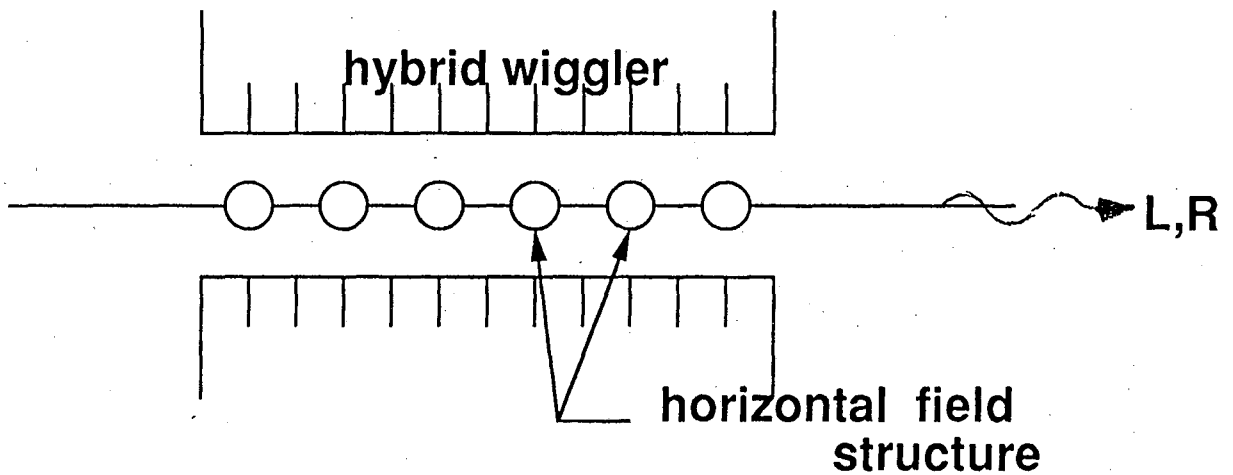

- Elliptically polarized beam is emitted on the mid-plane.
- Uses a conventional hybrid permanent magnet wiggler structure.
- Requires a A/C horizontal field structure to steer the beam above and below the midplane.

Hybrid Electromagnet Elliptical Wiggler Schematic

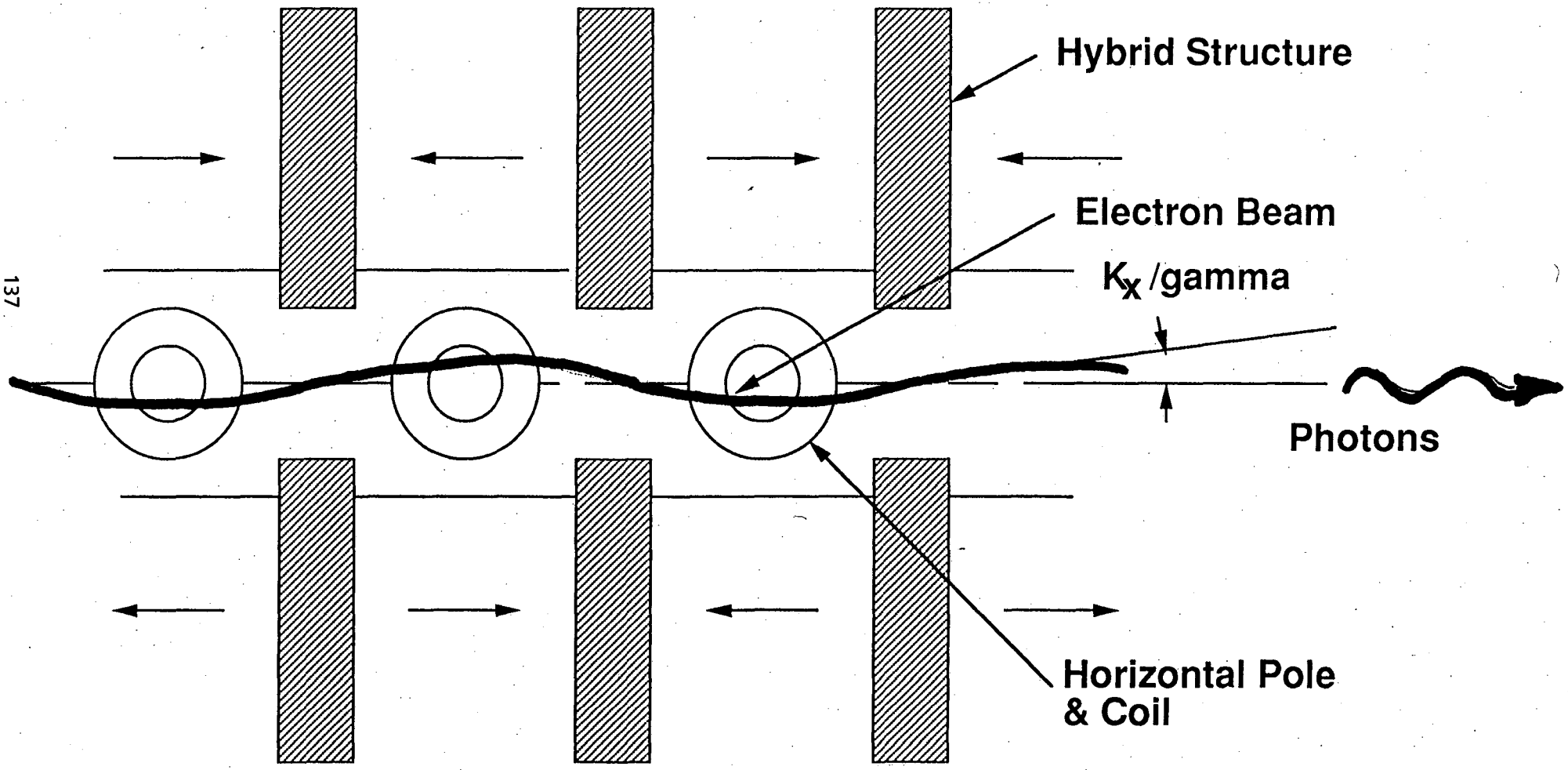

Vertical Section thru the Center

HEEW Photon Parameters - April, 1993

Critical Energy	3.0 keV
Maximum Photon Energy	10 keV
Minimum Photon Energy	50 eV
Horizontal Field Frequency	1 Hz
Vertical Deflection Parameter (Kx)	1.5 max.
Vertical Orbit Angles(+/- /Gamma)	0.51 mrad
Horizontal Opening Angle	+/- 9.65 mrad
Wiggler Period Length	20 cm
Number of Periods	13

Hybrid – Electromagnet Elliptical Wiggler

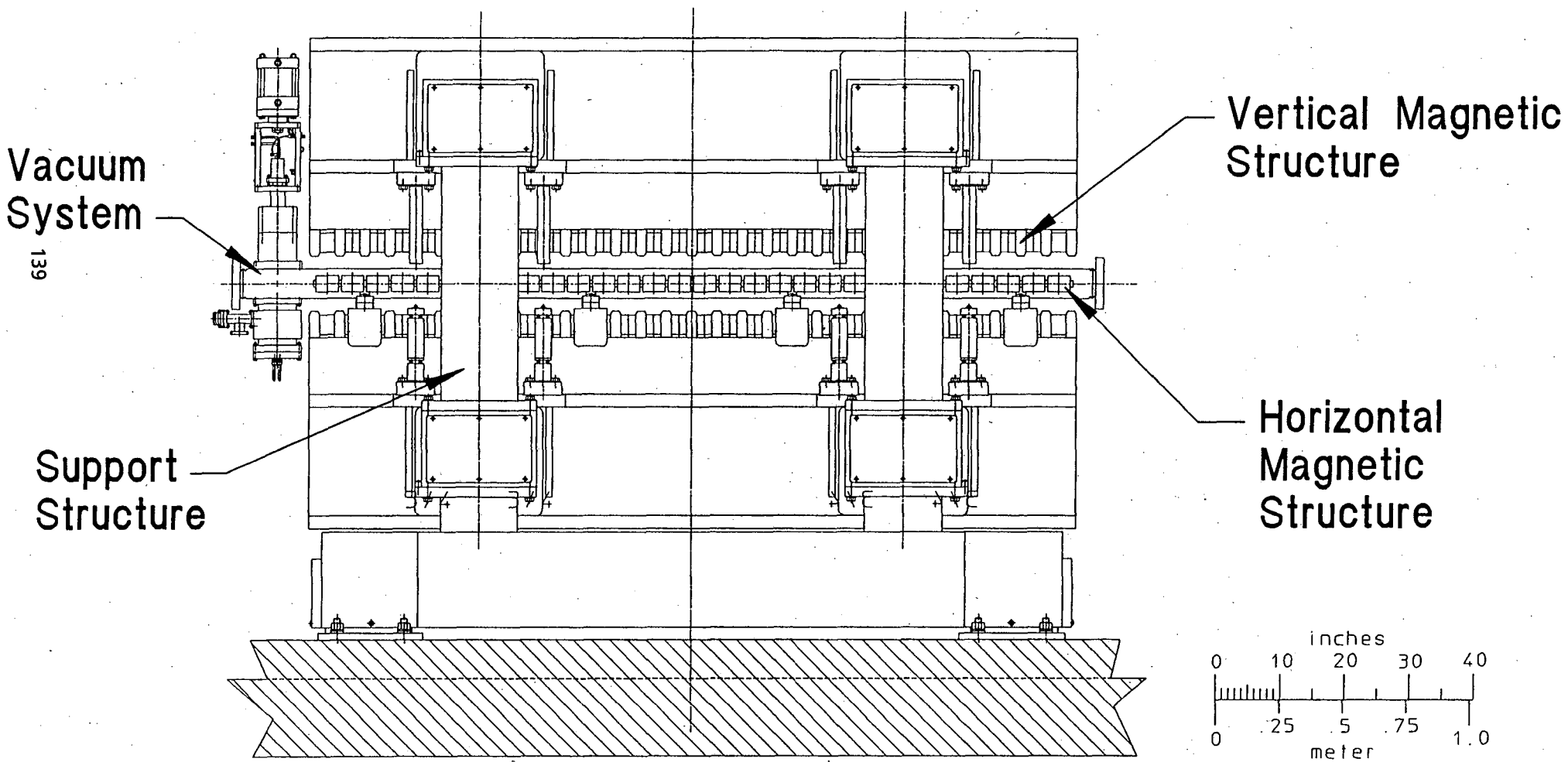

HEEW Side Sectional View

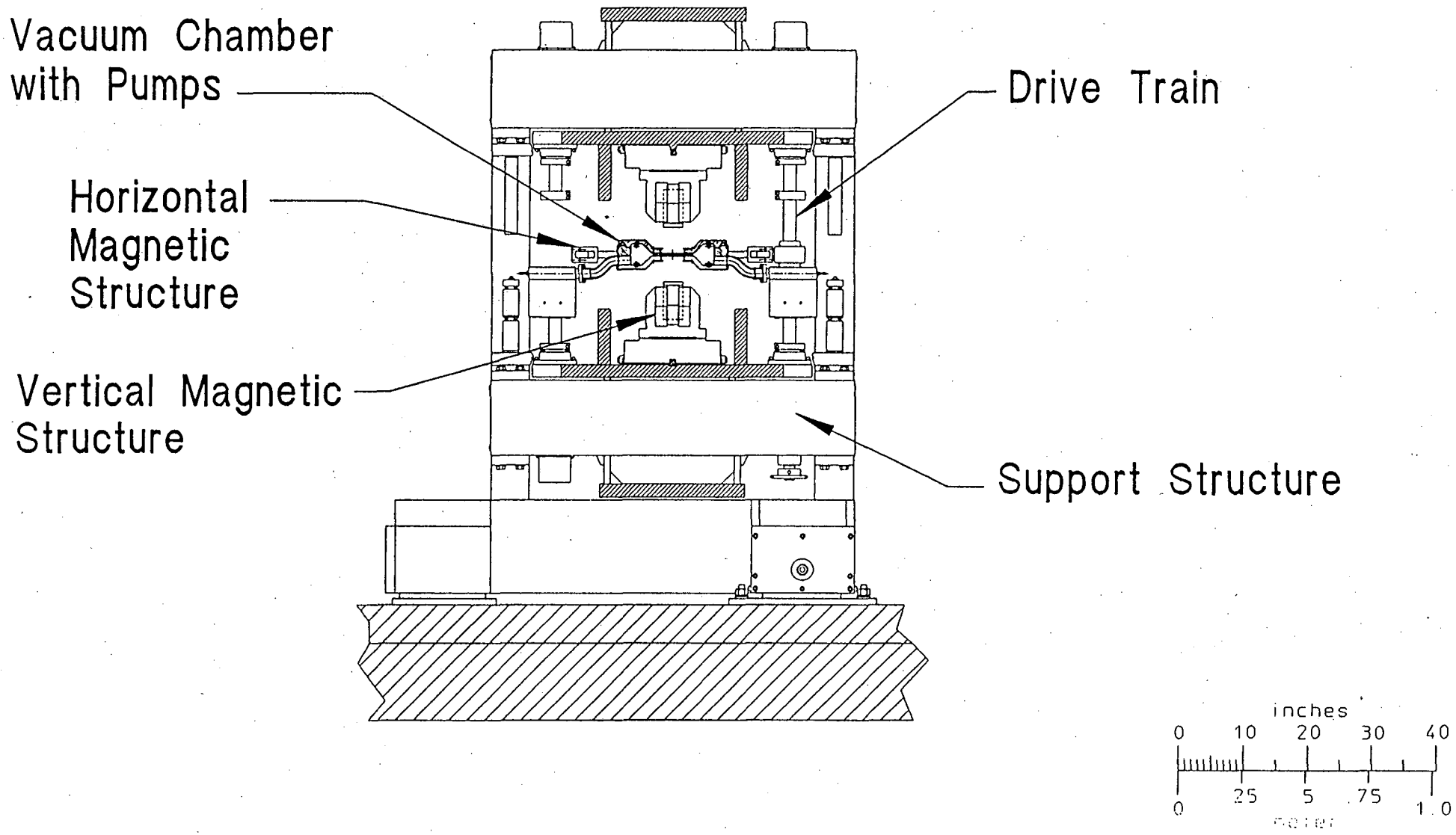

HEEW Sectional View at Horizontal Magnetic Structure

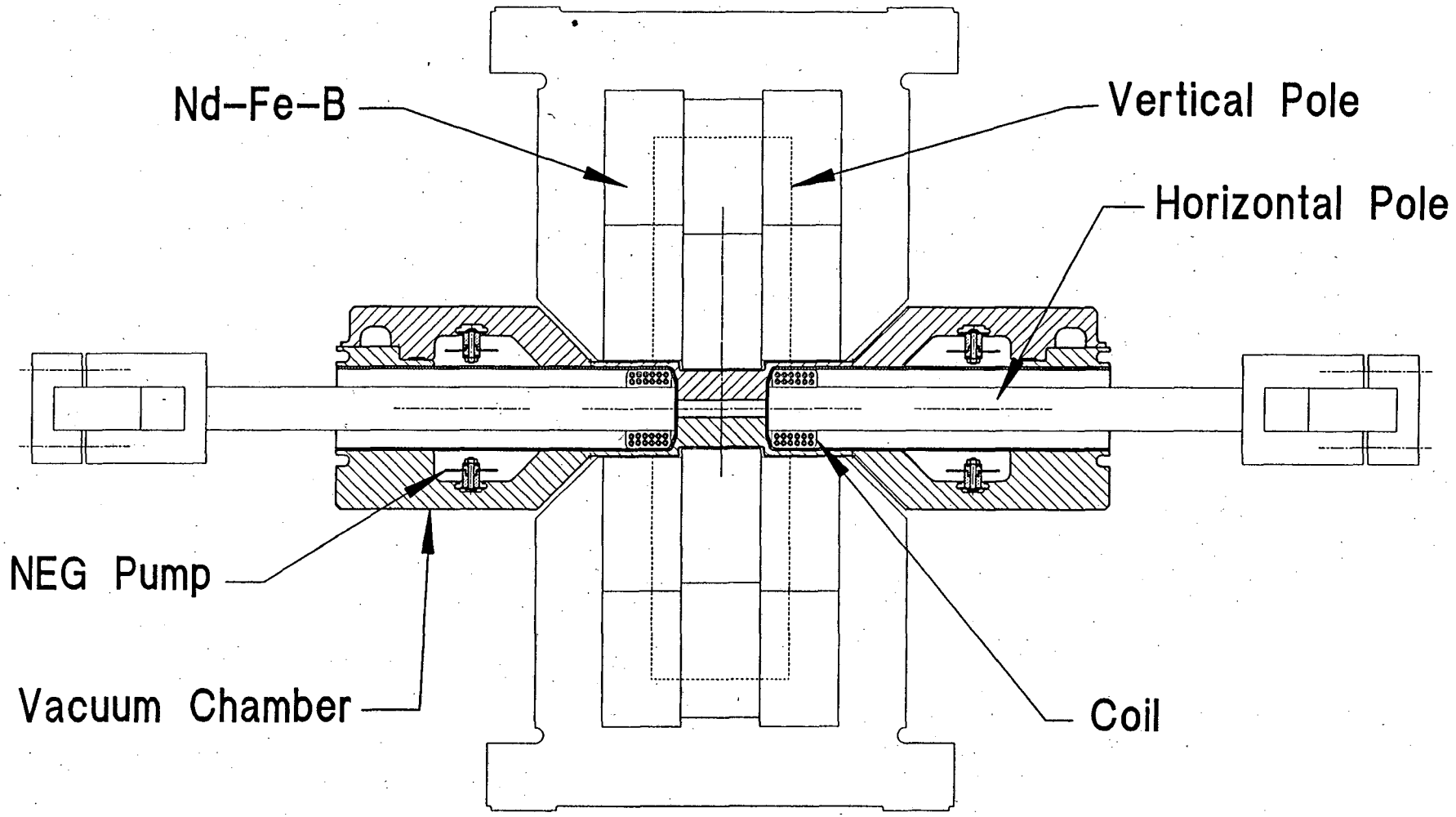

HEEW Horizontal Field Structure Parameters

Horizontal beam aperture	5.0 cm
Maximum Field Integral between Poles	5300 G cm
Peak Field	1306 G
Peak Pole Flux Density	2.05 T
Core Loss per Pole	0.10 W
Structure Core Loss	5.6 W

Horizontal Magnetic Field Structure Flux Distribution

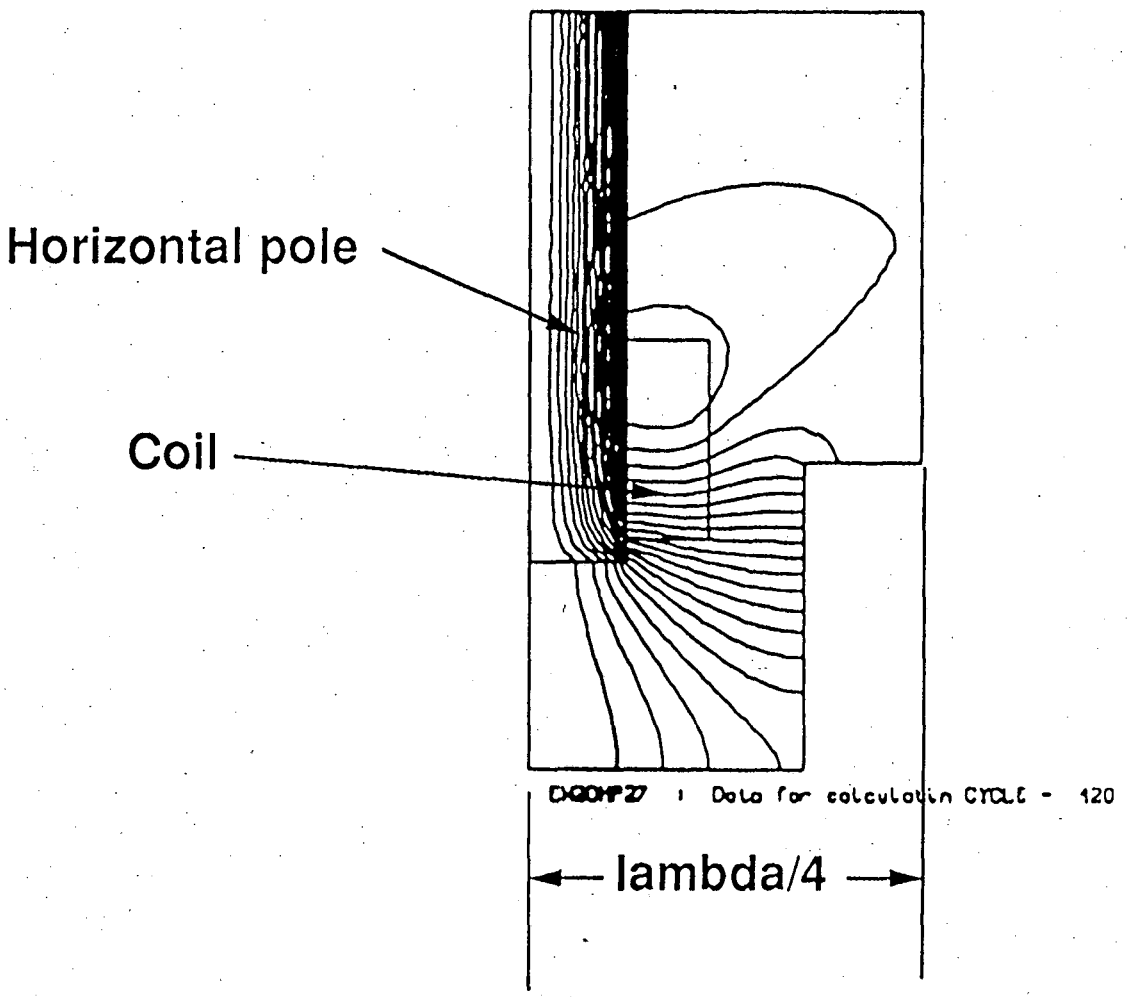

Horizontal Field Coil Parameters

Number of coils required	56 + 4 1/2 size coils
Conductor	1/8 OD X 1/16 ID Copper
Number of turns /coil	12
Current	500 A
Coil Resistance	1.56 mOhm
DC power/coil	387 W
DC voltage/coil	0.78 V
AC power/coil	194 W
Coil inductance	244 microHenry
AC voltage/coil	0.76 V
Coil time constant	0.156 s

Horizontal Field Coil Parameters (cont.)

Total DC power/ coils	22.4 kW
Total DC voltage	45.0 V
Total AC power/coils	11.3 kW
Total AC voltage	44.1 V
Coil cooling:	
Available pressure drop	60 psi
Flowrate/coil	0.105 gpm
Water temperature rise	7.0 deg. C

Vertical Field Structure Requirements

- Structure must achieve 2.0 T at the 1.4 cm minimum gap to achieve the 10 keV photon energy.

- Horizontal fan cannot exceed 9.7 mrad otherwise the photon beam will strike the inner wall of the sector vacuum chamber.

- Good photon flux for the side branch (between 2.5 and 7.5 mrad) - this implies reducing the 3rd harmonic of the field.

- Must accomodate the horizontal field structure.

HEEW Longitudinal Sectional View of the Vertical Magnetic Structure

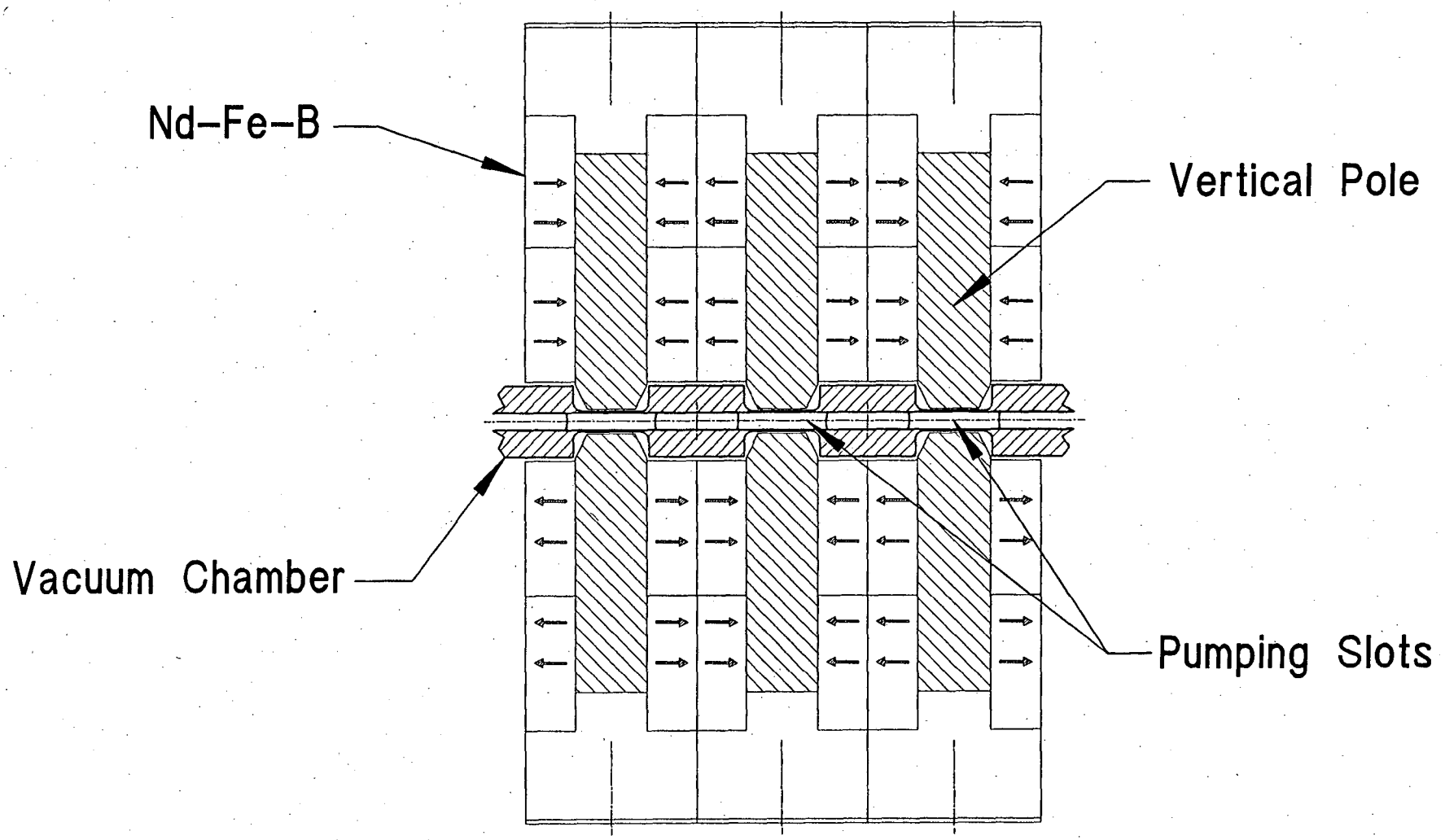

Vertical Magnetic Field Structure Flux Distribution

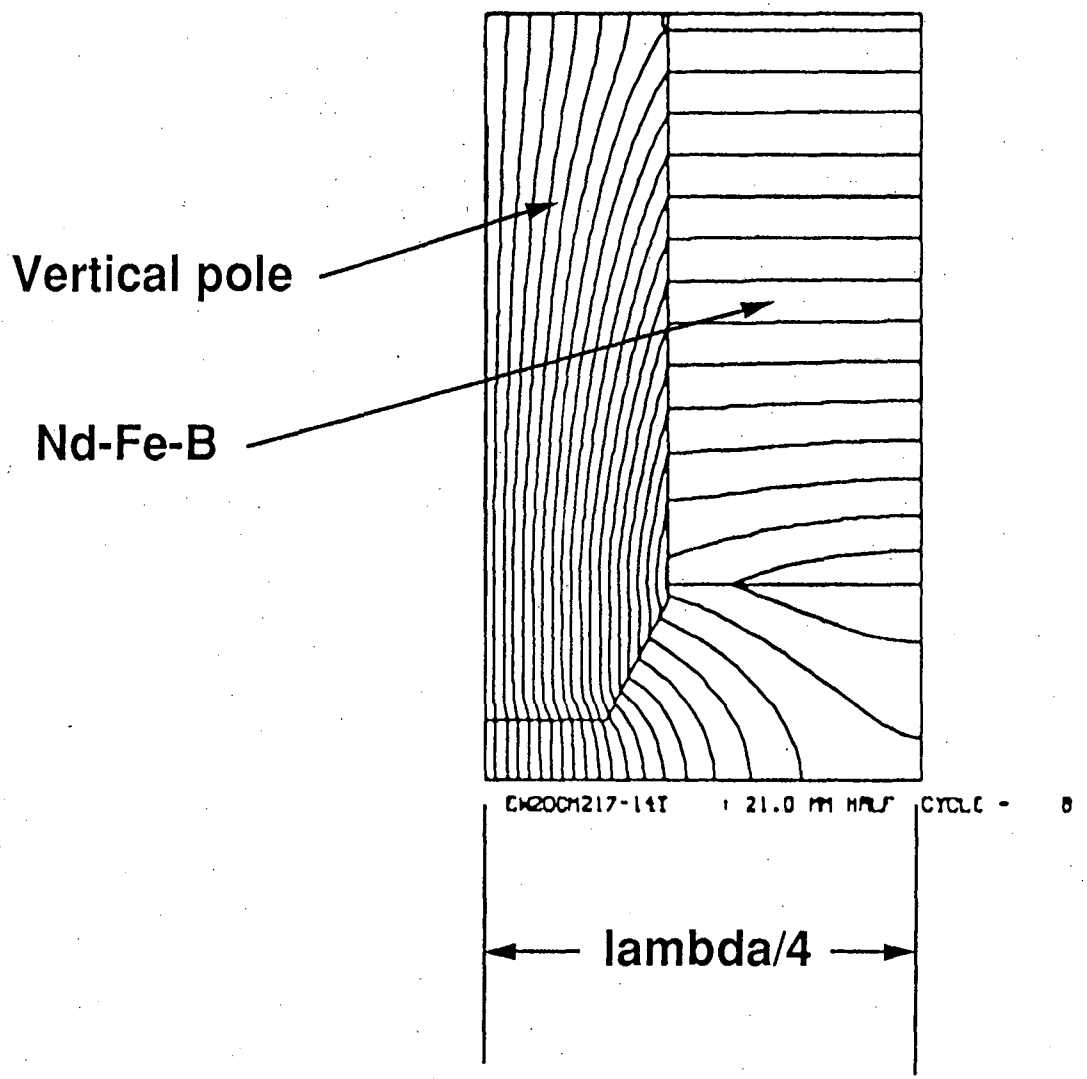

Vertical Field Structure Parameters

Peak vertical field	2.0053 T
1/4 period field integral	48,230 G cm
Normalized harmonics:	
1st	1.0
3rd	-0.254
5th	0.0286
7th	0.0296
9th	0.0263
Pole width	8.0 cm
Pole thickness	4.2 cm
Pole height	14.9 cm

Vertical Field Structure Parameters (cont.)

Number of full-field poles	54
Per pole eddy current heating @ 1 Hz	0.03 W
Nd-Fe-B/pole eddy current heating @ 1Hz	0.01 W
Vertical magnetic structure eddy current heating @ 1 Hz	2.35 W
Overall length of vertical magnetic structure	3.03 m

HEEW Near Midplane Plan View

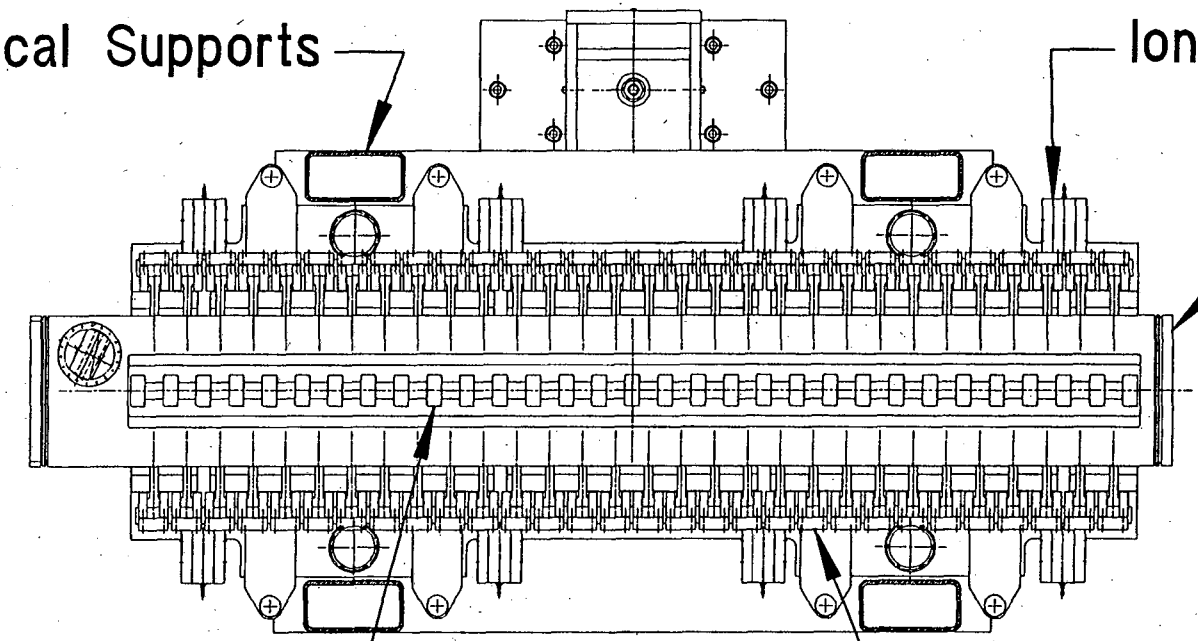

HEEW Sectional View at Vertical Magnetic Structure

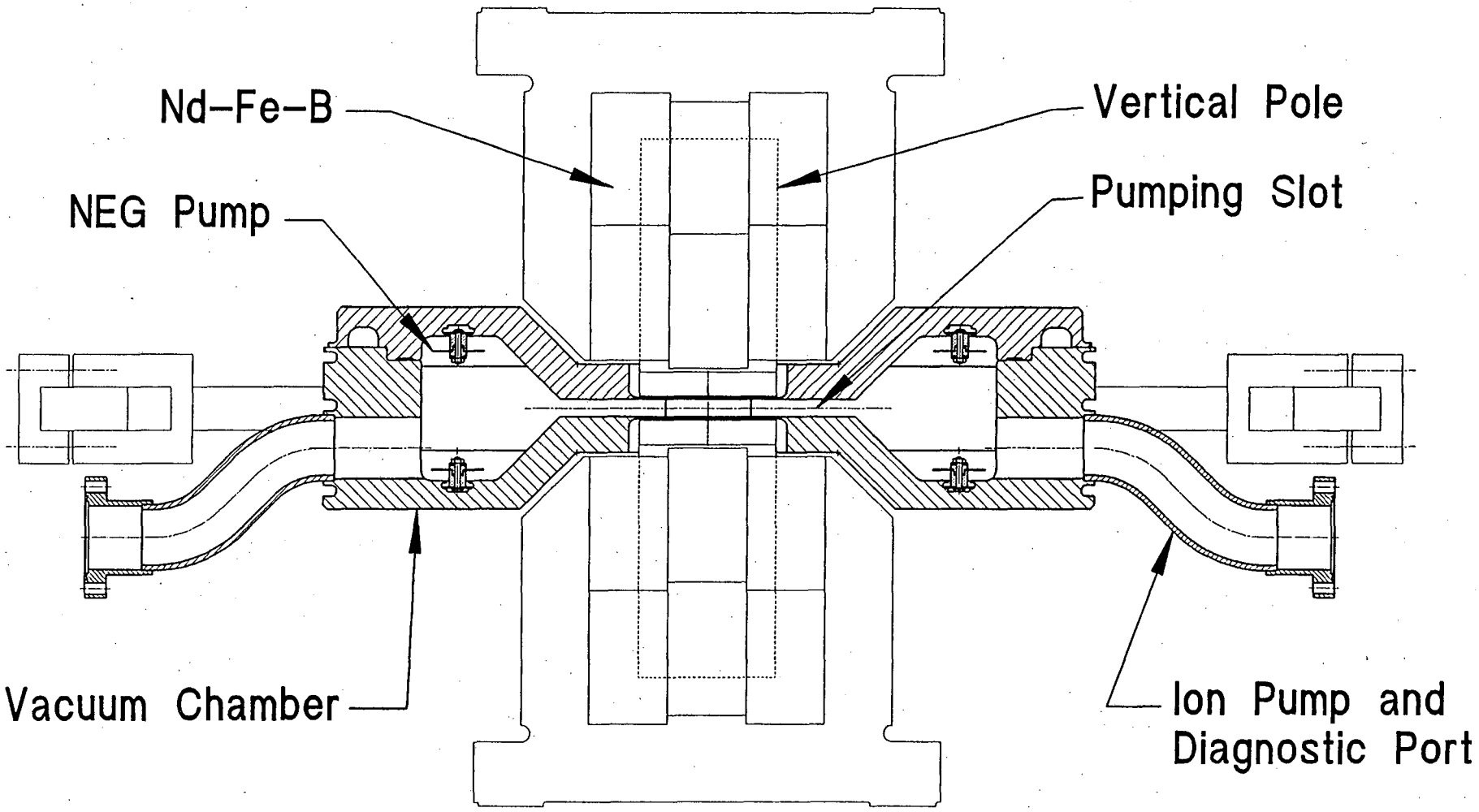

HEEW Sectional View at Horizontal Magnetic Structure

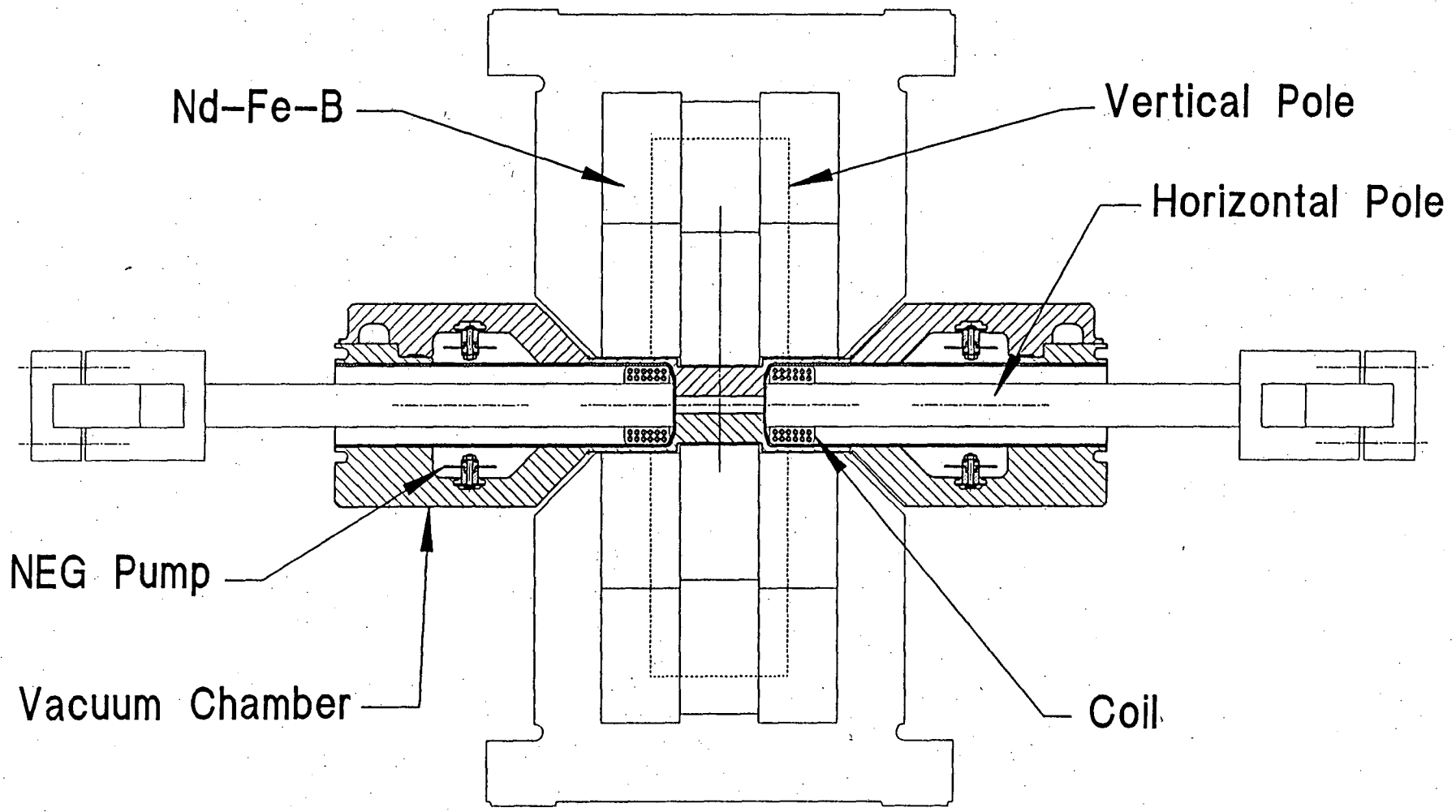

Vacuum System design

Beam aperture	1.0 cm X 5.0 cm
Vacuum chamber construction	5083-H321 Aluminum - welded
Vacuum chamber eddy current heating @ 1 Hz	40 W
Gradient magnet synchrotron light power impinging on the vacuum chamber	33 W
Gradient magnet synchrotron light absorbed on upstream photon stop	274 W
Elliptical wiggler beam impinging on the sector vacuum chamber slot lips (K_x = 1.0, B_y= 2.0 T)	176 W
Slot temperature rise with external vacuum chamber water cooling	3 deg. C

Plan for Elliptically Polarized I.D. Development

- Establish requirements.
- Evaluate design options.
    - carry out spectral calculations.
    - develop conceptual designs.
- Select approach & parameters and document (CDR).
- Carry out necessary modeling.
- Proceed with detail design and fabrication.

HEEW - Desired Users Input for Requirements

- Energy Range (present design for 50 eV to 10 keV):

- Wiggler horizontal opening angle (present design is for +/- 9.65 mrad):

- Frequency of polarization handedness change (present design is for 1 Hz):

3-D Magnetic Calculations

Ross Schlueter

Lawrence Berkeley Laboratory

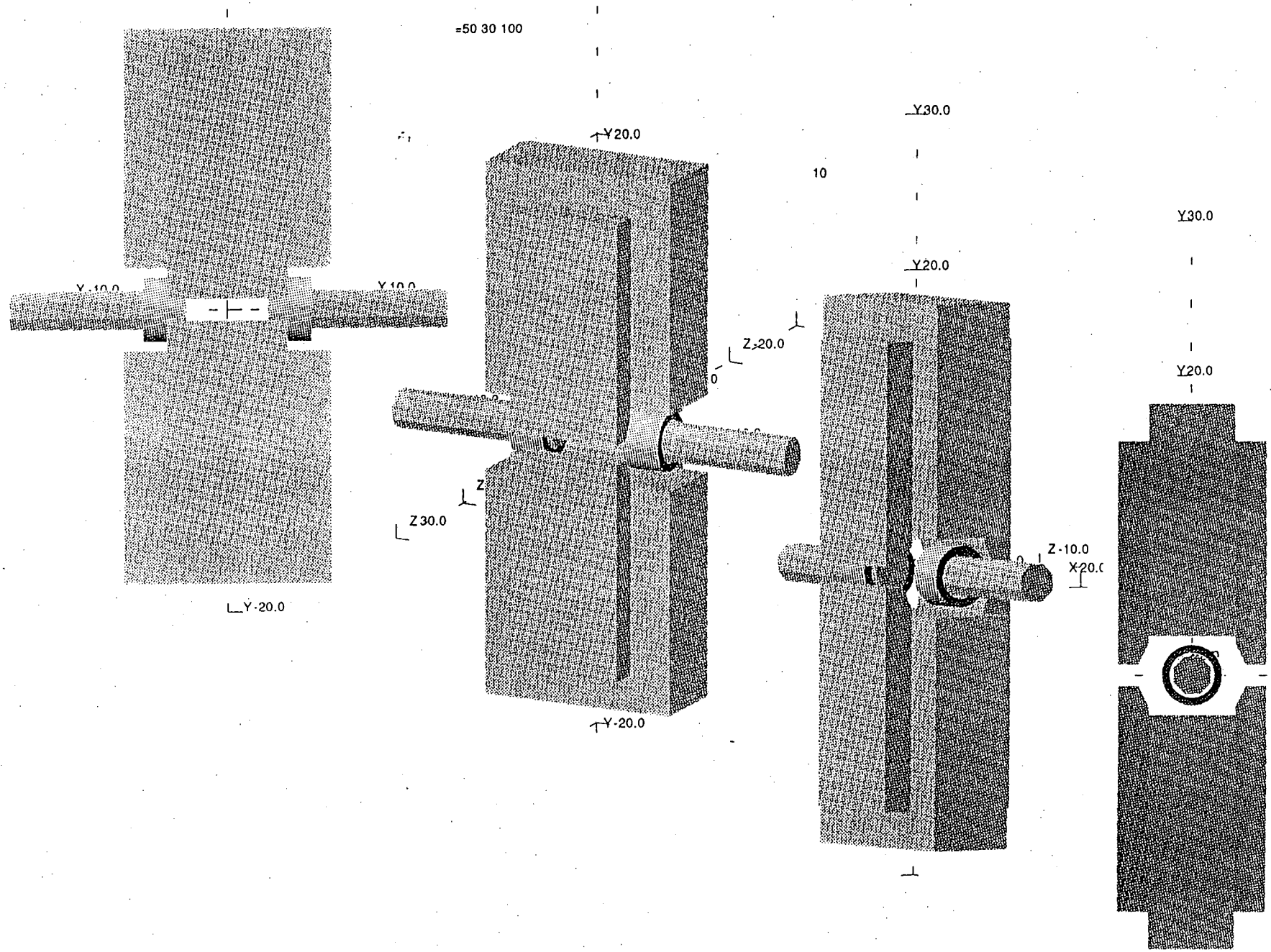
=50 30 100
Y-10.0
Y10.0
Y-20.0
Y20.0
Z-20.0
Z30.0
Y-20.0
10
Y30.0
Y20.0
Z-10.0
Y30.0
Y20.0

on-axis $\vec{B}$ vs. axial position

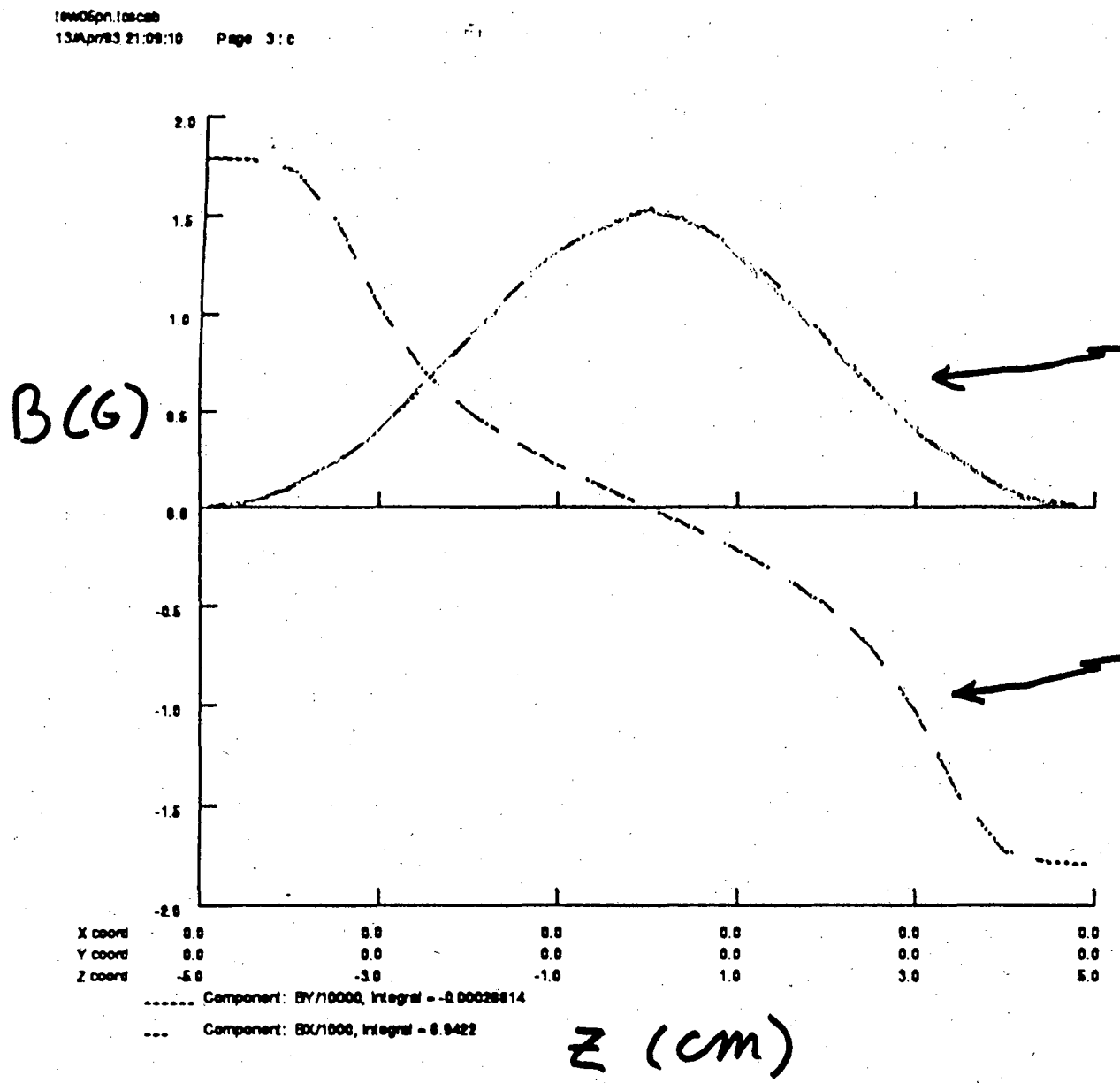

$B_x/10^3$ [G]

$B_y/10^4$ [G]

@ $I = 6.2$ kA

$\int_0^{\lambda/2} B_x \, dz = 6.9$ kG-c

VF/OPERA-3d

Beamlines for the Elliptical Wiggler

Phil A. Heimann

Lawrence Berkeley Laboratory

Beamlines for the Elliptical Wiggler

1 Grating Monochromator and Crystal Monochromator

- Operating Beamlines at the same time or in time sharing
- Effect of Optical Reflectivities on Circular Polarization Degree

2 Bring BL 10-1 from SSRL to ALS

- Layout of the Beamline
- Mod 1: Collecting Mirrors, 2 mrad -> 5 mrad
- Mod 2: Refocus Optics, sub-mm spot
- Flux and Resolution

3 Crystal Monochromator based on BL 9.3.1

- Layout in Sector 11
- Power: Multilayer Premonochromator
- Rotation of the Crystal Monochromator
- Flux and Resolution

4 Discussion

Operating the Beamlines at the same time or in time sharing

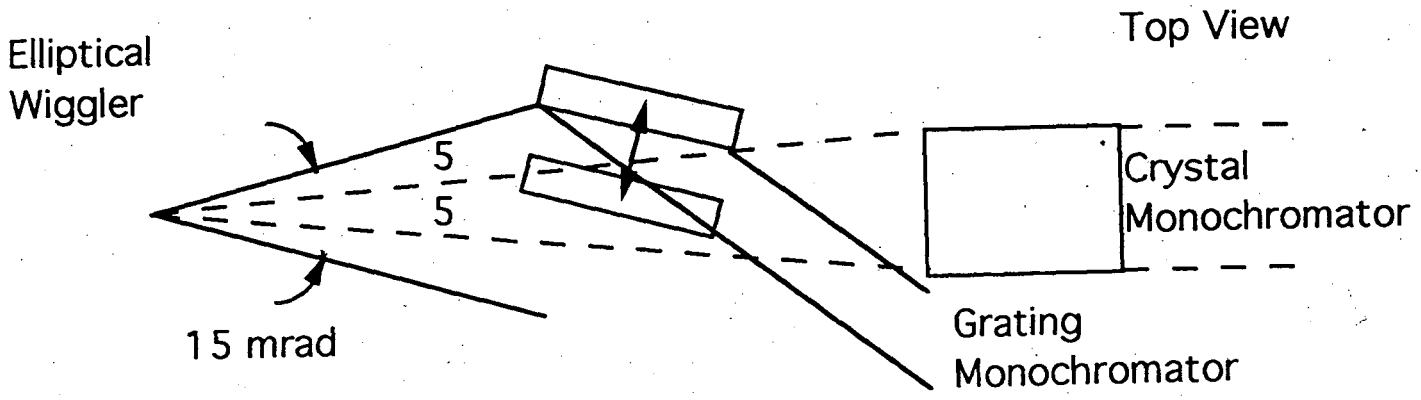

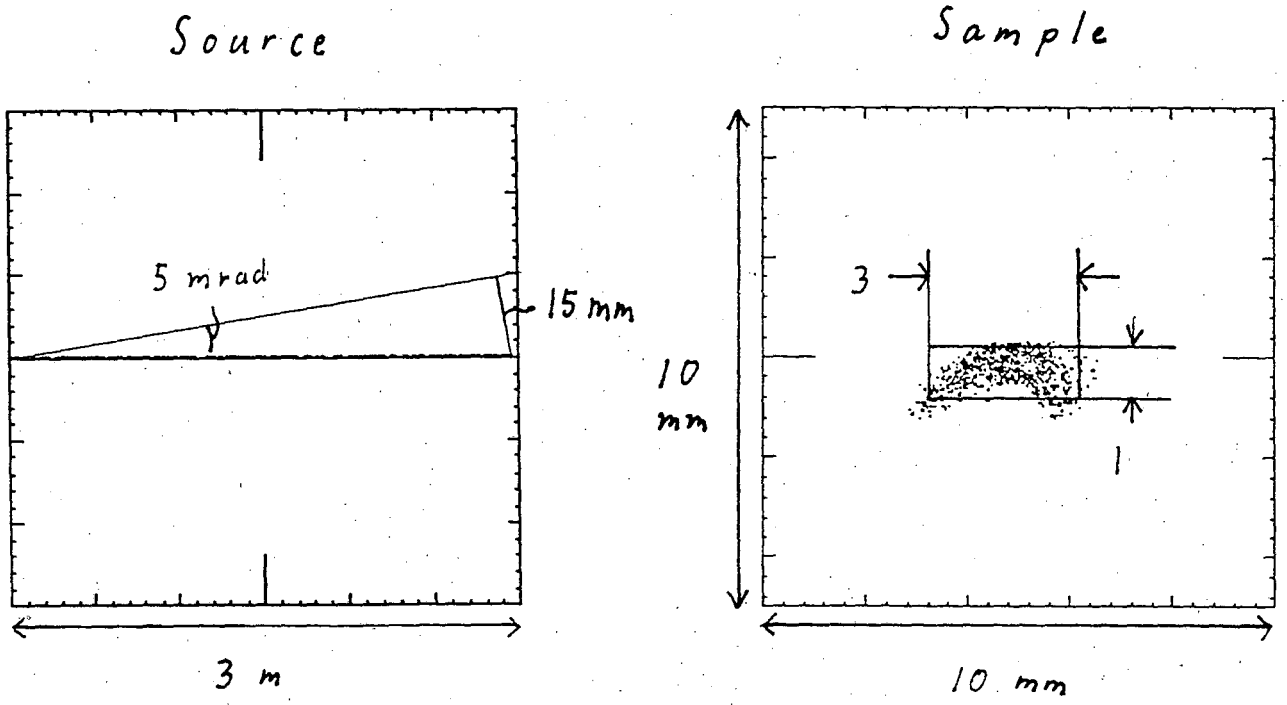

Off-axis collection has larger effective source size & results in a larger focus on the sample

Effect of Optical Reflectivities on Circular Polarization Degree

Mirror

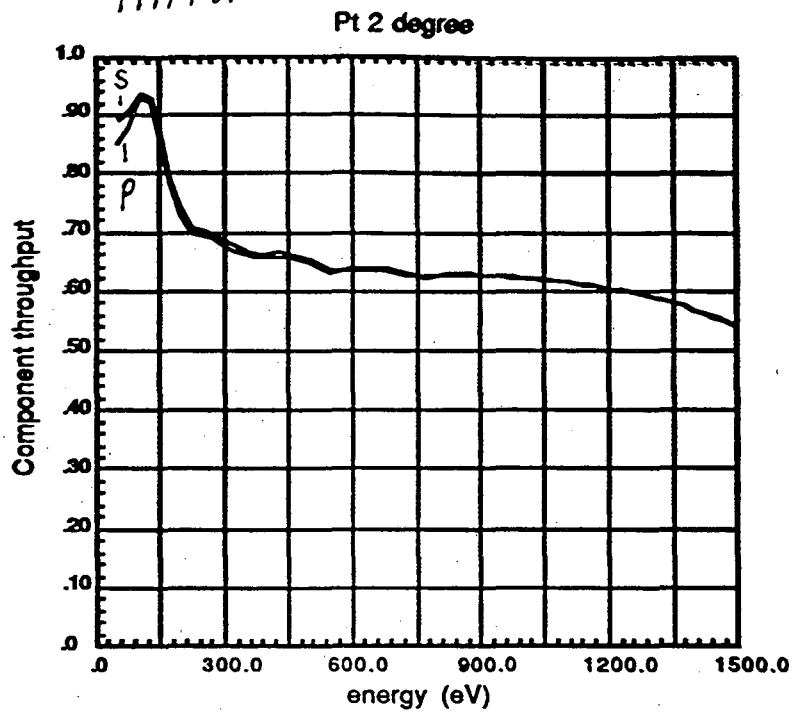

Grating Monochromator will have only Grazing Incidence Reflections

Crystal Si (1 1 1)

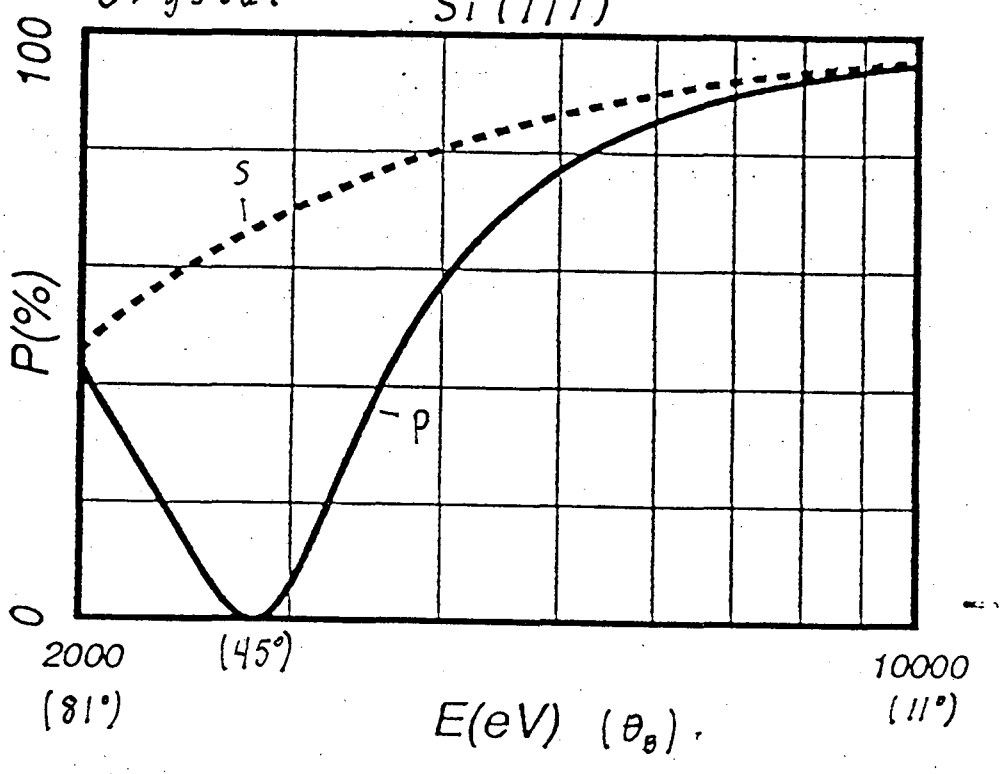

Phase Shift is also a Concern

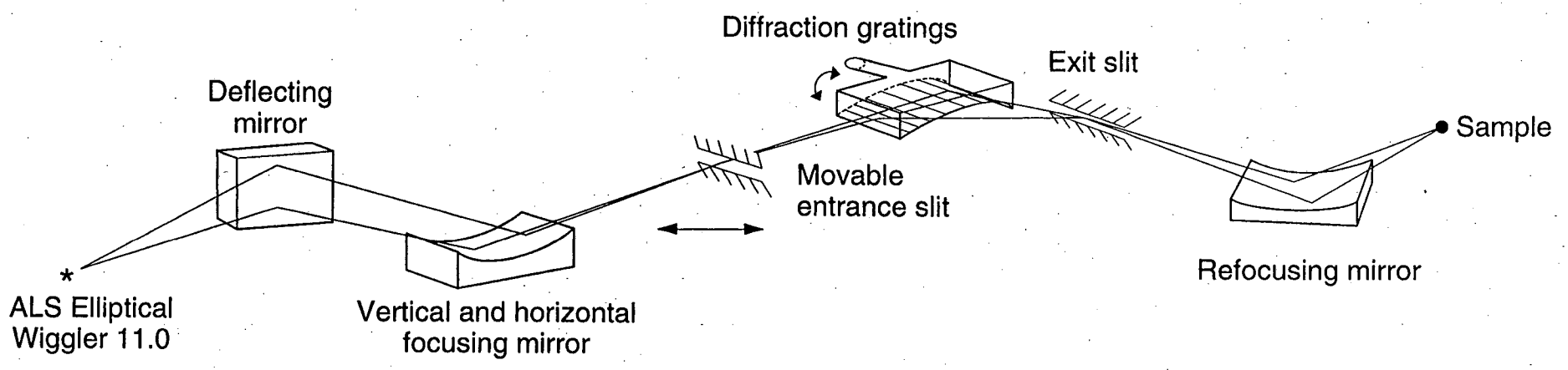

XBL927-5333C

Beamline 10-1

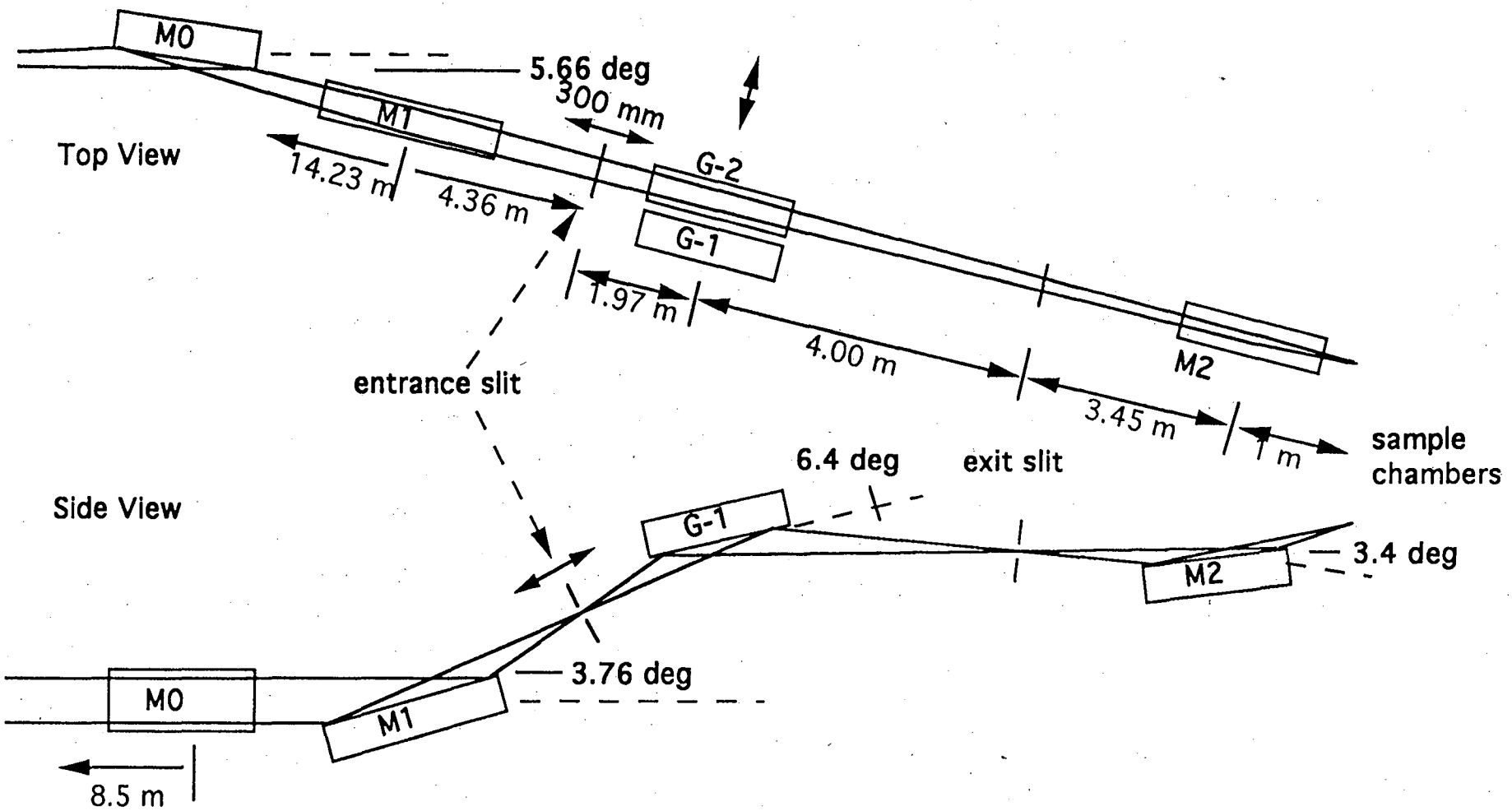

Raytrace of Elliptical Wiggler Through BL 10-1

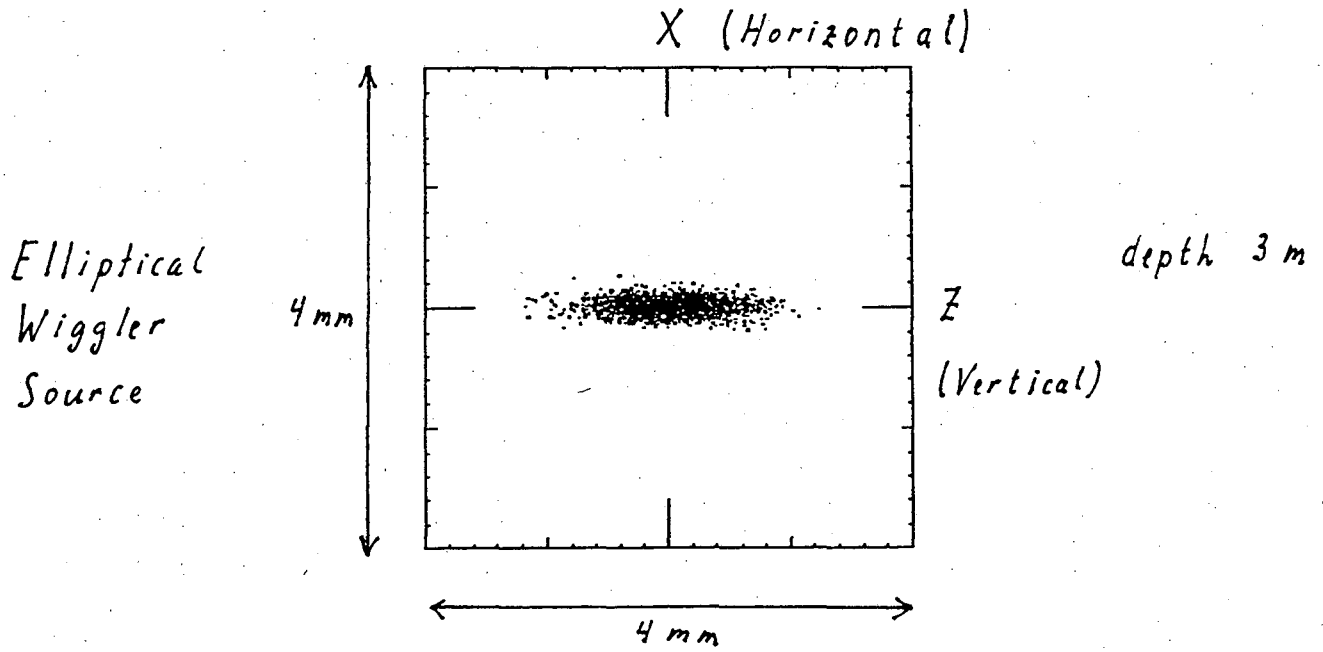

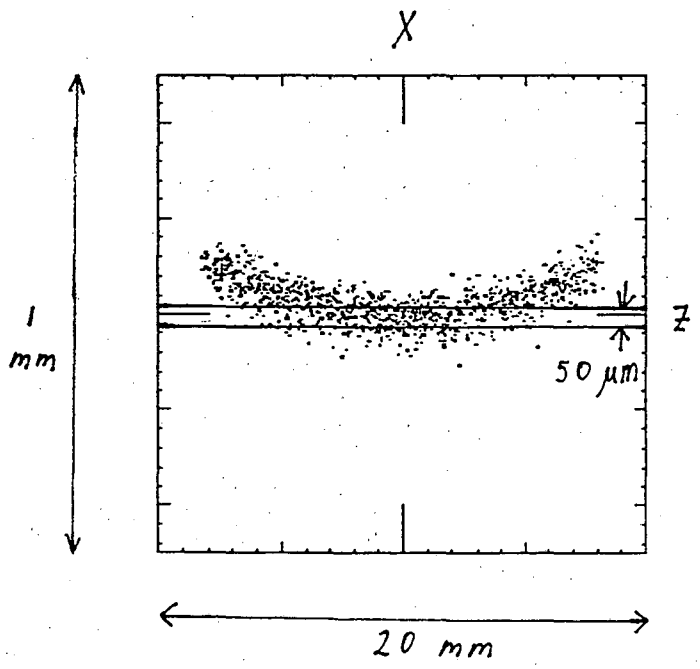

Entrance Slit at M1
Vertical Focus
37 % Transmission

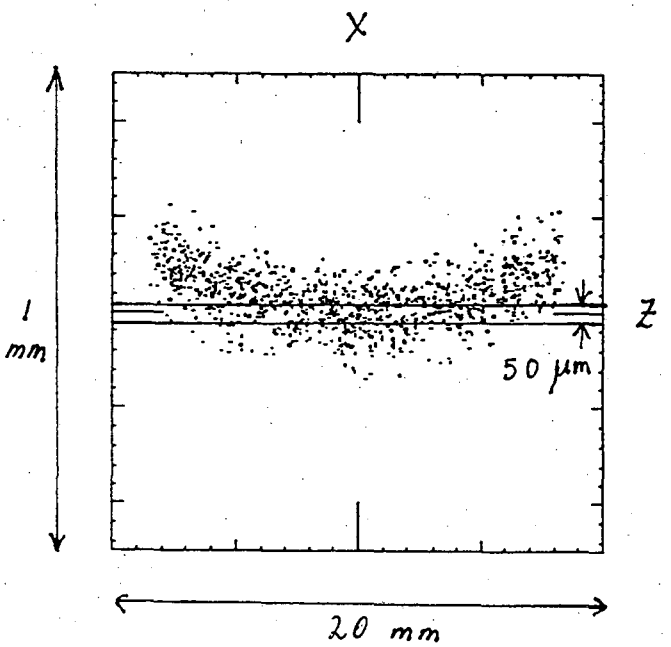

Entrance Slit at -150 mm

28 % Transmission

Exit Slit

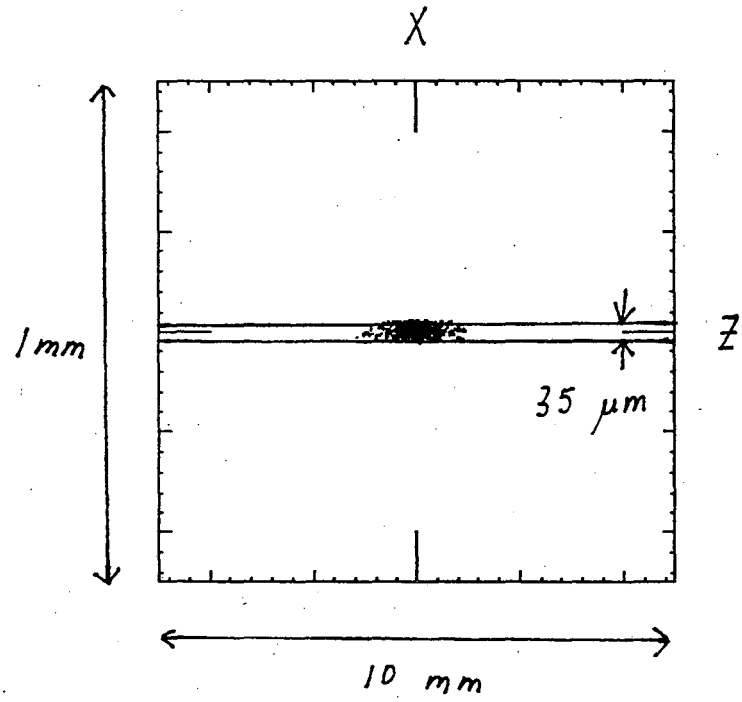

Sample

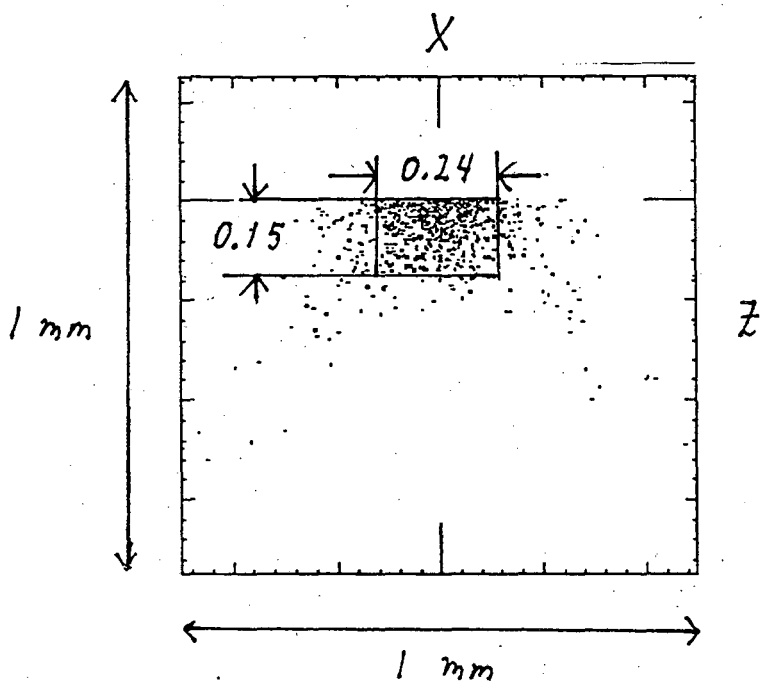

Actual focus at SSRL: $0.5 \times 1\ mm^2$

M. Samant

Difference:

i) SSRL source

ii) Mirror errors

Collecting Mirrors for 5 mrad ψ_H

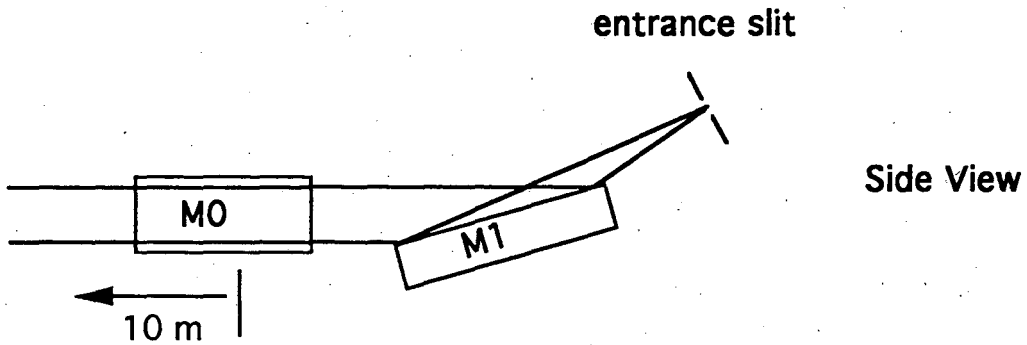

Mirror	Figure	θ	R(m)	Aperture (mm)
M0	Cylinder	87.5°	271.8	50 x 1150
M1	Sphere	88°	191.26	50 x 450

Entrance Slit

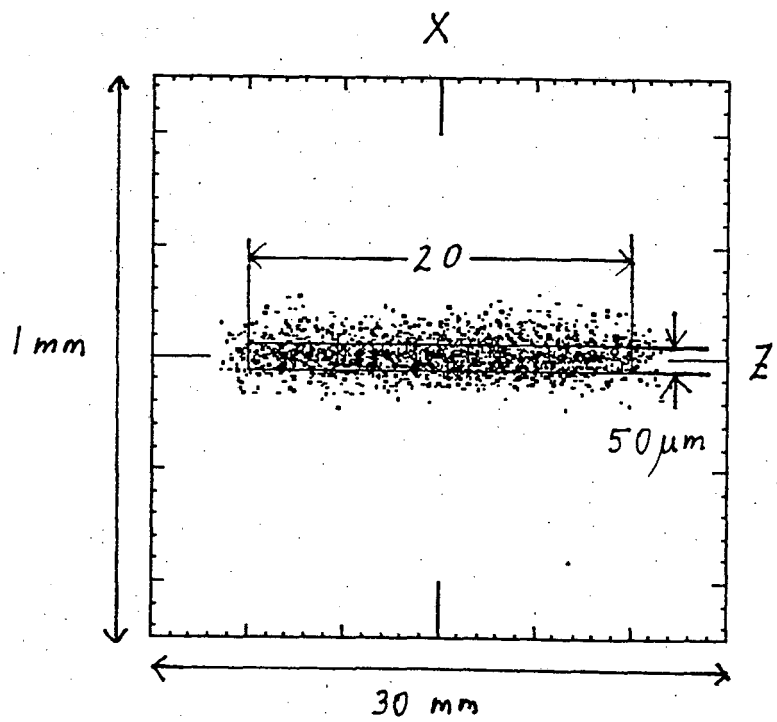

No line curvature

61 % Transmission

Modification 2: Refocus Optics

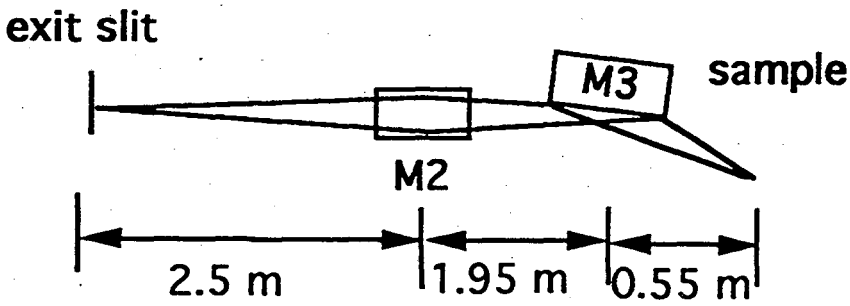

Top view

Mirror	Figure	θ	R (m)	Aperture (mm)
M2	Sphere	88°	71.634	50 x 150
M3	Elliptical Cylinder	88°	-	50 x 300

accepts 2 mrad ψ_H

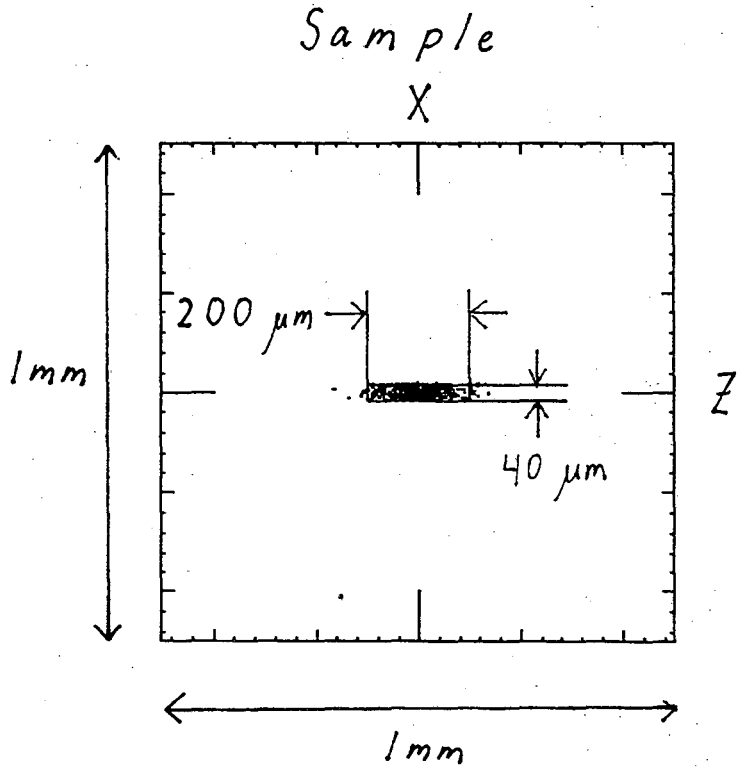

Resolution

N_2
$1s \rightarrow \pi^*$

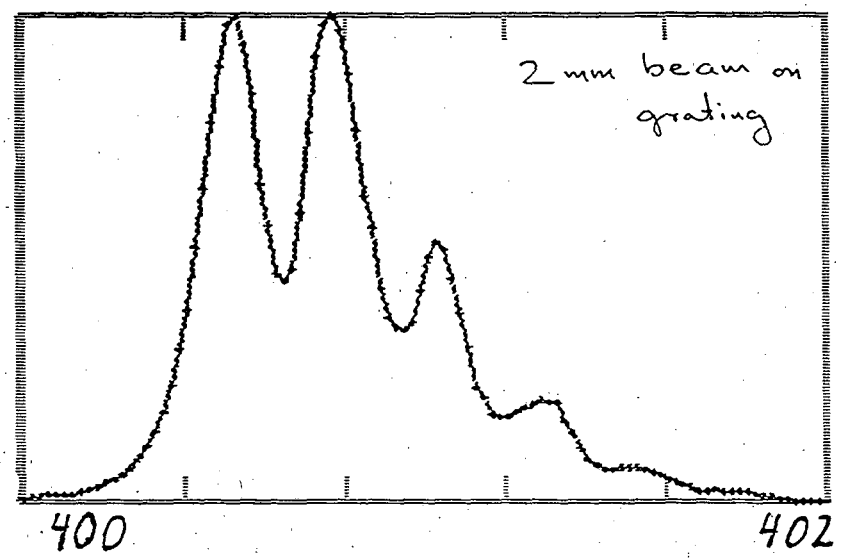

from
M. Samant

$$\Delta E \sim 80 \text{ meV} \qquad RP = \frac{E}{\Delta E} \sim 5{,}000$$

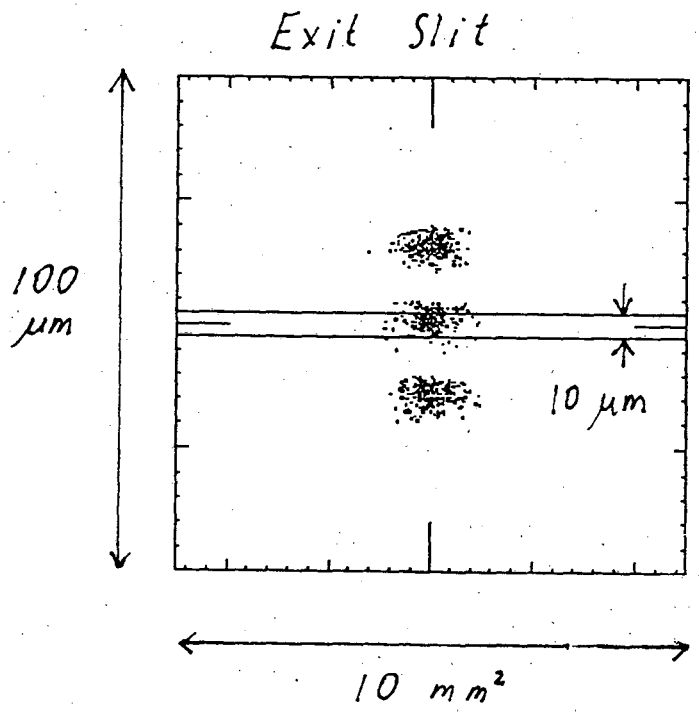

15 μm
Entrance Slit

$$\frac{E}{\Delta E} = \frac{243 \text{ eV}}{\pm 0.05 \text{ eV}} \sim 5000$$

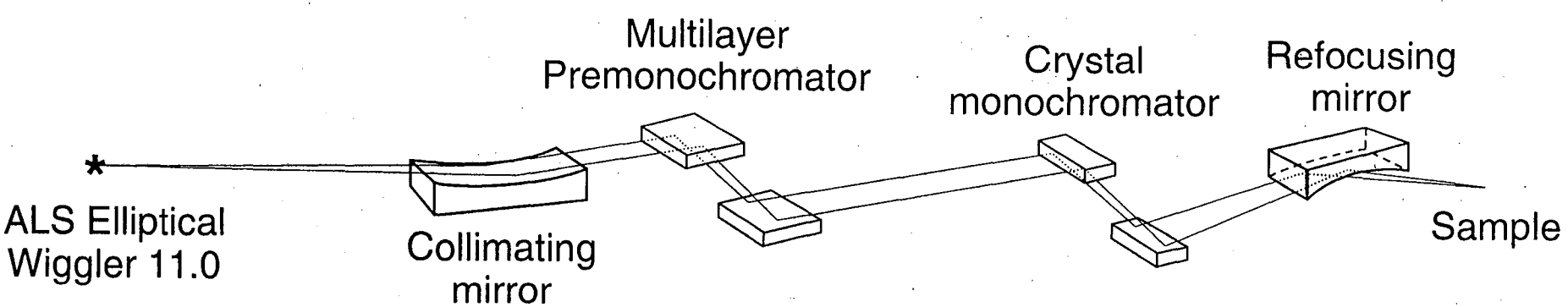
Multilayer
Premonochromator
Crystal
monochromator
Refocusing
mirror
ALS Elliptical
Wiggler 11.0
Collimating
mirror
Sample

XBL 934-4770

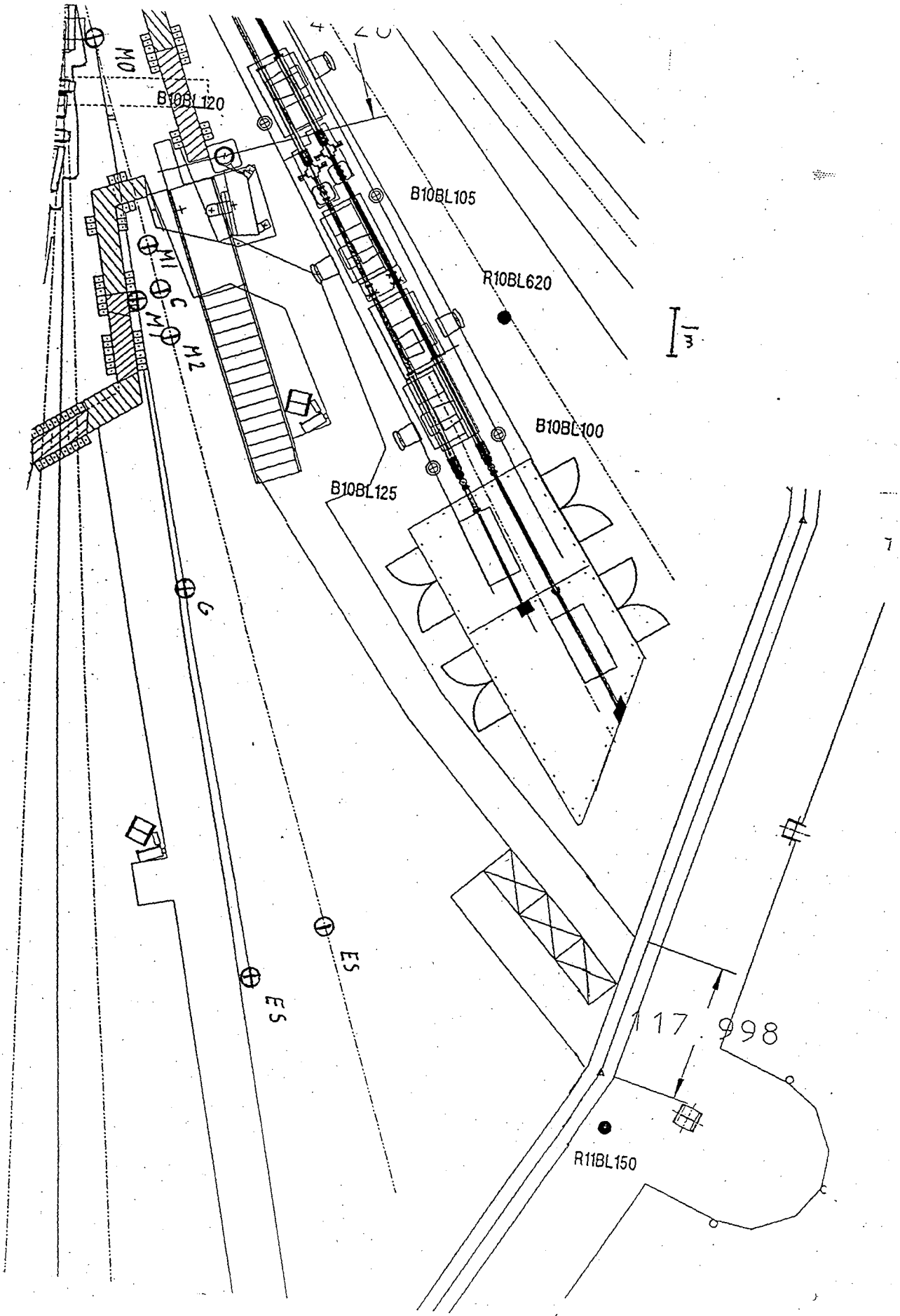
M0
B10BL120
B10BL105
R10BL620
M1
C
M2
B10BL100
B10BL125
G
ES
ES
117.998
R11BL150

Raytrace of Elliptical Wiggler Through Crystal Monochromator

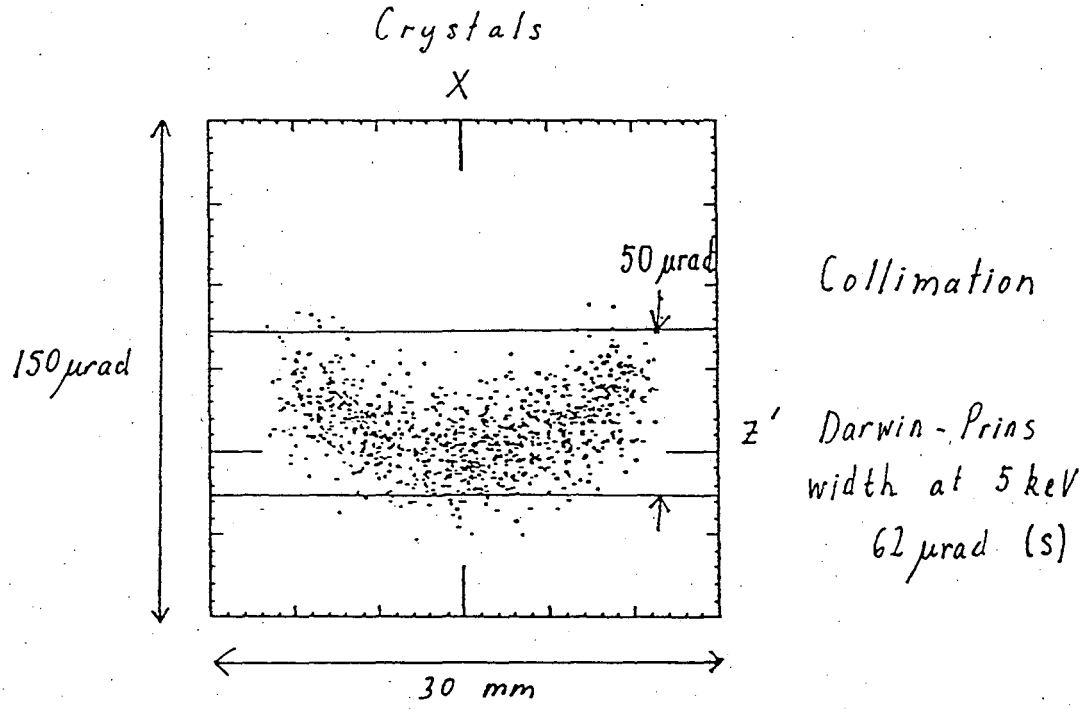

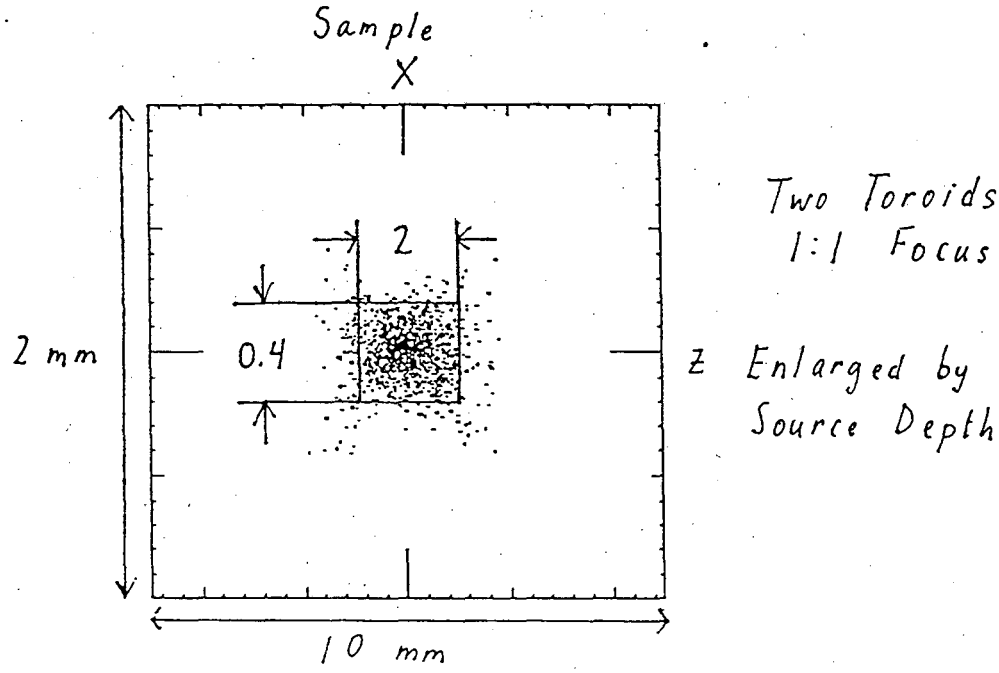

Power Considerations

Total Power	6.3 kW
Power in 5 mrad x 0.3 mrad	325 W
Absorbed by M1 Mirror	67 W
Reflected by M1 Mirror	258 W

Protect Crystals with Multilayer Premonochromator

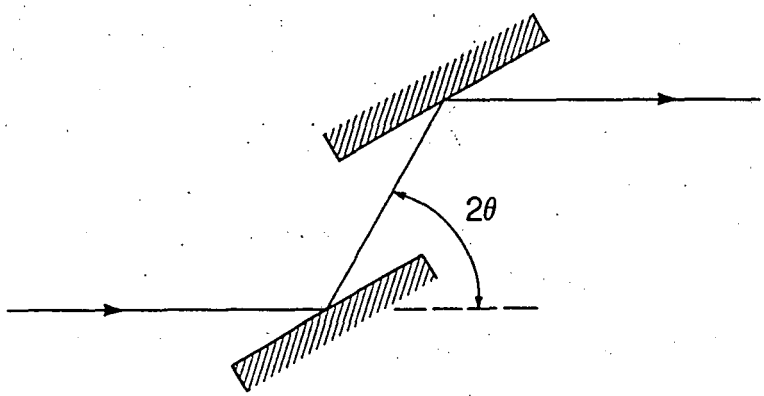

from Kortright & Digennaro SRI 88

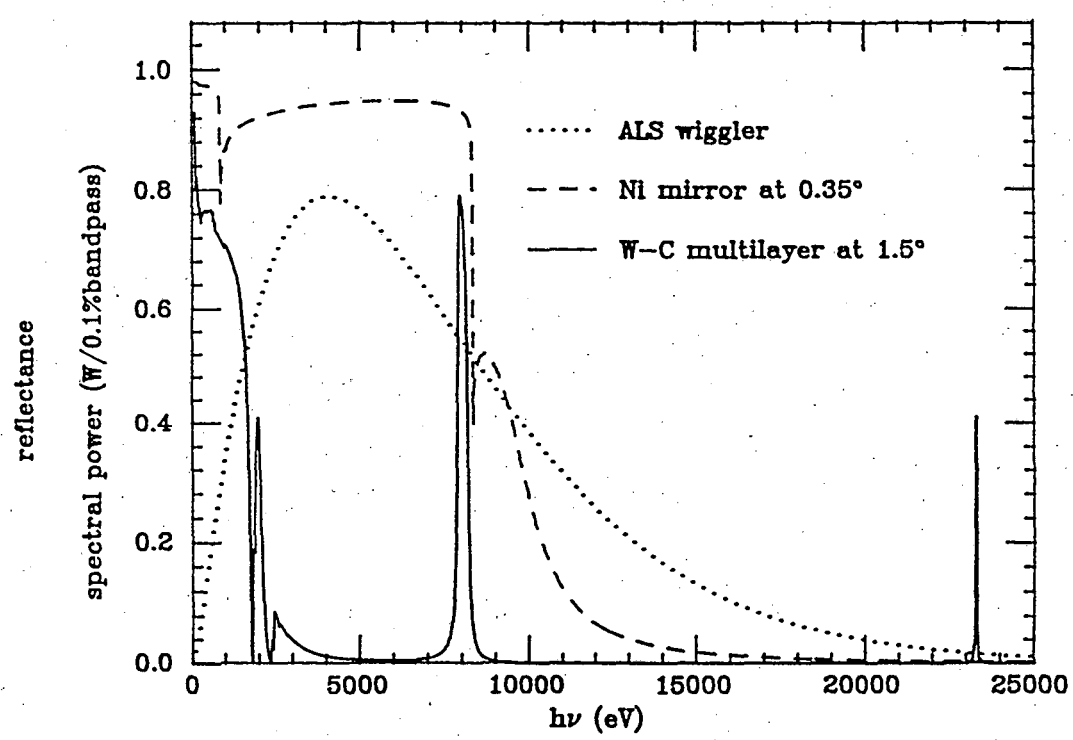

Power Reduced by ~ 1/100
Flux Reduced by ~ 1/10

From RADID

Crystal Monochromator Flux

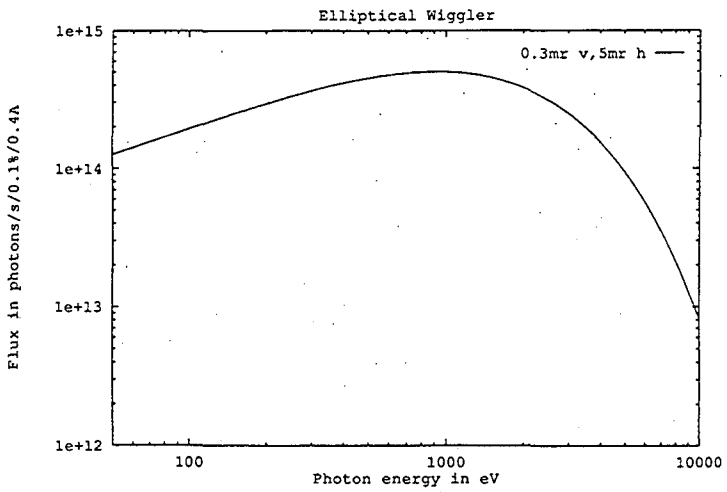

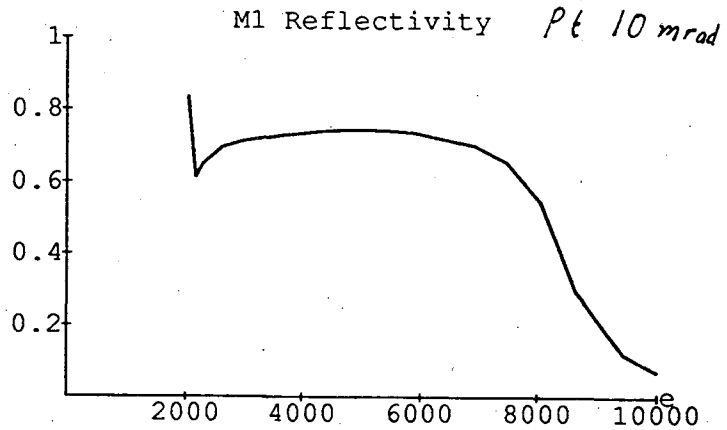

2 × Si(111)

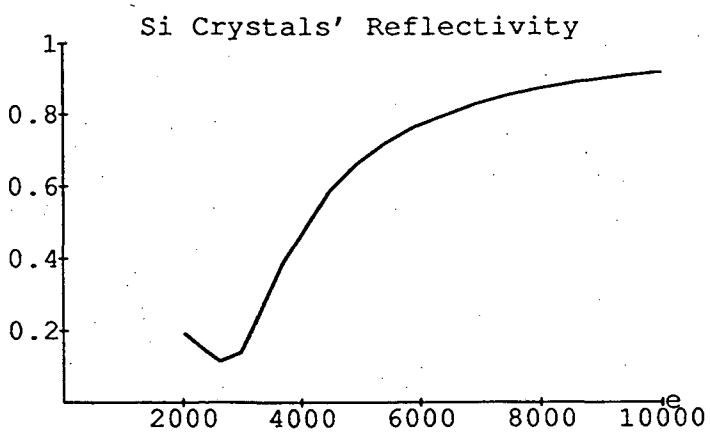

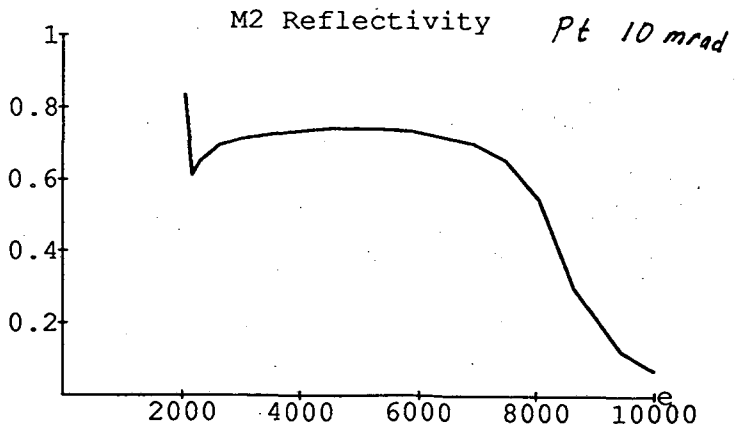

Crystal Monochromator Flux

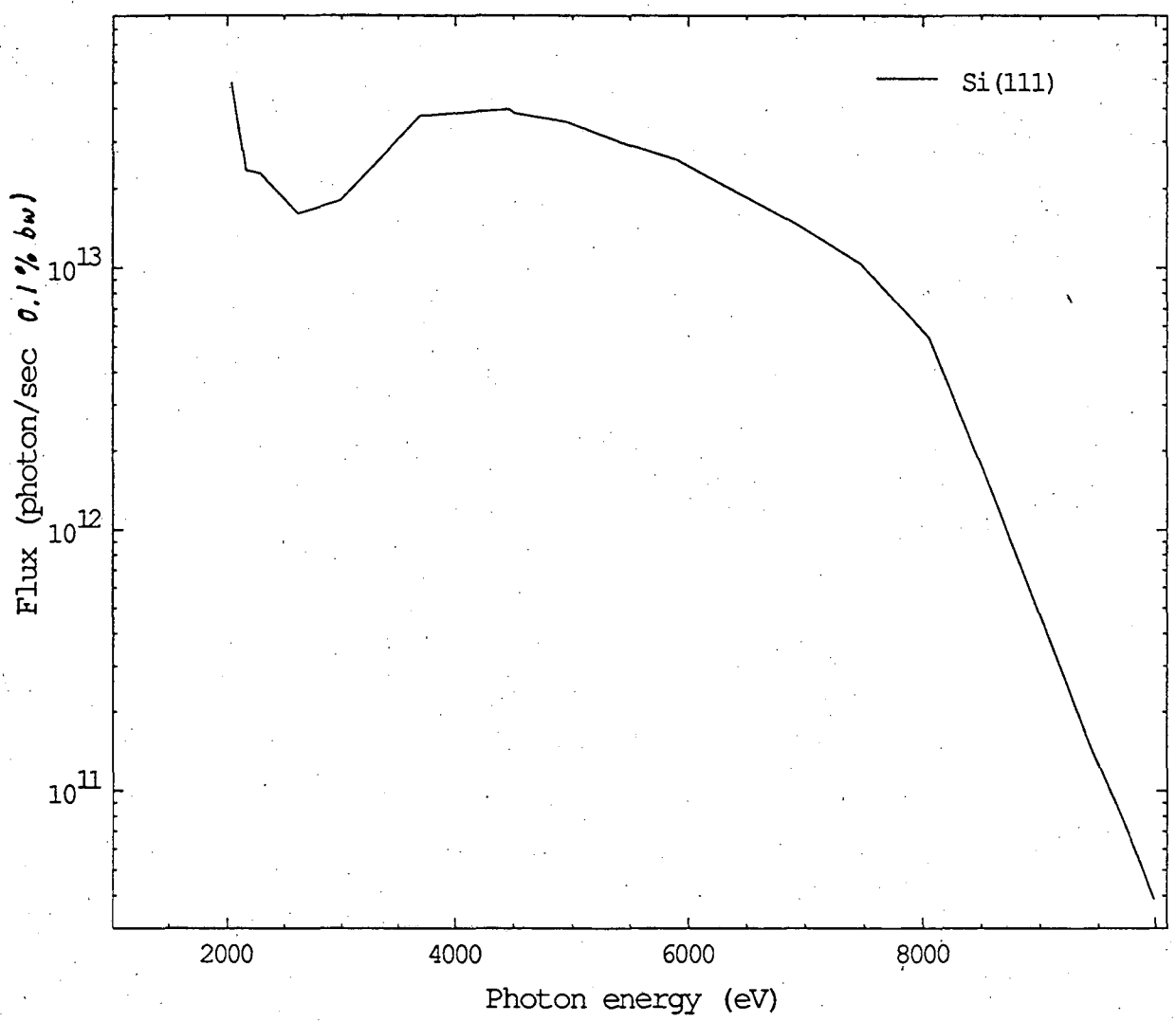

Neglecting:

Premonochromator ~ 0.1

Angular Acceptance of Crystals

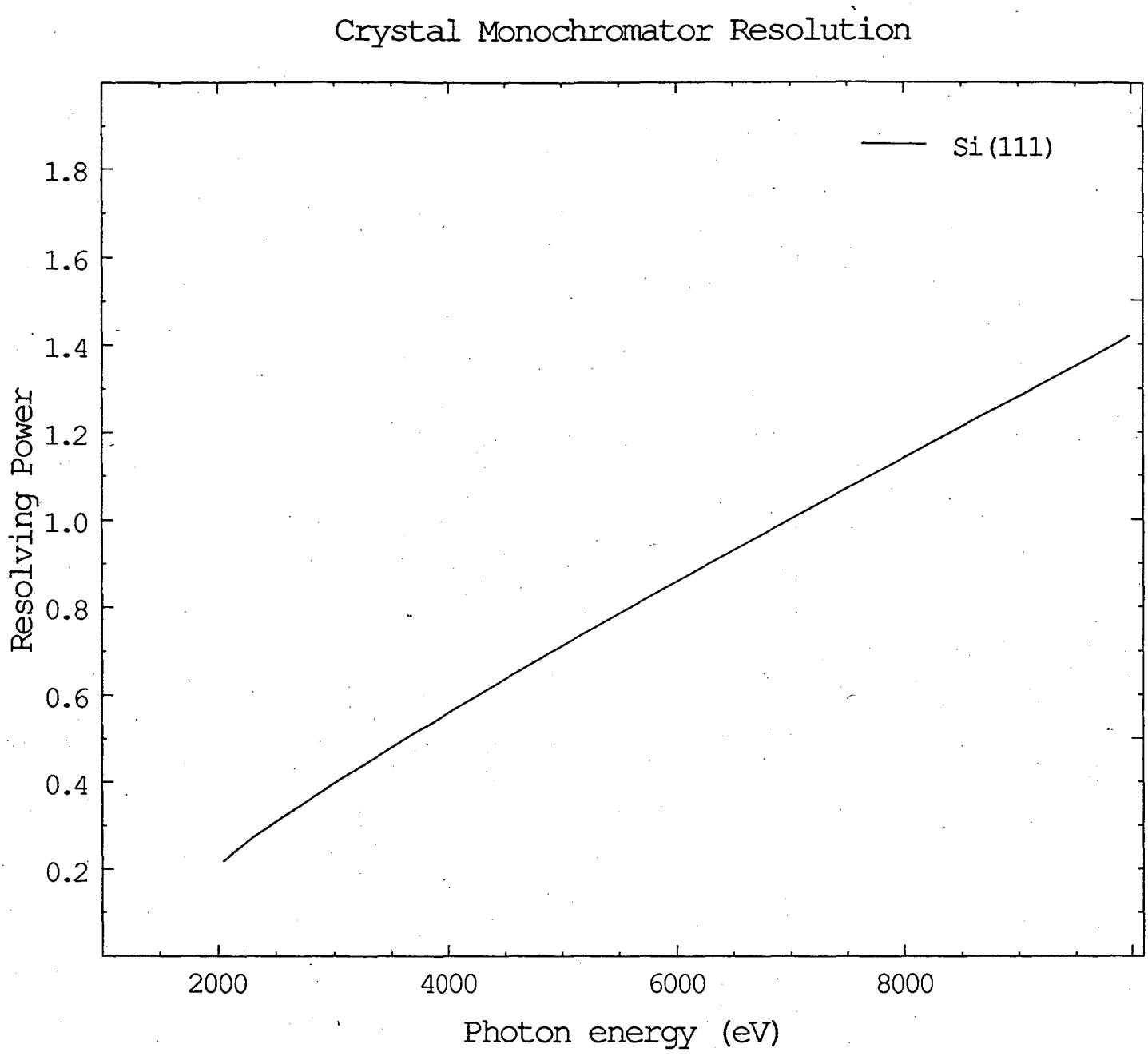

From Henke, Gullikson, Davis

Based on Calculated Rocking Curve Width For s- Polarization

4. Beamline Questions for Discussion

- Is it worthwhile operating both beamlines at the same time if the spot size for the grating monochromator beamline will be large?

- Is the IBM Beamline 10-1 or a similar SGM the ideal grating monochromator beamline for experiments using circular polarization

- What is minimum distance between last refocus mirror and sample?

- Is it necessary to reach 10 keV?

LAWRENCE BERKELEY LABORATORY
UNIVERSITY OF CALIFORNIA
TECHNICAL INFORMATION DEPARTMENT
BERKELEY, CALIFORNIA 94720

ABH593
LBL Libraries